

Doctoral Dissertation

**Finite Element (FE) Simulation of Masonry Wall Structures Considering
Mechanical Properties of Various Bricks**

各種レンガの力学特性を考慮した組積壁構造の有限要素解析

March, 2018

Muhammad Ridwan
14-9352-506-1

Graduate School of Science and Engineering,
Yamaguchi University

Acknowledgements

I would like to express deep appreciation to my advisor, Dr. Isamu Yoshitake from deep of my heart for his valuable guidance and expertise supervision continuously in last three years and four months. I am grateful to him for his interest, close supervision and encouragement along with his kind and supportive attitude in my PhD studies tenure and the time he has taken to finalize my research work and this dissertation. A great acknowledgement is due to Dr. Ayman Y. Nassif for his precious collaboration and suggestions in numerical investigations. His devotion to my research is a model for me.

My study presented in this dissertation was funded by Directorate General of Resources for Science Technology and Higher Education (DGRSTHE), Ministry of Research Technology and Higher Education of The Republic of Indonesia. My gratitude extends to DGRSTHE and Institute of Technology Padang that have made my study in field study Construction Materials, Departement Systems Design and Engineering, Graduate school of science and Engineering Yamaguchi University. My endless gratitude must be expressed to my fellow students at Construction Materials Laboratory deserve thanks for always being available to bounce ideas around and for simply creating a friendly atmosphere at the laboratory.

Finally, I am sincerely and deeply grateful to my family. Too much appreciation could never be expressed to my loving family. My parent Yulimar (alm.) and Aida Ibrahim, my loving wife Yessy Suryanty for her patience, understanding and support every day during my studies, my daughter Rahadatul Mardhiyah and my son Arif Abdul Aziz have always supported me. They have exemplified the meaning of true success, contentment found only in God.

I also thank my brother and sister, Nini Rahmi, Rozi Fidaus and Ulya Rahmi, for their encouragement. Additionally, I must express gratitude to my friends Desmon Hamid and Rahmat Zuhri, who have become part of my family. I could always count on them for support through the toughest and busiest moments of my graduate life.

Most importantly, I would like to thank Allah SWT for leading me and helping me find success in my studies. He gives me the true reason to strive forward day by day. Blessings I have seen in my life while in Yamaguchi have been more than coincidence. Ultimately, all thank goes to Him.

ABSTRACT

The main component of masonry wall structures in some developing countries are traditional clay brick. The traditional clay bricks are produced locally without following any technical inspection or standard, so the quality of bricks is quite different in regions. These bricks are used for houses and simple buildings, not only in village areas but also in the urban region.

Some developing countries like Indonesia are in a high risk seismic region. Many masonry houses have been damaged by severe earthquakes and the collapsed house have caused many injuries and deaths.

The research presented in this dissertation aims to analytically investigate structural behavior of masonry walls subjected to lateral loading, which are built with bricks various modulus. The study investigated on quality of clay brick on some developing countries and examined the effect of various quality bricks on elastic behavior of masonry structures. In addition, the study performed the FE simulation to examine the load-bearing capacity of the masonry wall subjected to out-of-plane lateral load.

The present dissertation consists of 5 chapters and contents of each chapter are shown below:

Chapter 1 "Introduction" describes the research background and purposes of the study. Main contents of this thesis are shown in this chapter.

Chapter 2 "Literature review" summarizes previous investigations dealing with masonry building structures in some developing country. In particular, this chapter describes previous researches dealing with the numerical simulations of the masonry wall structures.

Chapter 3 "Proposal of formulae for equivalent elasticity of masonry wall" addresses that bricks of low elastic modulus are occasionally employed in some developing countries. The purpose of this chapter is to quantify the equivalent elastic modulus of masonry structures made with various elasticity bricks. The study performed finite element (FE) simulations adopting the homogenization technique. The numerically estimated equivalent elastic moduli from the FE simulations were verified using previous test data. A new simplified formula for the equivalent modulus of elasticity for the masonry walls was proposed herein.

In Chapter 4 "New method for estimation of out-of-plane strength of masonry walls", the truss theory which is rarely used to analyze a masonry wall was used and discussed. This chapter proposes the fictitious truss method (FTM) to determine the elastic behavior of masonry walls subjected to lateral loading. The study employs a two-dimensional linear static model for masonry walls. The applicability of the FTM modeling is discussed by comparing to previous results. The result confirms that the FTM is a reliable method of assessing the out-of-plane strength of masonry walls owing to its conceptual accuracy, simplicity, and computational efficiency.

In Chapter 5 “Conclusions”, the main findings and knowledge’s obtained from the numerical investigations are summarized. In addition, this chapter addresses the future research in this research field.

|

抽象

発展途上国における壁状組積構造の主要な構成要素は、伝統的な粘土質レンガである。これらのレンガは大規模な工場製造ではなく、小規模な家内制手工業で製造されていることから、その品質管理にあたり適当な規準等もなく、地域ごとに品質が大きく異なる。このように製造されたレンガが、地方の家屋だけでなく都市部の住宅にも主要材料として使用されている。インドネシアのようないくつかの発展途上国は、地震のリスクが高い地域にある。多くのレンガ組積構造の住宅は地震によって深刻な損傷を受けており、崩壊した住宅によって多くの人命が失われることがしばしばである。本論文では、さまざまな弾性率のレンガを用いてつくられた壁状組積構造が水平荷重を受ける時の挙動を解析的に調べることを目的としている。この研究では、上記のような発展途上国で使用される粘土質レンガの品質を調べ、壁状組積構造の弾性挙動に及ぼすさまざまな品質のレンガの影響を調べた。さらにこの研究では、面外方向の水平荷重を受ける壁構造の耐荷重性能を調べるため有限要素解析を行った。

本論文は全5章で構成されており、各章の主な内容は以下のとおりである

.

第1章「序論」では，研究背景と目的について説明している．また，本論文の主な構成を示している．

第2章「既往の研究」では，発展途上国のレンガを使った壁状組積構造について検討した既往の研究をまとめている．この章では，特に壁状組積構造の数値シミュレーションを行った既往の研究を中心にレビューしている

第3章「組積壁構造の等価弾性係数の推定式の提案」では，先ずいくつかの途上国でしばしば低い弾性係数のレンガが使用されていることを示している．この章の目的は，さまざまな弾性係数を有するレンガでつくられた石積構造の等価弾性係数を定量化することである．この研究では，均質化法を使った有限要素（FE）シミュレーションを実施した．既往の試験データを用いて，FEシミュレーションに基づき数値的に推定された等価弾性係数を求めた．そして組積壁構造に適用できる等価弾性係数の簡易推定式を提案した．

第4章「組積壁構造の面外水平耐力の推定法」では，組積構造の解析にはほとんど使用されないトラス理論について検討を行った．この章では，面外方向の水平荷重を受ける組積壁状構造の弾性挙動を定める仮想トラス法（FTM）を提案している．この研究では，2次元線形静的モデルを採用している．提案するFTMの適用性について，既往の結果と比較しながら考察し

ている。比較結果より、FTMが解析精度・簡易性および計算効率に優れ、組積壁状構造の面外強度を評価する信頼できることを確認している。

第5章「結論」では、本研究の数値解析的検討から得られた主な知見等を要約している。さらに、この研究分野における今後の研究課題について述べている。

CONTENTS

ACKNOWLEDGEMENTS	i
ABSTRACT	ii
CONTENTS	viii
LIST OF FIGURES	xii
LIST OF TABLES	xvii
CHAPTER 1. INTRODUCTION	1
1.1. Background	1
1.2. Objectives.....	2
1.3. Outline of the dissertation	3
CHAPTER 2. LITERATURE REVIEW	7
2.1. Active seismic zone in the world	7
2.2. Non-engineered building construction in developing countries .	8
2.2.1. Typical non-engineered building construction.....	10
2.2.2. Conditions of non-engineered construction in developing countries	14
2.3. Types of masonry	19
2.3.1. Unreinforced masonry structures	19

2.3.2. Reinforced masonry structures	21
2.3.3. Confined masonry structures	22
2.4. Mechanical properties of masonry materials	23
2.4.1. Masonry units	24
2.4.2. Mortar	29
2.4.3. Masonry	33
2.5. Disposition of bricks or blocks	45
2.6. Types of Failure	47
2.6.1. In-Plane Failure of masonry wall.....	47
2.6.2. Out-of-plane failure of masonry wall	51
2.7. Model and methodology for analysis masonry wall	57
2.7.1. Discontinuous modelling of masonry	58
2.7.2. Continuous modelling of masonry.....	60
2.7.3. Finite element method	64

**CHAPTER 3. PROPOSAL OF FORMULAE FOR EQUIVALENT
ELASTICITY OF MASONRY WALL.....**

3.1. Outline	71
3.2. Investigation of the quality of bricks masonry	72
3.3. Overview FE simulation for homogenization.....	76
3.4. Purpose.....	78
3.5. Approach of the solution.....	79

3.5.1. Representative Element.....	79
3.5.2. Constitutive equation.....	84
3.6. Numerical simulations.....	86
3.6.1. Simulation model	86
3.6.2. Materials.....	88
3.6.3. Boundary condition	88
3.7. Equivalent elastic modulus calculation	90
3.8. Pre-simulation	91
3.9. Results and discussion.....	96
3.9.1. Equivalent elastic modulus.....	96
3.9.2. Poisson’s ratio and shear modulus	102
3.10. Verification and validation	103
3.11. Formula comparison.....	104
3.12. Summary	109

CHAPTER 4. NEW METHOD FOR ESTIMATION OF OUT-OF-PLANE STRENGTH OF MASONRY WALLS..... 111

4.1. Outline.....	111
4.2. Some proposed methods for analyzing masonry structure.....	112
4.3. Overview of out-of-plane strength of masonry structure	114
4.4. Material and Methods.....	118
4.4.1. Determination of truss geometry.....	118

4.4.2. Schematic of the FTM	122
4.4.3. Material models	124
4.5. Aspect ratio, slenderness ratio, and weight reduction	126
4.6. Results.....	128
4.6.1. Validation 1.....	128
4.6.2. Validation 2.....	134
4.6.3. Validation 3.....	138
4.7. Discussion.....	140
4.8. Summary.....	147
CHAPTER 5. CONCLUSIONS AND FUTURE RECOMMENDATION...	149
5.1. Conclusions.....	149
5.2. Recommendation	151
APPENDIX A	153
APPENDIX B	157
NOMENCLATURE.....	161
REFERENCES.....	167
RESEARCH ACHIEVEMENT.....	xix

LIST OF FIGURES

Figure 2.1 World earthquakes during the period of 2017.....	7
Figure 2.2 Typical Non-engineered buildings in Balasore, Dehradun, India. [Okazaki <i>et al.</i> , 2012]	10
Figure 2.3 Typical non-engineered buildings in Bandung City, Indonesia.....	11
Figure 2.4 Typical non-engineered buildings in Potohar Plateau and Plains of Punjab, Pakistan [Okazaki <i>et al.</i> , 2012].....	12
Figure 2.5 Typical non-engineered buildings in Puente Piedra, Carabayllo,Peru [Okazaki <i>et al.</i> , 2012]	12
Figure 2.6 Typical non-engineered buildings in Egypt Helwan City, El-Marg City	13
Figure 2.7 Typical non-engineered buildings in Balkot, Bhaktapur, Nepal.....	13
Figure 2.8 Typical non-engineered buildings in Yenikapi, Sirkeci, Turkey [Okazaki <i>et al.</i> , 2012]	14
Figure 2.9 Percentage of wall materials used in developing countries	15
Figure 2.10 Percentage of wall thickness used in developing countries	15

Figure 2.11 Buildings in Padang, Indonesia after earthquake September 30, 2009 (7.6 on Richter scale). Damages to an unconfined single story school building.....	17
Figure 2.12 Confined masonry: formwork present after construction of walls; note lack of columns on right side.	17
Figure 2.13 Typical earthquake damage: a house without vertical tie-columns and without top bond-beams in Attics (1988 Bovec earthquake).....	18
Figure 2.14 Unreinforced masonry	20
Figure 2.15 Reinforced masonry.....	21
Figure 2.16 Confined masonry.....	23
Figure 2.17 Typical stress-strain curve for compression in bricks.....	25
Figure 2.18 Relationship between compressive strength an elasticity module for bricks [Kaushik <i>et al.</i> 2007].....	25
Figure 2.19 Typical stress-strain curve for compression in mortar.....	30
Figure 2.20 Relationship between compressive strength an elasticity module for mortar [Kaushik <i>et al.</i> 2007].....	30
Figure 2.21 Correlation between stress-strain at masonry prism (Paulay and Priestley, [1992]).....	36
Figure 2.22 Mechanism of a collapse on the masonry prism [Paulay and Priestley, 1992].....	37
Figure 2.23 Testing arrangement of wallettes small walls, BS 5628 British 1992: (a) plane of failure parallel to bed joint, (b) plane of failure normal to bed, (c) Bond wrench shown in position before test and after bond failurejoint (Kalaf [2005]).....	40

Figure 2.24 Methods of testing shear strength in masonry construction [Paulay and Priestley, 1992]	44
Figure 2.25 Types of bond in masonry.	46
Figure 2.26 Typical sliding shear failure [Mistler, 2006].....	48
Figure 2.27 Typical shear failure [Mistler, 2006].....	49
Figure 2.28 Typical bending failure [Mistler, 2006].	51
Figure 2.29 Various types of wall support shapes and the associated out-of-plane flexure	53
Figure 2.30 Mechanics of internal moment resistance for the different types of bending.	53
Figure 2.31 Performance of URM walls subjected to out-of-plane load. [Paulay and Priestley,1992]	55
Figure 2.32 Moments and curvatures at center of face-loaded wall [Paulay and Priestley, 1992]	56
Figure 2.33 Advanced modelling approach (a) masonry sample; (b) detailed micro-modelling; (c) simplified micro-modelling; (d) macro-modelling [Lorenco,[1996].....	62
Figure 2.34 Homogenization of Masonry Material [Wu and Ha, 2006]	67
Figure 3.1 Average bricks compressive strength.....	74
Figure 3.2 Average mortar's thickness.....	75
Figure 3.3 Average plaster's thickness.....	75
Figure 3.4 Homogenization of masonry material.....	82
Figure 3.5 Model of masonry cells.....	83
Figure 3.6 Finite element Q4 used in numerical analysis	87

Figure 3.7 Load cases of imposed boundary displacement.....	89
Figure 3.8 Masonry as periodic composite material	91
Figure 3.9 Representative cells used.....	91
Figure 3.10 REO_1, mesh S1: 210 elements, 242 nodes, 484 DOF	92
Figure 3.11 REO_1, mesh S1: 760 elements, 819 nodes, 1638 DOF	92
Figure 3.12 REO_1, mesh S1: 760 elements, 819 nodes, 1638 DOF	93
Figure 3.13 Proposed model (RVE-1 and RVE-2)	93
Figure 3.14 Stress σ_y in REO_I along section 1-1 for various meshes, load case 2	94
Figure 3.15 Stress σ_y in REO_I along section 2-2 for various meshes, load case 2	95
Figure 3.16 Stress σ_y in REO_I along section 4-4 for various meshes, load case 2	95
Figure 3.17 Simulation results of equivalent elastic moduli of brick masonry	97
Figure 3.18 Degradation of Poisson's ratio.....	103
Figure 3.19 Equivalent elasticity of brick masonry	105
Figure 3.20 Comparison of equivalent elastic moduli based on Gumaste data (E_{mor} $> E_b$).	108
Figure 4.1 Establishing truss blocks and configuring the truss structure [Ridwan <i>et. al.</i> 2017].....	117
Figure 4.2 Truss shapes.....	119
Figure 4.3 Equivalent inertia of the effective cross section	119
Figure 4.4 Determination of the effective height of a truss element.....	121
Figure 4.5 Schematic of the proposed FTM.....	123

Figure 4.6 Stress–strain relationship of truss elements representing masonry walls	124
Figure 4.7 Setup of air bag (Herrera <i>et al.</i> [2016]).....	129
Figure 4.8 FTM model for Varela Rivera’s setup	132
Figure 4.9 Comparison of results for the first validation experiment	133
Figure 4.10 Hamoush’s test setup and FTM model.....	135
Figure 4.11 Comparison of results for the second validation experiment.....	137
Figure 4.12 Test setup for the third validation experiment.	139
Figure 4.13 Comparison of results for the third validation experiment.	146

LIST OF TABLES

Table 2.1. Compressive strength of mortar cubes 50 mm x 50 mm x 50 mm average of 3 cubes - according to ASTM C-270 [UNIDO, 1978a]	33
Table 2.2 Classification according to strength (SNI 15-2094-1991).....	38
Table 2.3 Correlation between modulus of elasticity of masonry and masonry compressive strength.....	42
Table 3.1 Moduli of elasticity for homogenization.....	79
Table 3.2 Material parameter for brick and mortar.....	88
Table 3.3 Material parameters for brick and mortar.....	94
Table 3.4 Homogenization model result from various researchers.....	98
Table 3.5 Percentage of change of simulation	100
Table 3.6 Examples of the calculations E_m	101
Table 3.7 Percentage of change of formula comparison.....	107
Table 3.8 Gumaste data and experiment and numerical results.....	109
Table 3.9 Comparison of Equivalent elastic moduli based on Gumaste data (E_{mor} > E_b).....	109
Table 4.1 Methods of analyzing masonry structures under out-of-plane loading	113
Table 4.2 Geometry, aspect ratio, and slenderness ratio of wall specimens.....	129
Table 4.3 Properties of SikaWrap 230-C (unidirectional) CFRP and Sikadur 330 resin.....	138
Table 4.4 Comparison of FTM with Varela Rivera's experimental results and various analysis methods.....	142

Table 4.5 Percentage of error of FTM method relative to Varela Rivera's
experiment and analysis method results 142

Table 4.6 . Comparison of FTM relative to Hamoush's experiment..... 145

CHAPTER 1. INTRODUCTION

1.1. Background

Masonry is composite building material around the world. Generally, depending on the availability of materials in the region, masonry bricks are made of clay, calcium silicate, limestone or natural stone, concrete, fiber composites or artificial materials. In some developing countries, traditional clay bricks are produced locally without following any technical inspection or standard and the quality varies from region to region. These bricks are used for houses and simple buildings, not only in village areas but also in the urban region.

In general, masonry structures are very good in resisting gravity loads, but do not perform well when subjected to lateral in-plane and out-of-plane loading, such as seismic loads caused by an earthquake. As countries locate in a high risk seismic

region, many masonry houses experienced severe damage during past earthquakes that caused many injuries and deaths. The houses collapsed gradually in brittle failure without ductility.

Based on the findings mentioned above, the mechanical characteristics of brick quality of masonry structure need to be studied.

1.2. Objectives

The study of masonry structures is still considered to have limited number of research activities and publications, compared to other civil- structural engineering research areas. Also, there have been very limited investigations and publications in the masonry area.

Therefore, the present research objective to investigate the performance mechanical characteristics of masonry walls subjected to lateral loading, which are built using bricks produced in local home industry. It supports the policy for contribution to standard for masonry rural houses and low-rise buildings.

The research significances are to address the problem of efficient and safe design of masonry houses and low-rise buildings in some developing countries. It aims to obtain the performance characteristics of masonry wall structure, built using local bricks, under lateral in-plane and out-of-plane loading, by using Finite Element (FE) simulation. The following objectives will be used to achieve the research aim:

- To deal with the quality of some developing countries clay bricks;
- To study of the effect of low quality of brick to elastic modulus of masonry;

- To study of the effect of loading on masonry wall under out-of-plane lateral load;
- To determine the load-bearing capacity and failure patterns of the masonry wall;

It will support the masonry modeling by using structural analysis software and the expected outcomes of this study are a simple model for predicting the strength of masonry wall.

The objective of this study is to quantify the equivalent elastic modulus of lower-stiffness masonry structures, when the mortar has a higher modulus of elasticity than the bricks, by employing finite element (FE) simulations and adopting the homogenization technique.

1.3. Outline of the dissertation

This dissertation contains five chapters. The outlines of each chapter are described below.

Chapter 1: Introduction

This chapter presents the research background and introduction to the topic, defines research problem, states the aim and outlines the method of investigation used in the study.

Chapter 2: Literature review

This chapter summarizes the experience of damage of masonry houses during the earthquakes in some developing countries. It reviews the

previous published literatures in the field of masonry wall structures and highlights the necessity and the scope of the current study. In particular, this chapter describes previous researches dealing with the numerical simulations of the masonry wall structures.

Chapter 3: Proposal of formulae for equivalent elasticity of masonry wall

This chapter presents the numerical simulation for investigation of equivalent elasticity of masonry structure. In this proposal addresses that bricks of low elastic modulus are occasionally employed in some developing countries. The purpose of this chapter is to quantify the equivalent elastic modulus of masonry structures made with various elasticity bricks. The study performed finite element (FE) simulations adopting the homogenization technique. The numerically estimated equivalent elastic moduli from the FE simulations were verified using previous test data. A new simplified formula for the equivalent modulus of elasticity for the masonry walls was proposed herein.

Chapter 4: New method for estimation of out-of-plane strength of masonry walls

This chapter proposes a model called the fictitious truss method (FTM) to determine the ability of masonry structures to withstand a lateral load within their elastic deformation capacities and introduces a two-dimensional linear static model for masonry walls. The model represents the effect of flexural interaction by computing the stress and strain in the axial direction of the material and by considering biaxial force effects on masonry elements. Pressure is applied to the surface

area of the wall sequentially to predict the ultimate tension and compression cracking.

The applicability of the FTM modeling is discussed by comparing to previous results. The result confirms that the FTM is a reliable method of assessing the out-of-plane strength of masonry walls owing to its conceptual accuracy, simplicity, and computational efficiency.

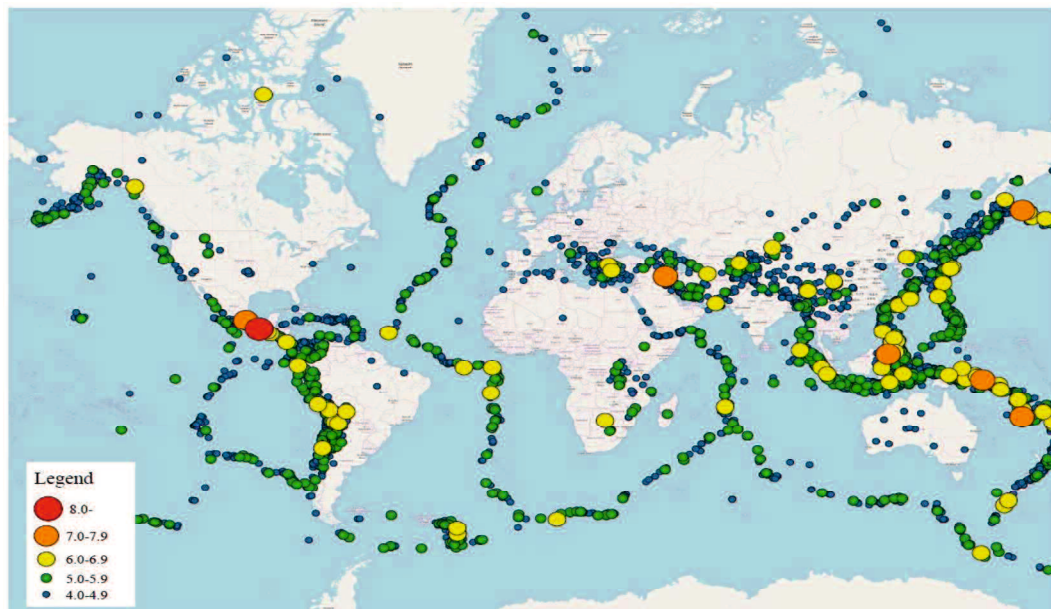
Chapter 5. Conclusions

This chapter summarizes the main findings and knowledge's obtained from the numerical investigations are summarized. In addition, this chapter addresses the recommendation and the future research in this research field.

CHAPTER 2. LITERATURE REVIEW

2.1. Active seismic zone in the world

Some developing countries are located in active seismic zones in the world. There are five active tectonic plates, earthquakes occurred daily in the region, with a magnitude of 5 in Richter scale or larger. Figure 2.1 shows the epicenters of recorded earthquakes during the period of 2017. A total of 11,594 earthquakes are plotted.



https://en.wikipedia.org/wiki/List_of_earthquakes_in_2017#/media/File:Map_of_earthquakes_in_2017.svg

Figure 2.1 World earthquakes during the period of 2017

This seismic has the potential to produce an earthquake with magnitude greater than 8.7. As example, the subduction zone in Sumatra is known for producing mega-thrust earthquakes such as the moment magnitude Mw 8.8-9.2 in 1833, the Mw 8.3-8.5 in 1861, the Mw 9.0-9.3 in December 2004, the Mw 8.7 in March 2005 and the Mw 8.4 in September 2007 [Irsyam *et al.*, 2008]. Based on the recent seismic activity, [Aydan *et al.*, 2007] identified a segment of the subduction zone facing Padang City that has not ruptured in the last 213 years. This seismic gap has the potential to produce an earthquake with magnitude greater than 8.7. The seismic gap is located in between the 1833 and 1861 fault ruptures, and it is estimated to have an approximate recurrence interval of 230 years [Zachariassen, 1999]. As a result, the potential earthquake rupture length in the Sumatra fault is not likely to exceed 100 km, so the maximum magnitude expected from such an event is estimated as Mw 7.5 [Natawidjaja, 2002; McCaffrey, 2009].

From previous seismic events, it has been seen that unreinforced masonry often presents an inadequate behavior to seismic actions, showing extensive cracking and disintegration due to combined inplane and out-of-plane loadings. This behavior is due to the low quality of materials,

2.2. Non-engineered building construction in developing countries

In general, buildings can be divided into two main categories, namely engineered buildings and non-engineered buildings, their percentages being quite different in developed, developing, and underdeveloped countries. Past destructive earthquakes showed that most of the disasters occurred to non-engineered buildings. In Indonesia, most dwellings (non-engineered buildings) constructed in small towns

and villages are built by referring to the tradition, their types suiting the culture and materials available in that area. The traditional houses generally have a good record or performance in past earthquakes. However, as the economic condition is prospering, there is a strong trend towards the construction of masonry houses and measure of status is associated with the owners of such masonry houses. Poor people tend to adopt such new habits and built “look like masonry” houses. Most of such masonry houses are built without considering the requirements for appropriate masonry construction

Most of the non-engineered constructions in developing countries, technically, are not properly constructed and most of the non-engineered constructions do not pay attention on the detailing, quality of materials, and quality of workmanship. Many building owners and craftsmen have limited knowledge on proper construction methods and they do not consider earthquake as a potential hazard. Most of the owners put deeper attention to the construction cost rather than building safely. Some of the craftsmen / masons have relatively insufficient formal education or training on proper building construction and gained their skills only from both the guidance from the foreman and their own experiences [Okazaki, *et al.*, 2012]

Therefore to reduce the earthquake risk in the future, all of those non-engineered construction should be reviewed if necessary. Since the non-engineered construction in developing countries has similarities as mentioned above.

2.2.1. Typical non-engineered building construction

Okazaki *et al.* [2012] have been survey on some developing countries have non-engineered houses that represent the current practice of non-engineered construction in various sites in the country.

- *India*

The most common non-engineered building in India is masonry building (of various types of bricks) with G + 1 story high. Most of the brick masonry building uses mud brick (adobe), CSEB and quarry stone. [Okazaki *et al.*, 2012]



Figure 2.2 Typical Non-engineered buildings in Balasore, Dehradun, India.

[Okazaki *et al.*, 2012]

- *Indonesia*

In general, there are three most common non-engineered constructions found in Indonesia, i.e. unconfined brick or concrete block masonry, confined masonry and reinforced concrete frame with infill masonry. Unconfined masonry building relies on the wall as the only load bearing structural elements (vertical and lateral). There is no confinement on this type of building and it is rarely found in Bandung

area. Confined masonry building relies on the masonry walls as the main load bearing structural elements. The confinement will contribute also to maintain the integrity of the wall when the loads are applied to the structures. Most of the confined masonry structures in Bandung are confined by reinforced concrete practical column/beams. Reinforced concrete with infill masonry wall building relies on the reinforced concrete columns and beams as the main load (both lateral and gravity) bearing structural elements [Okazaki *et al.*, 2012]



Figure 2.3 Typical non-engineered buildings in Bandung City, Indonesia
[Okazaki *et al.*, 2012]

- *Pakistan*

Three types of non-engineered building (confined masonry, unconfined masonry and reinforced concrete with infill masonry) are mostly adopted in non-engineered buildings in Pakistan.



Figure 2.4 Typical non-engineered buildings in Potohar Plateau and Plains of Punjab, Pakistan [Okazaki *et al.*, 2012]

- *Peru*

In Peru, there are three types of non-engineered buildings. Those are confined masonry building with horizontal and vertical confinements that support the bricks walls, unconfined masonry walls building without reinforced collar beam and reinforced confined elements and Concrete moment resistant frame with concrete shear walls or infill masonry.



Figure 2.5 Typical non-engineered buildings in Puente Piedra, Carabayllo, Peru [Okazaki *et al.*, 2012]

- *Egypt*

The most common types of non-engineered building in Egypt are reinforced concrete skeleton type buildings, wall bearing lime stone buildings and combined reinforced concrete and lime stone wall buildings.



Figure 2.6 Typical non-engineered buildings in Egypt Helwan City, El-Marg City
[Okazaki *et al.*, 2012]

- *Nepal*

In Nepal, there are two types of non-engineered brick masonry buildings, i.e. unconfined brick masonry buildings and reinforced concrete buildings with brick masonry infill.



Figure 2.7 Typical non-engineered buildings in Balkot, Bhaktapur, Nepal
[Okazaki *et al.*, 2012]

- *Turkey*

There are three types of non-engineered building in Turkey, i.e. reinforced concrete frame with clay hollow brick infill wall, unreinforced brick masonry and wooden structures.



Figure 2.8 Typical non-engineered buildings in Yenikapi, Sirkeci, Turkey
[Okazaki *et al.*, 2012]

2.2.2. Conditions of non-engineered construction in developing countries

Most of the buildings in Nepal, Pakistan, Indonesia, India, Peru, Turkey and Egypt utilize fired clay bricks as wall material, with one brick thickness (see Fig. 2.10). In terms of wall height to thickness ratio, the highest ratio is found in Indonesia (19.83), while the smallest is found in Egypt (9.00). [Okazaki *et al.*, 2012]

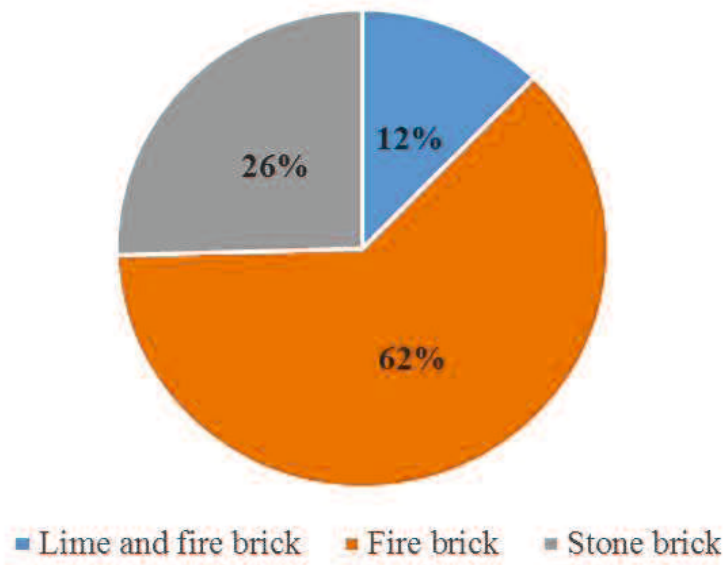


Figure 2.9 Percentage of wall materials used in developing countries

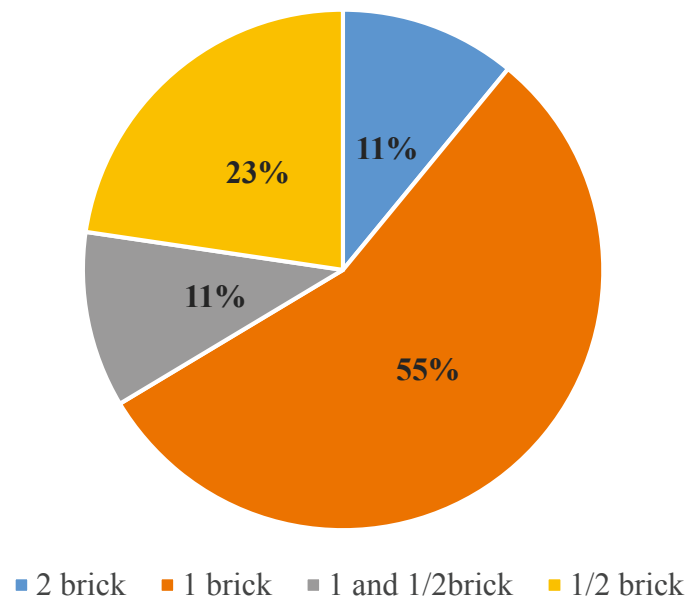


Figure 2.10 Percentage of wall thickness used in developing countries

Most of non-engineered constructions provide beams and few of them provide columns. This depends on the structural system adopted in the surveyed country. In Indonesia, most of the surveyed sites exhibit confined masonry, so both columns and beams are available. On the other hand, in Pakistan, Egypt, and India, where most of the selected sites are unconfined masonry, the buildings are only provided with beam/lintel. From all of the selected countries, it was found that most of non-engineered construction had poor detailing on the connection of the structural elements. [Okazaki *et al.*, 2012]

Most of countries have building regulation/codes and/or guideline on non-engineered construction at the national level, such as India, Indonesia, Pakistan, Peru and Nepal. Unfortunately, the building regulation/codes or guidelines on non-engineered structure are mostly not implemented by the countries, excepting for a few big cities. It was also found that some countries have problems on disseminating these regulations to the workers. In Turkey and Egypt, the non-engineered building code at the national level is not available. However, both countries have local offices in charge of building administration in the surveyed cities. In Turkey, the national building code is only for engineered structure. [Okazaki *et al.*, 2012]

Some mistakes are often found in many masonry houses or simple structures. In Fig. 2.11, fence wall built on not properly connected to the column and supporting beam. This wall was constructed without any column or tie beam. Such brick wall will collapse during earthquake because there is no lateral in plane stiffener in wall structures.



Source: https://www.researchgate.net/profile/I_Gede_Adi_Susila/publication/318085641/figure/fig2/AS:511433301557248@1498946609570/Figure-6-Buildings-in-Padang-Indonesia-after-earthquake-September-30-2009-76-on.png

Figure 2.11 Buildings in Padang, Indonesia after earthquake September 30, 2009 (7.6 on Richter scale). Damages to an unconfined single story school building

A masonry house (shown in Fig. 2.12) is considered to be a semi engineered structure, since the structural column and tie beam were not properly installed.



Source: <http://eqclearinghouse.org/co/20100112-haiti/wp-content/uploads/2010/03/3-Residential.jpg>

Figure 2.12 Confined masonry: formwork present after construction of walls; note lack of columns on right side.

There is no closed tie beam constructed at the upper part of the wall to confine the whole structure. It can be expected that some partial damages will occur during earthquake.

In Fig. 2.13, a simple reinforced concrete frame is placed at the corner of masonry house. The beam, which is retaining part of the wall structure, is not correctly connected with anchorage to end support. There are also no closed tie beam and column found in this structure. This type of house is classified as a non-engineered structure and will experience damage during an earthquake, especially at the corner of wall opening.



Source: http://db.world-housing.net/pdf_view/88/

Figure 2.13 Typical earthquake damage: a house without vertical tie-columns and without top bond-beams in Attics (1988 Bovec earthquake)

2.3. Types of masonry

Depending on the regions of the world, the building traditions of the country, masonry has different configurations as a structural element. These configurations vary from unreinforced masonry, too reinforced and confined masonry. The type of masonry used is related to the amount of seismicity, for example in countries with very low seismic activity, unreinforced masonry is used. On the other hand, in countries with mid to high seismic activity, reinforced or confined masonry is used [Blondet, 2005].

2.3.1. Unreinforced masonry structures

Unreinforced masonry is the typical configuration of masonry in countries with low or without seismic demand. It is characterized because it has no steel reinforcement and no reinforced concrete confinement.

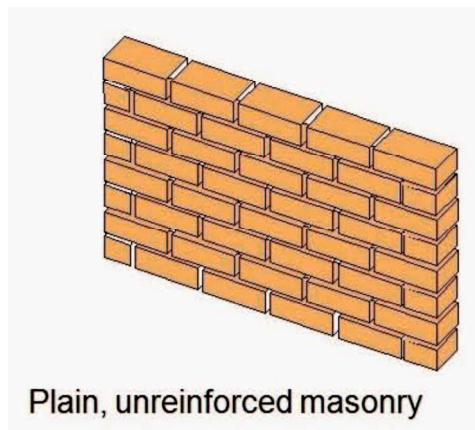
This type of masonry is a traditional form for construction of low-rise houses that has been extensively practiced in almost every part of the world. With the increased popularity and availability of reinforced concrete, improved masonry forms of construction, like confined and reinforced masonry became more common for low-rise houses. However, traditional houses with a load-bearing system of unreinforced burnt clay brick walls are still being constructed in many areas of Asia, the Indian Subcontinent and Latin America. This type of masonry is very vulnerable to the earthquake shaking. Many design codes [D.I.N., 2006] consider that this type of masonry is not earthquake resistant.

For this type of masonry general purpose mortar or thin layer mortar may be used. In case of using general purpose mortar, the recommended thickness of the

joints should be about 1.0 or 1.5 cm in order to avoid structural problems. For solid blocks a thin layer mortar may be used and this type of mortar is usually 1.0 or 2.0 mm thick. In Fig. 2.14, a simple scheme of unreinforced masonry is shown.



Source: <http://altbuildblog.blogspot.jp/2011/09/building-brick-house-in-mexico.html>

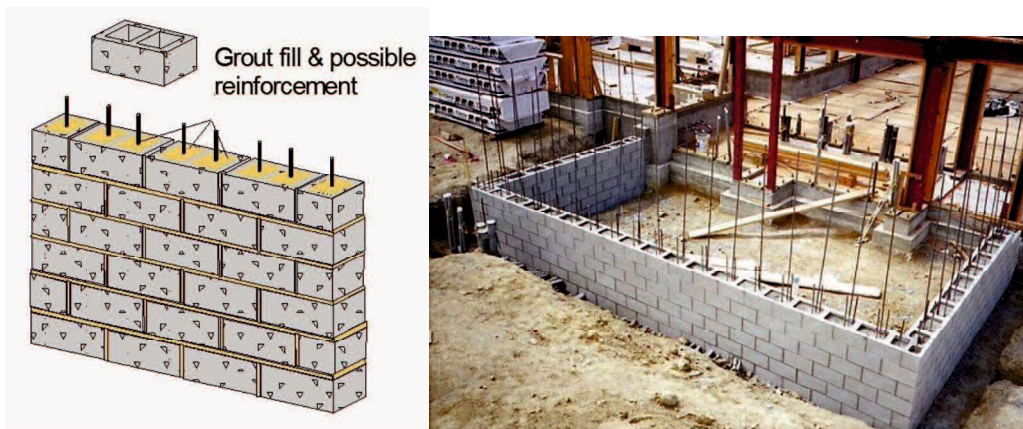


Source: <https://www.strukts.com/2012/08/masonry-structures/>

Figure 2.14 Unreinforced masonry

2.3.2. Reinforced masonry structures

This type of masonry is taken into account reinforcement by steel bars embedded in the mortar. This reinforcement is placed in the horizontal joints and/or in the brick holes and then filled with grout. The horizontal reinforcement helps to improve the resistance to horizontal loads (shear failure) and the vertical reinforcement helps to improve the flexural resistance. In seismic countries, this type of masonry is widely used and, sometimes, obligatory. Unfortunately, in most under developed countries, this type of masonry is not used well, especially because the grout filling for vertical bars is not well done. In Chile, there is a specific code to carry out the design of structures considering this type of masonry [I.N.N., 1997]. A general scheme of reinforced masonry is displayed in Fig. 2.15.



Source: a. <https://www.strukts.com/2012/08/masonry-structures/>.
b. <https://theconstructor.org/construction/tolerances-reinforced-masonry-construction/15244/>

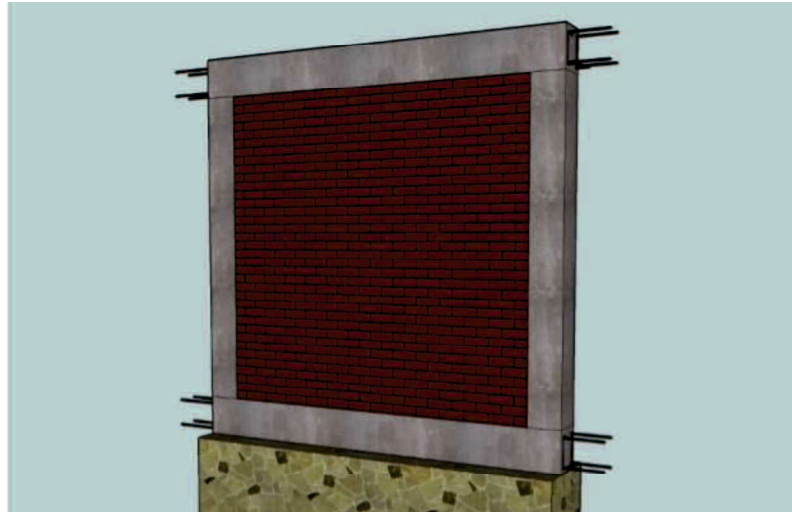
Figure 2.15 Reinforced masonry

2.3.3. Confined masonry structures

This is a special type of masonry which takes into account the confinement of the masonry within a reinforced concrete frame. This confinement is materialized with vertical tie columns and a horizontal bond beam. Normally, the codes define the requirements for the maximum area to be confined for a good structural performance. In seismic countries, this type of masonry structure is widely used and sometimes obligatory. In this type, the distribution of steel reinforcement on the intersections between tie columns and bond beams is very important.

It is also important to note that there are differences in this type of masonry, depending on how the wall is built. If the masonry is built before the reinforced concrete frame, then the structural system masonry is called “confined masonry”. If the masonry is built after the reinforced concrete frame, then the structural system is called “infilled frame”. This difference may lead to different structural behavior because of the “toothed wall edge” materialized in the “confined masonry” [Blondet, 2005].

In Chile, there is a specific code to carry out the design of structures considering this type of masonry [I.N.N., 1993]. A general scheme of confined masonry is displayed in Fig. 2.16.



Source <http://engineeringfeed.com/confined-masonry>
Figure 2.16 Confined masonry

2.4. Mechanical properties of masonry materials

Masonry is a nonhomogeneous material consisting of bricks and mortar in filled joints. Both have certain strengths and deformation capabilities. Only a proper balance between the right type of mortar and the right type of brick can give a good result for bearing walls. The strength value of brickwork is also strongly influenced by the workmanship.

Masonry is a complex material, because it is defined as a composition of bricks and mortar. The possibility of combining these elements with different qualities and geometry give masonry a wide range of alternatives of mechanical behavior and structural performance.

It is well known that masonry has a good performance when resisting and transmitting compressive loads and a poor performance to resist tensile demands.

In particular, the constituent elements of masonry (bricks and mortar) have a strong non-linear response when subjected to high demand loads and, normally,

have an anisotropic behavior. There is also a special issue to define the mechanical behavior of the contact zone between brick and mortar, which is highly non-linear. Moreover, normally earthquake loads demand a non-linear response in buildings and their structural components.

In order to understand better the structural behavior of masonry structures, the following paragraphs show a short description of some characteristics and properties of the constituent elements of masonry and their failure modes.

2.4.1. Masonry units

The properties of bricks vary in a wide range of values, depending on the quality of clay (or concrete in the case of blocks) or manufacture. Additionally, the mechanical behavior of bricks is not necessarily homogeneous and isotropic (especially for hollow or perforated bricks). This means that the properties are not the same in different directions and are also not the same in tension or compression. Normally, the behavior of bricks is described as elastic-brittle.

2.4.1.1. *Compressive strength of masonry units*

Compressive strength of masonry units was determined by a standardized procedure such as those of SNI 15-2094-1991, SNI 15-2094-2000, ASTM C-1314, and BS-3921 and. The compressive strength of masonry unit depends on the strength of the raw materials and shown higher value compared to the compressive strength of masonry [Paulay and Priestley, 1992; Drysdale *et al.*, 1994]. Typical stress-strain curve for compression in bricks is shown in Fig. 2.17.

To estimate the elasticity module E_b of clay bricks, [Kaushik *et al.*, 2007] recommends a range of values depending on the compression strength of the brick f_b . These values are:

$$150 \cdot f_b \leq E_b \leq 500 f_b \quad (2.1)$$

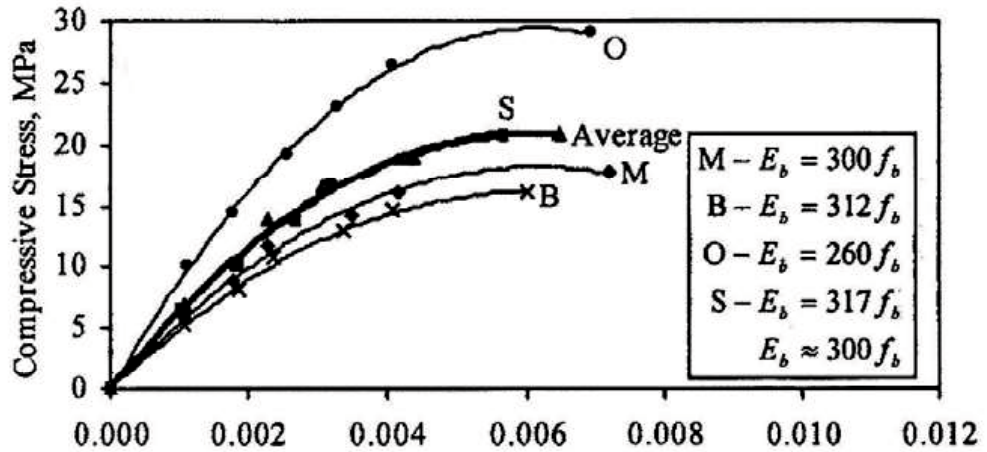


Figure 2.17 Typical stress-strain curve for compression in bricks

[Kaushik *et al.*, 2007]

This relationship is graphically showed in Fig. 2.18.

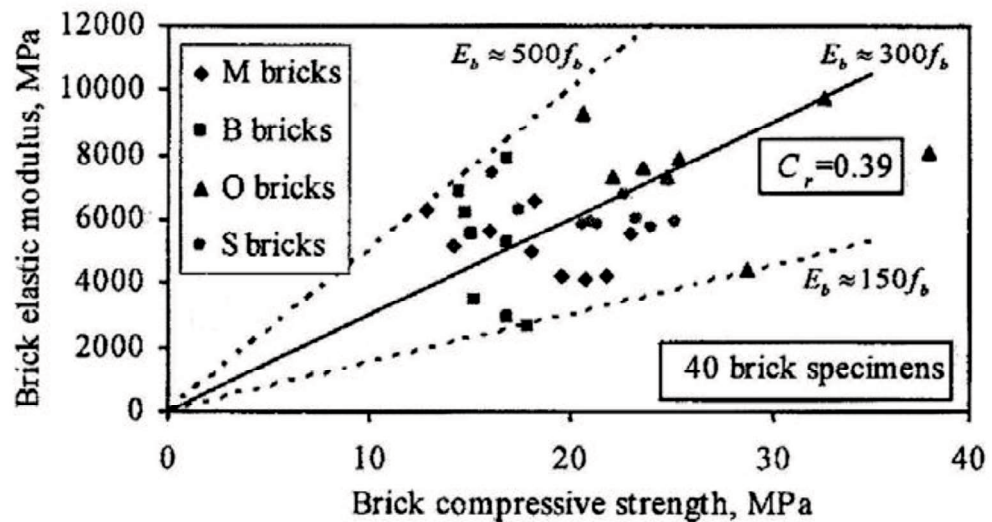


Figure 2.18 Relationship between compressive strength an elasticity module for bricks [Kaushik *et al.* 2007].

From theory of elasticity [Gere and Timoshenko, 1986], the shear elasticity module (G_m) is estimated as:

$$G_m = \frac{E_m}{2(1+\nu_m)} \quad (2.2)$$

Where “ ν_m ” is the Poisson’s module of mortar.

According to Mauerwerk-Kalender [Irmschler, *et al.* 2004], for calcium-silicate bricks the elasticity module can be estimated as:

$$E_b = 355 f_b \quad (2.3)$$

2.4.1.2. Tensile strength of masonry units

Tensile strength describes the capacity of a masonry material unit when subjected to a maximum tension. There are several tensile strength tests that depend on the applied loading such as flexural tensile strength, splitting tensile strength and direct tensile strength. The flexural tensile strength test or modulus of rupture test [ASTM C-67] was measured on masonry units subjected to an axial load that is applied incrementally to the center between the two supports at the end of the masonry units. The splitting tensile strength test [ASTM C-1006] was measured by applying a line-load at both surfaces and longitudinally parallel to the length of the masonry unit. The axial tensile strength test was carried out on cylindrical specimens where the ratio of height to diameter is 1. Steel plates glued with epoxy resin on the top and bottom faces of the cylinders were used to apply the tensile force.

In the absence of tensile strength tests of the masonry units, Hilsdorf [1967] reported some correlation between the compressive strength and the power of two-thirds yields the direct tensile strength:

$$f_{t,axial} = 0.26 f_{cb,cyl}^{0.67} \quad (2.4)$$

Other correlations are as follows :

$$f_{t,axial} = 0.72 f_{cb,splitting} \quad (2.5)$$

$$f_{t,axial} = 0.50 f_{cb,flexural} \quad (2.6)$$

Sahlin [1971] reviewed of test data the ratio of the tensile strength to the compressive strength of bricks is around 1:20 for solid brick and 1:30 for hollow bricks. It was mentioned that the ratio of modulus of rupture varies roughly between 10% and 30 % of the compressive strength of clay brick. The tensile strength value is around 30% to 40% of the modulus of rupture.

2.4.1.3. *Moisture content and absorption of masonry units*

The property of bricks that has the biggest influence on the mortar is the suction rate. The absorption in the clay brick unit produces a suction effect that can draw water from mortar. The suction rate must be controlled to prevent excessive removal of water from the mortar.

The water absorbed by the bricks leaves cavities in the mortar, which fill with air and result in a weakened mortar on setting. ASTM C-67 specifies it as the initial rate of absorption value (IRA), which is normally defined as the amount of water absorbed by a dry masonry unit when partially immersed in water to a depth of 3 mm for a given period of one minute. Several tests have indicated that IRA values

between 2.5 to 15 g/minute/dm² generally produce good bond strength with compatible mortar [Drysedale *et al.*, 1994; ASTM C-67]. Sahlin [1971] reported that masonry units with low suction (less than 10 g/minute/dm²) and reasonably rough surfaces, and mortar with reasonably high water retentivity more than 70% would probably give a good bond. Generally, the Indonesian brick has a high suction rate and the limit value of suction rate for Indonesia clay brick is not higher than 20 g/minute/dm² [UNIDO, 1978]. Bricks of low strength must be soaked for about one to two minutes to bring the suction rate down to suggested level. The moisture content and the water absorption of the masonry unit have a considerable effect on the characteristic of the masonry. Masonry quality was improved by wetting the clay brick units for approximately 5 to 8 minutes in a container of water, before placing the mortar.

Clay bricks absorb moisture from the environment that can cause complex chemical reactions. Several researchers have conducted tests and have plotted relationships between moisture expansion versus time for clay and shale bricks as discussed at Drysdale *et al.* [1994]. It is reasonable practice to assume that a linear relationship exists between expansion and the logarithm of time [Drysdale *et al.*, 1994].

2.4.1.4. Creep and shrinkage

A burnt clay product such as a brick has a very little movement itself but when combined with mortar some shrinkage of the brickwork can occur. The stronger the mortar the greater is the chance of such shrinkage becoming obvious. There are two kinds of shrinkage: free shrinkage and prevented shrinkage. Free shrinkage being a

term for how much shorter a bar of mortar becomes during curing, it shortens very much in the first hours and the shortening decreases with a higher amount of lime and a smaller amount of cement. Prevented shrinkage is the stress, which is created in the mortar if it is not allowed to shrink. This can, if the stress is stronger than the tension strength lead to cracks in the mortar. For lime mortars these forces grow very slowly and are very small. The more cement that is added a mortar the faster will the stress grow and the higher values it will reach. Mortars of cement-sand can give stress values of about 3 MPa within 3 to 4 days. When the amount of cement in a mortar increases the chance of cracks also increases. In reality, mortar is always prevented from shrinkage as it is kept in place by the bonding with the bricks.

2.4.2. Mortar

Mortar has many similarities with concrete, but difficulties arise from the different proportion of the components (cement, sand, lime and gypsum), which is the key point to determine its mechanical properties. In many cases, it is better to have a good bond between mortar and brick than a high resistance mortar.

Usually, depending on the type of brick, different types of mortar can be used: general purpose mortar, thin layer mortar or lightweight mortar. General purpose mortar is the traditional mortar used in joints with a thickness larger than 3,0 or 4,0 mm and in which only dense aggregate is used. Thin layer mortar is used normally when joints are 1.0 to 3.0 mm thick and when specific requirements must be fulfilled. Lightweight mortars are also designed to fulfil specific requirements of masonry and are made using special lightweight materials [Tomazevic, 1999].

A typical stress-strain curve for compression in bricks is shown in Fig. 2.19.

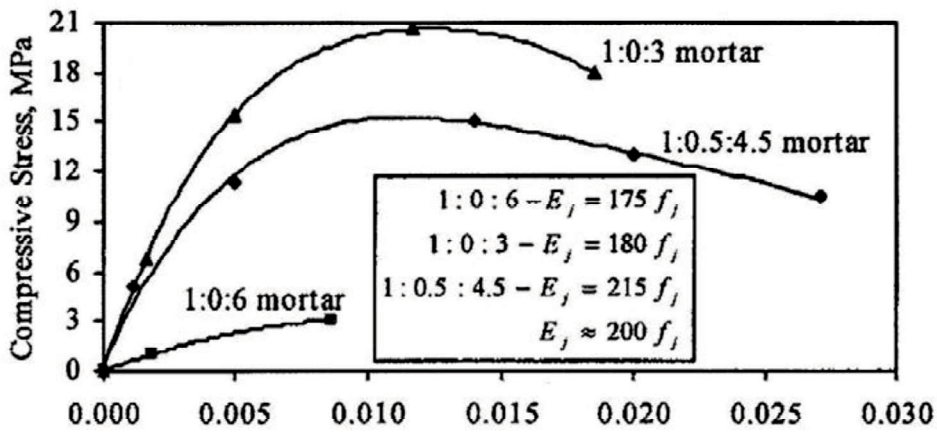


Figure 2.19 Typical stress-strain curve for compression in mortar [Kaushik *et al.*, 2007].

To estimate the elasticity module (E_m) of mortar, [Kaushik *et al.*, 2007] recommends a range of values depending on the compression strength of the mortar (f_m). These values are:

$$100 f_m \leq E_m \leq 400 f_m \quad (2.7)$$

This relationship is graphically showed in Fig. 2.20.

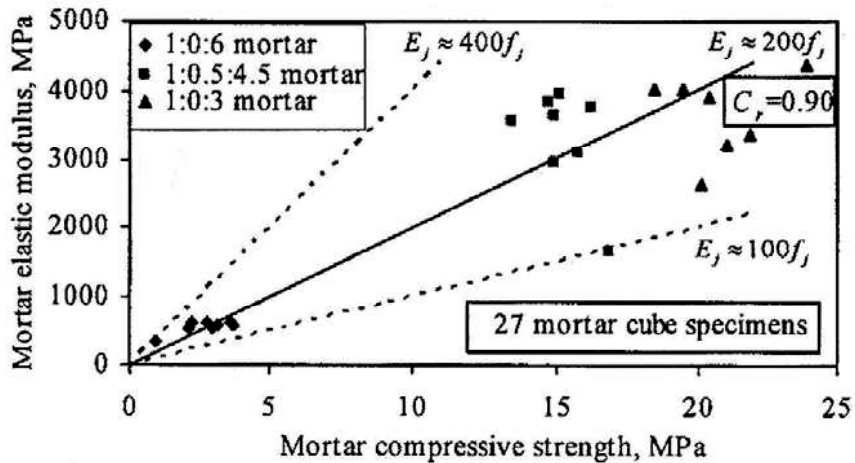


Figure 2.20 Relationship between compressive strength and elasticity module for mortar [Kaushik *et al.* 2007]

From theory of elasticity [Gere and Timoshenko, 1986], the shear elasticity module (G_m) is estimated as:

$$G_m = \frac{E_m}{2(1+\nu_m)} \quad (2.8)$$

Where “ ν_m ” is the Poisson’s module of mortar.

Although mortars form only a small proportion of brickwork as a whole, their characteristics have a significant influence on the quality of the brickwork. Batching and mixing are also an essential factor that has a great influence on both strength and workability of mortars. Mortar is used as a means of sticking or bonding bricks together and to take up all irregularities in the bricks. To do this the mortar must be well workable so that all joints are filling completely. There are two things of importance for the workability, stiffness and plasticity. The stiffness is dependent upon how much water there is added to the mortar. How much water to add depends on what one is to use the mortar for, and does not say anything about the quality, but it is a characteristic of the condition. The plasticity is a term for how easy the mortar can be formed. A binder rich mortar has a better plasticity than a binder poor mortar. The grading of the aggregate also has a certain influence on the plasticity, the closer the grading is to the ideal curve the better the plasticity.

The water content is calculated after the water is added to the dry mortar. The moisture in the aggregate is not considered in this calculation. The water content in the aggregate was about 20 % by weight.

Curing of mortar cubes: according to ASTM C-270, should be stored as follows:

Mortars where cement is the main binder, cubes must be cured in a relative humidity of 90 % or more and kept in the mold for from 48 – 52 hours, in such a manner that the upper surfaces shall be exposed to the moist air. Different mortar strengths are obtained by changing the aggregate ratio. Mortars, which only contain lime as a binder normally, have a strength of 0.5 to 1 MPa, cement-lime mortars strength varies from 1 to 10 MPa and pure cement mortar strengths ranges from 10 to 20 MPa. Table 2.1. is shown the compressive strength of mortar, that conducted by UNIDO in Indonesia.

Various types of cement can be used for mortar, such as ordinary Portland cement or Masonry cement. Ordinary Portland cement should conform to ASTM C-150 standard and Masonry cement should conform to ASTM C-207 standard. The sand for mortar should be clean, sharp and free from salt and organic contamination [Hendry *et al.*, 1997]. Most natural sand contains a small quantity of silt or clay. A small quantity of silt improves the workability. Specifications of sand should conform to ASTM C- 144 standard, prescribe grading limits for the particle size distribution. Mixing water for mortar should be clean and free from contaminants either dissolved or in suspension. Ordinary water will be suitable.

Table 2.1. Compressive strength of mortar cubes 50 mm x 50 mm x 50 mm
average of 3 cubes - according to ASTM C-270 [UNIDO, 1978a]

Mortar N	Mortar Composition					Compressive strength Average in kg/cm ²			
	Cement	Lime	Trass	Sand	r.c.	7 days	14 days	28 days	60 days
1		1	5			15	27	41	5
2	½	1	7			34	78	69	13
3	1			4		63	107	148	16
4		1		1	1	0	1	3	7
5		1		2		1	1	3	5
6	1	1		6		14	19	33	5
7		1		2	1	2	4	8	1
8	1			3		91	195	216	25
9	¼	1	5			7	13	23	2
1	1	1	1			7	18	31	3
1	1	1	1			16	33	45	6
1	1		6			27	47	54	8
1	1		4	1		50	74	102	11
1	1	1	7	3		16	26	34	4
1	1	1	9	3		16	29	47	5
1	½	1		4		9	12	17	2
1	1		2	2		75	105	123	14
1	1			2		214	312	303	40
1		1		3	1	0	1	3	9
2	½	1	5			45	77	109	11
2	½	1	4	6		8	13	21	2
2	1	1		4		45	63	77	7
2	½	1	1			22	50	71	9

Note : r.c. = red-cush

The modulus of elasticity of mortars, E_{mc} , can be related to its compressive strength, f'_{mc} , and may be approximated by $E_{mc} = 100 f'_{mc}$. Poisson's ratio of most hydraulic cement and lime mortars is on the order of 0.2 and increases rapidly as the uniaxial strength of the mortar is approached.

2.4.3. Masonry

Sometimes it is important to take into account the properties of masonry as a whole. The important thing in these cases is that the interaction between bricks and mortar and the geometrical disposition of the units is considered.

Clay-brick material with a relatively heavy specific gravity is capable of resisting axial load force but is weak in resisting tensile and shear load. In

accordance with its character clay brick becomes a structural element of low ductility. In the event of an earthquake an unreinforced masonry building often experiences damage so that unreinforced masonry construction is no longer recommended for buildings in seismic prone regions.

The tensile strength of masonry is very low, of the order of 1.5 to 2 % of its compressive strength. Normally brickwork strength is strongly correlated to the strength of the mortar. It appears that masonry strength may vary between the $1/3$ power and the $2/3$ power of the mortar strength when the elasticity modulus of brick and mortar are approximately equal [Sahlin, 1971].

Because of specific characteristics of each constituent masonry materials, especially the masonry unit, it is not easy to predict the mechanical characteristics of a specific masonry construction type by knowing only the characteristics of its constituent materials, mortar and masonry units. It is therefore of relevant importance that, for each type of masonry, experiments to correlate the strength characteristics of constituent materials with the characteristics of masonry are carried out [Tomažević, 1999]

2.4.3.1. *Masonry compressive strength*

The compressive strength of the masonry units was determined by a standardized procedure such as the prisms test [ASTM C-1314]; whole or half brick and capped with a sulphur pumice mixture [NZS-366 1963]; prisms test with minimum three courses [AS/NZS 4456.5- 1997], British Standard and Indonesian standard [SNI 15-2094-1991, SNI 15-2094-2000] which brick unit will be cut in half with a saw. Each cut part of the brick will be stacked on the other part and the

space between the two cut bricks are to be filled with 6 mm mortar. This test will investigate the compressive strength of the masonry in the normal direction of the mortar bed. ASTM C- 1314 prism tests recommended a height to depth ratio between 1.3 and 5.0. Recommendations have been made to the standards association NZ along these lines for a test based on ratio of height to least lateral dimension greater than or equal to 3

The compressive strength of a masonry wall is affected by some factors, such as workmanship, the properties of the masonry units, the thickness of mortar joints, the age of mortar and also the suction rate [Sahlin, 1971]. It is reported that increasing mortar joint thickness lowers the compressive strength and the normal joint thickness of 10 mm is recommended [Sahlin, 1971]. In their book, [Paulay and Priestley, 1992], as well as Drysdale *et al.* [1994], have concluded that the prism compressive strength of brick masonry (f'_m) is less compared with the unit compressive strength of a brick unit (f'_{cb}).

The brick masonry strength normally is about 25% to 50% of the masonry unit strength, the lower value referring to low strength mortar and the higher strength for high strength mortar. The compressive strength of masonry is substantially less than the masonry unit strength because of the influence of the mortar. The ratio also tends to decrease with increasing masonry unit's strength. In addition, the prism compressive strength of brick (f'_{pm}) bound with mortar is larger compared with the mortar strength (f'_{mc}) (Fig. 2.21). Collapse will occur because of vertical shearing of the brick unit rather than disintegration of the mortar. The cause is a result of improper brick and mortar laying. Because the lesser strength and value of the elasticity modulus of mortar than that of the brick unit caused the axial and

lateral tension (*Poisson's ratio*) of the mortar to become larger than the clay units. In line with the axial tension reaching the mortar's maximum strength (f'_{mc}), the mortar will experience a continued increasing of lateral shearing (Fig. 2.22a.). The joint effect of a lower elasticity modulus and a higher *Poisson's ratio* will tend to the lateral tensile strength of the mortar exceeding the lateral tension of the brick unit (Fig. 2.22b.). Because friction and adhesive strength on the mortar-brick joints force the lateral tension of the mortar and brick unit to change the lateral compressive strength on the mortar to equal to the lateral tensile strength on the brick unit (Fig. 2.22c.)

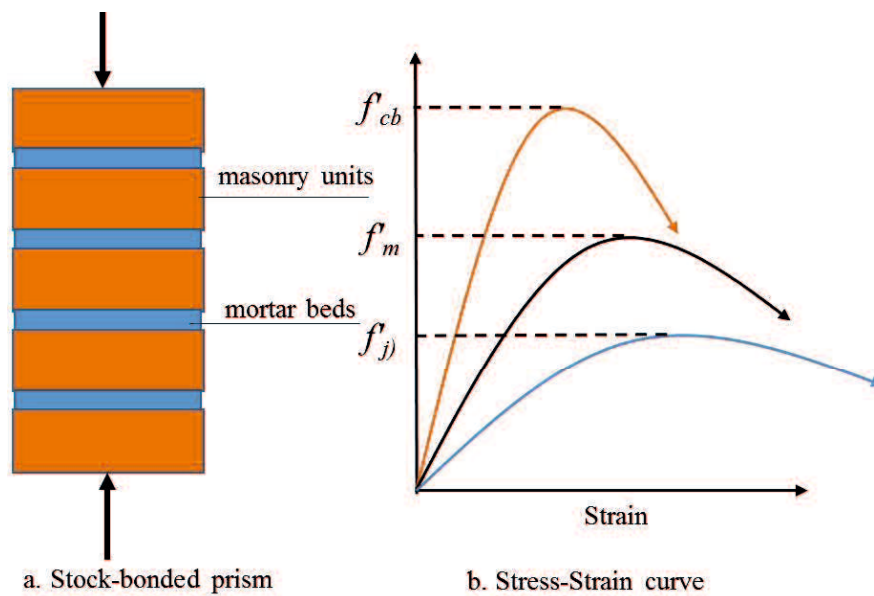


Figure 2.21 Correlation between stress-strain at masonry prism (Paulay and Priestley, [1992])

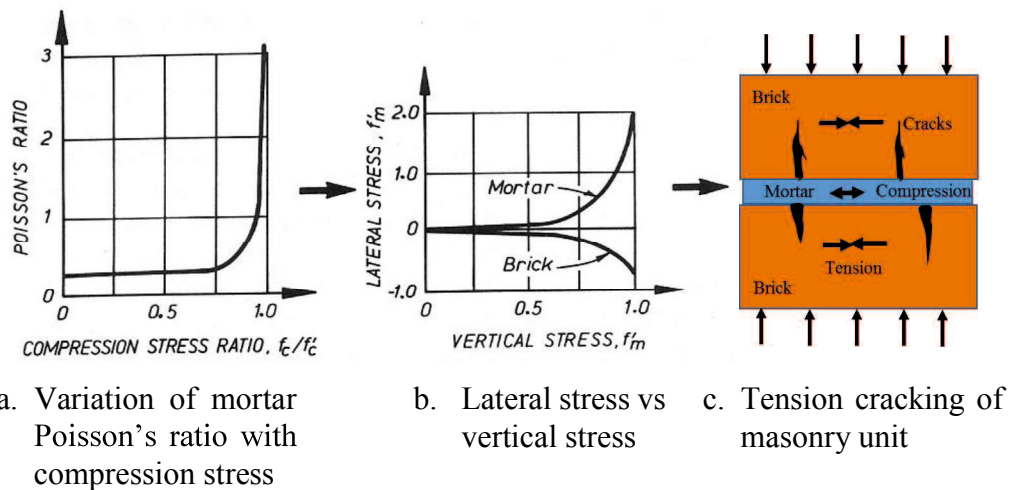


Figure 2.22 Mechanism of a collapse on the masonry prism [Paulay and Priestley, 1992]

The prism test recommends a height to thickness ratio of not more than 5 nor less than 1.3 [ASTM standard C-1314]. The specimen contains five stack-bond prisms and was tested in axial compression. The procedure of the compressive testing of the axially loaded prisms was in accordance with ASTM Test Method ASTM C-1314. ASTM standard E-518 prescribes a horizontal flexural test method for determining the bond strength of masonry.

In 1978, United Nations Development Program (UNDP) in cooperation with the Indonesian Directorate of Building Research focused on the extensive testing of brickwork specimens using local bricks and mortars. The aim of this research was to provide technical data for the establishment of the Indonesian Code of Practice for Brickwork Construction based on local practice. Compressive strength testing was conducted using a brickwork cube consist of 5 layers of bricks vertically and 2 layers horizontally. The specimens were tested after 7 days, 14 days, and 28 days (6 specimens each) and it was concluded that the compressive strength of brickwork had developed nearly 100% in 14 days. The compressive strength of brickwork varies between 2 to 3 MPa. The shear strength of brickwork is highly affected by

the bonding between the brick and mortar. Table 2.2 are shown the classification compressive strength of brick masonry in Indonesia:

Table 2.2 Classification according to strength (SNI 15-2094-1991)

Class	Average minimum compressive strength of 30 pcs tested bricks		Allowable coefficient of variation (%)
	kg/cm ²	MPa	
25	25	2.5	25
50	50	5	22
100	100	10	22
150	150	15	15
200	200	20	15
250	250	25	15

Similar specimens to those used for compressive strength were loaded diagonally and the shear strength of Indonesian brickwork ranges between 0.05 to 0.19 MPa and the data were found to be very variable. The flexural tensile strength of brickwork varies between 0.02 to 0.12 MPa [UNIDO, 1978b, 1979]. Since there were no available standard tests to evaluate the elastic modulus of brickwork in Indonesia, ASTM E-111 was adopted.

Recently, tests on the compressive strength of clay brick units were conducted in Indonesia by using solid clay bricks produced traditionally in home industries. The compressive strengths were conducted using the Indonesian standard and give lower quality bricks with average compressive strength of approximately 4 MPa. The compositions of the mortar mix consisted of 0.95 part of water: 1 part of cement: 4 part of sand. [Basoenondo *et al.*, 2003]. There are many local clay-brick suppliers in Indonesia that the quality and the compressive strength vary greatly.

A standardized clay brick quality and dimension are urgently needed for masonry units in Indonesia.

2.4.3.2. *Masonry flexural tensile strength*

The tensile strength of masonry describes the capacity of a material when subjected to maximum tension. The tensile strength is governed by the bond between the mortar and the units as this is typically less than the tensile strength of either of the constituent materials. Masonry bond strength easily affected by workmanship and can vary depending on the correct match between the mortar and the unit properties, particularly the water retention of the mortar and the suction of the masonry units.

Two types of loading options are provided for the flexural test, as shown in Fig. 2.23.:

- First, the specimens tested as horizontal beams with the transverse loads applied vertically
- Secondly, the specimen consists of at least five courses and tested in a vertical orientation and loaded in a manner that will induce equal and opposite's couples at the ends. [Bond-wrench method; ASTM C-1072]

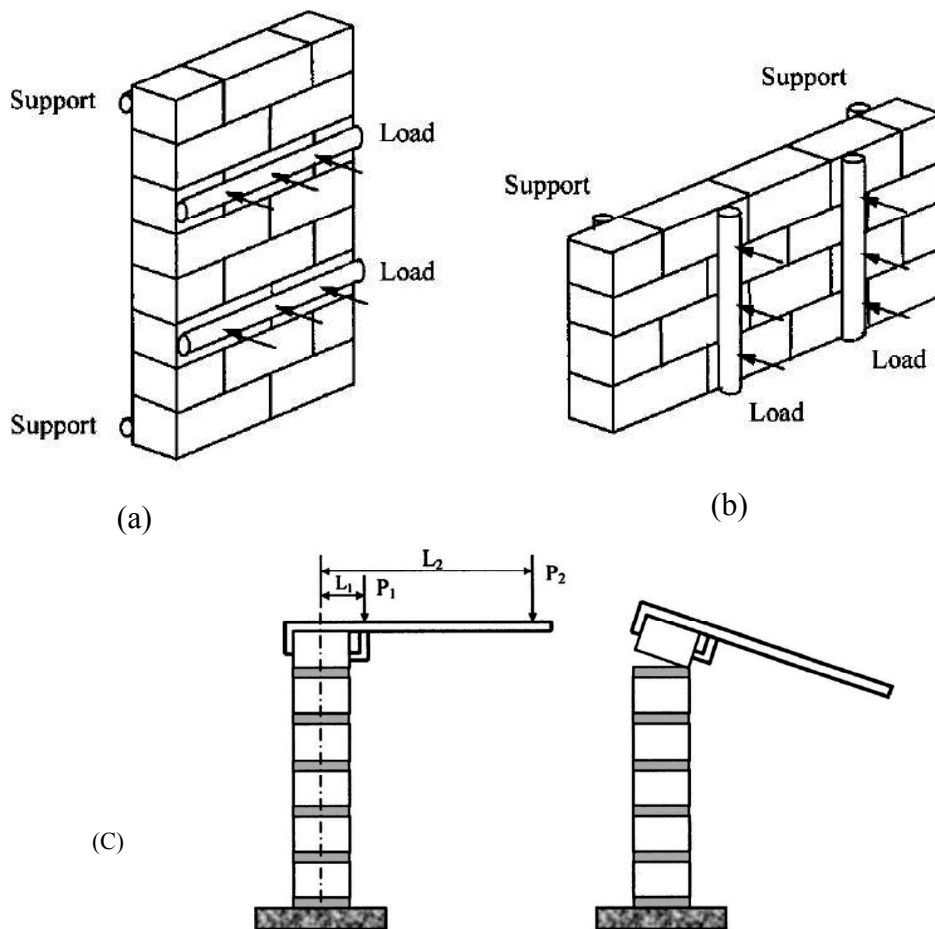


Figure 2.23 Testing arrangement of wallettes small walls, BS 5628 British 1992: (a) plane of failure parallel to bed joint, (b) plane of failure normal to bed, (c) Bond wrench shown in position before test and after bond failure joint (Kalaf [2005])

The Australian standard (SAA Masonry Code AS-3700) allows designers to assume a characteristic flexural tensile strength for masonry of 0.20 MPa. Hendry *et al.* [1997], reported the flexural tensile strength of clay brick ranges from about 0.2 to 0.8 MPa in the stronger direction.

Tomažević [1999] reported the correlation between the tensile, f_t , and compressive strength, f_m , of any type of masonry as:

$$0.03 f_m \leq f_t \leq 0.09 f_m \quad (2.9)$$

The flexural tensile strength value from the tests for unreinforced masonry walls can be used for in-plane lateral forces and out-of-plane bending conditions.

2.4.3.3. Masonry elastic modulus

The elastic modulus or Young's modulus was characterized by linear proportionality between stress and strain in the elastic condition. It may be determined from measurements obtained from compression tests of masonry prisms or a prismatic masonry test. The ideal combination of mortar and clay-brick is a clay-brick with elastic modulus equal to or nearly equal to that of the joint mortar. Young's modulus is a result of a comparison between strain and stress as follows:

$$E_m = \sigma / \varepsilon_m \quad (2.10)$$

The minimal test information concerning the strain-tension of clay units has resulted in the assumption that the behavior of clay bricks almost resembles linear elasticity material while concrete blocks are considered to behave in nonlinear way similar to the behavior of concrete in general. The modulus of elasticity of brick units also shows a very wide variety and basically depends on the type of material and value of the compressive strength. Typically, a secant modulus of elasticity, E_m , is described by the slope of the stress-strain curve between 5% and 33% of the masonry ultimate compressive strength of each prism test or prismatic test [FEMA-274 1997, UBC-97, ASTM E-111 and NEHRP, 2000].

Empirical linear relationships between the compressive elastic modulus and the equivalent compressive strength from some researches are usually assumed as follow:

$$E_m = k \cdot f'_m \quad (2.11)$$

Where k is a constant factor, E_m is elastic modulus of masonry in compression (MPa) and f'_m is specified compressive strength of masonry (MPa). Some of the correlations are shown in Table 2.3. and k factor for clay bricks vary in between $300 \leq k \leq 750$. This huge range factor is depended on the local raw material of clay brick.

Table 2.3 Correlation between modulus of elasticity of masonry and masonry compressive strength

No.	Reference	Elastic Modulus of Masonry in Compression
1	Paulay and Priestley [1992]	Concrete $E_m = 1000 f'_m$ Clay brick $E_m = 750 f'_m$
2	Drysdale <i>et al.</i> [1994]	Concrete $E_m = 750 f'_m$ Clay brick $E_m = 500-600 f'_m$
3	Sahlin [1971], Crisafulli <i>et al</i> [1995]	Clay brick $E_m = 300 f'_m$
4	FEMA 273 [1997]	Clay brick $E_m = 550 f'_m$
5	Tomažević [1999]	Clay brick $200 f_{cb} \leq E_m \leq 2000 f_{cb}$
6	NEHRP 2000	Clay brick $E_m = 750 f'_m$
7	Costigan <i>et al.</i> [2015]	NHL5 0:1:3 $E_m = 158f'_m$ $R^2 = 0.51$ NHL3.5 0:1:3 $E_m = 102f'_m$ $R^2 = 0.68$ NHL2 0:1:3 $E_m = 88f'_m$ $R^2 = 0.46$ CL90 0:1:3 $E_m = 82f'_m$ $R^2 = 0.48$ M6 1:0.5:4 $E_m = 231f'_m$ $R^2 = 0.63$

Without noticing the above differences, in a sensitive calculation towards the E_m value, attention should be paid to using a representative E_m value to avoid excessive strains, particularly considering the examples of clay bricks in Indonesia.

Normally, the test result showed significant variation on the Young's modulus of clay brick. In his text book [Drysdale *et al.*, 1994] has taken the maximum masonry compressive strain value as 0.003

2.4.3.4. Masonry Shear Strength

Shear specimens should be tested by a compression force applied along diagonal axis within the centroidal plane of the cross section. The diagonal compression test will be used to evaluate the masonry shear strength and the modulus of rigidity.

The basic form of the shear strength for unreinforced masonry is based on the Mohr Coulomb shear friction expression [Crisafulli *et al.* 1995; Hendry *et al.* 1997] as follow

$$\tau_m = \tau_o + \mu\sigma_n \quad (2.12)$$

Where τ_m = shear strength at the shear bond failure; τ_o = shear bond strength at zero normal stress due to the adhesive strength of mortar; μ = coefficient of internal friction between brick and mortar; and σ_n = the normal stress at the bed joint. From the above formula, it has shown that there is a relation between shear strength and the normal stress.

Hendry *et al.* [1997] reported the shear strength limit value of clay brick is about 2.0 N/mm². The shear strength depends on the mortar strength. For high strength mortar (1:1/4:3) which has compressive strength between 20 to 50 N/mm², the value of τ_o will be approximately 0.3 N/mm² and 0.2 N/mm² for medium strength mortar (1:1:6). The average value of μ is 0.4 to 0.6. Sahlin, [1971],

summarized that τ_o will be approximately 0.2 N/mm^2 and the average value of μ is 0.5.

In parametric form equation can be expressed:

$$V_n = f_n (f'_m, N) \quad (2.13)$$

Where V_n represents the design shear strength, f'_m is a measure of masonry material properties and N is the axial compression force.

Types of shear failure are divided into three categories i.e. failure along the mortar and brick unit joints, failure of shear load and diagonal tensile cracks. Some methods of testing shear strength are shown in Fig. 2.24.

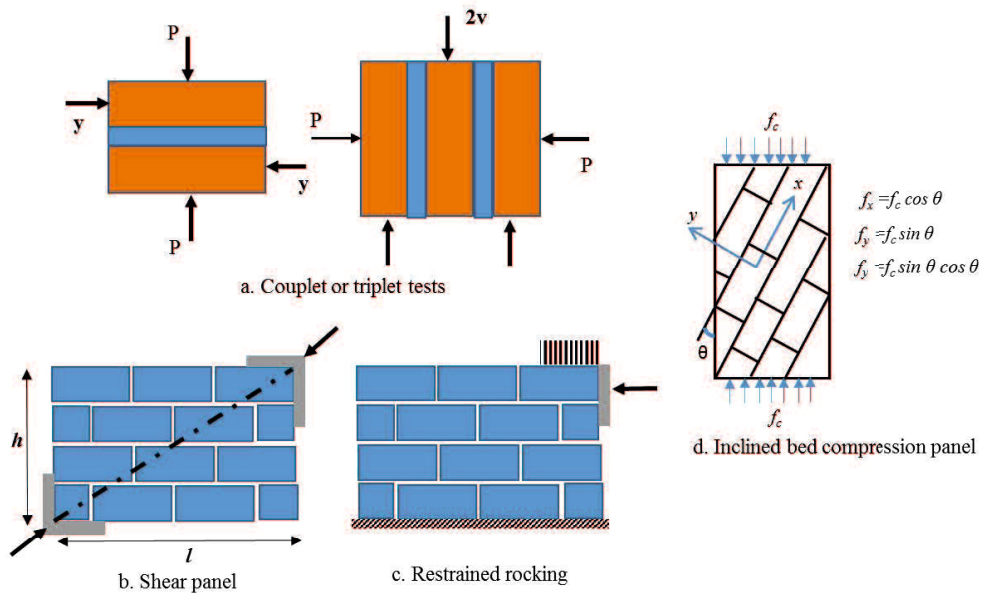


Figure 2.24 Methods of testing shear strength in masonry construction [Paulay and Priestley, 1992]

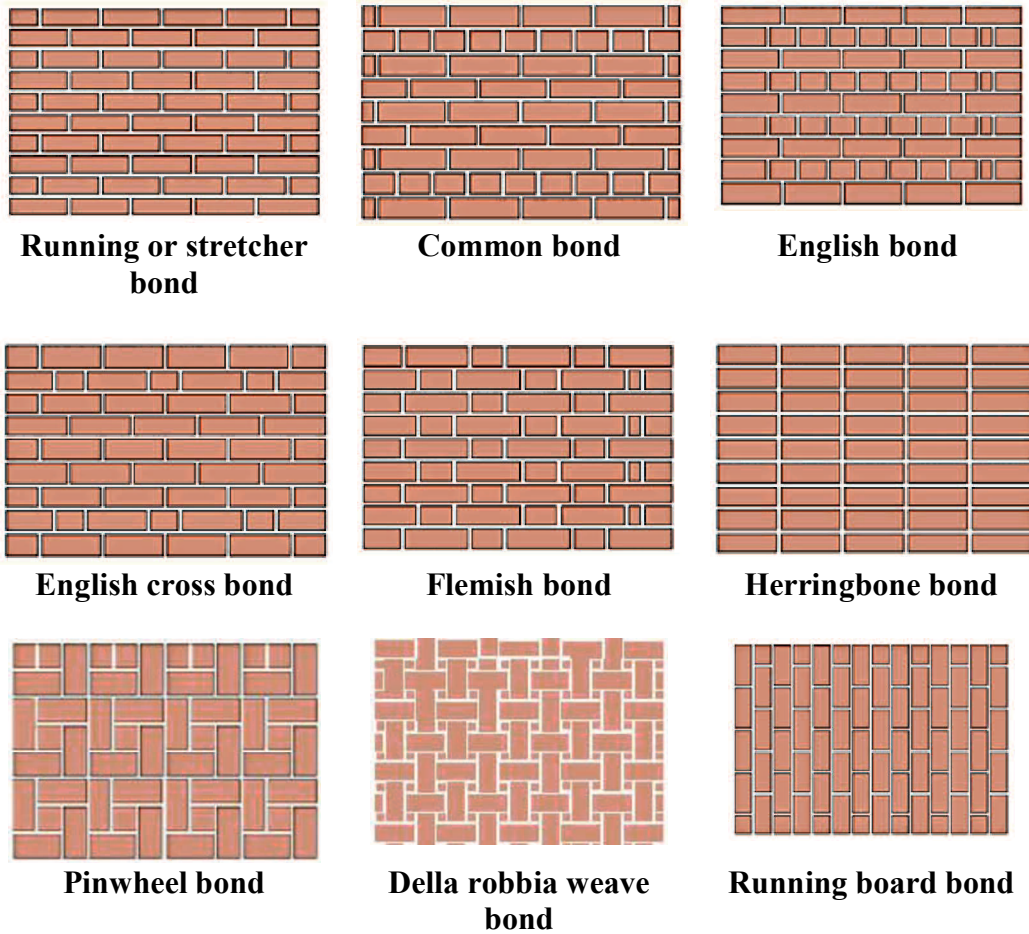
2.4.3.5. Masonry Shear Modulus

Masonry shear modulus of modulus of rigidity may be obtained from measurements of diagonal deformations in racking test specimens. In the absence of sufficient data, shear modulus, G_m , can be assumed vary from 6% to 25% of the Elastic modulus (Young's modulus). The shear modulus of elasticity, G_m , was taken from the coefficient from Alcocer and Klinger [1994] in between 0.1 – 0.3 times E_m (0.1 for high-strength units and 0.3 for weaker units). The shear modulus of uncracked unreinforced masonry can be estimated as $G_m = 0.4 E_m$ in compression [FEMA 273] After cracking the shear stiffness is reduced substantially as sliding along bed joints develops or as diagonal tension cracks open. Some researchers reported that G_m value can be estimated through $= 400 f'_m$ [Fattal and Cattaneo, 1977; Paulay and Priestley, 1992]

Tomažević [1999] reported the correlation between the tensile and compressive strength for any type of masonry: $1000 f_{ts} \leq G_m \leq 2700 f_{ts}$. Most result indicated a G_m value close to $2000 f_{ts}$.

2.5. Disposition of bricks or blocks

Another important factor to take into accounts for the determination of the behavior of masonry is the disposition of bricks or type of bond. Masonry is an organized disposition of bricks bonded with mortar and the way the bricks are organized may determine the structural response of the wall. A general description of some of the most recognized types of bond are those shown in Fig. 2.25. It is possible to find some variations in these types of bonds, with regard to the vertical joints, which may or may not be filled with mortar.



Source : http://www.waltonsons.com/wp/?page_id=1093

Figure 2.25 Types of bond in masonry.

For the model defined in this work, the “running type of bond” will be used. This model is the most common model in Germany and the typical model in Chile. In fact, in Chile it is hard to find masonry of any other type of bond other than “running”. Moreover, all the laboratory tests considered to make an evaluation of the proposed model have this type of bond.

2.6. Types of Failure

2.6.1. In-Plane Failure of masonry wall

Various in-plane examples of unreinforced masonry walls subjected to seismic lateral loads can be seen in several text books [e.g. Paulay and Priestley, 1992]. The in-plane capacity of the wall depended on the relative strength of the masonry and the mortar. The level of the axial load significantly controls the type of failure. There are several failure conditions for in-plane masonry walls due to the form of construction and the combine effects of axial load and bending, as follows [Tomažević, 1999]:

Anthonie, *et al.* [1994] reported the in-plane tests of unreinforced masonry walls with different aspect ratios. The cyclic test result showed that the more slender walls perform a rocking mechanism while the stockier walls failed by diagonal cracking. The slender walls can fail by diagonal cracking when subjected to larger axial loads.

Bruneau [1995] has reported after 1995 Kobe (Hansin-Awaji) Earthquake that the in-plane behavior of the few of the building was excellent. It has been concluded, component wise, by Badoux *et. al.* [2002] that rocking can be a stable non-linear response in slender URM walls providing they have a significant lateral deformation capacity. Doherty [2000] considers that URM buildings may still be satisfactory in medium earthquake risk zones if anchorage and out-of-plane failures of the walls could be prevented. This is because medium levels of earthquakes are not strong enough to cause significant in-plane damage to the building that could jeopardize its stability. In fact, those URM buildings which rocked about their

foundation survived during the 15th August 1950 Assam earthquake [Arya, 1992], despite their other weaknesses. Masonry walls resisting in-plane loads usually exhibit the following three modes of failure:

2.6.1.1. *Sliding shear failure*

Sliding shear failure, along head or bed joint because of low normal stresses and/or low friction coefficients, which may be due to poor quality of the mortar

A wall with poor shear strength (especially in the horizontal joint), loaded predominantly with horizontal forces can exhibit this failure mechanism. The aspect ratio for these walls is usually 1:1 or less (1:1,5; vertical : horizontal). This failure is characterized with a horizontal crack in one of the bed joints, as shown in Fig. 2.26 [Mistler, 2006].

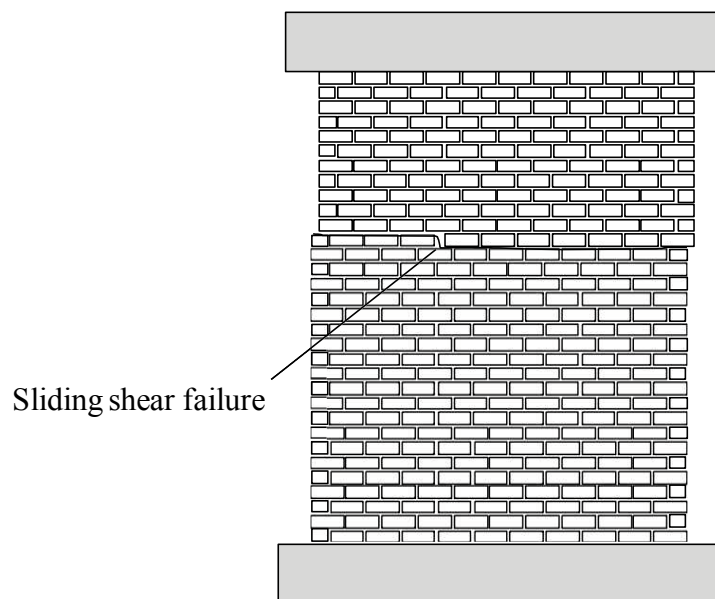


Figure 2.26 Typical sliding shear failure [Mistler, 2006]

2.6.1.2. *Shear failure*

Shear failure, takes place where the principal tensile stresses developed in the wall under a combination of vertical and horizontal loads, exceeds the tensile strength of masonry materials. The crack propagation either follows the mortar joints or passes through the masonry units, or both. Shear failure should be avoided as it will cause a limited/lower ductility for URM-walls. The strength and stiffness of the URM-wall will degrade rapidly following formation of a diagonal shear crack.

Shear failure is exhibited when a wall is loaded with significant vertical as well as horizontal forces. This is the most common mode of failure. The aspect ratio for such walls is usually about 1:1. Shear failure can also occur in panels with a larger aspect ratio, i.e. 2:1, in cases with big vertical loads. This failure is characterized by a diagonal crack, which crosses joints and bricks or follows the line of bed and head joints (see Fig. 2.27) [Mistler, 2006].

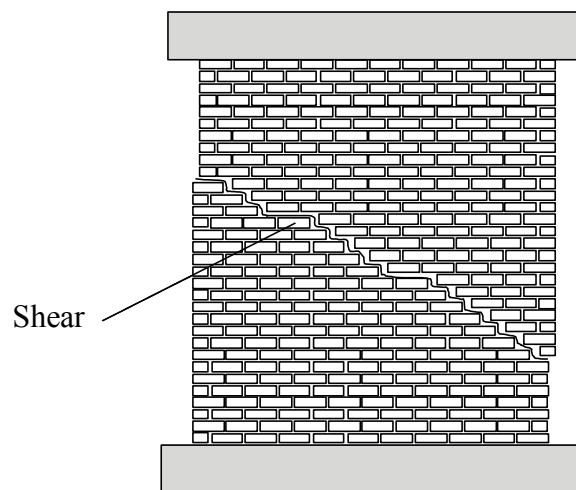


Figure 2.27 Typical shear failure [Mistler, 2006].

Lenczer [1972] has reported that the shear strength of a bearing wall, in the case of slip failure mode, can be calculated as

$$\tau_b = \tau_{bo} + \mu\sigma_n \quad (2.14)$$

where τ_b = shear strength at the shear bond failure; τ_{bo} = shear bond strength at zero normal stress due to the adhesive strength of mortar; μ = coefficient of internal friction between brick and mortar; and σ_n = normal stress.

2.6.1.3. Bending failure

Flexural failure, crushing of compressed zones at the ends of the URM wall usually takes place, indicating the flexural mode of failure. It happens when the shear resistance still strong enough when compared to the shear demands.

This type of failure can occur where walls have improved shear resistance. For larger aspect ratios i.e. 2:1 bending failure can occur due to small vertical loads, rather than high shear resistance. In this mode of failure the masonry panel can rock like a rigid body (in cases of low vertical loads). This failure is characterized by a toe-crushing on the lower side of the wall and/or an opening on the other side. For a better understanding see Fig. 2.28. [Mistler, 2006].

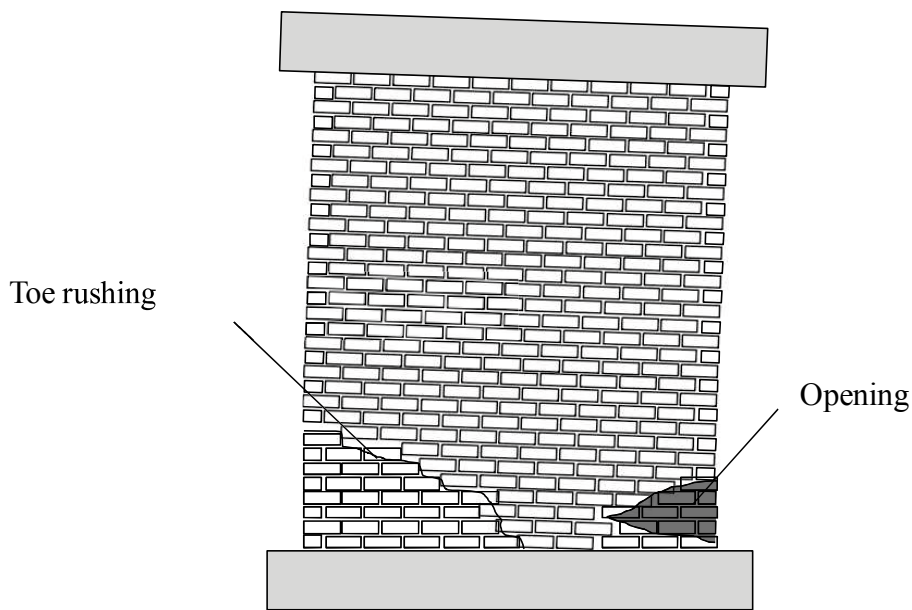


Figure 2.28 Typical bending failure [Mistler, 2006].

2.6.2. Out-of-plane failure of masonry wall

When an unreinforced masonry (URM) building is subjected to horizontal shaking during a seismic event, most of its walls inevitably experience a combination of in-plane and out-of-plane response. Past research into seismic response of URM structures has focused primarily on walls' in-plane shear behavior, since it provides the primary load path for transfer of the building's lateral seismic force to its foundation [e.g. König *et al.*, 1988; Anthoine *et al.*, 1994; Andreaus, 1996; Magenes and Calvi, 1997; Tomažević and Klemenc, 1997; Paquette and Bruneau, 2003; Vasconcelos and Lourenço, 2009]. However, whilst out-of-plane action is not typically considered to be part of the building's seismic load path, walls still require sufficient capacity to avoid out-of-plane collapse; as even local failure can pose significant danger to life safety, and furthermore, failure of loadbearing walls could potentially trigger partial or complete collapse of the

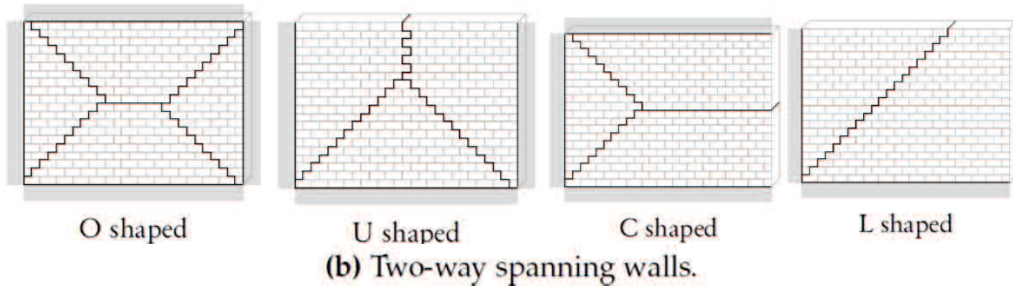
overall structure by compromising its gravity or lateral in-plane load resistance paths.

In the last studies have also found, however, that a large proportion of out-of-plane collapse during earthquakes occurred in instances where the walls were not designed to withstand such actions, and furthermore, that failure was preventable if the walls were properly designed and constructed according to the relevant design codes [Scrivener, 1993; Page, 1995].

Nonetheless, the topic of seismic out-of-plane response is one that is still not fully understood; Paulay and Priestley [1992] describing it as “one of the most complex and ill-understood areas of seismic analysis”, and numerous others highlighting the need for further research into the seismic behavior of URM buildings [Bruneau, 1994; Brunsdon, 1994; Calvi, 1999; Maffei *et al.*, 2000; Abrams, 2001]. Considering Australia’s large amount of seismically vulnerable URM building stock, it is therefore of significant interest both nationally and internationally that we conduct research to improve our understanding of seismic out-of-plane wall response, and facilitate development of the corresponding design and assessment techniques.

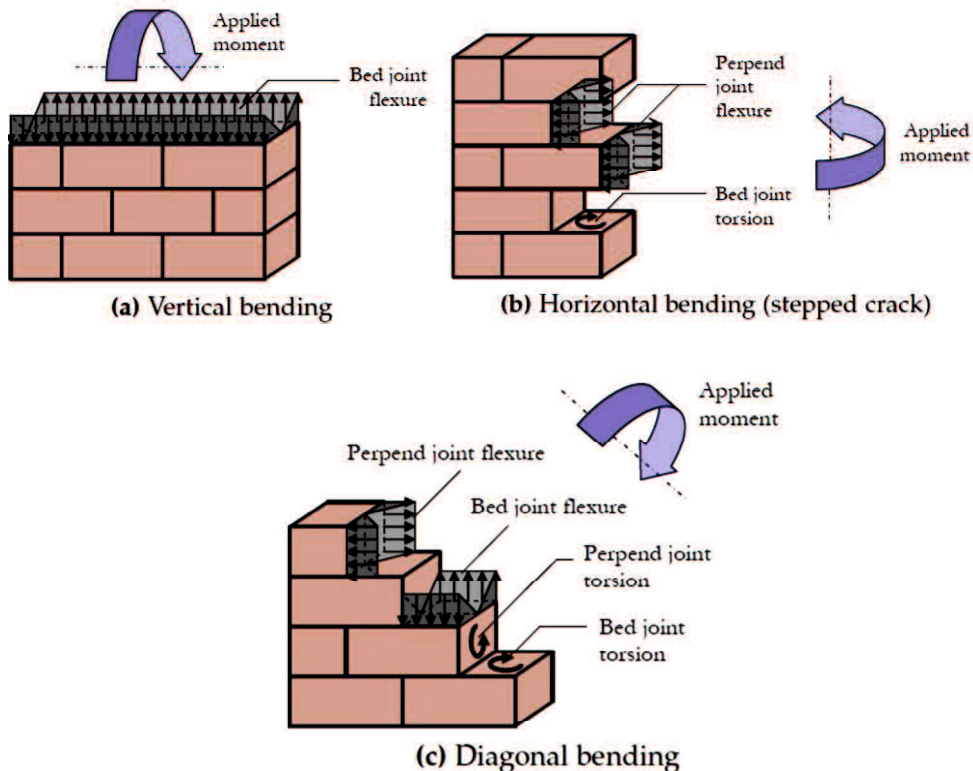
When a wall is subjected to out-of-plane face loading due to either earthquake or wind, it undergoes flexure (bending). Orientation of the internal stresses within the wall and the resulting crack pattern developed is dictated by the position of its supported edges, as shown in Fig. 2.29. One-way spanning walls (Fig. 2.29a) undergo uniaxial bending, which can be classified as either vertical or horizontal depending on the orientation of the span. This results in cracks that run parallel to

the panel's supports and the axis of internal bending. Behavior of two-way spanning walls (Fig. 2.29b), which include any class of walls supported on at cracking patterns.



Source: <https://digital.library.adelaide.edu.au/dspace/handle/2440/77089>

Figure 2.29 Various types of wall support shapes and the associated out-of-plane flexure



Source: <https://digital.library.adelaide.edu.au/dspace/handle/2440/77089>

Figure 2.30 Mechanics of internal moment resistance for the different types of bending.

Least one vertical edge and one horizontal edge, is especially complex, due to the anisotropic nature of the masonry material and the structural indeterminacy of the wall configurations [Drysdale *et al.*, 1994]. Such walls undergo biaxial bending, whereby the internal flexural stresses act in both the horizontal and vertical directions. As a result, two-way panels characteristically develop crack patterns exhibiting a combination of vertical, horizontal and diagonal crack lines. In turn, the internal moments along the different types of crack lines can consist of a combination of flexure (normal stress) and torsion (shear stress) (Fig. 2.30). The majority of past experimental and theoretical research dealing with seismic out-of-plane response has been focused on vertically spanning URM walls [Ewing and Kariotis, 1981; Doherty *et al.*, 2002; Griffith *et al.*, 2004]. By contrast, two-way URM walls have received only limited attention [e.g. Jaramillo, 2002], even though they are most commonly encountered in practice. This topic will hence form the primary focus of this dissertation.

During the seismic loads, the lateral inertia forces will induce both in-plane and out-of-plane forces at the URM walls. These out-of-plane forces can cause the URM buildings to be more unstable and vulnerable to out-of-plane failures. Loading perpendicular to the masonry wall causes bending of the wall and the effect will be determined by the boundary conditions. If the boundary conditions spanned between floor levels or between orthogonal URM walls, the performance of out-of-plane failure can be assumed to act as a one-way slab (see Fig. 2.31). In the other case that the boundary conditions are spanned between floor levels and also between orthogonal URM walls, the performance can be assumed to act as a two-way slab.

The capacities of the URM wall to out-of-plane forces depend on the ratio of height of the wall to the thickness, the boundary conditions, the types of the floor diaphragm, the compressive stress and the tensile strength of the masonry. The tensile strength of the masonry is low. The performance of the brick wall structure for the out-of-plane action is very brittle and it will crack under light lateral floor response mainly due to lack of adequate wall ties. Several potential URM elements fail due to out-of-plane forces such as parapet walls, veneers, flexibility of the horizontal diaphragm, and unanchored load bearing walls. The out-of-plane failure mechanism can be seen in Fig. 2.32.

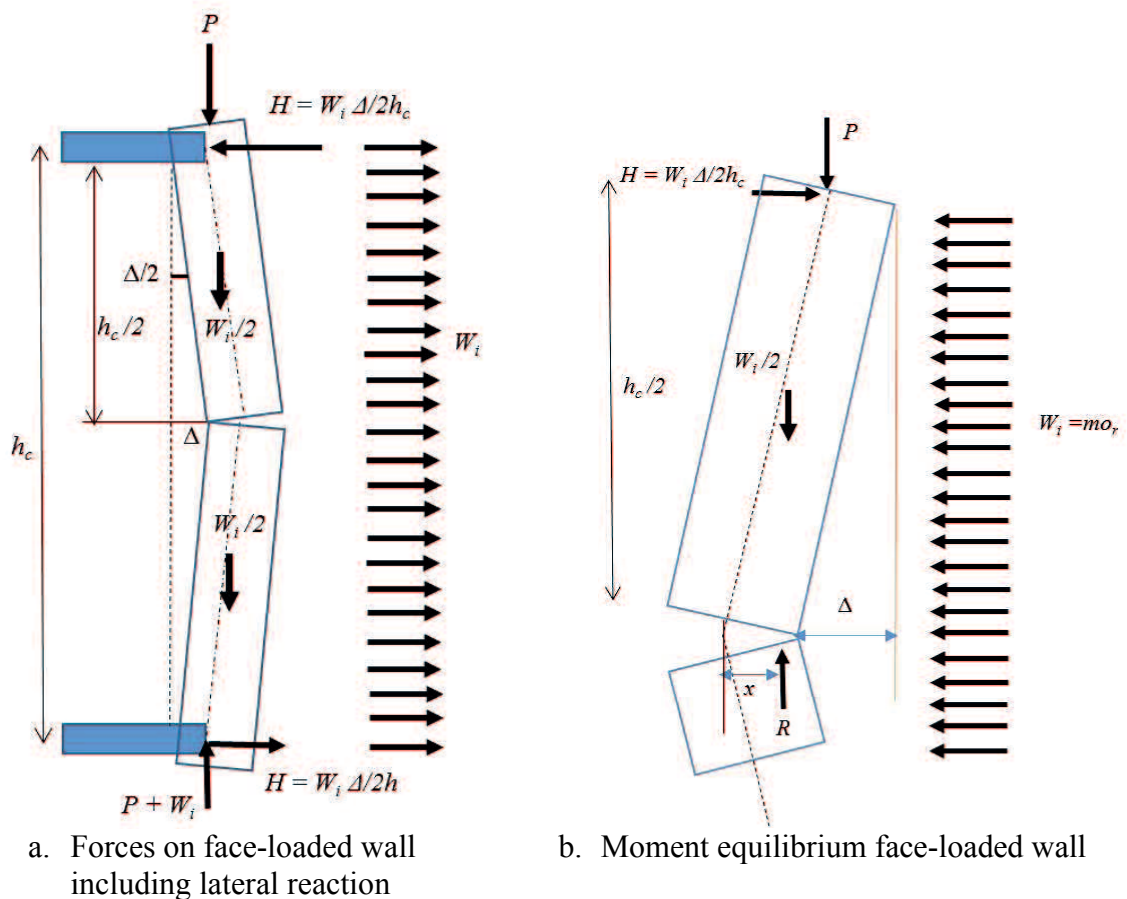


Figure 2.31 Performance of URM walls subjected to out-of-plane load. [Paulay and Priestley, 1992]

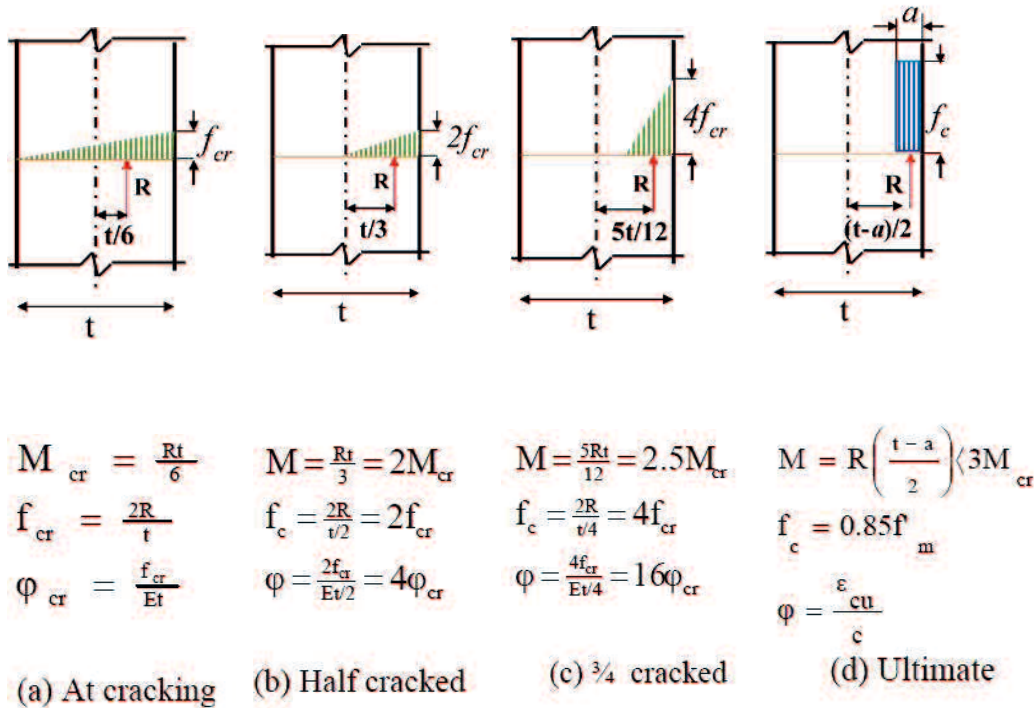


Figure 2.32 Moments and curvatures at center of face-loaded wall [Paulay and Priestley, 1992]

In the early 70's, Paulay and Priestley of the University of Canterbury carried out some experimental investigations on the unreinforced masonry walls subjected to static cyclic loading concerned particularly with the ductility capability, stiffness degradation and load capacity. Priestley, 1985b, stated that the response of unreinforced masonry walls to out-of plane (face-load) seismic excitation is one of the most complex and ill-understood area of seismic analysis. In the early 1980s, the ABK Joint Venture in the USA performed most extensive researches on the out-of-plane performances of URM walls. The results still become the main sources for seismic design guidelines of masonry building in the USA.

FEMA – 273 stated that the stiffness of out-of-plane URM walls should be neglected in analytical models of the global structural system if in-plane walls exist. The dynamic stability of the out-of-plane performance also depends on the ratio of

height of the wall to the thickness of URM wall and the value of the site spectral acceleration. Bruneau [1994] reported that the out-of-plane collapse of walls could be rapid and explosive in nature. In addition, damage incurred to URM buildings with flexible floor and roof diaphragms can be attributed to their insufficient or total lack of in-plane stiffness and integrity [Simsir *et al.*, 2004]. The situation is further worsened by inherent weaknesses of the materials and commonly observed bad workmanship in these buildings.

2.7. Model and methodology for analysis masonry wall

During the last forty years, an enormous growth in the development of numerical tools for structural analysis has been achieved. Nowadays, the finite element method is usually adopted in order to achieve sophisticated simulations of the structural behavior. A description of the material behavior, which yields the relation between the stress and strain tensor in a material point of the body, is necessary for this purpose. This mathematical description is commonly named a constitutive model and an important objective of today's research is to obtain robust numerical tools, capable of predicting the behavior of the structure from the elastic domain until total failure, due to excessive cracking and rigidity degradation.

In the analysis of masonry structure, the existence of (mortar) joints is the major source of weakness and material non-linearities. Different levels of refinement have been used for the structural analysis. Depending on the degree of accuracy and the simplicity desired, the following modelling strategies can be used [Lorenco, 1996]

- Detailed micro modelling : both units and mortar are discretized and modeled with continuum elements whereas the unit-mortar interface is represented by discontinuum elements.
- Simplified micro-modelling : expanded unit are modeled with continuum elements, while the behavior of the mortar joints and unit mortar interface is lumped in discontinuum line interface elements.
- Macro-modeling : unit mortar joints and unit mortar interface are smeared out in a homogenous anisotropic continuum.

2.7.1. Discontinuous modelling of masonry

Lately, a considerable attention has been given to rational assessment methodologies, to be directly consistent with the discontinuous nature of structural masonry.

The discontinuities in continuous systems are in fact interfaces between dissimilar materials and joints or fractures in the material. A survey of the literature [Tzamtzis 2003] on finite element modelling of cracks and joints shows that three main approaches are common for a representative analysis: the discrete crack and the smeared crack approach or the use of joint or interface elements.

Discrete crack approach represents the crack as a separation of nodes. When the stress or strain at a node, or the average in adjacent elements, exceeds a given value, the node is redefined as two nodes and the elements on either side are allowed to separate increasing the number of equations to be solved and extends the bandwidth of the stiffness matrix.

In the smeared crack approach, cracks and joints are modelled in an average sense by an appropriate modification of the material properties at the integration points of regular finite elements.

Smeared cracks are convenient when the crack orientations are not known beforehand, because the formation of a crack involves no re-meshing or new degrees of freedom. However, they have only limited ability to model sharp discontinuities and represent the topology or material behavior in the vicinity of the crack.

The method is attractive if global analysis of large-scale masonry structures is required. It does not make a distinction between individual bricks and joints, but treats masonry as an anisotropic composite such that joints and cracks are smeared out. An inherent limitation of the smeared crack approach is that discrete cracks are smeared out over an entire element and the crack opening is modelled by the continuous displacement approximation functions of the conventional finite element approach. In view of this limitation, as well as other problems such as mesh-dependency due to tensile and compressive softening and difficulties of model calibration, smeared crack models should only be used with caution for the analysis of discontinuous structures.

The Interface smeared crack approach combines the advantages of the discrete and smeared approaches described above, treating cracks discretely like joint elements, but, like smeared crack elements.

Most of the crack models available have only limited ability to model sharp discontinuities present in many structural systems

2.7.2. Continuous modelling of masonry

The first step toward carrying out such analyses is to develop adequate constitutive models. In the case of masonry, when using the continuum model approach, three levels of approximation might be applied: micro-models, simplified or detailed, and macro-models [Rots 1991]:

2.7.2.1. *Micro-modelling*

Micro-modeling when units are represented by continuum elements whereas the behavior of the mortar joints and unit-mortar interface is lumped in discontinuous or interface elements. A complete micro-model must include all the failure mechanisms of masonry, namely, cracking of joints, sliding over one head or bed joint, cracking of the units and crushing of masonry.

In the micro-model, each component of masonry – unit, mortar (simplified), and unit/mortar joint (detailed) – must be represented by different finite elements. The employment of a micro-model to analyse an entire building becomes prohibitive, since it would result in a large number of finite elements, and consequently require a lot of computer resources to run the analyses.

Two approaches can be used: the first one is the simplified or layer model, without taking into account the interface (friction law) between brick unit elements and mortar elements (Fig. 2.33b), and the second one detailed or interface model,

by introducing a normal and tangential contact surface instead of mortar layers (Fig. 2.33c).

These kinds of detailed and simplified micro-models have very accurate results provided that there are suitable input data. This type of analysis is the most advanced level of numerical simulation for masonry elements. It is very appropriate for simulating out-of-plane behavior of masonry, but for in-plane behavior this type of approach is not justified due to the high complexity compared to similar results as in easier approaches.

However, if there is a high interest in observing local behavior and interaction with other elements or material this technique may be the only one that leads to coherent results.

2.7.2.2. *Macro-modelling*

Macro-modelling use an anisotropic continuum model that establishes the relation between average stresses and average strains in masonry, considering composite masonry as a homogeneous material.

Units and joints are not represented anymore and the geometry of masonry constituents (units and joints) is lost (Fig. 2.33d). An adequate macro-model must include anisotropic elastic and inelastic behavior.

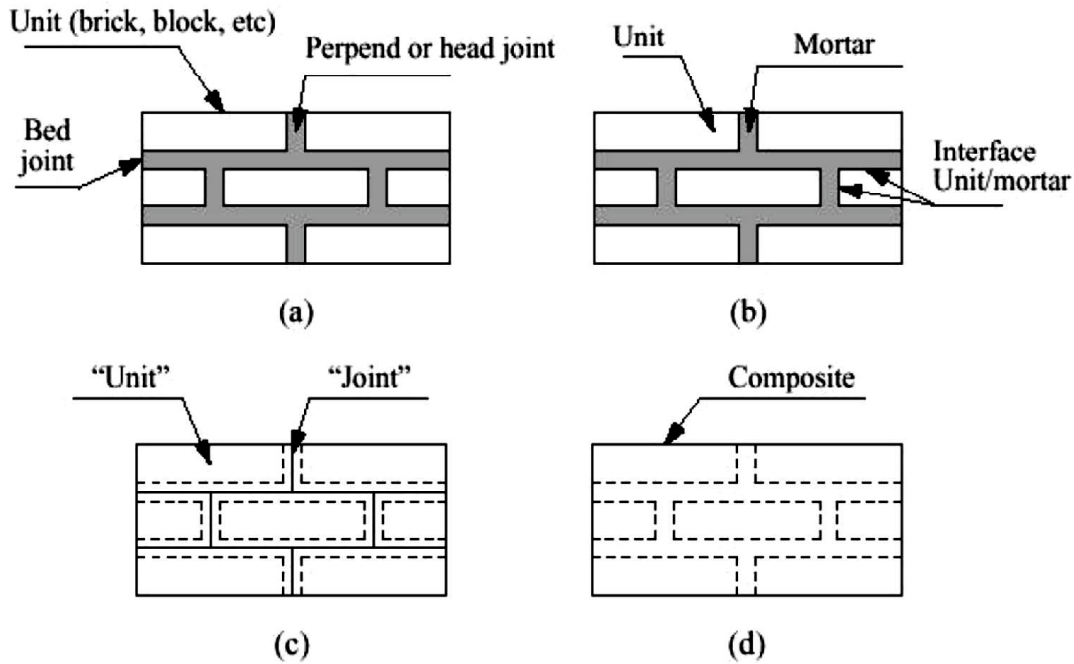


Figure 2.33 Advanced modelling approach (a) masonry sample; (b) detailed micro-modelling; (c) simplified micro-modelling; (d) macro-modelling [Lorenzo,[1996]

This type of analysis is the most suitable from the point of view of balance between involved time and accuracy of the results. Macro-modelling requires an extra process, homogenization [Salamon 1968]. Homogenization of masonry is a step that has been widely treated in articles [Pande *et al.*, 1989, Lourenço *et al.*, 2001, Lourenço 1998, Wang *et al.*, 2006] proposing complicated energy and deformation compatibility equations. Even so, the obtained results must be seriously calibrated after this homogenization, in order to obtain a good correlation with the experimental tests.

The most convenient approach is to use a macro-model in which the material behavior characteristic parameters to be borrowed from concrete models. Because of the non-symmetrical behavior in tension and compression, typically for a concrete material calibration at least uniaxial compression and uniaxial tension

experimental tests are needed. Default values which consider the bi-axial behavior of concrete are available in the scientific literature [Dassault Systèmes, 2010] based on large experimental campaigns. If an accurate post-failure/cracking behavior is desired than other experiments may be required. Unlike concrete elements, due to their inherent inhomogeneous character masonry pose an anisotropic behavior. At least theoretically the material mechanical properties should be defined taking into account their directionally dependent character.

The uniaxial compression test consist in compressing the material specimen. By recording the load and displacement, applying simple formulas one can extract the stress-strain curve. Uniaxial tension test is much more difficult to perform and only the pre-failure response can be obtain with enough confidence even for mortar specimens. In case of masonry specimens this kind of test is not available, and one can make only assumption about the tensile failure strength of the masonry material. The scientific literature recommends a value of 7%–10% of the compressive strength. The choice of tensile cracking stress is very important, because in almost all cases the failure mode is govern by tensile behavior. Use of low cracking stresses will cause numerical problems.

In case of brittle material, calibration of the post-cracking behavior depend on the reinforcement present. For masonry behavior law, a stress-displacement tension stiffening model is recommended with typical values less than 0.05 mm. In case of reinforced masonry, if the reinforcing layer is strong enough, the stress-strain tension stiffening model is more appropriate. For numerical models with an acceptable mesh network could be assumed that the strain softening after cracking

brings the stress to zero at a total strain 10 times the strain at failure. This results a zero stress at a total strain of about 0.001 or less [Dassault Systèmes, 2010].

To understand the post-cracking shear behavior combined tension and shear experiments are used. Unfortunately these experiments are quite difficult to perform. Without experimental results one may assume with a good confidence that the shear retention factor goes linearly to zero at the same crack opening strain used for the tension stiffening model. For defining the failure ratios which gives the biaxial yield and flow parameters biaxial experiments are required to calibrate [Dhanasekar *et al.*, 2010, page 1981]. High scattering of the masonry mechanical characteristics, impose for the statistical interpretation of the experimental results many experimental specimens on the same techniques. In our case were experimentally study three different techniques for masonry walls retrofitting and only three specimen for each of these. On this observation, the experimental results have more a qualitative values offering an indicative results values for the strength and displacement characteristics of the retrofitted walls.

2.7.3. Finite element method

Numerical simulation is a cost-effective method for investigating the behavior of masonry structures. The numerical simulation has become a widely used method for investigating behaviors of structures under static loading,

2.7.3.1. Continuum model and discrete model

The continuum model considers the masonry material as a continuum medium, and is applicable to analysing a large-scale masonry wall in some early investigations [Anthoine 1995, De Buhan and De Felice 1997, Pegon and Anthoine 1997]. Research showed that after varying the bond pattern, neglecting the head joints, or assuming plane stress states, reasonable estimates of the global elastic behavior of masonry were obtained. However, as Anthoine [1995] indicated, a careful examination of the elastic stresses that develop in the different constitutive materials shows that the situation might be quite different in the non-linear range (damage or plasticity). To obtain reliable equivalent material properties of masonry material, homogenization is critical in numerical analysis.

The discrete model has been developed to perform linear and nonlinear analyses of masonry structures. It is computationally intensive, making it a time-consuming method, and is therefore generally only suitable for simulating the fracture behaviors of small specimens [Ma *et al.*, 2001]. In this study, the specimens are full-scaled masonry walls made of cored brick and mortar joint. Therefore, to avoid the calculating problem, the homogenized model is preferable, which is discussed in the following section.

2.7.3.2. Homogenized model

The homogenization technique has been used in the past to derive the equivalent material properties and failure characteristics for solid brick masonry. Considerable research has been conducted in the last decade to investigate the complex mechanical behavior of solid brick masonry structures using various

theoretical and numerical homogenization techniques [Anthoine 1995, Luciano and Sacco 1997, Ma *et al.*, 2001, Milani *et al.*, 2006a, Milani *et al.*, 2006b, Wu and Ha, 2006, Zucchini and Lourenco, 2004]. It has been shown that using homogenized material properties can give a reliable estimate of masonry response under both static and dynamic loading. However, substantially less computational time is required to perform the analysis of masonry structures as compared with distinct model in which bricks and mortar joints are separately discretized.

Recently, the homogenization technique has been used to derive equivalent material properties of hollow concrete block masonry [Wu and Hao, 2007b], in spite of this, no study has been conducted to analyse the response of masonry structure constituted by cored brick units jointed with mortar using the homogenization technique. Due to the complex geometric properties of the cored brick unit, it is very complicated and time consuming to use the distinct model to perform the analysis on this kind of masonry structure. Therefore, it is of importance if the equivalent material properties of this masonry structure can be derived. As masonry is a composite structure constituted by bricks and mortar, using the discrete method to compute large scale of masonry walls often requires a significant amount of time. The homogenized technique, which is used to derive the behavior of the composite from geometry and behavior of the basic cell, has been developed to simplify the computation. Some homogenization models of URM structures has been investigated by researchers [Anthoine, 1995, Cecchi and Di Marco, 2002, ElGawady *et al.* 2006a, Luccioni *et al.*, 2004, Milani *et al.*, 2006a, Wu and Ha, 2006, Zucchini and Lourenco, 2004] in recent years.

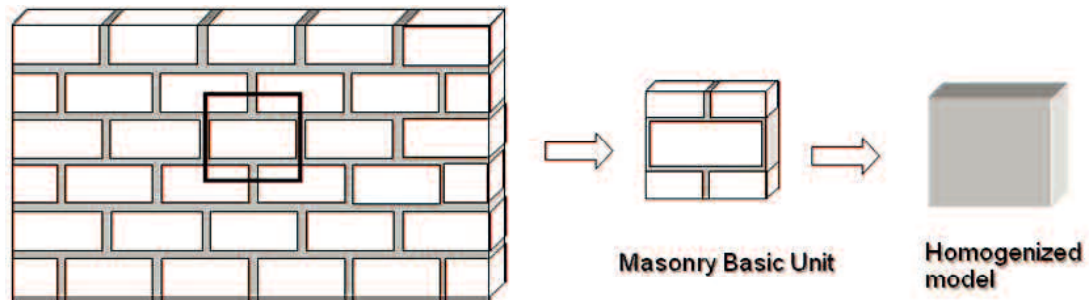


Figure 2.34 Homogenization of Masonry Material [Wu and Ha, 2006]

The homogenization approach is shown above in Figure 2.29. Determining the basic cell is the first stage of homogenization. The basic cell contains all the geometric and constitutive information of the masonry, and is modelled to calculate the equivalent elastic constants and failure modes of masonry structures. Its volume depends on the bonding formats and retrofitting modes. Header bond shown in Figure 2.4 is commonly used for homogenization. More complex bond types require cells with greater dimensions, which are divided into small elements to calculate the constants. Some recent research [Cecchi *et al.*, 2004; Cecchi *et al.*, 2005] began to focus on homogenizing CFRP retrofitted masonry structures. Firstly, the reinforcement and masonry were homogenized separately, then the homogenization of reinforced masonry was obtained by integrating the constitutive function of masonry and reinforcement along the thickness of the wall [Cecchi *et al.*, 2005]. Moreover, the authors developed a numerical finite element single-step homogenization procedure, which can be used as an example for modelling retrofitted masonry walls.

2.7.3.3. Homogenization Technique

Homogenization techniques have been used to derive the equivalent material properties of masonry for many years. Homogenization techniques can be used to derive the equivalent material properties of a composite from the geometry and behavior of the representative volume element. Masonry is a composite structure constituted by bricks and mortar. Thus, the homogenization technique can be used to derive the equivalent material properties of masonry unit. In this section, a highly detailed finite element model was used to model a two-dimensional basic cell to derive the equivalent material properties for a homogenous masonry unit. Various load cases were applied to the basic cell surfaces to derive average stress-strain relationships of the homogenous masonry unit under different stress states. The average elastic properties and failure characteristics of the homogenous masonry unit are obtained from the simulated results.

Traditionally, laboratory tests are performed to obtain average stress and strain relationships of a specimen, required to find the homogenized properties of composite materials such as concrete with aggregates and cement. However, for masonry structures, it is often too difficult to conduct the laboratory test. To overcome this difficulty, the numerical homogenization method was used in this study to derive its equivalent material properties. Fig. 2.29 shows the homogenization process for a basic cell, which contains all the geometric and constitutive information of the masonry wall. The basic cell was modelled, separately, with individual components of mortar and brick. Constitutive relations of the basic cell can be set up in terms of average stresses and strains from the

geometry and constitutive relationships of the individual components. The average stress and strain $\bar{\sigma}_{ij}$ and $\bar{\varepsilon}_{ij}$ are defined by the integral over the basic cell as dV

$$\bar{\sigma}_{ij} = \frac{1}{\Omega} \int_{\Omega} \sigma_{ij} d\Omega \quad (2.15)$$

$$\bar{\varepsilon}_{ij} = \frac{1}{\Omega} \int_{\Omega} \varepsilon_{ij} d\Omega \quad (2.16)$$

where Ω is the volume of the basic cell, σ_{ij} and ε_{ij} are stress and strain components in an element. By applying various displacement boundary conditions on the surfaces of the basic cell, the equivalent stress-strain relationships of the basic cell were established. In addition, the equivalent material properties of the basic cell were derived from the simulated stress-strain curves. However, to simulate the performance of the basic cell under different loading conditions in a finite element program, the material properties of mortar and brick should be determined.

CHAPTER 3. PROPOSAL OF FORMULAE FOR EQUIVALENT ELASTICITY OF MASONRY WALL

3.1. Outline

Some developing countries use brick low elastic modulus for society building. While most of the previous research efforts focused on masonry structures built using bricks of the considerably higher elastic modulus. The research efforts reported in this chapter aim at quantification of the equivalent elastic modulus of lower stiffness masonry structures when the mortar has the higher modulus of elasticity than the bricks making use of finite element (FE) simulations adopting the homogenization technique.

The reported numerical simulations adopted two-dimensional Representative Volume Elements (RVE) using quadrilateral (Q4) elements. The equivalent elastic moduli of composite elements with various bricks and mortar

were quantified. The numerically estimated equivalent elastic moduli from the FE simulations were verified using previously established test data. Hence, a new simplified formula for calculating the equivalent modulus of elasticity of such masonry structures is here proposed.

3.2. Investigation of the quality of bricks masonry

Brick masonry (BM) is a building construction method in which a two-phase composite material is formed of regularly distributed brick and mortar [Ma et.al. 2001]. Normally, bricks (clay bricks) contain the following ingredients: silica (sand) around 50% to 60% by weight, alumina (clay) around 20% to 30% by weight, lime around 2 to 5% by weight, iron oxide $\leq 7\%$ by weight and Magnesia less than 1% by weight [Punmia, *et al.*, 2003]

Usually, the bricks show higher values for compressive strength and stiffness than the mortar. However, the opposite is true in some of the developing countries. For example, the mechanical properties of bricks in some areas of Indonesia show significantly lower values than those of mortar because construction materials are sometimes manufactured in family-run industries [Indra *et al.* 2013]. This is due to culture, economics, source and material of the bricks. In spite of the use of low-quality bricks, the design code for masonry structures in Indonesia (SNI-2094-2000) is based on the design code of other countries, namely, the DIN 105 standard of Germany and the ASTM C 67-94 standard of the USA.

Hence, most investigations are focused on bricks showing higher strength and when compared to the mortar used in masonry structures. However, as mentioned above, this is not always the case [Gumaste *et al.* 2006; Indra *et al.* 2013]

in some developing countries. It was reported in [Indra *et al.* 2013] that bricks in Payakumbuh, located in the West Sumatera Province of Indonesia had a significantly low compressive strength of 2.9 MPa on an average. Similarly, Putri [2014] reported a brick strength of 2.5 MPa in Padang city. Elhusna *et al.* [2014] observed that the compressive strength of bricks in Bengkulu Province was within the range of 2.4–6.7 MPa. Wisnumurti *et al.* [2014] investigated the strength of bricks from four different areas in East Java. According to their investigations, the compressive strength was within the range of 0.55–0.9 MPa, and the modulus of elasticity of the low-quality bricks was within the range of 279–571 MPa. In addition, Basoenondo [2008] reported that the compressive strength and the modulus of elasticity of bricks in the West Java Province were 0.5–2.87 MPa and 220–540 MPa, respectively. It is noteworthy that the test was based on the American standard ASTM E-111 owing to the lack of an Indonesian standard for the evaluation of the elastic modulus of bricks.

Most of the non-engineered constructions at countries use baked clay or stone masonry for the wall materials. Brick sizes in Turkey, Nepal, Indonesia, Peru and Pakistan are relatively similar, meanwhile in India and Egypt bricks have different sizes compared to the others. Peru has the highest brick compressive strength, while Turkey has the smallest brick compressive strength compared to the other countries. Test results from sites in each country showed that some do not have adequate strength for the brick (see Fig. 3.1). [Okazaki *et al.*, 2012]

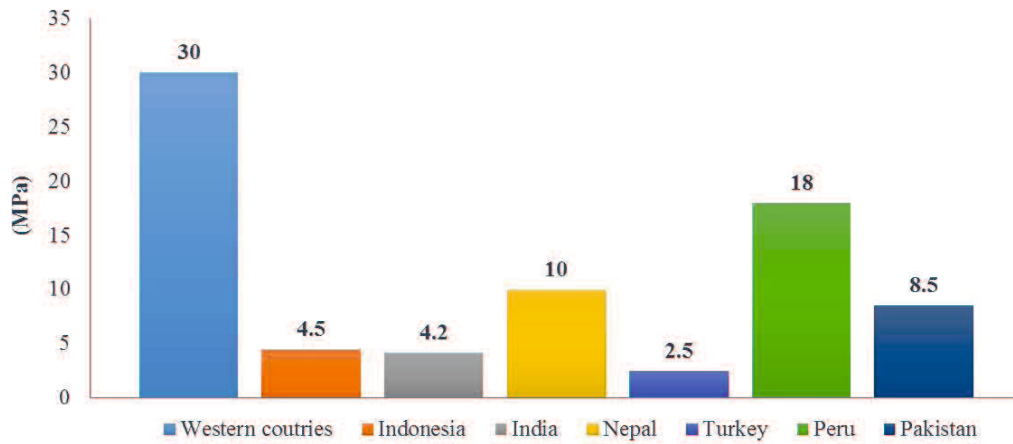


Figure 3.1 Average bricks compressive strength

General-purpose bricks in western countries have higher strength and stiffness than mortar, as discussed by Gumaste *et al.* [2006]. They reported that bricks in India have a relatively lower strength (3–20 MPa) and elastic modulus (300–15000 MPa). Similarly, Indonesian bricks have lower strength and stiffness [Basoenondo, 2008].

The general theory is based on the assumption that mechanical properties of brick elements are higher than those of mortar [Paulay, 1992]. In most cases, the ideal elasticity used in the design refers to formulas specified in overseas regulations. These assumptions may result in inappropriate design for the construction of masonry structures using Indonesian bricks.

Most of the countries use ordinary Portland cement as plaster and mortar cementing agent. Pakistan found to have the highest mortar strength, even though the mix is similar with other countries. On the other hand, Peru has different mortar mix compared to the other countries, but it produce the same compressive strength. The mortar thickness in Egypt is found to be the thickest (25 mm), while Turkey and Pakistan have the thinnest mortar layer (10-20 mm and 11.5mm respectively). The common plaster mix is either 1:6

or 1:4 (pc : sand) , except in Peru where the mix is 1:1. Turkey has the thickest plaster (20-30 mm), while Nepal has the thinnest plaster (10 mm) (see Fig. 3.2). [Okazaki *et al.*, 2012]

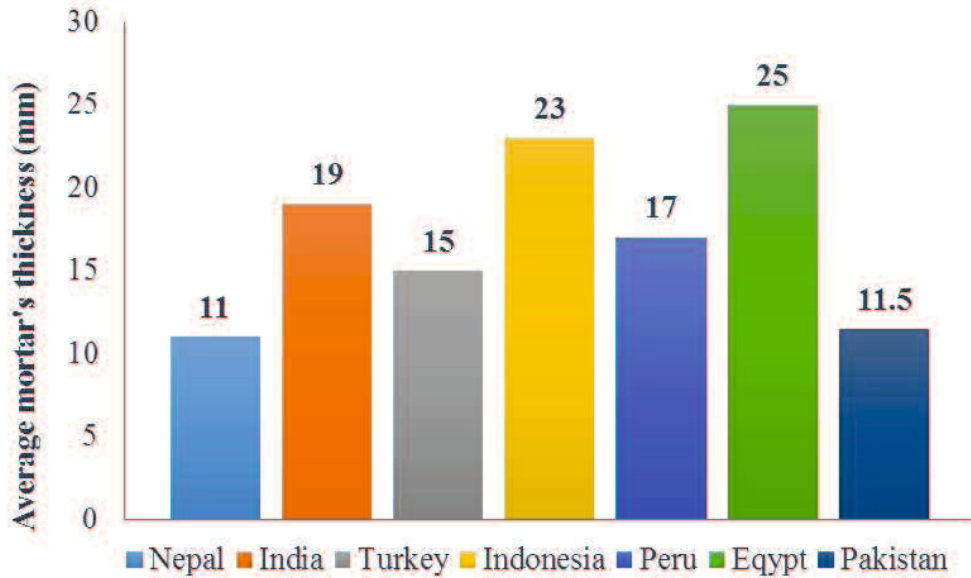


Figure 3.2 Average mortar's thickness

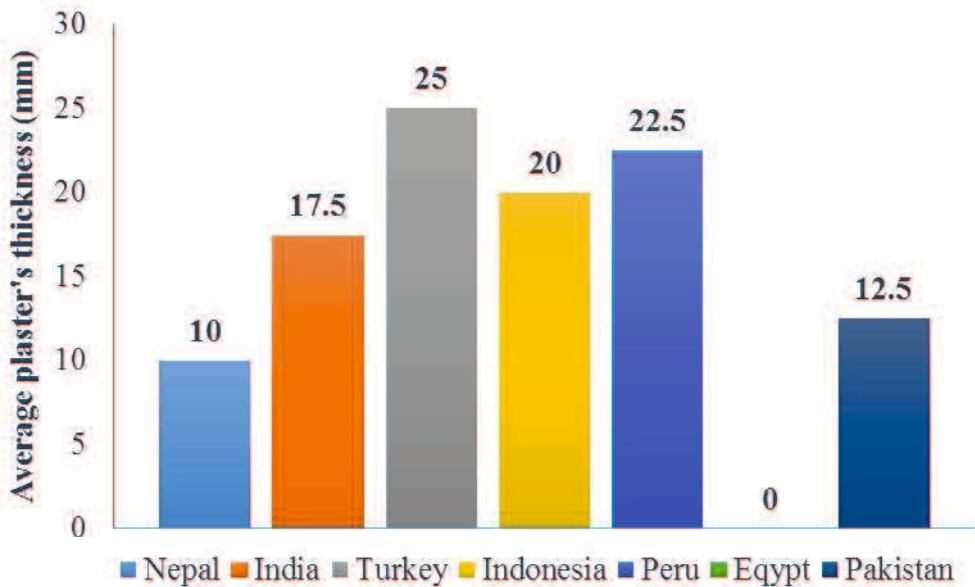


Figure 3.3 Average plaster's thickness

3.3. Overview FE simulation for homogenization

Finite element (FE) simulations are often used to analyze and design such masonry structural systems. The challenges in numerical modeling of the behavior of large-scale masonry systems have led to the development of techniques such as homogenization [Lourenço, *et al.* 2007]. Lourenço *et al.* [2007] reviewed the recent trends in homogenization techniques. They discussed different homogenization techniques available in published literature, and special attention was paid to the micromechanical-based model and the one based on polynomial expansion of the micro-stress field.

The techniques of homogenization are based on establishing constitutive relations in terms of averaged stresses and strains from the geometry and constitutive relations of the individual components.. The popularity of such techniques has increased in the masonry community during the last decade [Ma *et al.* 2001; Lourenço *et al.* 2007; Pande *et al.* 1989; Pietruszczak *et al.* 1992; Anthoine, 1995; Pegon, and Anthoine, 1997; Luciano and Sacco 1997; Anthoine, 1997; Zucchini and Lourenço, 2002].

The techniques of masonry homogenization can be classified into three types: traditional homogenization, numerical homogenization, and micromechanical and microstructural models. Pande *et al.* [1989], Hendry [1990], and Pietruszczak and Niu [1992] used the traditional homogenization with an empirical approach to estimate the volume ratio effects on the physical and the mechanical properties of bricks and mortar. Equivalent elastic properties were determined for a brick-mortar system made with equally spaced layers. In addition, a simplified geometry to

represent the complex geometry of the representative cell was adopted so that a close-form solution to the homogenization problem would be possible. This method is suitable for modeling the linear elastic behavior and for a relatively simple modeling of the nonlinear behavior of masonry structures.

Anthoine [1995], Mistler *et al.* [2007], Pegon and Anthoine [1997], Luciano and Sacco [1997], Ma *et al.* [2001], Zucchini and Lourenço [2002], and Anthoine [1997] developed the numerical homogenization theory, which is applicable to FE simulations of masonry wall structures. It is used to apply the homogenization theory for masonry wall consisting of the periodic arrangement of unit and mortar as cell. Owing to the complexity of a masonry basic cell, it is necessary to use the finite element method to obtain a numerical solution to problems. This approach is suitable for analyzing the nonlinear behavior of the complex masonry basic cell by solving the problem for all possible macroscopic loading histories.

Luciano and Sacco [1997], Ma *et al.* [2001], and Zucchini and Lourenço [2002] proposed a theory based on the micromechanical and macro-structural concepts. Their model contained representative volume elements and constitutive elements for all geometries. Although this approach is very useful, its applications are limited because it is difficult to determine several parameters in the micromechanical model for macroscopic analysis.

Homogenization typically has two different models, namely discrete and continuum models. Mohebkhah *et al.* [2008] used discrete models for nonlinear static analysis. They performed simulations using the model for analyzing the fracture behavior of small laboratory panels and verified the model with

experimental data. Lourenço *et al.* [1998] used continuum models to analyze masonry structures. The model is appropriate for analyzing anisotropic elastic and inelastic behaviors; it is also suitable for nonlinear static analysis, such as in case of large-scale masonry walls.

The generalization of the homogenization procedure for out-of-plane behavior of masonry [Milani *et al.*, 2006] can be applied to periodic composite materials. There are two or more units of masonry, such as stones, bricks, and hollow bricks. Mistler *et al.* [2007] examined the effect of the elastic properties on a brick masonry structure. They used the numerical homogenization technique to confirm the effectiveness of the generalization of the homogenization procedure. Pegon and Anthoine [1997] developed a homogenization theory for studying the macroscopic nonlinear behavior of masonry. Lourenço *et al.* [1996] used a micromechanical model of homogenization for three-dimensional numerical simulations.

3.4. Purpose

The study developed a representative volume element system using multi-parametrical representations of the elastic properties of masonry. It was observed that typical mortar has a lower elasticity than bricks in the homogenization process (Table 3.1).

The purpose of the present study is to numerically determine the equivalent elastic modulus of a brick masonry construction, assuming that the elastic modulus of mortar (E_{mor}) is higher than that of bricks (E_b) and otherwise. The analysis in the present study was based on a numerical simulation using the homogenization

technique. The fundamental model is a two-dimensional (2D) representative volume element (RVE) formulation. The proposed analytical approach can significantly contribute to a safer analysis and design of masonry structural systems built with low-quality bricks in various developing countries, such as Indonesia.

Table 3.1 Moduli of elasticity for homogenization

Author (s)	E_{brick} (MPa)	E_{mortar} (MPa)
Stefanou, <i>et al.</i> 2015	6740	1700
Cluni and Gusella 2004	12500	1200
Cecchi and Di Marco 2002	1000	$E_{mor}/E_b < 1$
Zucchini and Lourenço 2002	20000	$1 < E_b/E_{mor} < 1000$
Rekik <i>et al.</i> 2015	10000	0.49
Pande <i>et al.</i> 1989	11000	$E_b/E_{mor} = 1.1-11$
Anthoine 1995	11000	2200
Lee, <i>et al.</i> 1996	22000	7400
Gabor, <i>et al.</i> 2006	13000	4000
Lorenco 1996	20000	2000

3.5. Approach of the solution

3.5.1. Representative Element

The representative volume element (RVE) is a typical unit of masonry; it was selected to represent brick masonry. I considered a masonry wall Ω , consisting of a periodic arrangement of masonry units and mortar joints, as shown in Fig. 3.4. The periodicity allows Ω to be regarded as the repetition of the RVE [Lourenço *et al.* 2007].

Ma *et al.* [2001] stated that a masonry RVE should include all the participating materials, constitute the entire structure in a periodic and continuous distribution, and be the minimum unit satisfying the first two conditions.

In order to start developing the procedure to find a representative size, an RVE should be properly defined. First some definitions of the RVE, used by scientists for different purposes follow.

- An RVE is the minimal material volume, which contains enough statistically mechanisms of deformation processes. The increasing of this volume should not lead to changes of evolution equations for field-values, describing these mechanisms [Trusov and Keller, 1997].
- The RVE must be chosen "sufficiently large" compared to the microstructural size for the approach to be valid. The RVE is the smallest material volume element of the composite for which the usual spatially constant "overall modulus" macroscopic constitutive representation is a sufficiently accurate model to represent mean constitutive response [Drugan and Willis, 1996].
- The RVE is a model of the material to be used to determine the corresponding effective properties for the homogenized macroscopic model. The RVE should be large enough to contain sufficient information about the microstructure in order to be representative, however it should be much smaller than the macroscopic body. This is known as the Micro-Meso-Macro principle [Hashin, 1983]

- The RVE is defined as the minimum volume of laboratory scale specimen, such that the results obtained from this specimen can still be regarded as representative for a continuum [van Mier, 1997].
- The RVE is very clearly defined in two situations only: i) unit cell in a periodic microstructure, and ii) volume containing a very large (mathematically infinite) set of microscale elements (e.g. grains), possessing statistically homogeneous and ergodic properties [Ostoja and Starzewski, 2001].

Bringing together all these definitions, one can define RVE as a representation of the material to be used to determine the corresponding effective properties for the homogenized macroscopic model with a size which is small enough compared to the macroscopic body and large enough compared to the microstructural size. An RVE should contain sufficient information about the microstructure and be a good representation of a continuum

Several methods are available in the literature in order to determine the RVE size. Bulsara et al. [1999] in their work used a simulation scheme which generated statistically similar realizations of the actual microstructure of a ceramic-matrix composite. This was done on the basis of a radial distribution function which was obtained by a stereological method and image analysis. They conducted a systematic investigation of the RVE size with respect to the transverse damage initiation for one fiber volume fraction.

Ashihmin and Povyshev [1995] determined the statistical properties of stress using an imitation model. The model is based on finite-element simulations. They obtained the statistical criterion for metals representative volume determination.

The RVE cell is classified into two types: RVE-1 and RVE-2 in this study. The cell dimensions of these two types of cells are the same; however, the arrangement of bricks and mortar in the cells are different. Ma *et al.* [2001] compared both RVEs, and observed that their stress–strain curves under the condition of vertical compression without applying horizontal restrains are the same. Figure 3.5 shows an RVE. It provides a valuable dividing boundary between the discrete and continuum models. Equivalent stress–strain relations of the RVE were homogenized by applying a compatible, distributed displacement loading along the vertical and horizontal directions and a positive–negative horizontal displacement loading on the top and bottom of the RVE surfaces [Ma *et al.* 2001].

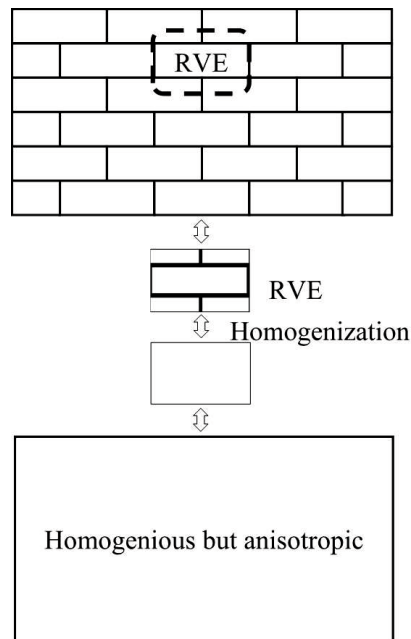
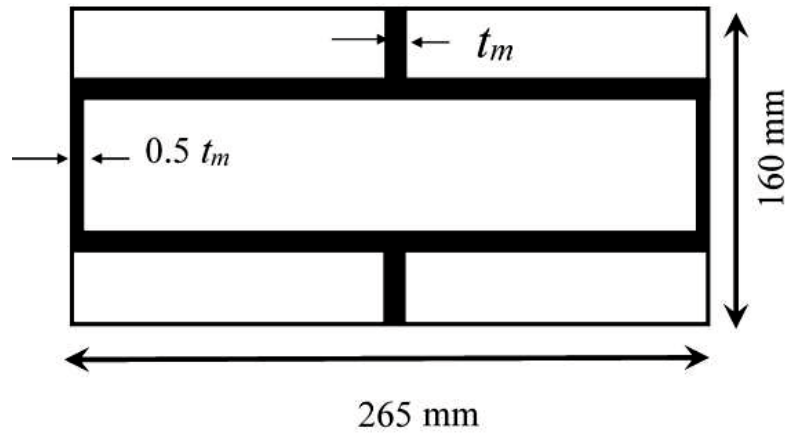
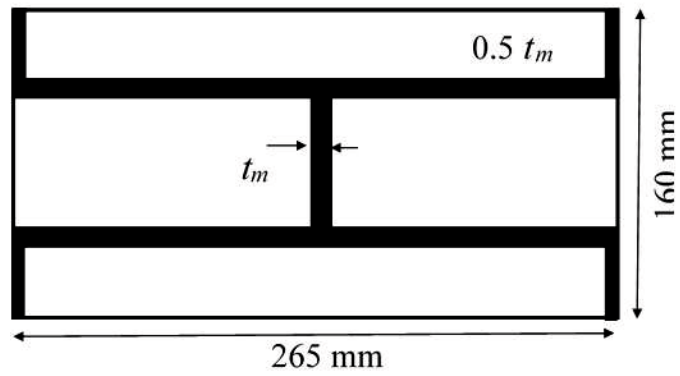


Figure 3.4 Homogenization of masonry material



(a) RVE-1



(b) RVE-2

Figure 3.5 Model of masonry cells

The average stress and strain can be calculated via the following equations.

$$\bar{\sigma}_{ij} = \frac{1}{|\Omega|} \int_{\Omega} \sigma_{ij} d\Omega \quad \text{and} \quad (3.1)$$

$$\bar{\varepsilon}_{ij} = \frac{1}{|\Omega|} \int_{\Omega} \varepsilon_{ij} d\Omega, \quad (3.2)$$

where Ω is volume of the RVE cell.

The elastic parameters of the RVE can be derived from the simulated stress–strain relation.

Then a statistical analysis, which is based on the Chi-square criterion (Eq. 3.3), is used to determine the size of the RVE.

$$R^2 = \sum_{i=1}^n \frac{(D_i - \bar{D})^2}{\bar{D}} \quad (3.3)$$

where D_i is the normalized average value of the stress in the current unit cell; \bar{D} is average of D_i ; n is the number of realizations for the current size.

3.5.2. Constitutive equation

Isotropic, linear-elastic materials were used for both the brick and mortar. The constitutive stress–strain relations are presented in the following matrix.

$$\begin{Bmatrix} \sigma_x \\ \sigma_y \\ \tau_{xy} \end{Bmatrix} = \frac{E}{1-\nu^2} \begin{bmatrix} 1 & \nu & 0 \\ \nu & 1 & 0 \\ 0 & 0 & \frac{1-\nu}{2} \end{bmatrix} \begin{Bmatrix} \varepsilon_x \\ \varepsilon_y \\ \gamma_{xy} \end{Bmatrix} \quad (3.4)$$

Here, E and ν are the Young's modulus and Poisson's ratio, respectively, which were applied for each material, individually. Five independent material properties (E_x , E_y , ν_x , ν_y , G) are used to constitute the equation for the isotropic material under the plane stress condition, which is expressed as Eq. (3.5):

$$\begin{Bmatrix} \bar{\sigma}_{xx} \\ \bar{\sigma}_{yy} \\ \bar{\tau}_{xy} \end{Bmatrix} = \begin{bmatrix} \frac{\bar{E}_{11}}{1-\bar{\nu}_{12}\bar{\nu}_{21}} & \frac{\bar{E}_{11}\bar{\nu}_{21}}{1-\bar{\nu}_{12}\bar{\nu}_{21}} & 0 \\ \frac{\bar{E}_{22}\bar{\nu}_{12}}{1-\bar{\nu}_{12}\bar{\nu}_{21}} & \frac{\bar{E}_{22}}{1-\bar{\nu}_{12}\bar{\nu}_{21}} & 0 \\ 0 & 0 & \bar{G} \end{bmatrix} \begin{Bmatrix} \bar{\varepsilon}_{xx} \\ \bar{\varepsilon}_{yy} \\ \bar{\gamma}_{xy} \end{Bmatrix}. \quad (3.5)$$

The effective properties of the brick masonry structure can be calculated from Eq. (3.5), and a set of numerical solutions were derived under certain boundary conditions. The numerical simulation results were combined using a nonlinear regression process.

The power function equation is used in this study. The power function equation describes many scientific and engineering phenomena. In engineering, It is often written in power function form as

$$y = ax^b \quad (3.6)$$

The method of least squares is applied to the power function by first linearizing the data (the assumption is that b is not known). If the only unknown is a , then a linear relation exists between x^b and y . The linearization of the data is as follows.

$$\ln(y) = \ln(a) + b \ln(x) \quad (3.7)$$

The resulting equation shows a linear relation between $\ln(y)$ and $\ln(x)$.

Let

$$z = \ln y$$

$$w = \ln (x)$$

$$a_0 = \ln a \text{ implying } a = e^{a_0}$$

$$a_1 = b$$

we get

$$z = a_0 + a_1 w \quad (3.8)$$

$$\begin{aligned}
a_1 &= \frac{n \sum_{i=1}^n w_i z_i - \sum_{i=1}^n w_i \sum_{i=1}^n z_i}{n \sum_{i=1}^n w_i^2 - \left(\sum_{i=1}^n w_i \right)^2} \\
a_0 &= \frac{\sum_{i=1}^n z_i}{n} - a_1 \frac{\sum_{i=1}^n w_i}{n}
\end{aligned} \tag{3.8a,b}$$

Since a_0 and a_1 can be found, the original constants of the model are

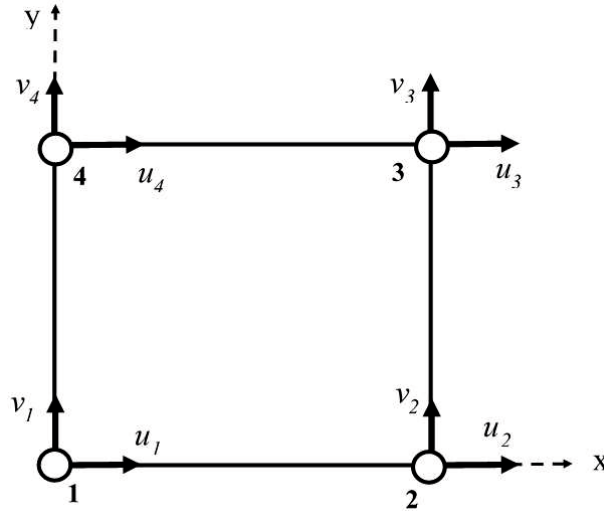
$$\begin{aligned}
b &= a_1 \\
a &= e^{a_0}
\end{aligned} \tag{3.9}$$

3.6. Numerical simulations

3.6.1. Simulation model

The physical models of the RVEs (RVE-1 and RVE-2) used in the present numerical simulation are shown in Fig. 3.5. Both were used to obtain the differences in elasticity, Poisson's ratio, and shear moduli between the RVE-1 and RVE-2. For each RVE cell, three boundary conditions (BCs) and a displacement load were applied; the FE simulation was realized through the FE program SAP2000-V17. The three BCs will be explained in Section 3.6.3. Then, the values of E , ν , and G were calculated using Eqs. (3.9) – (3.12). The elasticity and Poisson's ratio were used as baseline data, and various data measurements for elasticity were obtained from the FE simulation.

Figure 3.6 shows the quadrilateral (Q4) finite element with four nodes and eight degrees of freedom (DOF) used to discretize the problem in the numerical



investigation.

Figure 3.6 Finite element Q4 used in numerical analysis

The RVE-1 and RVE-2 cells consisted of 3,360 elements, 3,485 nodes, and 6,970 DOF. The brick and the mortar were discretized individually. The dimensions of the cell were $250 \times 120 \times 65$ mm, and the assumed thickness of the mortar was 15 mm.

Ma *et al.* [2001] also applied both the models and obtained the same numerical results. The numerical results in the present study indicated that the RVE was able to represent the material properties at the unit volume level. Thus, all subsequent calculations were performed with the RVE-1 model as the RVE.

3.6.2. Materials

The material properties for the validation of the model were obtained from the experimental and simulation results published by Pegon, and Anthoine [1997] and Ma *et al.* [2001] (**Table 3.2**). These material properties are used to ensure applying FE program for the RVE model. Then, the material properties of mortar have higher and lower elasticity than the brick can be used to the simulation

Table 3.2 Material parameter for brick and mortar.

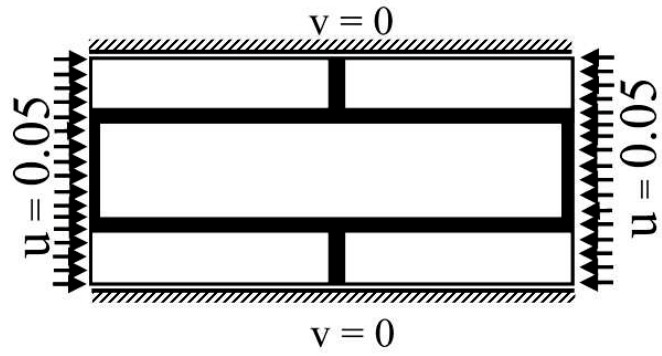
Material	$E_x=E_y$ (MPa)	$\nu_x = \nu_y$	$G=E/2(1+\nu)$ (MPa)
Brick	11000	0.2	4580
Mortar	2200	0.25	880

E_x, E_y = Young's modulus [MPa], G = Kirchhoff's modulus [MPa], ν_x, ν_y = Poisson's ratios.

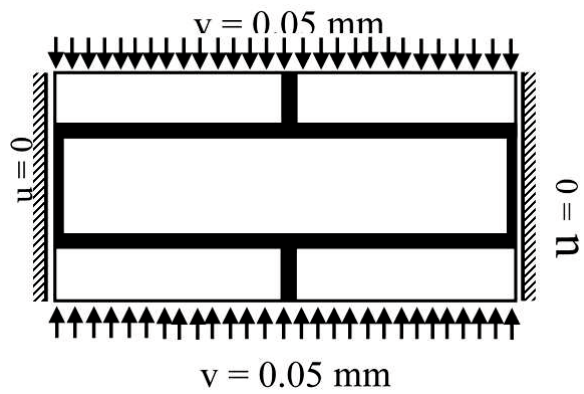
3.6.3. Boundary condition

Ma *et al.* [2001] simulated various BCs. Three state groups of BCs were applied to the RVE model. These included the compression–compression stress state, the compression–tension state, and the compression–tension–shear stress state. Each group had six BC cases. Ma *et al.* [2001] stated that the elastic modulus could be obtained from the abovementioned groups using three BC cases. Figure 3.7 shows the three load cases and the boundary displacements that were used in present study. There were certain displacement boundary conditions:

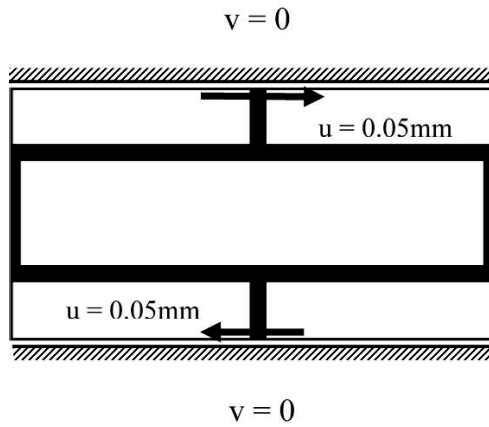
- 1) $u \neq 0, v = 0, \bar{\varepsilon}_{xx} \neq 0, \bar{\varepsilon}_{yy} = 0, \text{ and } \bar{\gamma}_{xy} = 0$, were used for horizontal compression.
- 2) $v \neq 0, u = 0, \bar{\varepsilon}_{yy} \neq 0, \bar{\varepsilon}_{xx} = 0, \text{ and } \bar{\gamma}_{xy} = 0$ were used for vertical compression.
- 3) $u \neq 0, v = 0, \bar{\varepsilon}_{xx} = 0, \bar{\varepsilon}_{yy} = 0, \text{ and } \bar{\gamma}_{xy} \neq 0$ were used for horizontal shear.



(a) Load case 1: horizontal compression



(b) Load case 2: vertical compression force



(c) Load case 3: horizontal shear force

Figure 3.7 Load cases of imposed boundary displacement

A displacement of approximately 0.05 mm was applied to the non-zero side of the cell. The zero-displacement side was constrained to achieve simplicity in calculations and homogenization of the linear static materials.

3.7. Equivalent elastic modulus calculation

The average values of stress and strain can be calculated by employing Eqs. (3.1) and (3.2) as well as the FE simulation results. The effective material parameters of the masonry structure can be estimated as these for an equivalent, homogeneous orthotropic material by using Eqs. (3.9)–(3.12) [Ma *et al.* 2001]:

$$\bar{\nu}_{yx} = \frac{\bar{\sigma}_{xx}^{(2)}}{\bar{\sigma}_{yy}^{(2)}}, \bar{\nu}_{xy} = \frac{\bar{\sigma}_{yy}^{(1)}}{\bar{\sigma}_{xx}^{(1)}}, \quad (3.9)$$

$$\bar{E}_{xx} = \frac{\bar{\sigma}_{xx}^{(1)}(1-\bar{\nu}_{xy}\bar{\nu}_{yx})}{\bar{\epsilon}_{xx}^{(1)}} = \bar{\sigma}_{xx}^{(1)} \frac{1-\frac{\bar{\sigma}_{xx}^{(2)}\bar{\sigma}_{yy}^{(1)}}{\bar{\sigma}_{yy}^{(2)}\bar{\sigma}_{xx}^{(1)}}}{\bar{\epsilon}_{xx}^{(1)}}, \quad (3.10)$$

$$\bar{E}_{yy} = \frac{\bar{\sigma}_{yy}^{(2)}(1-\bar{\nu}_x\bar{\nu}_y)}{\bar{\epsilon}_y^{(2)}} = \bar{\sigma}_{xx}^{(2)} \frac{1-\frac{\bar{\sigma}_{xx}^{(2)}\bar{\sigma}_{yy}^{(1)}}{\bar{\sigma}_{yy}^{(2)}\bar{\sigma}_{xx}^{(1)}}}{\bar{\epsilon}_{yy}^{(2)}}, \quad (3.11)$$

$$\bar{G} = \frac{\bar{\tau}_{xy}^{(3)}}{\bar{\gamma}_{xy}^{(3)}}. \quad (3.12)$$

The superscript index ($i = 1, 2$) denotes the BC case. Subsequently, the simulations were performed with a wide range of elasticity and Poisson's ratio values. Then, nonlinear regression was applied to determine the trend line of the simulation and the basis of the formulation. The formula can represent the case $E_{mor} > E_b$ as well as the case where $E_{mor} < E_b$. The equivalent elastic modulus is the average value of E_{xx} and E_{yy} in the simulation (Eqs. (3.10), (3.11))

To ensure the accuracy of the results, the validation and verification were performed by comparing the results with the numerical and experimental results

obtained in other research works [Ma *et al.* 2001],[Mistler *et al.* 1992],[Zavalis *et al.* 2014]. The simulation results were analyzed to develop the empirical formula proposed in this work.

3.8. Pre-simulation

The result studies of Kuczma *et al.* [2005] can be used for pre-validation the simulation before applying the proposed model to ensure the accuracy of the model and ensure the software. Kuczma *et al.* [2005] tried comparing models with multiple dimensions and number of elements. Their analysis is based on a numerical homogenization technique and performed on a 2D representative volume element (RVE, here denoted by REO, Fig. 3.8 and Fig. 3.9). They solved some relevant boundary value problems for the REO by making use of the finite element method.

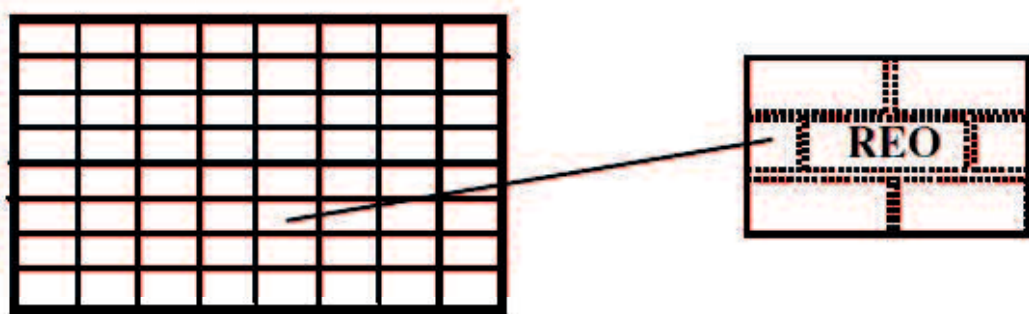


Figure 3.8 Masonry as periodic composite material

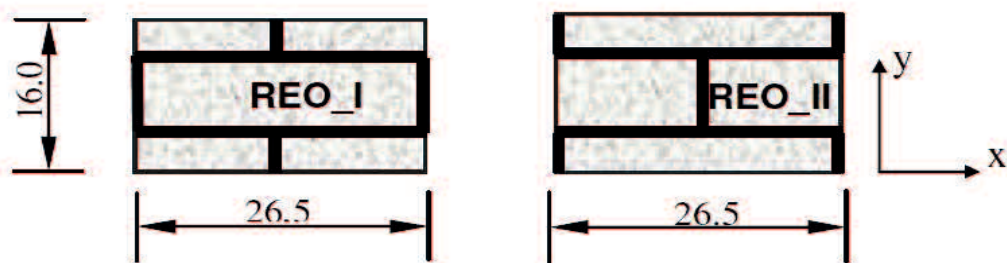


Figure 3.9 Representative cells used

Numerical simulations of the behavior of masonry that will be carried out on selected representative cells. For the representative cells REO_I and REO_II used three meshes, (Figs. 3.10-3.12). They used S1:as 210 elements, 242 nodes, 484 DOF, S2:as 760 elements, 819 nodes, 1638 DOF and S3 as 1456 elements, 1537 nodes, 3074 DOF.

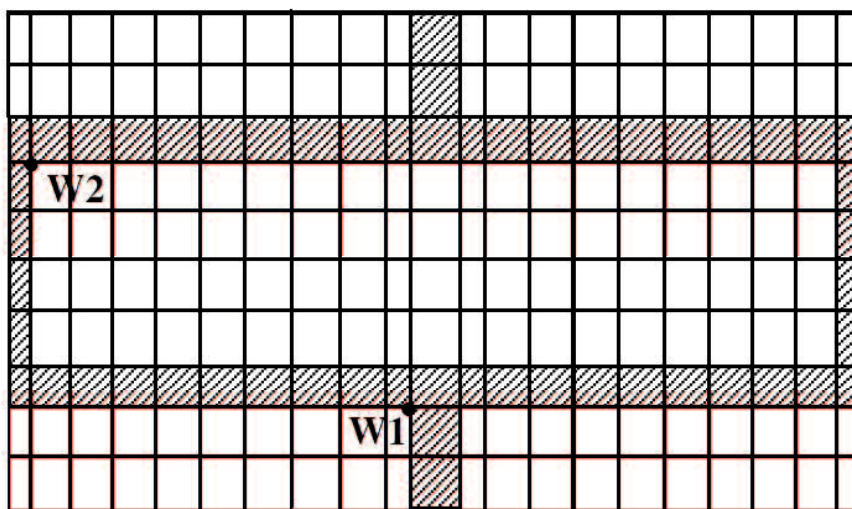


Figure 3.10 REO_1, mesh S1: 210 elements, 242 nodes, 484 DOF

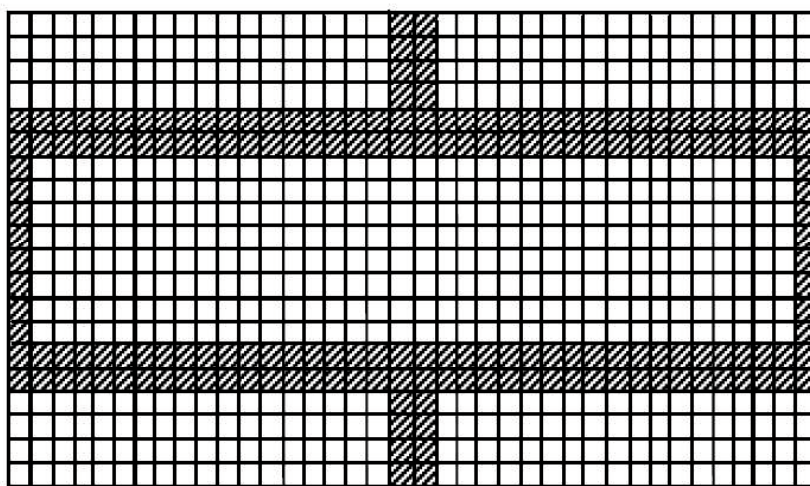


Figure 3.11 REO_1, mesh S1: 760 elements, 819 nodes, 1638 DOF

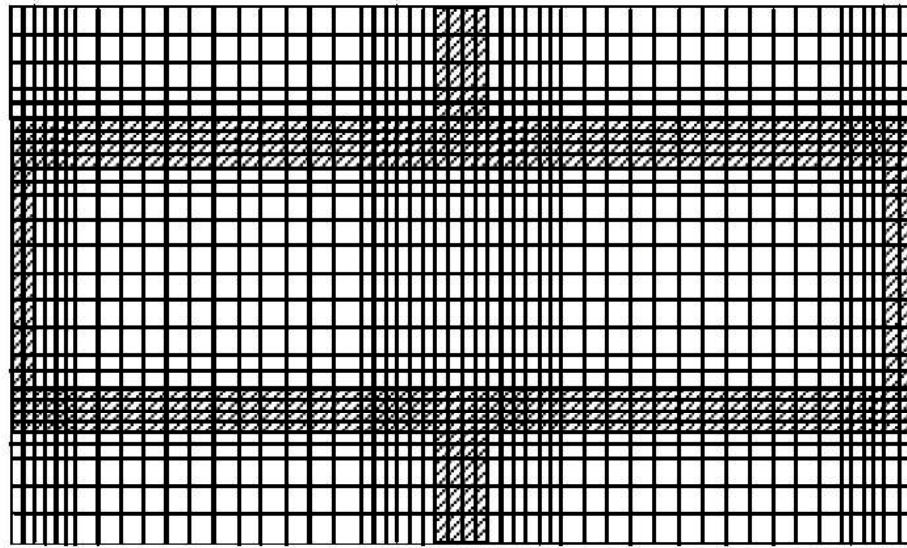


Figure 3.12 REO_1, mesh S1: 760 elements, 819 nodes, 1638 DOF

Proposed model is

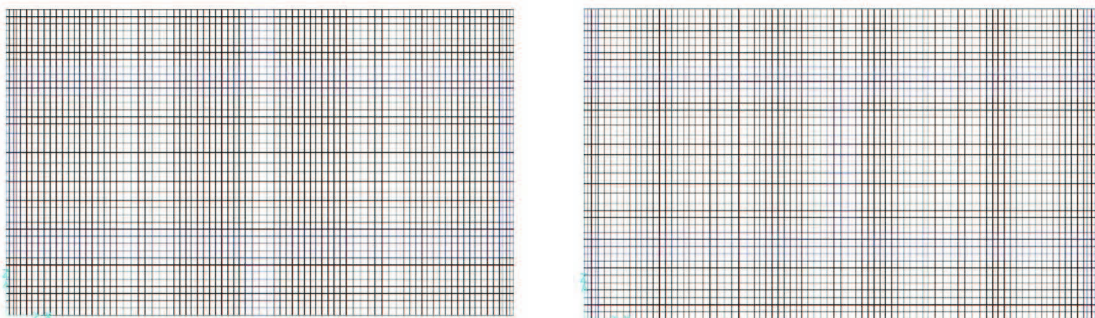


Figure 3.13 Proposed model (RVE-1 and RVE-2)

The RVE-1 and RVE-2 cells consisted of 3,360 elements, 3,485 nodes, and 6,970 DOF (Fig. 3.13)

As can be seen, bricks and mortar joints are discretized individually. The dimensions of the brick are 25 x 12 x 6.5 cm and the assumed thickness of (bed and head) mortar joints is 1.5 cm. The material parameters for brick and mortar were

taken from literature [Anthoine, 1995; Ma *et al.*, 2001] and are summarized in Table 3.2a. On the surface of REO_I and REO_II we have selected two characteristic points w1 and w2, at which we will observe changes in displacements and stresses for various cases of loads and meshes.

Table 3.3 Material parameters for brick and morta

Material	f_c	$E_x = E_y$	$\nu_x = \nu_y$	$G = E/2(1 + \nu)$
Brick	\approx	11000	0,2	4580
Mortar	\approx	220	0,2	88

Kucma's study have considered three load cases of imposed boundary displacements (section 3.6.3)

Distributions of stresses along characteristic cross-sections for various meshes are shown in Figs. 3.11 to 3.13. As can be observed, these solutions exhibit good convergence properties. All the graphs in Figs 3.14 to 3.16 correspond to the load case 2.

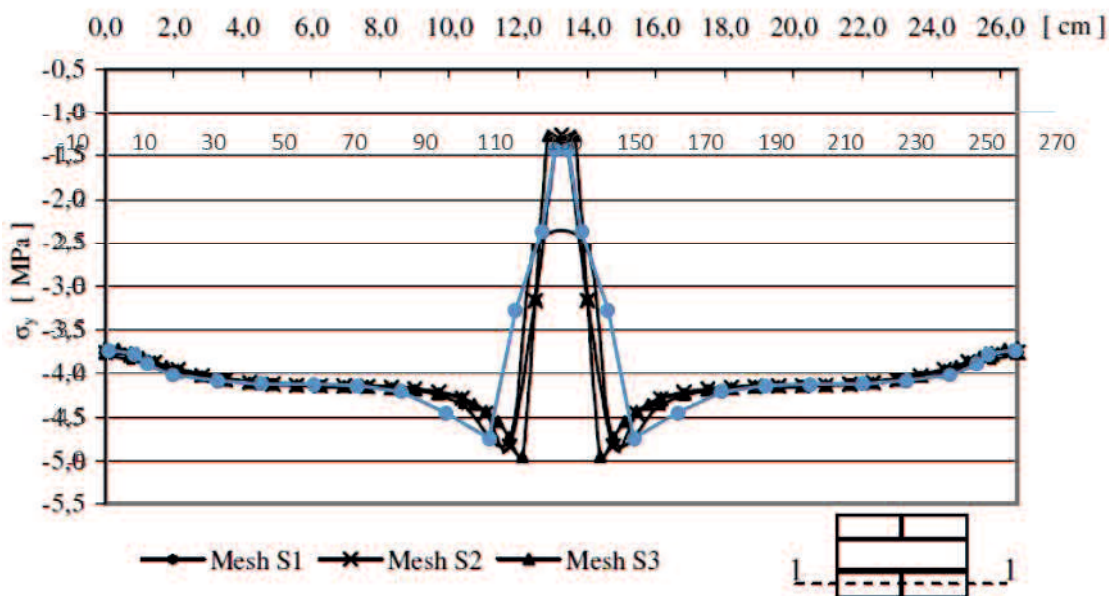


Figure 3.14 Stress σ_y in REO_I along section 1-1 for various meshes, load case 2

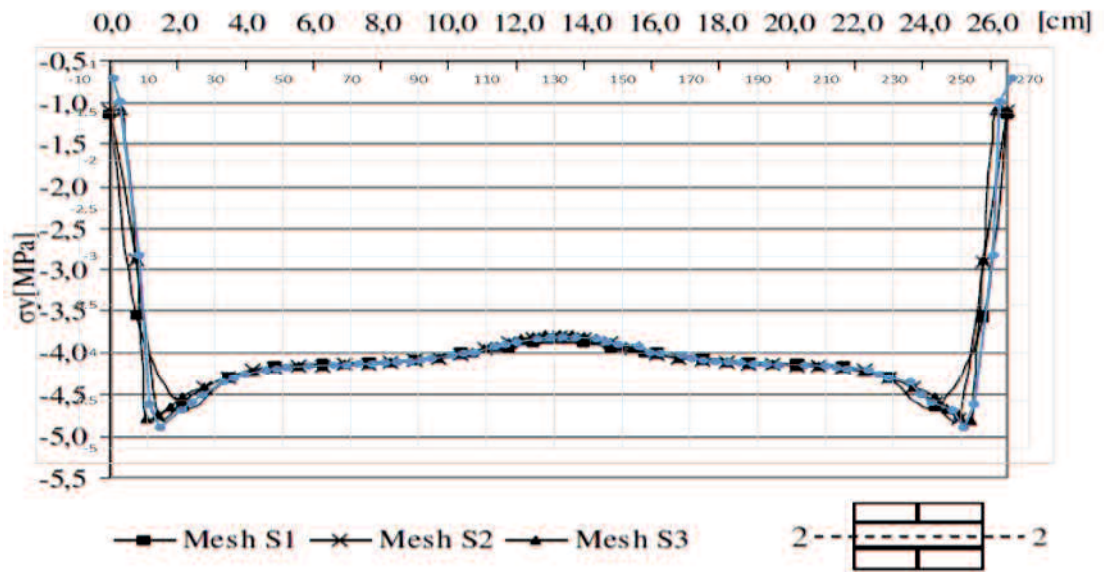


Figure 3.15 Stress σ_y in REO_I along section 2-2 for various meshes, load case 2

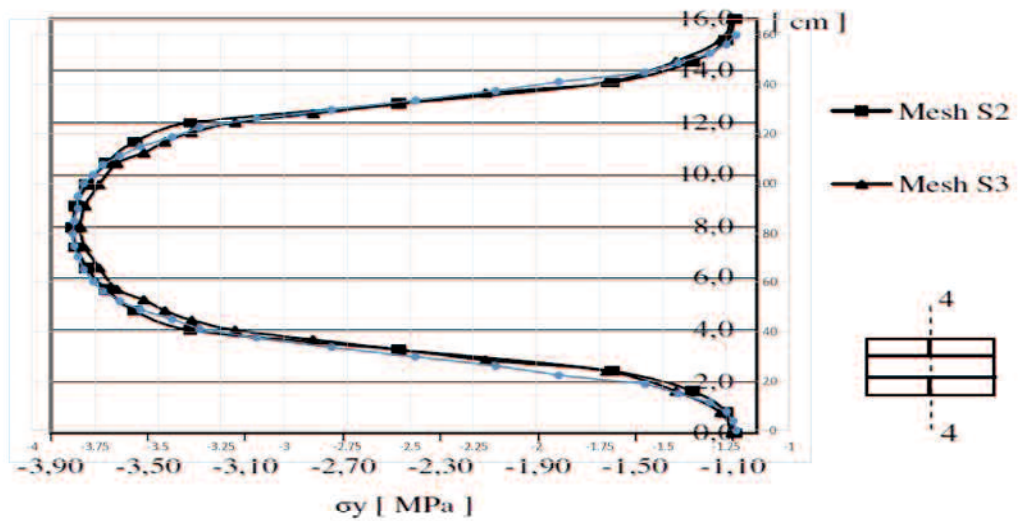


Figure 3.16 Stress σ_y in REO_I along section 4-4 for various meshes, load case 2

This pre-simulation (blue color) result looks quite acceptable when compared with the results of the Kucma's study. So, That for the next simulation process can be used the same model and methodology.

3.9. Results and discussion

3.9.1. Equivalent elastic modulus

In this study, the elasticity values of the brick are 1,000 MPa, 2,000 MPa, 5,000 MPa, and 10,000 MPa. The elasticity values of mortar are 0.2 to 5 times the elasticity of the brick. Poisson's ratio was assumed to be 0.25, where $\nu_x = \nu_y$. Each of these data was applied to every load case (RVE-1 and RVE-2).

The results of RVE1 and RVE2 calculations can be found in Appendix A

The elastic modulus of the mortar and brick are the main input data in the numerical simulation. The ratio of the elastic modulus of mortar to that of the brick is called the ratio of mortar (R_{mor}). The value of R_{mor} changes depending on the elasticity of both the materials, bricks and mortar, in the unit cell.

Additionally, the value of R_{mor} was also influenced by the dimensions of the two elements. The Indonesian code for masonry (SNI 15-2094-2000) regulates the dimensions of bricks with diverse sizes, which are 65 ± 2 to 80 ± 3 mm in height, 92 ± 2 to 110 ± 2 mm in width, and 190 ± 4 to 230 ± 5 mm in length. Changes in the thickness of either the brick or mortar affect the value of R_{mor} . Here, the thickness of the mortar is set to $t_m \leq 0.5h_b$, where h_b is the thickness of brick. Therefore, by using a mortar thickness of $0.5h_b$, the ratio of the volume of the mortar would reach its maximum value. It could reach up to 47 % if volume of mortar divided by RVE unit when the dimensions of bricks are $h_b = 65$ mm, $l_b = 250$ mm, and $w_b = 110$ mm.

The change in the volume ratio influences the stress–strain distribution in the unit cell. Therefore, it will affect the value of the Poisson's ratio and that of the equivalent elasticity of the masonry structure. Thus, for the case $E_{mor} > E_b$ or $R_{mor} > 1$, higher mortar elasticity increases the equivalent elastic modulus of the masonry structure.

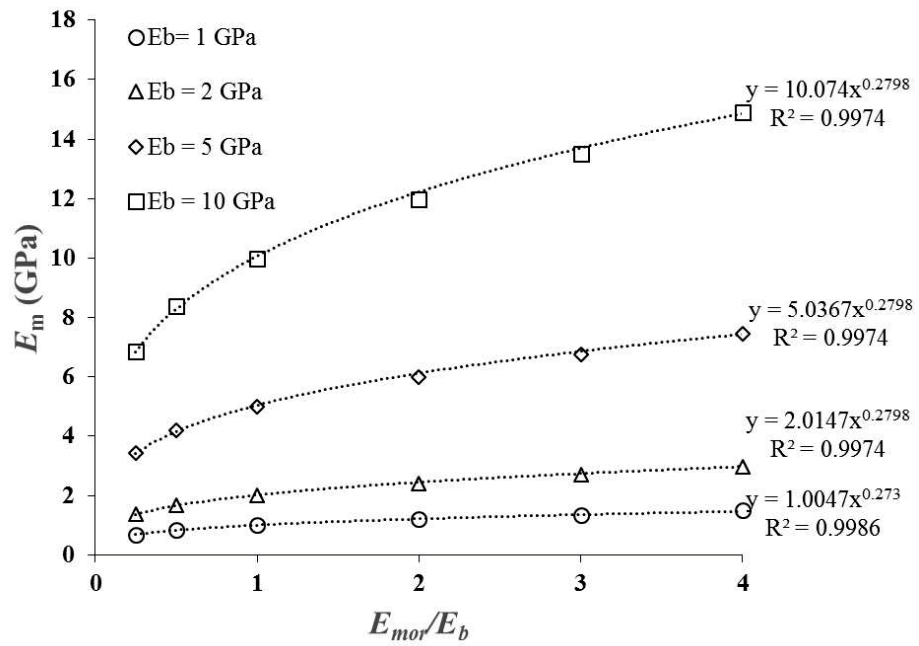


Figure 3.17 Simulation results of equivalent elastic moduli of brick masonry

Table 3.4 Homogenization model result from various researchers

Model (MPa)	\bar{E}_x	\bar{E}_y	$\bar{\nu}_x$	$\bar{\nu}_y$	$\bar{G}(0.4 \bar{E}_m)$
This Research					
RVE (B)	7882	6120	0.1600	0.2046	4520(2450)
RVE (A)	7882	6121	0.1604	0.2044	4441(2450)
Ma, <i>et al.</i> 2001					
	7899	6274	0.270	0.310	2884
Mistler, <i>et al.</i> 1992					
3D model	7958	6777	0.164	-	2583
2D Plane Stress	7882	6592	0.159	-	2682
2D generalized plane strain	7971	6811	0.165	-	2584
2D plane strain	8157	6963	0.194	-	2584
Wang, <i>et al.</i> , 2007					
FEM, Stack bond [Anthoine, 1995]	8530	6790	0.196	-	2580
FEM, running bond [Anthoine, 1995]	8620	6770	0.2	-	2620
Periodic model stack bond	8568	6850	0.191	-	2594
Periodic model stack bond	8574	6809	0.197	-	2620
Periodic model running bond	8574	6809	0.197	-	2620
Multilayer method [Pande <i>et al.</i> 1989]	8525	6906	0.208	-	2569
Wo-step method [Pietruszczak <i>et al.</i> 1992]	9,187	6,588	0.215	-	2658

Figure 3.17 shows the simulation results and regression curves between the R_{mor} and E_m where E_m is the equivalent elastic modulus of the masonry structure. It is remarkable that the coefficient of correlation is established at a value of 0.9974. The best equation of R_{mor} is power trend line with the power value is 0.2798. This value did not change for various E_b ; however, there is only a slight difference in the elasticity value of the brick. Based on the results, the proposed equations for the equivalent elastic modulus in the simulation are presented below:

$$E_m = E_b(R_{mor})^{\delta+\theta}, \quad (3.13)$$

where $R_{mor} = \frac{E_{mor}}{E_b}$.

The superscript δ denotes the geometric properties of the cells, and θ is a disparity value from the geometric properties to the ratio of the elastic modulus of mortar.

The value δ is given by the following equation:

$$\delta = 0.33 \left(\rho_{mor} + \bar{\nu} + \frac{t_m}{h_b} \right), \quad (3.14)$$

where ρ_{mor} is the volume ratio of mortar to the area of the cell, $\rho_{mor} = \frac{t_m(t_m+h_b+l_b)}{t_m(t_m+h_b+l_b)+(h_b l_b)}$; $\bar{\nu}$ is the average Poisson's ratio (brick and mortar); $\bar{\nu} = 0.5(\nu_{mor} + \nu_b)$; $\frac{t_m}{h_b}$ is the ratio of the thickness of the mortar to that of the brick

The disparity value θ can be calculated as follows:

If $R_{mor} > 1$, the following expression can be used:

$$\theta = 0.002(R_{mor}^2 + R_{mor} + 1). \quad (3.15)$$

If $R_{mor} < 1$, the following expression can be used:

$$\theta = 0.002 \left(\left(\frac{1}{R_{mor}} \right)^2 + \frac{1}{R_{mor}} + 1 \right). \quad (3.16)$$

The simulation results obtained from using this formula are suitable for cases of ratios from 0.2 to 5.0. Figure 3.14 shows simulation results using brick elasticity values of 1, 2, 5, and 10 GPa. The result confirms that the elasticity of the masonry structure increases in accordance with the mortar ratio R_{mor} . Figure 3.12 also shows that the the gradient of each curve is different for each R_{mor} .

The percentage of change (Poc) was applied to quantify the changes of gradient in each curve. The Poc is an index of how much a quantity has increased or decreased with respect to the original amount. Therefore, the Poc can be obtained from the Eq. (3.17).

$$Poc = \frac{E_m - E_b}{E_b} 100\% \quad (3.17)$$

Table 3.5 provides the percentage of change for the curves in Fig. 3.14, where for any change in R_{mor} for each E_b , it remains the same. To obtain the equivalent elastic modulus of the masonry structure with a different gradient, Eq. (3.18) can be employed:

$$E_{m,(poc)} = E_b(1 + Poc). \quad (3.18)$$

Table 3.5 Percentage of change of simulation

E_b (MPa)	Percentage of change (Poc) %					
	R_{mor}					
	0.25	0.5	1	2	3	4
1000	-31.42	-15.98	0	19.62	35.05	61.98
2000	-31.42	-15.98	0	19.62	35.05	61.98
5000	-31.42	-15.98	0	19.62	35.05	61.98
10000	-31.42	-15.98	0	19.62	35.05	61.98

This illustrates that the elasticity of the masonry structure will increase linearly with an increase in R_{mor} for each E_b . Table 3.6 lists some examples of E_m . The results indicate that the gradient for each value of E_b and R_{mor} is different, but at the same R_{mor} , the Poc is the same. This indicates that an increase in the R_{mor} value influences the stress distribution of the elements in the cells and increases the equivalent elastic modulus of the masonry structure. Conversely, a decrease in the

elasticity of mortar would minimize the equivalent elastic modulus of the masonry structure. From the above discussion, we can conclude that it is beneficial to increase the elasticity of the bricks if the elasticity of mortar is higher than the elasticity of the bricks.

Table 3.6 Examples of the calculations E_m .

Case	R_{mor}	Poc (%)	E_b (MPa)	Calculation $E_m = E_b \times (1 + Poc\%)$ MPa
$R_{mor} > 1$	4	61.98	1000	1620
			2000	3240
			5000	8099
			10000	1698
	3	35.05	1000	1351
			2000	2701
			5000	6753
			10000	13505
	2	19.62	1000	1196
			2000	2392
			5000	5981
			10000	11962
$R_{mor} < 1$	0.5	-15.98	1000	840
			2000	1680
			5000	4201
			10000	8402
	0.25	-31.42	1000	686
			2000	1372
			5000	3429
			10000	6858

3.9.2. Poisson's ratio and shear modulus

Poisson's Ratio describes the transverse strain; therefore, it is obviously related to shear. The Shear Modulus, usually abbreviated as G , plays the same role in describing shear as the Young's Modulus does in describing the longitudinal strain. It is defined as $G = \text{shear stress}/\text{shear strain}$.

The shear modulus G can be calculated in terms of E and ν : $G = E/2(1 + \nu)$. As ν ranges from 1/4 to 1/3 for most rocks, therefore that G is approximately calculated as $0.4E$.

The average Poisson's ratio decreased linearly as the R_{mor} value increased. The equivalent Poisson's ratio can be expressed as follows:

if $R_{mor} < 1$, the following expression can be used :

$$\bar{\nu}_m = \bar{\nu} - 0.01\left(\frac{1}{R_{mor}}\right); \quad (3.19)$$

if $R_{mor} > 1$, the following expression can be used:

$$\bar{\nu}_m = \bar{\nu} - 0.01R_{mor} \quad . \quad (3.20)$$

The Poisson's ratio of the masonry structure decreased by approximately 0.01 times the R_{mor} value owing to the assumption that the Poisson's ratio of the brick is smaller than that of mortar.(Fig. 3.18)

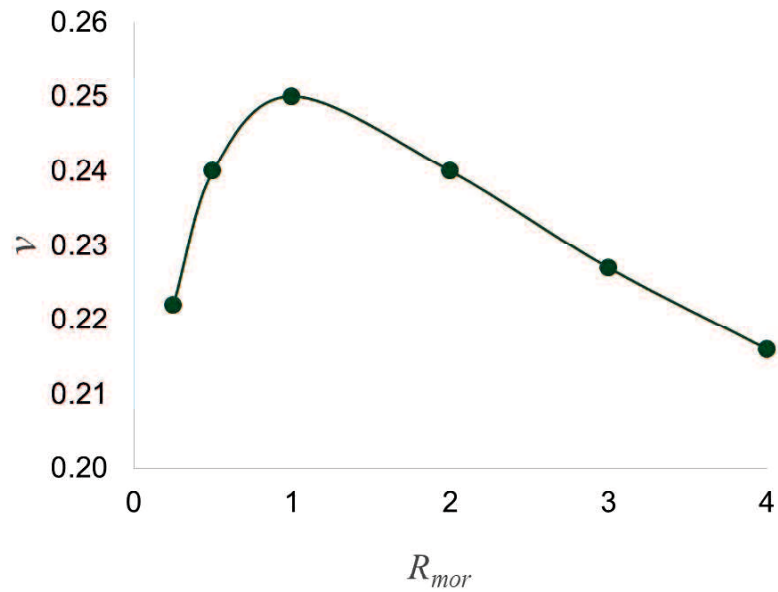


Figure 3.18 Degradation of Poisson's ratio

In present study, the shear modulus was obtained from the simulation results using Eq. (12). The range of the estimated G was 60–70 % of E_m because of the lower Poisson's ratio estimated in the simulation.

The vertical deformation (y direction) and the lateral deformation (x direction) are different owing to Poisson's effect. The effect may lead to the increase of the equivalent \bar{G} . Using Eqs. (3.19) and (3.20), the equivalent shear modulus \bar{G} can be expressed as in Eq. (3.21).

$$\bar{G} = \frac{E_m}{1.3(1+\bar{\nu})} \quad (3.21)$$

3.10. Verification and validation

The numerical simulation results were compared to the results of the simulation conducted by Wang *et al.* [2007], Ma *et al.* [2001], and Mistler *et al.* [2007], as given in Table 3.3. It is evident that the 2D plane stress analysis results reported by Mistler *et al.* [2007] are similar to those in the present work.

However, \bar{E}_y , $\bar{\nu}_y$, and \bar{G} present slight differences because the input data used were different. It should be noted that the average horizontal elastic modulus of the masonry structure was greater than that in the vertical direction. The calculated average value of the equivalent elasticity agreed very well with the experimental data obtained by Mistler *et al.* [2007] on the 2D plane stress, and by Ma *et al.* [2001]. By employing the same input data, listed in Table 3.2, the value of \bar{E}_x is equal to Mistler's result and slightly different from Ma's result. The differences in the results value range is 7.5 % while the value of Poisson's ratio ν_x is relatively similar. The value of G is different and is slightly increase, because of the diminution of the Poisson's ratio value.

3.11. Formula comparison

In the previous investigations, many formulae have been proposed for the determination of material parameters. These formulae addressed to isotropic materials. Zavalis *et al.* [2014] have cited some formulas developed by Matysek [1999] (such as Eq. (3.22)), Brooks [1999] (Eq. (3.23)), and Ciesielski [1999] (Eq. (3.24)). However, they were originally derived to be used in the modeling of masonry structures. It is noteworthy that the values of elastic moduli obtained from other researchers are similar to the results obtained in the numerical simulations reported in the present study.

$$E_m = \frac{1.25\xi+1}{1.25\xi+\beta} E_b, \quad (3.22)$$

where ξ is the ratio of the height of bricks to the thickness of the mortar joints, and β is the ratio of brick's elastic modulus to that of the mortar.

$$\frac{1}{E_m} = \frac{0.86}{E_b} + \frac{0.14}{E_{mor}}, \quad (3.23)$$

where E_b and E_{mor} are the elastic moduli of the bricks and mortar, respectively.

$$E_m^i = \frac{1.20E_b^i E_{mor}^i}{0.2E_b^i + E_{mor}^i}, \quad (3.24)$$

where E_b^i and E_{mor}^i are the medium elastic moduli of the brick and mortar in section i , respectively.

The equivalent elasticities (E_m) estimated through the proposed formula were compared to the modulus derived from the previous formulae, Eqs. (3.22)–(3.24). Figure 3.19 shows that these previous formulae underestimate the equivalent elasticity of the masonry structures with low-modulus bricks. It is noteworthy that the proposed formula is applicable for the elasticity ratio of $R_{mor} < 1$.

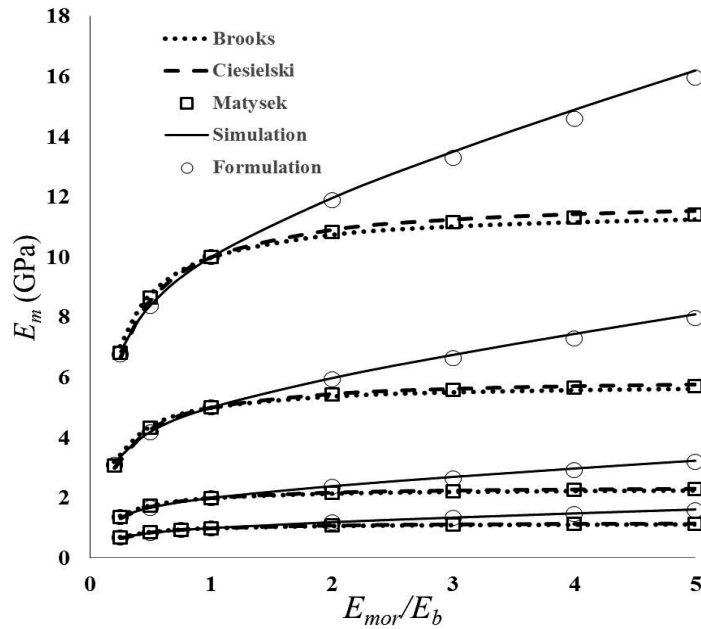


Figure 3.19 Equivalent elasticity of brick masonry

Equations (3.22)–(3.24) have a *Poc* behavior similar to that of the simulation results (Table 3.5). There same percentage of change can be observed for any E_b , as presented in Table 3.7 However, there are differences for the case of $R_{mor} > 1$. By using Eqs. (22)–(24), when $R_{mor} = 2$, the E_m value has only increased by approximately 7.53 % to 9.09 % and for $R_{mor} = 5$, the E_m value has increased by approximately 12.6 % to 15.38 %. For the case of $R_{mor} = 2$, E_m increased by approximately 19.48–19.79 %, and when $R_{mor} = 5$, E_m increased by approximately 61.68–62.71 %.

For $R_{mor} < 1$, the *Poc* presents similar values between the proposed and the previous formulae, particularly with the Ciesielsky and Matysek formula; however, there was a slight difference with respect to the Brooks formula. This indicates that for the case of $R_{mor} < 1$, the proposed formula can be used as well.

Any increase in the ratio of mortar increased the elasticity of masonry. This is consistent with the data obtained by Drougkas *et al.* [2015], and Gumaste *et al.* [2006] which also examined the $E_{mor} > E_b$ case as shown in Table 3.7

Table 3.7 Percentage of change of formula comparison

		Percentage of change (Poc) %						
Ref.	E_b (MPa)	R_{mor}						
		0.25	0.50	1.00	2.00	3.00	4.00	5.00
Brooks	1000	-29.58	-12.28	0.00	7.53	10.29	11.73	12.61
Ciesielski		-33.33	-14.29	0.00	9.09	12.50	14.29	15.38
Matysek		-31.86	-13.48	0.00	8.45	11.59	13.24	14.24
Simulation		-31.41	-16.00	0.00	19.48	34.85	48.68	61.68
Formulation		-33.34	-16.99	0.00	19.79	34.60	48.34	62.71
Brooks	2000	-29.58	-12.28	0.00	7.53	10.29	11.73	12.61
Ciesielski		-33.33	-14.29	0.00	9.09	12.50	14.29	15.38
Matysek		-31.86	-13.48	0.00	8.45	11.59	13.24	14.24
Simulation		-31.43	-15.98	0.00	19.62	35.05	48.94	61.98
Formulation		-33.34	-16.99	0.00	19.79	34.60	48.34	62.71
Brooks	5000	-29.58	-12.28	0.00	7.53	10.29	11.73	12.61
Ciesielski		-33.33	-14.29	0.00	9.09	12.50	14.29	15.38
Matysek		-31.86	-13.48	0.00	8.45	11.59	13.24	14.24
Simulation		-31.60	-15.98	0.00	19.62	35.05	48.94	61.98
Formulation		-32.23	-16.99	0.00	19.79	34.60	48.34	62.71
Brooks	10000	-29.58	-12.28	0.00	7.53	10.29	11.73	12.61
Ciesielski		-33.33	-14.29	0.00	9.09	12.50	14.29	15.38
Matysek		-31.86	-13.48	0.00	8.45	11.59	13.24	14.24
Simulation		-31.43	-15.98	0.00	19.65	35.05	48.93	61.98
Formulation		-33.34	-16.99	0.00	19.79	34.60	48.34	62.71

Table 3.9 and Fig. 3.19 illustrate the comparison results of the equivalent elastic moduli based on data obtained by Gumaste *et al.* [2006] (see Table 3.8). Table 3.8 and Fig. 3.20 also demonstrate a comparison between the equivalent

elastic moduli results derived from the proposed formula to those derived from the formulas proposed by Gumaste, Brooks, Matystek, and Ciesielsky.

Results from the Gumaste formula were almost similar to the simulation, the difference was lower than 1 %. On the other hand, the estimation using the proposed formula was 3–8 % higher than the results of Ciesielski, Eq. (22), Brooks, Eq. (23), and Matystek, Eq. (24). Although numerical values obtained by Gumaste were very similar to those of the proposed formula, the experimental research is still required. To compensate for the lower brick strength in some countries, such as Indonesia and India, the proposed formula resulting from the investigation could be employed. The formula is appropriate for the calculation of the variable elasticity of low-quality masonry structures. In addition, the proposed formula is suitable for numerical applications on further large-scale masonry structures.

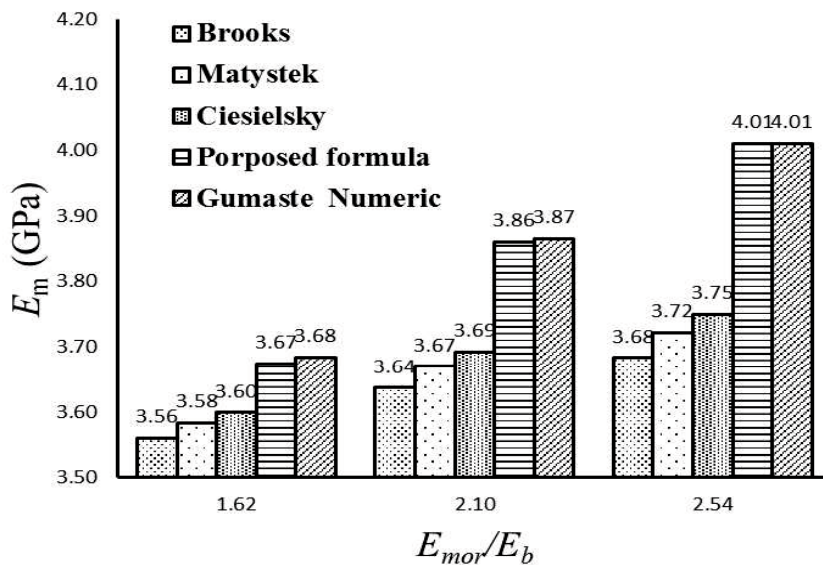


Figure 3.20 Comparison of equivalent elastic moduli based on Gumaste data ($E_{mor} > E_b$).

Table 3.8 Gumaste data and experiment and numerical results

Ref.	Data								Results	
	E_b (MPa)	E_{mor} (MPa)	ν_b	ν_{mor}	h_b (mm)	l_b (mm)	t_b (mm)	t_{mor} (mm)	E_{ex} (MPa)	E_{num} (MPa)
Gumaste <i>et al.</i> [2013]	3370	8570	0.15	0.2	75	230	105	12	3317	4005
	3370	5450	0.15	0.2	75	230	105	12	3789	3684
	3370	7080	0.15	0.2	75	230	105	12	3677	3865

Table 3.9 Comparison of Equivalent elastic moduli based on Gumaste data ($E_{mor} > E_b$)

E_{mor}/E_b	Numeric		Formula		
	Gumaste	Porposed	Brooks	Matystek	Ciesielsky
1.62	3.68	3.67	3.56	3.58	3.60
2.10	3.87	3.86	3.64	3.67	3.69
2.54	4.01	4.01	3.68	3.72	3.75

3.12. Summary

Most of the design formulae for calculating the equivalent elasticity of brick masonry structures are applicable only for the case where $E_{mor} < E_b$. The present study was focused on masonry structures with low-quality bricks, i.e. $E_{mor} > E_b$. This paper presented numerical simulations to derive formulas for the equivalent elasticity of brick masonry structures. The accuracy of the formulas was discussed and verified by using experimental secondary data. The equivalent elasticity obtained using the newly developed formulas was estimated with high accuracy, resulting in a discrepancy of less than 1 % compared to the numerical results derived by Gumaste.

CHAPTER 4. NEW METHOD FOR ESTIMATION OF OUT-OF-PLANE STRENGTH OF MASONRY WALLS

4.1. Outline

This chapter proposes a method called the fictitious truss method (FTM). Here the truss method is used to determine the ability of masonry structures to withstand a lateral load within their elastic deformation capacities and introduces a two-dimensional linear static model for masonry walls. The background of FTM model selection is rarely used to analyze a masonry wall, especially a masonry wall under a load in the out-of-plane direction.

The FTM model represents the effect of flexural interaction by computing the stress and strain in the axial direction within the material and by considering

uniaxial force effects on masonry elements. Pressure is applied to the surface area of the wall sequentially to predict the ultimate tension and compression cracking.

FTM modeling is validated using previously obtained results for confined and unconfined masonry walls and for reinforced and unreinforced masonry walls. The FTM is a reliable method of assessing the out-of-plane strength of masonry structures owing to its conceptual accuracy, simplicity, and computational efficiency.

4.2. Some proposed methods for analyzing masonry structure

Many theories have been proposed to investigate the strength and behavior of masonry structures in the out-of-plane direction, as shown in Table 4.1. However, these theories are based on and limited to certain experimental configurations. Most studies on the out-of-plane behavior of masonry walls have been experimental works and thus time-consuming and expensive [Noor-E-Khuda *et al.*, 2016]. It has been concluded that the method that most accurately predicts the out-of-plane strength of confined walls is the bidirectional strut method. This method is an iterative procedure based on two-way arching action.

The present study proposes a new method of using a truss as a structural element of a masonry wall in order to analyze the out-of-plane strength of a masonry structure. The aim of present study is a model oriented to the determination of out of-plane resistance. The proposed fictitious truss method (FTM) provides practitioners and academics with analytical results and can be modified for a variety of masonry walls.

Table 4.1 Methods of analyzing masonry structures under out-of-plane loading

Analysis Method		Reference.
Yield line method	unreinforced wall	[Drysdale <i>et al.</i> 1988],[Martini <i>et al.</i> 1997]
	reinforced wall	[Zhang <i>et al.</i> 2001]
	confined wall	[Varela-Rivera <i>et al.</i> 2011, Varela-Rivera <i>et al.</i> 2012a, Varela-Rivera <i>et al.</i> 2012b]
The failure line method	unreinforced wall	[Drysdale <i>et al.</i> 1988]
	unconfined wall	[Varela-Rivera <i>et al.</i> 2011, Varela-Rivera <i>et al.</i> 2012a, Varela-Rivera <i>et al.</i> 2012b]
The modified yielding line method	surrounded by steel frame	Dawe and Seah [Dawe <i>et al.</i> 1989] it cited from [Moreno-Herrera <i>et al.</i> 2016]]
The compressive strut method	confined wall	[Varela-Rivera <i>et al.</i> 2011, Varela-Rivera <i>et al.</i> 2012a]
	infill walls	[6]
The spring-strut and the bidirectional strut method	confined walls	[Varela-Rivera <i>et al.</i> 2011, Varela-Rivera <i>et al.</i> 2012a, Varela-Rivera <i>et al.</i> 2012b, Moreno-Herrera <i>et al.</i> 2016]

The truss model is rarely used in calculations for a masonry wall structures, but several truss models have been extensively used for analysis of the nonlinear behavior of masonry infills. A truss model for masonry structures was proposed by Lu *et al.* [2014] in research on a nonplanar reinforced concrete wall. Recently, Moharrami *et al.* [2015] used the truss model for the analysis of masonry structures employing nonlinear truss modeling, which was used in the analysis of shear failure in the in-plane direction of the wall.

4.3. Overview of out-of-plane strength of masonry structure

The masonry wall is widely used for its low cost in low-rise construction in various countries. Additionally, a ring beam around a masonry structure (confined masonry) wall is recommended for the prevention of injuries and casualties that might occur in the unexpected collapse of a masonry wall. One form of masonry wall collapse is due to loading in the out-of-plane direction, which can occur, for example, in an earthquake or a flood. However, there is no indication that many masonry walls have collapsed under wind pressure after the completion of their construction [Drysdale *et al.* 1988], which can be considered evidence of the adequacy of their construction.

There is a connection between walls and reinforced concrete, given the different deformations of the two materials in response to loading. This is strongly dependent on the type of masonry used for infill. Masonry can be built using different kinds of units (e.g., solid or hollow), unit materials (e.g., clay or concrete), and mortar, depending on the region. The infill wall and the confinement are usually connected with mortar (unreinforced masonry) using an anchor and reinforcement (reinforced masonry).

Research on out-of-plane loading has included experiments and theoretical analysis using different analytical methods, but there has been far less research on out-of-plane loading of masonry walls than on in-plane loading of masonry walls. Some experimental studies have been performed on out-of-plane behavior of masonry reinforced walls [Noor-E-Khuda *et al.* 2016, Gilstrap *et al.* 1998, Zhang *et al.* 2001], unreinforced masonry walls [Drysdale *et al.* 1988, Griffith *et al.* 2007],

infill masonry walls [Abrams *et al.* 1996, Henderson *et al.* 2003, Tu *et al.* 2010] and confined masonry walls [Varela-Rivera *et al.* 2011, Varela-Rivera *et al.* 2012a, Varela-Rivera *et al.* 2012b]. Based on these studies the main variables that affect the out-of-plane behavior of masonry walls are the aspect ratio (height divided by length), wall support conditions, wall slenderness ratio (height divided by thickness), axial load, in-plane stiffness of surrounding elements, wall openings, and unit type. Moreover, the out-of-plane behavior of confined walls is different than that observed for unreinforced, reinforced, and infill walls. The difference is mainly associated with construction procedures and wall reinforcement details. The differences between infill and confined walls are as follows. Firstly, confined walls consist of unreinforced panels surrounded by flexible reinforced concrete confining elements. The wall panels are constructed first, and later the confining elements are constructed. Infill walls consist of unreinforced or reinforced masonry walls surrounded by stiff concrete or structural steel frames [Moreno-Herrera *et al.* 2012]. The frames are constructed first, and later the masonry panels are constructed. This type of construction causes gaps between the frames and the masonry panels. Construction gaps delay the formation of arching action [Abrams *et al.* 1996, Dawe *et al.* 1989].

The aspect ratio and slenderness ratio [Drysdale *et al.*, 1988; Varela-Rivera *et al.*, 2012a; Moreno-Herrera *et al.*, 2012; Agnihotri *et al.* 2013] have been shown to affect the strength of unreinforced masonry (URM). Some researchers have used finite element (FE) theory and software to analyze masonry walls under out-of-plane loading. Drysdale *et al.* [1988] used FE elastic plate analysis, Noor-E-Khuda *et al.* [2016] used the explicit FE method and a layered shell model, and La-Mendola

et al. [2014] and Milani *et al.* [2013] used commercial FE software. The FE method is very helpful, but it is complex and requires considerable cost.

On the other hand, numerical modeling of the out-of-plane response of infill frames was reviewed by Asteris *et al.* [2017], whose in-depth literature review included some models of out-of-plane responses for infill frames. There are flexural-action-based models and arching-action-based models.

Cavalery *et al.* [2009] investigated modeling of the out-of-plane behavior of masonry walls. This investigation concluded that the responses of compressed sections were related to the moment of curvature of the masonry. Two types of masonry walls were used: calcarenite and clay brick. The flexural responses of masonry cross sections were determined using a numerical procedure, including nonlinearity owing to the $\sigma - \varepsilon$ law in compression and the assumption of limit-tension material.

Some researchers have also investigated near-surface-mount-reinforced masonry walls. [La-Mendola *et al.* 2014; Dizhur *et al.* 2014; Willis *et al.* 2010, Anil *et al.* 2012; Ismail *et al.* 2016]. They used fiber-reinforced polymer (FRP), carbon-fiber-reinforced polymer (CFRP) strips, and polymer-textile-reinforced mortar to reinforce a masonry wall. These materials are used to improve the out-of-plane performance of a URM wall. Near-surface-mount-reinforced masonry walls are very helpful in increasing the strength of masonry but are strongly affected by the type of reinforcement used.

URM panels in reinforced concrete frames were investigated by Tu *et al.* [2010] and Furtado *et al.* [2016]. Tu *et al.* [2010] investigated the out-of-plane behavior of URM walls in shaking table tests. They used an analytical model for analysis. Furtado *et al.* evaluated the combination of in-plane and out-of-plane behaviors by comparing two infill masonry walls subjected to monotonic out-of-plane loading and cyclic out-of-plane loading.

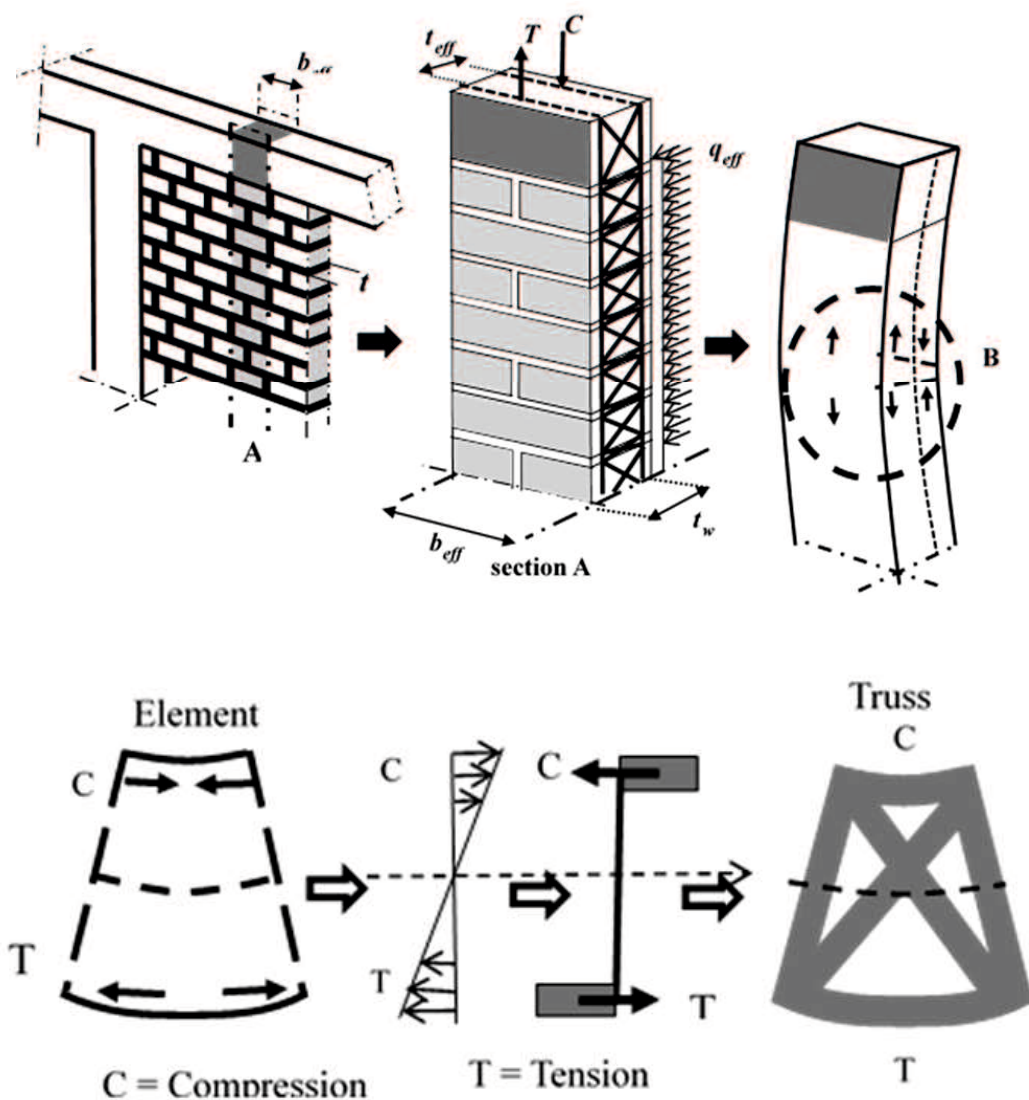


Figure 4.1 Establishing truss blocks and configuring the truss structure [Ridwan *et al.* 2017]

4.4. Material and Methods

The FTM creates patterns of stress distribution in a flexural element structure. The geometry of the FTM is obtained by centralizing and simplifying the force acting on a wall. The elements establish truss blocks and then configure the truss structure as indicated in Fig. 4. 1.

4.4.1. Determination of truss geometry

A truss model requires cross-sectional dimensions and determination of the geometry of truss elements as well as applicable material models. The first step is establishing the dimensions of the truss and of the truss elements considering the real dimensions of the masonry structure. In the cross section of the masonry structure, t_w is the thickness of the masonry and is not directly used in the FTM models.

The FTM makes the following assumptions. The thickness of the masonry wall is the initial height of the truss model (t_w). The effective cross section of the truss element is a square shape ($a \times b_{eff}$), the cross section is the effective area of compression stress in a flexural beam, the aspect ratio is less than one (i.e., $H/L < 1$), and the truss is fictitious. The truss can be calculated as a numerical value until early fracture, and buckling can be ignored. If reinforcement is used, its arrangement must be regular.

The shape of the truss model is shown in Fig. 4.2. There are three types of shapes: v_t is a vertical truss, h_t is a horizontal truss, and d_t is a diagonal truss. A diagonal truss can be a single diagonal or double diagonal truss.

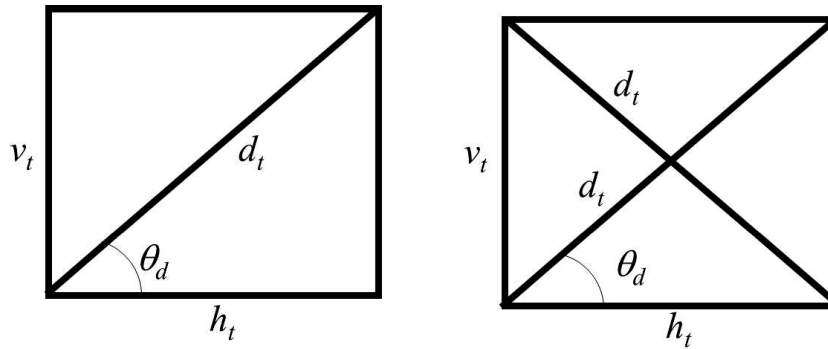


Figure 4.2 Truss shapes

The truss geometry defines the geometry of the vertical cross section of the brick and determines the height of the masonry wall. Each block truss is the representative geometry of the brick and mortar. The height of the truss (v_t) is the effective width of a cross section of the masonry wall (t_{eff}), while the width (h_t) of the truss is the effective thickness of the mortar or unit masonry. b_{eff} is the width of the unit load to be used. t_{eff} is obtained from the equivalent inertia of the effective cross section, as shown in Fig. 4.3 and by solving equation (4.1) below:

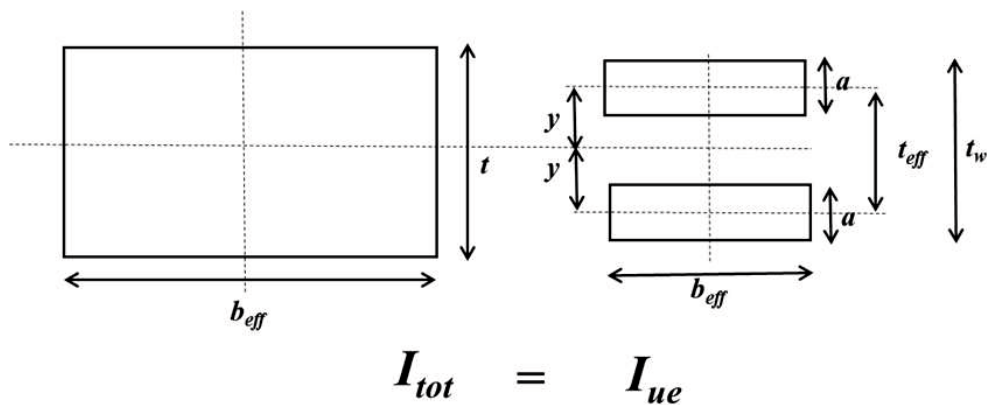


Figure 4.3 Equivalent inertia of the effective cross section

$$I_{tot} = I_{ue}, \quad (4.1)$$

where $I_{tot} = \frac{1}{12} b_{eff} t^3$ and I_{ue} is the inertia unit equivalent of the masonry element which can be solved with the provision that $A_1 = A_2$ and the equation

$$I_{eq} = \sum_1^n I_n + \sum_1^n (A_n y_n^2) \quad (4.2)$$

y is thus obtained if $n = 2$ as

$$y = \sqrt{\frac{I_{tot} - 2I_n}{2A_n}}. \quad (4.3)$$

The result is that t_{eff} is $2y$

The total height of the vertical truss elements is $t_w = 2y + a$; however, the height used in the analysis (t_{eff}) is $2y$ as indicated in Fig. 4.3. Figure 4.4 shows the determination of the effective height of a truss element that has parameters for the equivalent stress of the block parameter.

The total stress area in compression is $A_c = a b_{eff}$. In accordance with SNI 03-2847-2013, the depth of the equivalent stress block (a) is obtained as $a = \beta_l c$, where c is the distance from the center of mass to the top and $\beta_l = 0.85$. β_l is a function of the strength class of materials: $\beta_l = 0.85$ for $f'_{me} < 30$ MPa, and is reduced by 0.008 for every increase of 1 MPa in compressive strength; it should not be less than 0.65. Therefore, $a = 0.85c$ and $\alpha = 1$ for actual compressive strength, and 0.85 for the compressive strength equivalent. b_{eff} is the length of the brick or the length of the effective area of pressure used as the effective width. $A_c = A_t = a b_{eff}$ is used for a masonry wall without reinforcement and $A_t = A_r$ is used for a

masonry wall with reinforcement, where A_t is the area of tension, A_c is the area of compression, and A_r is the area of reinforcement. Typical cross-sectional dimensions used in the FTM are shown in Fig. 4.1.

The geometric dimension of the mortar part is the same for the brick and unit parts. The material parameters should be set according to the properties of each material, and the material modeling assumption in tension and compression is isotropic, linear, elastic material. An elastic material may show linear or nonlinear behavior. In this study, we assume linear behavior. For linear elastic materials, stresses are linearly proportional to strains ($\sigma = E\varepsilon$) as described by Hooke's law. The law is applicable for material properties that are independent of coordinates (homogeneous) and material properties that are independent of the rotation of the axes at any point in a body or structure (isotropic materials). Here only two elastic constants (modulus of elasticity E and Poisson's ratio ν) are needed for linear elastic materials.

The FTM can be used to determine the strength of a confined or unconfined masonry structure in the out-of-plane direction

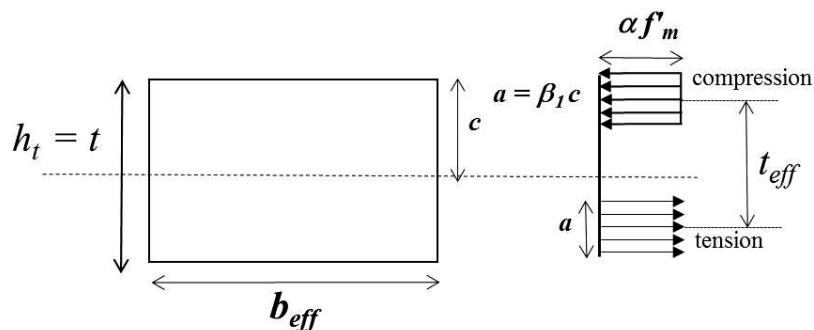


Figure 4.4 Determination of the effective height of a truss element

4.4.2. Schematic of the FTM

The FTM determines the out-of-plane strength of a masonry wall structure and involves the following steps:

- Check that the aspect ratio (H/L) of the masonry structure is less than 1.0.
- Provide material properties including the elasticity, specific gravity, Poisson's ratio, compressive strength, tensile strength, and others.
- Determine the widely assumed pressure area (b_{eff}).
- Determine the effective height of the element truss ($a = \beta_1 c$).
- Arrange $A_c = A_t = a b_{eff}$ to obtain y (Eqs. 1, 2, 3).
- Determine the effective thickness of the truss structure $t_{eff} = 2y$.
- Obtain the model and its dimensions by determining the boundary conditions of the masonry structure.
- Analyze the FTM structure to obtain the element truss force.
- Apply the load (P_{eq}) gradually until there is cracking in areas of tension and compression.

All loads are applied as concentrated equivalent loads acting on the truss joints. The FTM is schematically shown in Fig. 4.5 and Appendix B

The FTM may not be applicable physically, but it can be performed numerically. The element truss force can be analyzed using classical mechanics methods, other methods typically used to calculate truss structures, or using FE software. After determining the truss element and truss structure, the loading can be applied gradually while checking the strain in compression and the tension truss element condition.

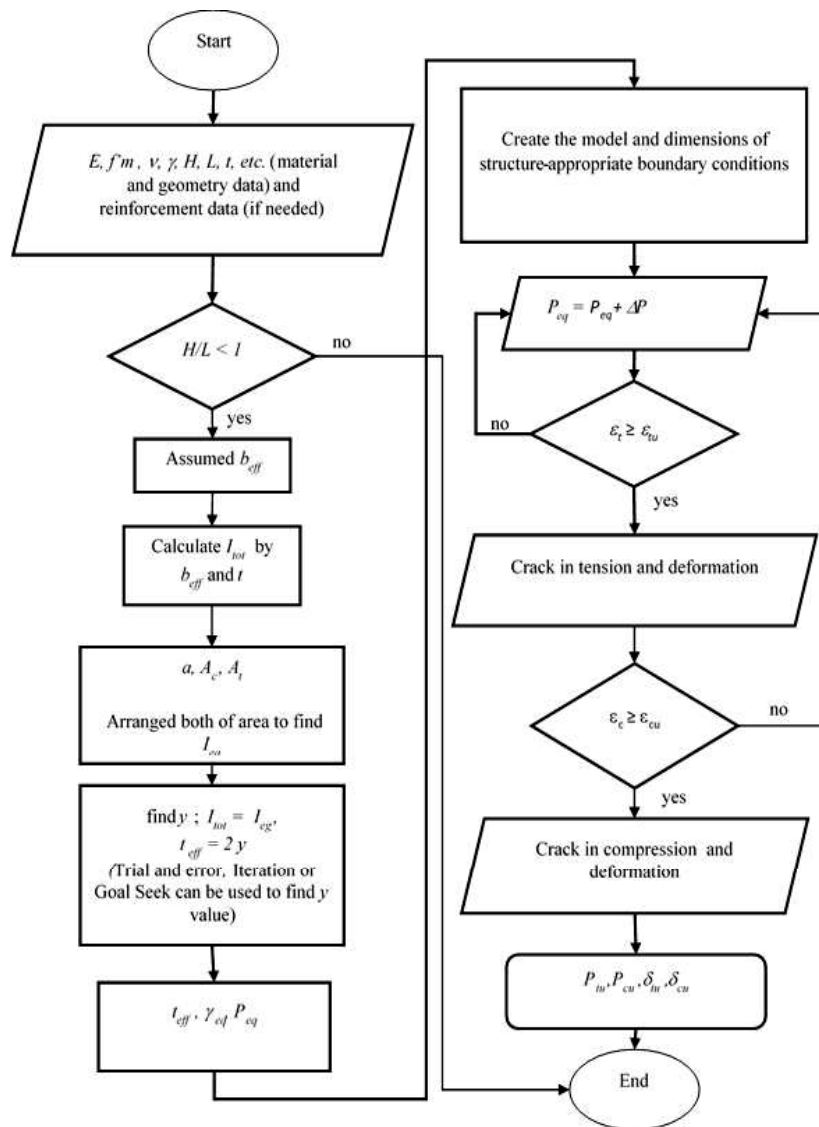


Figure 4.5 Schematic of the proposed FTM

4.4.3. Material models

The stress–strain relationship of truss elements representing masonry walls is shown in **Fig. 4.6**. The tensile strength and compressive strength of the mortar and the units are interconnected. In the present study, the vertical and horizontal truss elements are the studied variables while the diagonal truss element distributes forces to the vertical and horizontal truss elements.

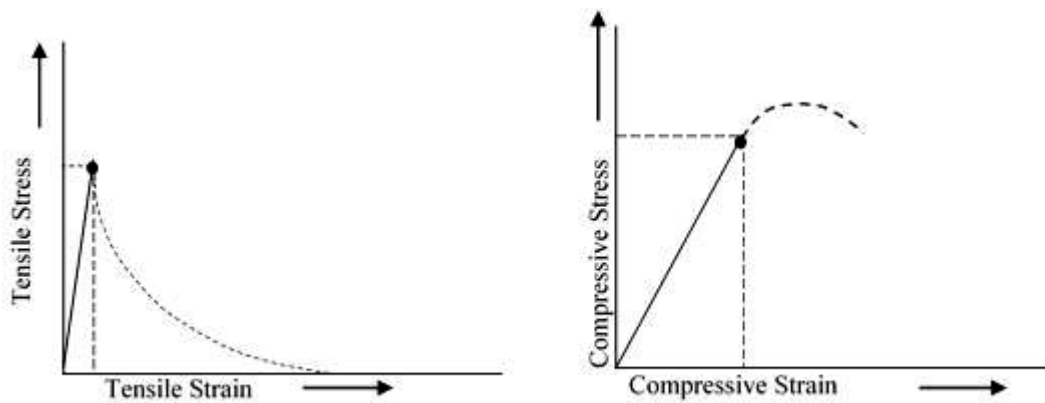


Figure 4.6 Stress–strain relationship of truss elements representing masonry walls

The material model of masonry is linear and elastic for brittle material; likewise for units and mortar. The failure criterion of the FTM model is the maximum principal strain by uniaxial loading on a truss member. The Hooke's law concept $\varepsilon = \frac{\sigma}{E}$ can be applied to predict when either of the principal strains resulting from the principal stresses ($\sigma_{1,2}$) meets or exceeds the maximum strain corresponding to the yield strength (σ_y) of the material in uniaxial tension or compression.

The FTM requires the force acting on a truss element to be in the critical region of the mid-span of the truss structure, where there is tension and compression on either side. Tension and compression may occur in mortar and brick in structural elements. It is therefore necessary to choose either brick or mortar as the material when determining the strength of masonry structures.

Almeida *et al.* [26] investigated hollow bricks and the brick–mortar interfaces under uniaxial tension for hollow bricks sourced from Portugal and Spain. Testing various brick types revealed a similar uniaxial response in tension and compression (Fig. 4. 6). Figure 4.6a shows the relationship between tension stress and strain. Stress increases linearly to a peak value before gradually and nonlinearly decreasing. The present paper focuses only on the behavior until the peak tensile load is reached. The same behavior is seen for both raw materials and materials such as FRP, CFRP, and steel. Almeida *et al.* [2002] found that elongation values for hollow brick obtained with different peak tensile loads ranged from 3 to 10 μ while those for mortar were less than 5 μ . The tensile stress values ranged over 2.75–3.82 and 1.93–2.25 N/mm², respectively, for the hollow brick and mortar. In the present study, the tensile stress was assumed to be 3 and 2 N/mm², respectively, for the hollow brick and mortar, and the tensile strain was assumed to be 0.001. Figure 4.6b shows the relationship between compression stress and strain.

Kaushik *et al.* [2007] found cracking at strain values from 0.0023 to 0.00375. Based on these data, the present study used 0.003 as the cracking point for masonry

elements. Kaushik *et al.* stated that the values of E_b , E_j , and E_m for masonry walls are approximately.

$$E_b \approx 300 f_b, \quad (4.4)$$

$$E_j \approx 200 f_j, \quad (4.5)$$

$$E_m = 550 f'_m. \quad (4.6)$$

Corresponding coefficients of variance were 0.35, 0.32, and 0.3 respectively. These results are in line with the basic formula used by Eurocode 6 [2005] regarding the characteristic compressive strength of masonry. Following the above research, E_b , E_j , and E_m for masonry can be used in the present study; however, the present study considers the elastic linear range.

4.5. Aspect ratio, slenderness ratio, and weight reduction

A masonry structure comprising multiple walls subjected to out-of-plane loading has an aspect ratio (AR). The present study does not consider $AR \geq 1$ except for the case of the one-way vertical wall (with a plane of failure parallel to the bed joints). This is because several previous studies [La Mendola *et al.* 2014] revealed that structural rigidity is higher in the horizontal direction than in the vertical direction if $AR \geq 1$. However, the approach of using $P = (0.3AR + 0.7) P$ can be invoked for $AR > 1$.

The slenderness ratio also affects the masonry structure. The thickness of a masonry wall (t) affects the stiffness and strength of the wall. In the present study, t is a variable that has been resolved in various stages used in determining the

stiffness and strength of a masonry wall. The stages seek the equivalent thickness of the wall (t_{eff}), which represents the truss.

In structural analysis using, for example, FE software, self-weight is calculated automatically. A solid element is used as the truss element. Therefore, the specific gravity of the truss must be adapted to the specific gravity of the solid masonry elements. This can be achieved by multiplying the specific gravity by a factor ξ for masonry elements:

$$\gamma_{eq(u)} = \xi \gamma_u \quad (4.7)$$

$$\gamma_{eq(m)} = \xi \gamma_m \quad (4.8)$$

where $\xi = \frac{b_{eff} t}{2a \left(\frac{t_{eff}}{\sin \theta} + t_{eff} + b_{eff} \right)}$, γ_{eq} is the specific gravity equivalent of a unit or

of mortar, ξ is the specific gravity factor, γ_u is the specific gravity of the unit, and γ_m is the specific gravity of the mortar. Geometrically, the self-weight of a truss element affects the behavior of masonry structures. The load given to the structure is therefore an additional external load. For instance, if the thickness of the wall is (t) = 120 mm, the width of the unit load to be used is (b_{eff}) = 210 mm, the depth of the equivalent stress block is (a) = 51 mm, and the effective width of a cross section of the truss model is (t_{eff}) = 69.13 mm, then the value of the specific gravity factor (ξ) is 0.655. This value has a significant influence on the self-weight of masonry structure.

4.6. Results

The FTM was validated using the results of analysis of out-of-plane masonry structures conducted in previous studies. Truss analysis can be performed by using matrix methods as for a two-dimensional truss using the direct stiffness method. In this study, this is performed using SAP2000 software [2015]. The basic data are entered in accordance with the constitutive modeling approach. Both truss shapes were used and validated for masonry wall structures subject to out-of-plane loading. Material properties from the literature were used as input data in analyzing the FTM structure with FE software.

4.6.1. Validation 1

The first validation of the FTM was conducted for a model used by Varela-Rivera *et al.* [2011], namely six confined masonry walls with reinforced concrete. The specifications of the materials and dimensions of the walls are given in Table 4.2. Each wall was comprised of hollow blocks in a half-running bond pattern. The dimensions of the concrete confining elements were 0.15 x 0.2 m × 0.4 m for E-1, E-2, E-4, and E-5, and 0.12 m × 0.2 m × 0.4 m for E-3 and E-6. Each wall was confined by reinforced concrete around its perimeter. A load was applied to the masonry wall using air bags with dimensions of 1.2 m × 3 m (Fig. 4.7).

The air bags were filled gradually until the ultimate cracking of the masonry walls. The thickness of mortar connecting the blocks of masonry units was 10 mm.

Table 4.2 Geometry, aspect ratio, and slenderness ratio of wall specimens

Wall specimen		E-1	E-2	E-3	E-4	E-5	E-6
f_c (MPa)		14.79	19.16	19.8	15.31	17.39	21.67
f_j	(MPa)	2.89	2.34	2.47	2.79	2.66	2.26
f_p	(MPa)	5.47	5.47	4.09	5.47	5.47	4.09
f_m	(MPa)	2.84	2.84	2.45	2.84	2.84	2.45
f_{tpe}	(MPa)	0.14	0.14	0.11	0.14	0.14	0.11
f_{tpa}	(MPa)	0.44	0.44	0.36	0.44	0.44	0.36
E_c	(MPa)	9,614	10,943	11,124	9,782	10,425	11,638
Length	L (m)	3.67	3.77	3.77	2.85	2.95	2.95
Height	H (m)	2.72	2.88	2.88	2.72	2.72	2.72
Thickness	t (m)	0.15	0.15	0.12	0.15	0.15	0.12
H/L		0.74	0.76	0.76	0.95	0.92	0.92
H/t		18.13	19.2	24	18.13	18.13	22.67

Data taken from Varela-Rivera *et al.* [2011]

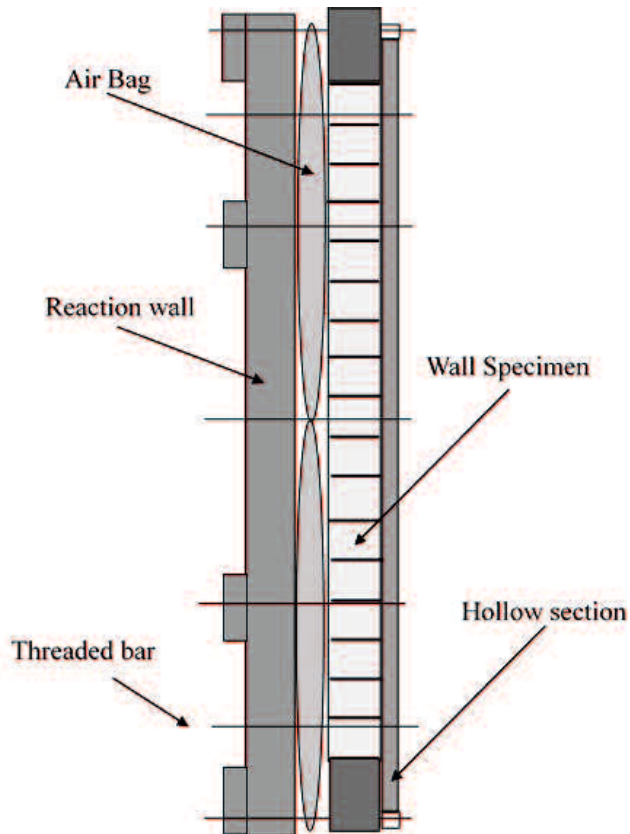
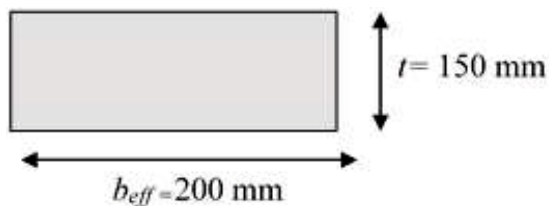


Figure 4.7 Setup of air bag (Herrera *et al.* [2016])

The results of this numerical experiment (W_e) were compared with those obtained by Varela *et al.* [2012a, 2012b] using the spring–strut method (W_{ss}), and were previously compared with the results of previous studies conducted by Varela-Rivera *et al.* [2011] using the yield-line method (W_{yl}), failure-line method (W_{fl}), and compressive strut method (W_{cs}). The yield-line method (W_{yl}) is theoretically not recommended for brittle materials such as masonry, but is still used to predict the out-of-plane strength of walls [Drysdale *et al.* 1988]. The failure-line method (W_{fl}) is a modification of the yield line method based on the idea that, prior to the formation of the final failure cracking pattern, some cracks are already formed, and their contribution to the internal work should not be included. For this reason, the failure line method predicts lower strength than the yield line method. The compressive strut method (W_{cs}) was proposed by Abrams *et al.* [1996] for infill walls surrounded by concrete frames. In Abrams’ work, an infill wall was subjected to uniform pressures. It was assumed that, after the formation of a given cracking pattern, a wall was divided into segments.

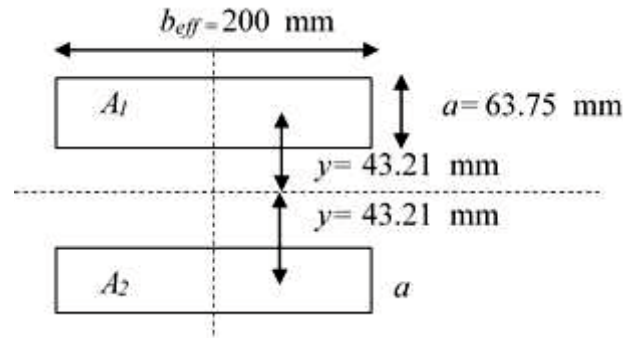
The structure and description of the walls and the FTM model proposed here are presented in Fig. 4.8. Results of FTM analysis are denoted by W_t and W_c . FTM results are presented and incorporated in Fig. 4.9.

The example calculations of b_{eff} and t_{eff} are as follows:



$$I_{tot} = \frac{1}{12} b_{eff} t^2 = 56,250,000 \text{ mm}^4$$

$$c = 0.5 t, \beta = 0.85 \rightarrow a = c\beta = 75 \times 0.85 = 63.75 \text{ mm}$$



$$I_{eq} = \sum I_n + \sum A_n y^2$$

$$I_{eq} = 56,250,000 = I_{tot}$$

n	$I_n = 1/12 b_{eff} \cdot a^3 \text{ (mm}^4\text{)}$	$A_n = b_{eff} \cdot a \text{ (mm}^2\text{)}$	y^2	$\text{(mm}^4\text{)}$
1	4,318,066.406	12,750	1,867.21	28,125,000
2	4,318,066.406	12,750	1,867.21	28,125,000
Σ	8,636,132.813		$I_{eq} =$	56,250,000

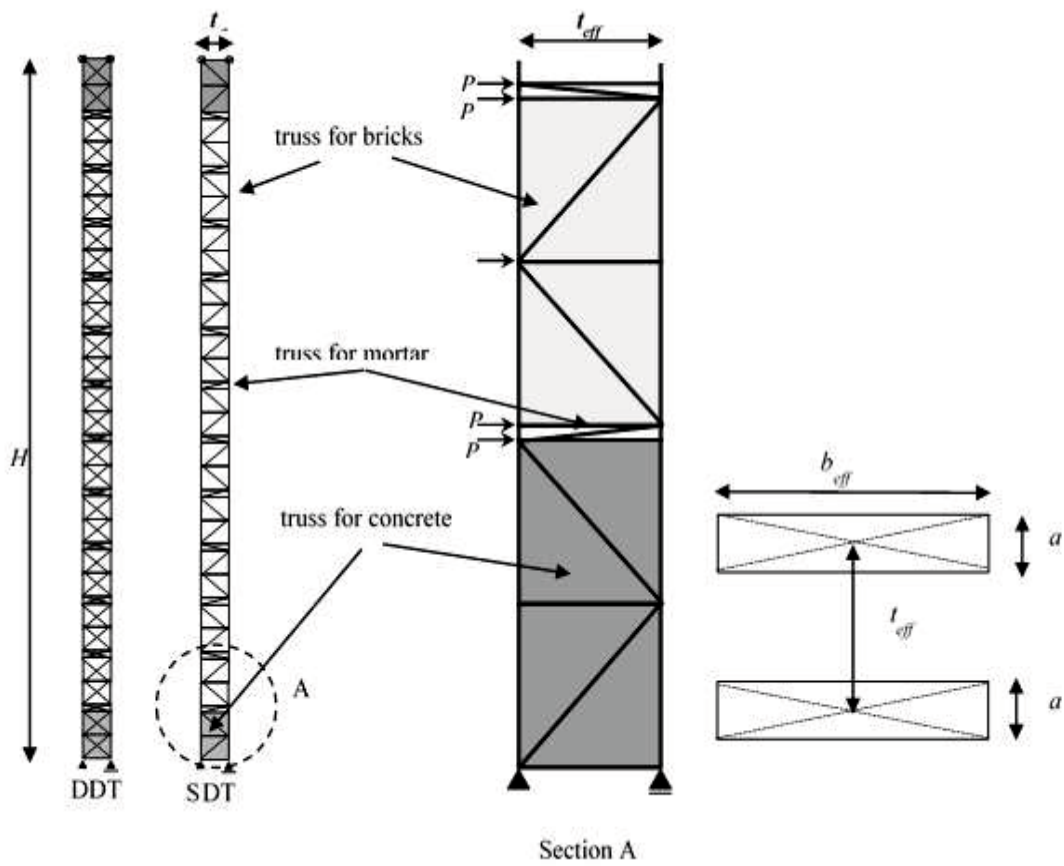
y is calculated by using the “goal seek” command in Microsoft Excel

software or by Equation 3:

$$y = \sqrt{\frac{I_{tot} - 2I_n}{2A_n}} = 43.21 \text{ mm}$$

The result is that $y = 43.21 \text{ mm}$; hereafter, $t_{eff} = 2y = 86.42 \text{ mm}$ and $t_w = 150.17 \text{ mm}$.

FTM results are explained further in the Discussion section.



	t	b_{eff}	a	y	t_{eff}
	mm	mm	mm	mm	mm
E1	150	200	63.75	43.21	86.42
E2	150	200	63.75	43.21	86.42
E3	120	200	51.00	34.57	69.14
E4	150	200	63.75	43.21	86.42
E5	150	200	63.75	43.21	86.42
E6	120	200	51.00	34.57	69.14

Figure 4.8 FTM model for Varela Rivera's setup

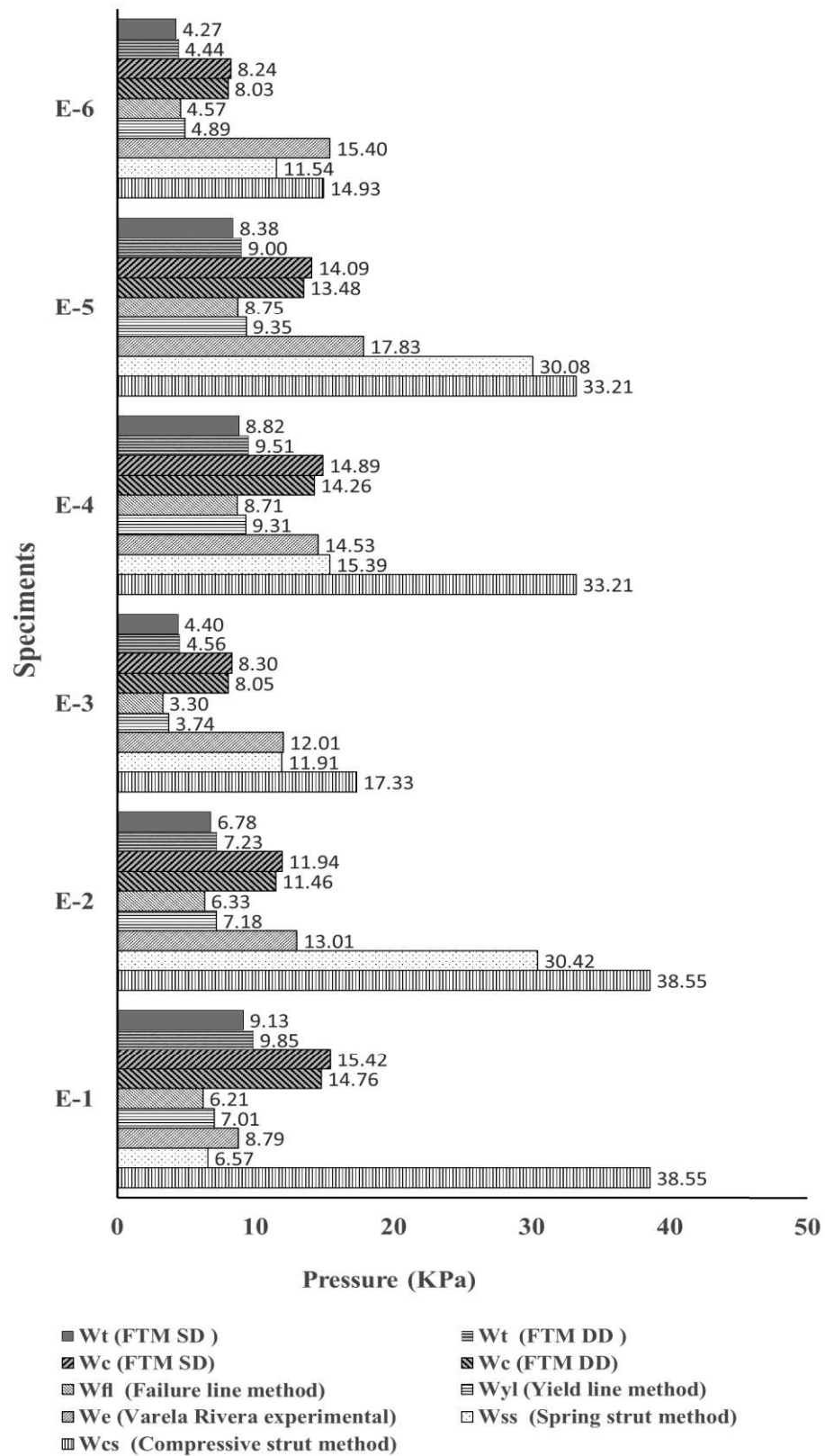
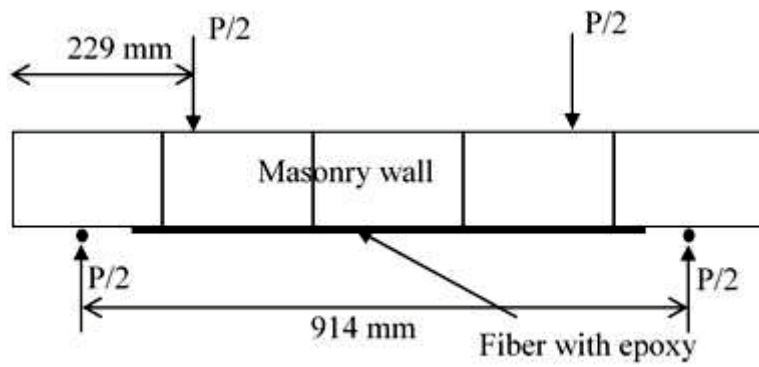


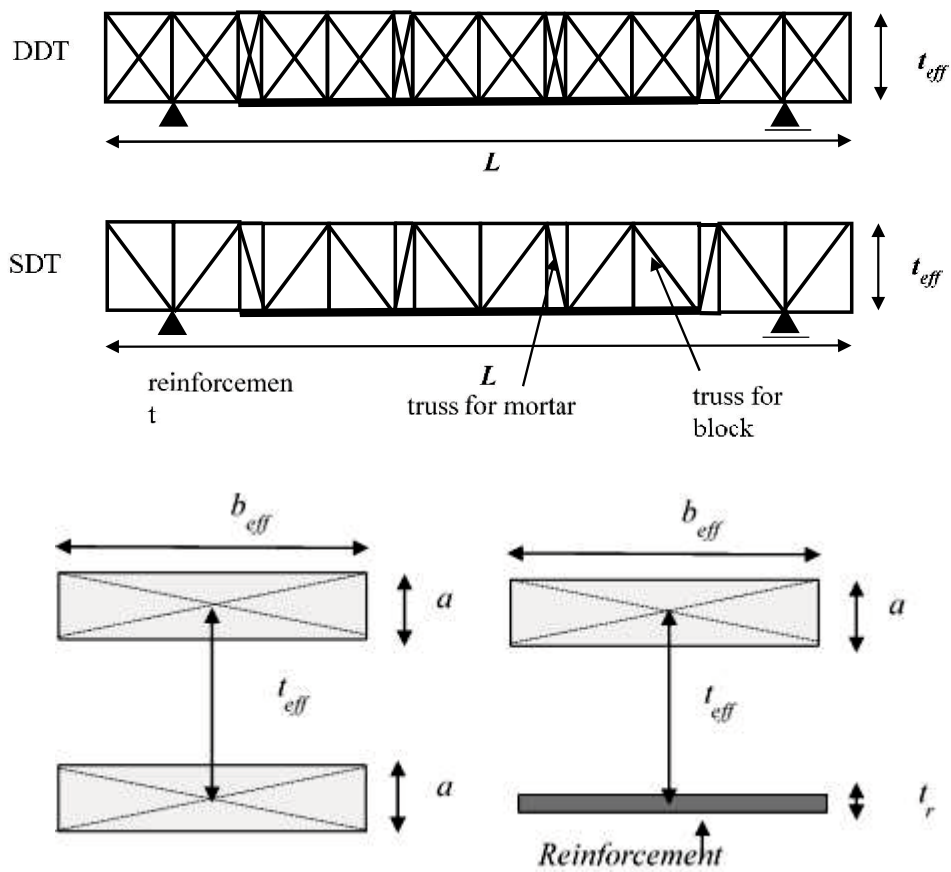
Figure 4.9 Comparison of results for the first validation experiment

4.6.2. Validation 2

The second validation of the FTM was conducted for a model used by Hamoush *et al.* [2002], who investigated the behavior of a surface-reinforced masonry wall under out-of-plane loading. The wall was reinforced with FRP and had dimensions of 900 mm × 600 mm × 200 mm. There were 18 specimens in total. Specimens had a single or double layer of FRP and a distance from the fiber to the support of 0, $d/2$, or $d/4$, where d is the span from the support to the first of point load on the masonry wall specimen. Specimens were constructed with hollow bricks made from mortar with a thickness of 25 mm. A single hollow block unit had two holes. The dimensions of a hollow block were 400 mm × 200 mm × 200 mm. The thickness of the HB was the effective compressed zone in this validation. The web fiber used in the validation was constructed with Tyfo Hi-Clear epoxy resin with an ultimate tensile strength of 414 MPa, ultimate elongation of 2.0%, elastic modulus of 27,580 MPa, and design thickness of 0.4 mm per layer. The Hamoush test setup and FTM model are shown in Fig. 4. 10.



a. Hamoush test setup



L (mm)	H (mm)	t (mm)	b_{eff} (mm)	a (mm)	y (mm)	t_{eff} (mm)
600	900	200	200	85.00	38.89	77.78

b. FTM model

Figure 4.10 Hamoush's test setup and FTM model.

The height (t_{eff}) of the truss was the center distance between the top and bottom of the hollow block.

Several methods can be used to analyze the FTM, such as the consistent deformation method, matrix method, finite element method, or FE software. Here, we analyzed the FTM structure using FE software using material properties taken from the literature as input data. The results of this validation are presented in Fig. 4.11. The FTM results compared with the three experimental specimen results are explained in the Discussion section.

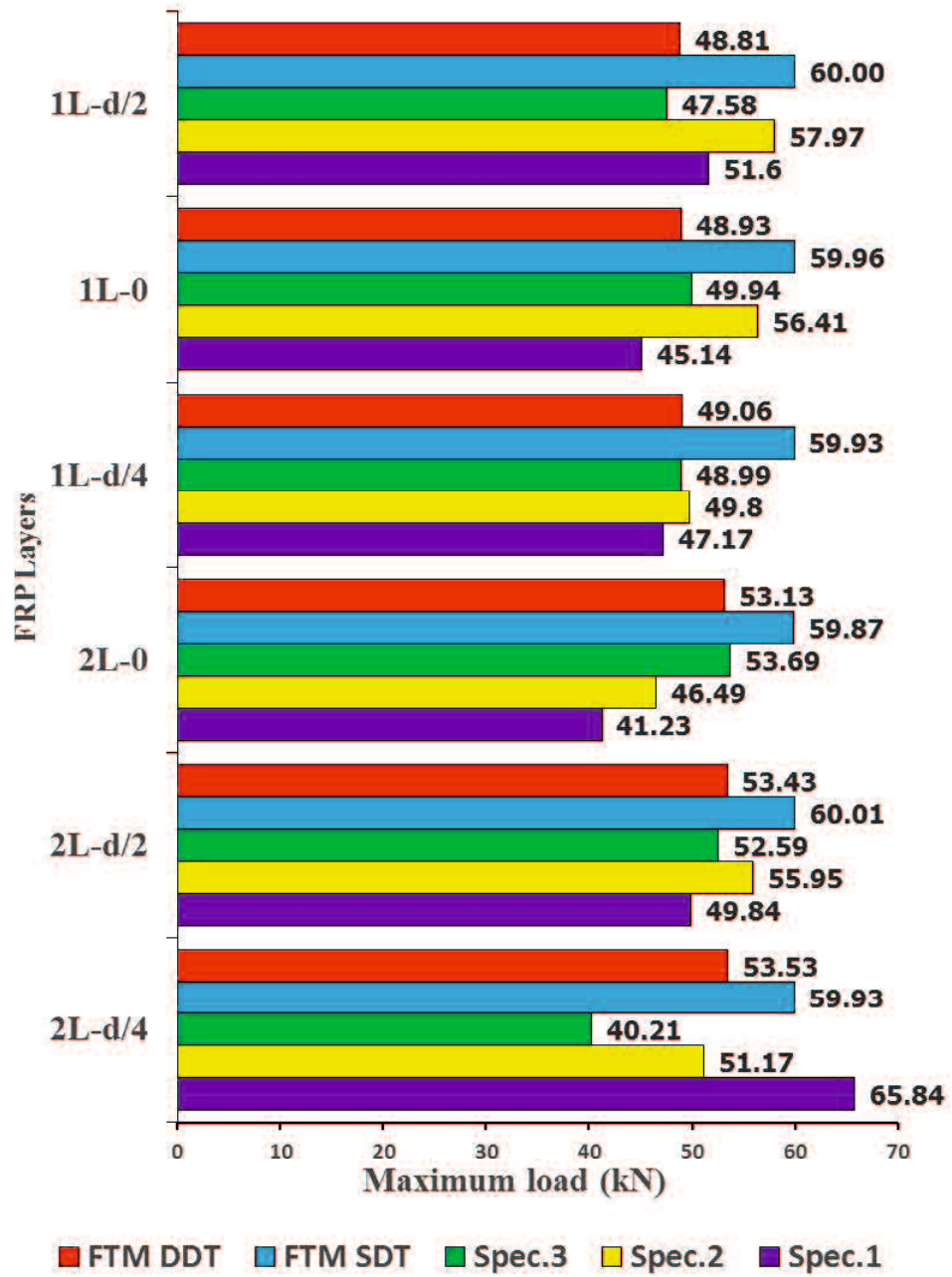


Figure 4.11 Comparison of results for the second validation experiment

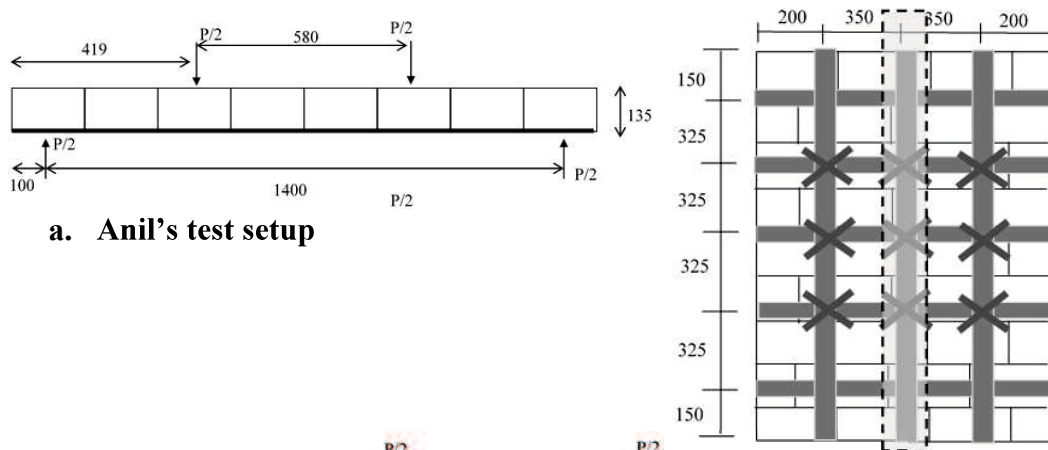
4.6.3. Validation 3

The third validation of the FTM was conducted for low-quality brick considered by Anil *et al.* [2012]. The brick had a strength of 2.5 MPa, hollow ratio of 65%, and dimensions of 185 mm × 185 mm × 135 mm. The mortar was of higher strength (5.2–7.1 MPa). The dimensions of the masonry walls were 1,600 mm × 1,100 mm × 135 mm. CFRP was coated on the side adjacent to the load side to retrofit the walls. The properties of the CFRP are given in Table 4.3. The test setup is presented in Fig. 4.12.

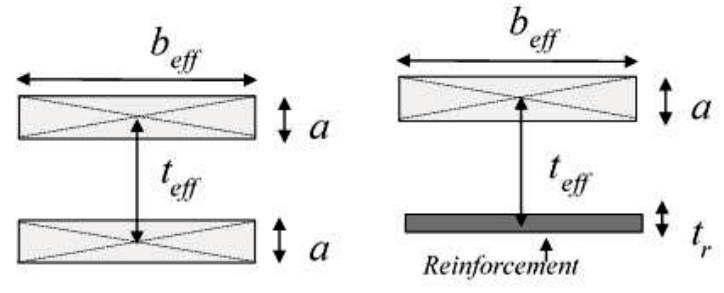
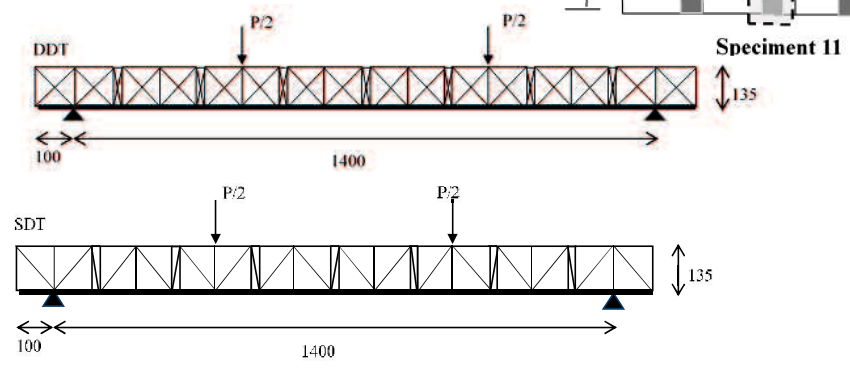
Table 4.3 Properties of SikaWrap 230-C (unidirectional) CFRP and Sikadur 330 resin

Properties of CFRP	Remarks of CFRP
Thickness (mm)	0.12
Tensile strength (MPa)	4100
Elastic modulus (MPa)	231,000
Ultimate tensile strain (%)	1.7%
Properties of Resin	Remarks of Resin
Tensile strength (MPa)	30
Elastic modulus (MPa)	3800

(Data taken from Anil *et al.* [2012])



a. Anil's test setup



L (mm)	H (mm)	t (mm)	b_{eff} (mm)	a (mm)	y (mm)	t_{eff} (mm)
1100	1600	135	185	37.29	52.50	105.00

b. FTM model

Figure 4.12 Test setup for the third validation experiment.

The CFRP was used in diverse arrays with different anchor arrangements and different combinations of vertical, horizontal, and diagonal arrangements. The CFRP arrangements were applied to 11 samples. Five sample results obtained using

the FTM in this validation were satisfactory, as presented in Fig. 4.13. The results are close to the experimental values.

4.7. Discussion

The use of FTM to analyze a confined masonry wall under out-of-plane loading was convincing in the first validation. The maximum pressure generated by the FTM (i.e., the strength of the wall) is given in Fig. 4.9 and on Table 4.4. W_t and W_c are the pressures required to produce forces on the tension truss and compression truss, respectively, that cause the wall to fail. Experimental results obtained by Varela-Rivera *et al.* [2011] and displayed in Fig. 4.9 revealed that specimens with similar aspect and slenderness ratios (E-1 and E-2; E-4 and E-5) have a lower out-of-plane strength than specimens with lower in-plane stiffness (E-1 and E-4). In the case of specimens with similar aspect ratios and in-plane stiffness (E-2 and E-3; E-5 and E-6), W_e is greater for specimens with smaller slenderness ratios (E-2 and E-5). The difference is related to the greater axial compressive strength of the block. The same behavior is seen in the above results obtained using the FTM. In contrast, the yield-line method and failure-line method underestimate W_e .

The FTM provides the strength resulting from a compression crack W_c and the strength resulting from a tension crack W_t . W_c represents the value of the strength resulting from an experimental crack W_e (E-2, E-3, E-4 and E-5); W_e is similar to W_c . The strength of masonry using W_{cs} (the compressive strut method) and W_{ss} (the spring-strut-method) overestimated W_e ; this comparison is similar to that for W_t and W_c obtained in FTM analysis. These results are consistent with the

effects of the slenderness ratio of a masonry structure in that the thickness of the masonry structure affects the pressure needed for the structure to fail. W_t and W_c were slightly greater than W_{yl} and W_e .

The FTM provided a value close to the experimental result (W_e) and the result of the spring–strut method (W_{ss}). However, W_c was a greater than W_e while W_t was lower than W_e for specimen E-1 owing to the difference in the rigidity of confinement. The rigidity of confinement depends on the reinforcement factor; this will be considered in the next FTM study.

W_t appears almost identical to W_{yl} and W_{fl} . This indicates that the previous method of obtaining W_{yl} and W_{fl} can only be used at one stage of cracking. The previous method can be applied only to a confined masonry wall. The above comparison reveals that FTM is useful in analyzing the strength of confined masonry walls.

The percentage of error (PoE) comparison between FTM and experimental and analysis results can be seen in Table 4.5. It is shown that for W_e (E-1) relative to FTM (W_t), PoE values are 3.9-12.1%; for E-2, E-4, and E-5 relative to W_c , PoE values are 1.9-20.9%; for W_{yl} relative to W_t , PoE values are 0.7-21.8%; for W_{fl} (E-2, E-4, E-5 and E-6) relative to W_t , the PoE values are 1.2-14.2%; for W_{ss} (E-4 and E-6) relative to W_c , PoE values are 3.3%, 7.4%, and 28.6%, and only W_{cs} relative to W_t or W_c have PoE values greater than 30%.” From these results it is seen that the first crack of a masonry structure can be caused by tensile stress or compressive stress.

Table 4.4 Comparison of FTM with Varela Rivera's experimental results and various analysis methods

Wall specimen (kPa)		E-1	E-2	E-3	E-4	E-5	E-6
W_e (Varela Rivera experiment)		8.79	13.01	12.01	14.53	17.83	15.40
W_{yl} (Yield line method)		7.01	7.18	3.74	9.31	9.35	4.89
W_{fl} (Failure line method)		6.21	6.33	3.30	8.71	8.75	4.57
W_{cs} (Compressive strut method)		38.55	38.55	17.33	33.21	33.21	14.93
W_{ss} (Spring strut method)		6.57	30.42	11.91	15.39	30.08	11.54
Double Diagonal	W_t (FTMDD)	9.85	7.23	4.56	9.51	9.00	4.44
	\mathcal{D} (mm)	13.22	14.89	18.72	12.82	12.26	15.07
	W_c (FTMDD)	14.76	11.46	8.05	14.26	13.48	8.03
	\mathcal{D} (mm)	19.81	23.60	33.08	19.21	18.37	27.30
Single Diagonal	W_t (FTMSD)	9.13	6.78	4.40	8.82	8.38	4.27
	\mathcal{D} (mm)	12.67	14.29	17.08	12.28	11.81	14.88
	W_c (FTMSD)	15.42	11.94	8.30	14.89	14.09	8.24
	\mathcal{D} (mm)	21.40	25.15	32.27	20.74	19.85	28.73

Table 4.5 Percentage of error of FTM method relative to Varela Rivera's experiment and analysis method results

Wall specimen (kPa)	E-1	E-2	E-3	E-4	E-5	E-6
W_e (Varela Rivera experiment)	8.79	13.01	12.01	14.53	17.83	15.40
W_t (FTMDD)	9.85	7.23	4.56	9.51	9.00	4.44
% of error	12.06	44.41	62.06	34.53	49.53	71.20
W_t (FTMSD)	9.13	6.78	4.40	8.82	8.38	4.27
% of error	3.85	47.88	63.40	39.33	52.98	72.27
W_c (FTMDD)	14.76	11.46	8.05	14.26	13.48	8.03
% of error	67.95	11.88	32.95	1.88	24.38	47.83
W_c (FTMSD)	15.42	11.94	8.30	14.89	14.09	8.24
% of error	75.4	8.3	30.9	2.5	20.9	46.5
Yield line method						
Wall specimen	E-1	E-2	E-3	E-4	E-5	E-6
W_{yl} (Yield line method)	7.01	7.18	3.74	9.31	9.35	4.89
W_t (FTMDD)	9.85	7.23	4.56	9.51	9.00	4.44
% of error	40.52	0.72	21.83	2.18	3.76	9.29
W_t (FTMSD)	9.13	6.78	4.40	8.82	8.38	4.27
% of error	30.22	5.56	17.54	5.31	10.33	12.69

Wc (FTMDD)	14.76	11.46	8.05	14.26	13.48	8.03
% of error	110.60	59.67	115.33	53.13	44.20	64.30
Wc (FTMSD)	15.42	11.94	8.30	14.89	14.09	8.24
% of error	119.95	66.23	122.06	59.92	50.75	68.52
Failure line method						
Wall specimen	E-1	E-2	E-3	E-4	E-5	E-6
Wfl (Failure line method)	6.21	6.33	3.30	8.71	8.75	4.57
Wt (FTMDD)	9.85	7.23	4.56	9.51	9.00	4.44
% of error	58.62	14.25	38.08	9.22	2.84	2.94
Wt (FTMSD)	9.13	6.78	4.40	8.82	8.38	4.27
% of error	47.00	7.13	33.21	1.22	4.18	6.57
Wc (FTMDD)	14.76	11.46	8.05	14.26	13.48	8.03
% of error	137.73	81.11	144.04	63.68	54.09	75.80
Wc (FTMSD)	15.42	11.94	8.30	14.89	14.09	8.24
% of error	148.28	88.55	151.66	70.94	61.08	80.32
Compressive strut method						
Wall specimen	E-1	E-2	E-3	E-4	E-5	E-6
Wcs (Compressive strut method)	38.55	38.55	17.33	33.21	33.21	14.93
Wt (FTM DD)	9.85	7.23	4.56	9.51	9.00	4.44
% of error	74.4	81.2	73.7	71.4	72.9	70.3
Wt (FTM SD)	9.13	6.78	4.40	8.82	8.38	4.27
% of error	76.3	82.4	74.6	73.5	74.8	71.4
Wc (FTM DD)	14.76	11.46	8.05	14.26	13.48	8.03
% of error	61.7	70.3	53.5	57.1	59.4	46.2
Wc (FTM SD)	15.42	11.94	8.30	14.89	14.09	8.24
% of error	60.0	69.0	52.1	55.2	57.6	44.8
Spring strut method						
Wall specimen	E-1	E-2	E-3	E-4	E-5	E-6
Wss (Spring strut method)	6.57	30.42	11.91	15.39	30.08	11.54
Wt (FTM DD)	9.85	7.23	4.56	9.51	9.00	4.44
% of error	49.93	76.23	61.74	38.19	70.08	61.56
Wt (FTM SD)	9.13	6.78	4.40	8.82	8.38	4.27
% of error	38.95	77.71	63.09	42.72	72.13	63.00
Wc (FTM DD)	14.76	11.46	8.05	14.26	13.48	8.03
% of error	124.70	62.31	32.38	7.37	55.18	30.38
Wc (FTM SD)	15.42	11.94	8.30	14.89	14.09	8.24
% of error	134.68	60.76	30.27	3.26	53.14	28.59

In the second validation, FRP was used to provide tension on the truss element. Results obtained with FTM show that the addition of FRP strengthens masonry structures, which is in line with the results of experiments. The FRP would fail before cracking appears in the area of compression [Hamoush *et al.* 2002]. The FTM reveals that the tensile load does not reach a maximum and that there is cracking as a result of compressive strain.

Figure 4.11 and Table 4.6 shows that cracking, as a result of the truss tension obtained with the FTM, is similar to the experimental result. The percentage of error in this validation for all comparisons was between 0.82 and 27.01%.

The addition of the FRP layer provides a peak load before cracking that is higher than that for a single layer along with an increase in the loading capacity. Similarly, the two layers reduce the deformation of the structure. Apparently, retrofitting using a single layer and retrofitting using a double layer are similar under tension of the truss element, but the double layer provides different compressive strengths for the compression of the truss element. A double layer of FRP increases structural integrity, especially when the FRP layers extend to the supports [Hamoush *et al.* 2002]. Various installations of a single layer of FRP strengthen the system only slightly.

Figure 4.13 and Table 4. 7 compares the results obtained using FTM with the experimental and analytical results of Anil *et al.* [2012] in the third validation experiment. The FTM was used in cases with and without CFRP.

Table 4.6 . Comparison of FTM relative to Hamoush’s experiment

Distance of fiber to support			Spec.1	Spec.2	Spec.3	Aver.	FTM SD	% of error	FTM DD	% of error
2L-d/4	Max. load	kN	65.84	51.17	40.21	52.41	59.93	14.4	53.53	2.15
	δ .	mm	2.47	2.1	1.75	2.11	3.17	50.4	2.62	24.2
2L-d/2	Max. load	kN	49.84	55.95	52.59	52.79	60	13.7	53.43	1.21
	δ .	mm	3.33	2.71	4.49	3.51	3.38	3.62	2.63	25.2
2L-0	Max. load	kN	41.23	46.49	53.69	47.14	59.87	27	53.13	12.7
	δ .	mm	2.69	3.22	3.53	3.15	3.34	6.13	2.63	16.5
1L-d/4	Max. load	kN	47.17	49.8	48.99	48.65	59.93	23.2	49.06	0.83
	δ .	mm	2.87	3.76	3.25	3.29	3.17	3.77	3.67	11.4
1L-0	Max. load	kN	45.14	56.41	49.94	50.5	59.96	18.8	48.93	3.1
	δ .	mm	4.05	2.6	3.05	3.23	5.36	65.7	3.69	14.2
1L-d/2	Max. load	kN	51.6	57.97	47.58	52.38	60	14.6	48.81	6.82
	δ .	mm	2.75	3.23	2.76	2.91	5.48	88.1	3.72	27.8

The diagonal modeling of CFRP in this validation is not applicable because the diagonal combination of CFRP strips is not handled in the two-dimensional FTM; it could be applied in three-dimensional FTM. Therefore, only certain reinforcements are used in this case, namely the reinforcements of samples 1, 8, 9, 10, and 11.

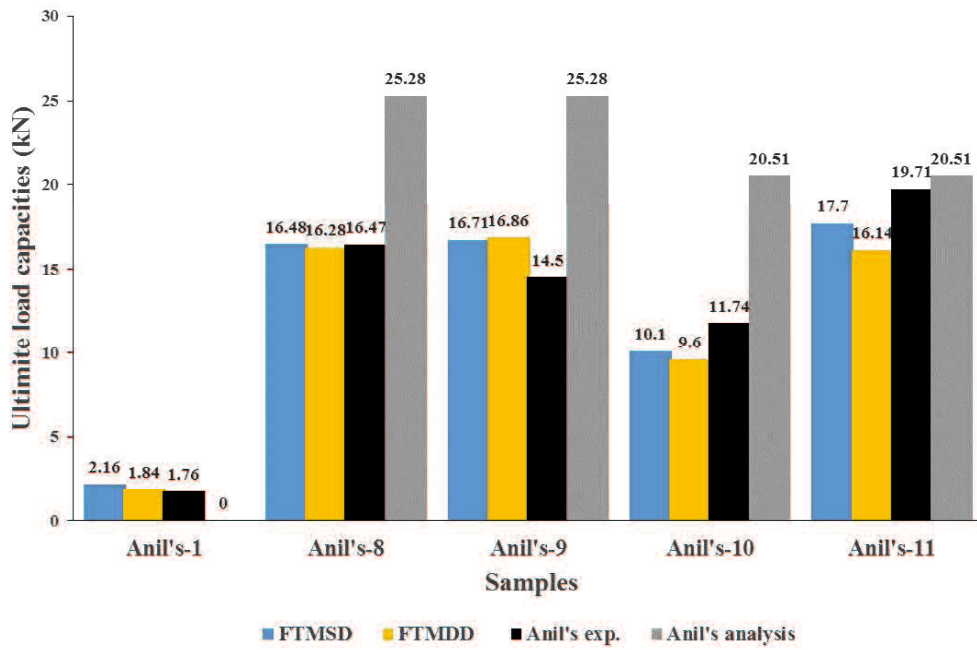


Figure 4.13 Comparison of results for the third validation experiment.

Table 4.7. Comparison of FTM to Anil experiment an analysis results

			Anil's experiment	Anil's Analysis	FTMSD	% of error	FTMDD	% of error
Anil's-1	Load	kN	1.76	-	2.16	22.67	1.84	4.27
	δ	mm	0.91		3.72		3.58	
Anil's-8	Load	kN	16.47	25.28	16.48	0.07	16.28	1.16
	δ	mm	8.14		24.56		29.05	
Anil's-9	Load	kN	14.5	25.28	16.71	15.22	16.86	16.28
	δ	mm	5.83		23.32		22.66	
Anil's-10	Load	kN	11.74	20.51	10.1	13.98	9.6	18.21
	δ	mm	7.1		20.77		22.75	
Anil's-11	Load	kN	19.71	20.51	17.7	10.18	16.14	18.09
	δ	mm	10.93		33.15		31.19	

Sample 1 did not use CFRP and cracked at low load in sample 10. FTM values overestimated the load capacities compared with experimental values. For sample numbers 8, 9, and 11, FTM underestimated the load capacity results found by analysis. The average overestimation of samples 1 and 10 were around 4.27% (FTMDD) and 13.98% (FTMSD) of the load capacity values, and the average underestimation of samples 8, 9, and 11 were between 0.07% (FTMSD) and 13.98% (FTMSD) of the load capacity values. The load capacity then increased as CFRP was applied and the truss element was compressed. FTM provided results similar to the experimental results, although there were slight differences owing to the modeling of the anchor in the FTM models. The analysis of Anil *et al.* [2012] overestimated the results obtained using FTM and the results obtained in experiments. Anil *et al.* [2012] did not record an analysis of sample 1

4.8. Summary

FTM was applied to a wide variety of planar masonry structures, both confined and unconfined as well as both with and without reinforcement. The structures corresponded to a simple beam, distributed load, and concentrated load.

Furthermore, FTM has been validated with several types of structures such that FTM produces satisfactory results and there is expected to serve as a tool for evaluating the strength of a masonry wall under out-of-plane loading

CHAPTER 5. CONCLUSIONS AND FUTURE RECOMMENDATIONS

5.1. Conclusions

Most of the design formulae for calculating the equivalent elasticity of brick masonry structures are applicable only for the case where $E_{mor} < E_b$. The present study was focused on masonry structures with low-quality bricks, i.e. $E_{mor} > E_b$. This dissertation presented numerical simulations to derive formulas for the equivalent elasticity of brick masonry structures. The accuracy of the formulas was discussed and verified by using experimental secondary data. The equivalent elasticity obtained using the newly developed formulas was estimated with high accuracy, resulting in a discrepancy of less than 1 % compared to the numerical results derived by Gumaste. The conclusions of this investigation are summarized as follows:

- The proposed formula is a new, simplified formula; we performed finite element (FE) simulations, adopting the homogenization technique. It can be used to calculate the equivalent modulus of elasticity of such brick masonry structures.

- The conventional formula may underestimate the equivalent elasticity of the masonry structures made with mortar that has a higher modulus than bricks.
- The proposed formula is applicable in various calculations of the equivalent elasticity of masonry structures. In particular, the formula can be suitable for the estimation of the equivalent elasticity of bricks with low elastic modulus. Furthermore, the proposed formula can be applied for bricks with high elastic modulus.
- The equivalent elasticity estimated via the proposed formula increases in accordance with the increase in elastic modulus ratio of mortar.
- The proposed formula can be employed for masonry structures in countries that use bricks of low elastic moduli.

FTM was applied to a wide variety of planar masonry structures, both confined and unconfined as well as both with and without reinforcement. The structures corresponded to a simple beam, distributed load, and concentrated load. The following conclusions are drawn from the results of validation tests on FTM.

- FTM can be applied to various conditions of masonry structure models subject to out-of-plane loading. Specifically, FTM can be applied to a structure having an aspect ratio less than 1.
- FTM produces satisfactory results if the reinforcement of the masonry structure is uniform in direction and runs parallel to the span of the structure. However, diagonal reinforcement is difficult to model using FTM.
- FTM overcomes problems faced by previous methods because it reproduces compression and tension failures.

5.2. Recommendations

In further studies, it is suggested that the experimental research be extended, particularly to masonry structures that are composed of mortar with a higher modulus of elasticity than that of bricks.

The FTM's effectiveness in in-plane mechanical properties and three-dimensional modelling of walls will be investigated further in future work.

Strength is needed for poor quality existing structures specifically brick materials. Some elements of the buildings, such as the wall, connection, column, and beam need to be strengthened to have a proper behavior of building when subjected to a future earthquake.

Quality control or inspection is needed from the local authority to control the implementation of building's guideline or code and good construction practice.

This dissertation supports the policy for contribution to the development of the Indonesian National Standard for masonry rural houses and low-rise buildings by the Ministry of Public Works - The Republic of Indonesia

APPENDIX A

Data		Mortar	Brick	case	S_x	S_y	strain	v_x	v_y	E_x	E_y	G	Average E	Average ν	Average G	
1	A	10000	10000	AH	-4.0250	-1.0060	-0.0004	0.2499	0.2500	10000	10001	7337.4414	10000	0.2500	7358.0260	
	Poisson			0.25	0.25	AV	-1.6670	-6.6670	-0.0006		10000	10001				
	f'comp			10	10	AS	4.3300	0.0006								
	B					BH	-4.0250	-1.0060	-0.0004	0.2499	0.2500	10000				10001
				BV	-1.6670	-6.6670	-0.0006			10000	10001					
				BS	4.3300	0.0006										
2	A	20000	10000	AH	-4.9108	-1.1502	-0.0004	0.2342	0.2459	12264	11665	8433.3447	11965	0.2400	8459.1614	
	Poisson			0.25	0.25	AV	-1.9027	-7.7361	-0.0006		12264	11665				
	f'comp			15	10	AS	4.9396	0.0006								
	B					BH	-4.9113	-1.1489	-0.0004	0.2339	0.2459	12266				11666
				BV	-1.9027	-7.7361	-0.0006			12266	11666					
				BS	4.9601	0.0006										
3	A	30000	10000	AH	-5.7227	-1.2195	-0.0004	0.2131	0.2418	14384	12640	8973.0689	13505	0.2273	9019.4222	
	Poisson			0.25	0.25	AV	-2.0143	-8.3292	-0.0006		14384	12640				
	f'comp			20	10	AS	5.2274	0.0006								
	B					BH	-5.7233	-1.2176	-0.0004	0.2127	0.2414	14388				12610
				BV	-2.0060	-8.3081	-0.0006			14388	12610					
				BS	5.2686	0.0006										
4	A	40000	10000	AH	-6.5128	-1.2650	-0.0004	0.1942	0.2384	16460	13349	9334.3605	14894	0.2161	9399.9868	
	Poisson			0.25	0.25	AV	-2.0856	-8.7480	-0.0006		16460	13349				
	f'comp			40	10	AS	5.4184	0.0006								
	B					BH	-6.5136	-1.2629	-0.0004	0.1939	0.2379	16465				13301
				BV	-2.0730	-8.7150	-0.0006			16465	13301					
				BS	5.4800	0.0006										
5	A	10000	20000	AH	-6.9048	-1.6395	-0.0004	0.2374	0.2492	17215	16393	12005.0459	16804	0.2434	11966.7172	
	Poisson			0.25	0.25	AV	-2.7134	-10.8897	-0.0006		17215	16393				
	f'comp			10	15	AS	7.0732	0.0006								
	B					BH	-6.9034	-1.6413	-0.0004	0.2378	0.2491	17211				16397
				BV	-2.7135	-10.8934	-0.0006			17211	16397					
				BS	7.0554	0.0006										
6	A	10000	30000	AH	-9.5186	-2.0805	-0.0004	0.2186	0.2461	23867	21138	15416.2163	22502	0.2324	15333.1880	
	Poisson			0.25	0.25	AV	-3.4363	-13.9626	-0.0006		23867	21138				
	f'comp			10	20	AS	9.0295	0.0006								
	B					BH	-9.5151	-2.0835	-0.0004	0.2190	0.2459	23858				21144
				BV	-3.4340	-13.9668	-0.0006			23858	21144					
				BS	8.9976	0.0006										
7	A	10000	40000	AH	-11.9219	-2.4019	-0.0004	0.2015	0.2427	30048	24815	18058.9828	27429	0.2221	17930.8710	
	Poisson			0.25	0.25	AV	-3.9579	-16.3069	-0.0006		30048	24815				
	f'comp			10	20	AS	10.5103	0.0006								
	B					BH	-11.9159	-2.4052	-0.0004	0.2019	0.2423	30033				24821
				BV	-3.9520	-16.3106	-0.0006			30033	24821					
				BS	10.4674	0.0006										
8	A	5000	10000	AH	-3.4524	-0.8197	-0.0004	0.2374	0.2492	8608	8196	6002.4954	8402	0.2434	5983.3483	
	Poisson			0.25	0.25	AV	-1.3567	-5.4449	-0.0006		8608	8196				
	f'comp			10	10	AS	3.5366	0.0006								
	B					BH	-3.4517	-0.8206	-0.0004	0.2377	0.2491	8605				8199
				BV	-1.3567	-5.4467	-0.0006			8605	8199					
				BS	3.5277	0.0006										
9	A	2500	7500	AH	-2.3796	-0.5201	-0.0004	0.2186	0.2461	5967	5285	3854.0430	5625	0.2324	3831.6510	
	Poisson			0.25	0.25	AV	-0.8591	-3.4906	-0.0006		5967	5285				
	f'comp			10	10	AS	2.2574	0.0006								
	B					BH	-2.3788	-0.5209	-0.0004	0.2190	0.2459	5964				5286
				BV	-0.8585	-3.4917	-0.0006			5964	5286					
				BS	2.2494	0.0006										
10	A	2500	2500	AH	-1.0060	-0.2520	-0.0004	0.2505	0.2501	2499	2500	1835.2076	2499	0.2503	1836.6734	
	Poisson			0.25	0.25	AV	-0.4170	-1.6670	-0.0006		2499	2500				
	f'comp			7.5	10	AS	1.0830	0.0006								
	B					BH	-1.0060	-0.2520	-0.0004	0.2505	0.2501	2499				2500
				BV	-0.4170	-1.6670	-0.0006			2499	2500					
				BS	1.0830	0.0006										
11	A	2500	5000	AH	-1.7262	-0.4099	-0.0004	0.2374	0.2492	4304	4098	3001.2712	4201	0.2434	2991.6904	
	Poisson			0.25	0.25	AV	-0.6783	-2.7224	-0.0006		4304	4098				
	f'comp			7.5	5	AS	1.7683	0.0006								
	B					BH	-1.7259	-0.4103	-0.0004	0.2377	0.2491	4303				4099
				BV	-0.6784	-2.7233	-0.0006			4303	4099					
				BS	1.7638	0.0006										
12	A	2200	11000	AH	-3.0770	-0.4923	-0.0004	0.1600	0.2046	7887	6120	4507.5879	7003	0.1824	4474.6966	
	Poisson			0.25	0.2	AV	-0.8090	-3.9543	-0.0006		7887	6120				
	f'comp			14	52	AS	2.6070	0.0006								
	B					BH	-3.0753	-0.4934	-0.0004	0.1605	0.2044	7882				6121
				BV	-0.8086	-3.9554	-0.0006			7882	6121					
				BS	2.6026	0.0006										

Data		Mortar	Brick	case	S_x	S_y	strain	v_x	v_y	E_x	E_y	G	Average E	Average ν	Average G		
13	A	10000	2000	AH	-1.4587	-0.2599	-0.0004	0.1782	0.2356	3703	2782	1923.9589	3240	0.2066	1940.7003		
	Poisson			0.25	0.25	AV	-0.4276	-1.8149	-0.0006			3703				2782	
	fcomp			50	14	AS	1.1139	0.0006									
	B			BH	-1.4589	-0.2595	-0.0004	0.1779	0.2349	3704	2769	1957.4417					
				BV	-0.4243	-1.8060	-0.0006			3704	2769						
14	A	20000	2000	AH	-2.2298	-0.2826	-0.0004	0.1267	0.2268	5739	3139	2150.2612	4432	0.1765	2183.0692		
	Poisson			0.25	0.25	AV	-0.4580	-2.0197	-0.0006			5739				3139	
	fcomp			50	15	AS	1.2370	0.0006									
	B			BH	-2.2301	-0.2824	-0.0004	0.1266	0.2258	5741	3110	2215.8772					
				BV	-0.4519	-2.0012	-0.0006			5741	3110						
15	A	30000	2000	AH	-3.2953	-0.2990	-0.0004	0.0907	0.2222	8556	3354	2367.0519	5746	0.1584	2413.6595		
	Poisson			0.25	0.25	AV	-0.4753	-2.1395	-0.0006			8556				3354	
	fcomp			50	15	AS	1.3580	0.0006									
	B			BH	-2.9966	-0.2990	-0.0004	0.0998	0.2211	7766	3308	2460.2670					
				BV	-0.4673	-2.1140	-0.0006			7766	3308						
16	A	1000	1000	AH	-0.4030	-0.1010	-0.0004	0.2506	0.2504	1001	1000	733.7441	1001	0.2505	733.7441		
	Poisson			0.25	0.25	AV	-0.1670	-0.6670	-0.0006			1001				1000	
	fcomp			10	10	AS	0.4330	0.0006									
	B			BH	-0.4030	-0.1010	-0.0004	0.2506	0.2504	1001	1000	733.7441					
				BV	-0.1670	-0.6670	-0.0006			1001	1000						
17	A	1000	10000	AH	-2.9805	-0.6005	-0.0004	0.2015	0.2427	7512	6204	4536.9447	6857	0.2221	4493.8244		
	Poisson			0.25	0.25	AV	-0.9895	-4.0767	-0.0006			7512				6204	
	fcomp			10	10	AS	2.6405	0.0006									
	B			BH	-2.9790	-0.6013	-0.0004	0.2018	0.2423	7508	6205	4450.7042					
				BV	-0.9880	-4.0777	-0.0006			7508	6205						
18	A	1000	12500	AH	-3.5373	-0.6608	-0.0004	0.1868	0.2394	8955	6938	5045.7099	7945	0.2130	5002.7876		
	Poisson			0.25	0.25	AV	-1.0865	-4.5392	-0.0006			8955				6938	
	fcomp			10	10	AS	2.9193	0.0006									
	B			BH	-3.5352	-0.6617	-0.0004	0.1872	0.2388	8950	6939	4959.8653					
				BV	-1.0840	-4.5399	-0.0006			8950	6939						
19	A	50000	10000	AH	-7.2934	-1.2995	-0.0004	0.1782	0.2356	18516	13910	9619.7670	16198	0.2066	9703.4743		
	Poisson			0.25	0.25	AV	-2.1378	-9.0744	-0.0006			18516				13910	
	fcomp			40	10	AS	5.5693	0.0006									
	B			BH	-7.2942	-1.2974	-0.0004	0.1779	0.2349	18522	13844	9787.1817					
				BV	-2.1214	-9.0299	-0.0006			18522	13844						
20	A	10000	50000	AH	-14.1494	-2.6432	-0.0004	0.1868	0.2394	35819	27752	20182.8238	31782	0.2130	20011.1618		
	Poisson			0.25	0.25	AV	-4.3459	-18.1568	-0.0006			35819				27752	
	fcomp			10	20	AS	11.6774	0.0006									
	B			BH	-14.1408	-2.6466	-0.0004	0.1872	0.2388	35799	27757	19839.4997					
				BV	-4.3360	-18.1597	-0.0006			35799	27757						
21	A	4000	2000	AH	-0.9822	-0.2300	-0.0004	0.2342	0.2460	2453	2333	1686.6513	2392	0.2400	1822.0465		
	Poisson			0.25	0.25	AV	-0.3805	-1.5472	-0.0006			2453				2333	
	fcomp			7.5	10	AS	0.9879	0.0006									
	B			BH	-0.9823	-0.2298	-0.0004	0.2339	0.2458	2453	2330	1957.4417					
				BV	-0.3798	-1.5453	-0.0006			2453	2330						
22	A	6000	2000	AH	-1.1445	-0.2439	-0.0004	0.2131	0.2418	2877	2528	1794.6224	2701	0.2273	1803.8799		
	Poisson			0.25	0.25	AV	-0.4029	-1.6658	-0.0006			2877				2528	
	fcomp			7.5	10	AS	1.0455	0.0006									
	B			BH	-1.1447	-0.2435	-0.0004	0.2127	0.2414	2878	2522	1813.1374					
				BV	-0.4012	-1.6616	-0.0006			2878	2522						
23	A	8000	2000	AH	-1.3026	-0.2530	-0.0004	0.1942	0.2384	3292	2670	1866.8717	2979	0.2161	1879.9942		
	Poisson			0.25	0.25	AV	-0.4171	-1.7496	-0.0006			3292				2670	
	fcomp			7.5	10	AS	1.0837	0.0006									
	B			BH	-1.3027	-0.2526	-0.0004	0.1939	0.2379	3293	2660	1893.1167					
				BV	-0.4146	-1.7430	-0.0006			3293	2660						
24	A	2000	2000	AH	-0.8050	-0.2010	-0.0004	0.2497	0.2498	2000	2000	1467.4883	2000	0.2498	1100.6162		
	Poisson			0.25	0.25	AV	-0.3330	-1.3330	-0.0006			2000				2000	
	fcomp			7.5	10	AS	0.8660	0.0006									
	B			BH	-0.8050	-0.2010	-0.0004	0.2497	0.2498	2000	2000	733.7441					
				BV	-0.3330	-1.3330	-0.0006			2000	2000						
25	A	10000	5000	AH	-2.4554	-0.5751	-0.0004	0.2342	0.2459	6132	5832	4216.6855	5981	0.2400	4229.5936		
	Poisson			0.25	0.25	AV	-0.9513	-3.8681	-0.0006			6132				5832	
	fcomp			10	10	AS	2.4698	0.0006									
	B			BH	-2.4557	-0.5744	-0.0004	0.2339	0.2458	6133	5826	4242.5016					
				BV	-0.9495	-3.8634	-0.0006			6133	5826						
				BS	2.4801	0.0006											

Data		Mortar	Brick	case	S_x	S_y	strain	v_x	v_y	E_x	E_y	G	Average E	Average ν	Average G	
26	A	20000	5000	AH	-3.2564	-0.6325	-0.0004	0.1942	0.2384	8230	6674	4667.1928	7447	0.2161	4700.0046	
	Poisson			0.25	0.25	AV	-1.0428	-4.3740	-0.0006			8230				6674
	fcomp			10	10	AS	2.7092	0.0006								
	B					BH	-3.2568	-0.6314	-0.0004	0.1939	0.2379	8232				6650
27	A	15000	5000	AH	-2.8613	-0.6098	-0.0004	0.2131	0.2418	7192	6320	4486.5181	6753	0.2273	4509.7055	
	Poisson			0.25	0.25	AV	-1.0071	-4.1646	-0.0006			7192				6320
	fcomp			10	10	AS	2.6137	0.0006								
	B					BH	-2.8617	-0.6088	-0.0004	0.2127	0.2415	7194				6305
28	A	30000	5000	AH	-4.0344	-0.6639	-0.0004	0.1646	0.2332	10281	7187	4933.4608	8725	0.1986	4983.9703	
	Poisson			0.25	0.25	AV	-1.0895	-4.6713	-0.0006			10281				7187
	fcomp			10	10	AS	2.8506	0.0006								
	B					BH	-4.0349	-0.6629	-0.0004	0.1643	0.2325	10284				7146
29	A	25000	5000	AH	-3.6467	-0.6497	-0.0004	0.1782	0.2356	9258	6955	4809.8678	8099	0.2066	4851.7304	
	Poisson			0.25	0.25	AV	-1.0689	-4.5372	-0.0006			9258				6955
	fcomp			10	10	AS	2.7846	0.0006								
	B					BH	-3.6471	-0.6487	-0.0004	0.1779	0.2349	9261				6922
30	A	30000	20000	AH	-8.9706	-2.1903	-0.0004	0.2442	0.2482	22332	21960	16021.4361	22144	0.2461	16049.4733	
	Poisson			0.25	0.25	AV	-3.6256	-14.6104	-0.0006			22332				21960
	fcomp			10	10	AS	9.4165	0.0006								
	B					BH	-8.9712	-2.1887	-0.0004	0.2440	0.2481	22335				21949
31	A	20000	20000	AH	-8.0500	-2.0130	-0.0004	0.2501	0.2500	19999	19999	16021.4361	19999	0.2500	15346.1601	
	Poisson			0.25	0.25	AV	-3.3330	-13.3330	-0.0006			19999				19999
	fcomp			10	10	AS	9.4165	0.0006								
	B					BH	-8.0500	-2.0130	-0.0004	0.2501	0.2500	19999				19999
32	A	15000	20000	AH	-7.5293	-1.8683	-0.0004	0.2481	0.2503	18713	18553	13626.8324	18633	0.2493	13609.4544	
	Poisson			0.25	0.25	AV	-3.0945	-12.3632	-0.0006			18713				18553
	fcomp			10	10	AS	8.0439	0.0006								
	B					BH	-7.5288	-1.8693	-0.0004	0.2483	0.2503	18711				18556
33	A	5000	20000	AH	-5.9609	-1.2009	-0.0004	0.2015	0.2503	15000	18784	9029.4940	15303	0.2240	8965.4454	
	Poisson			0.25	0.25	AV	-3.0945	-12.3632	-0.0006			15000				18784
	fcomp			10	10	AS	5.2552	0.0006								
	B					BH	-5.9580	-1.2026	-0.0004	0.2019	0.2423	15016				12410
33	A	200	1000	AH	-0.2333	-0.0325	-0.0004	0.1395	0.2046	601	559	410.9298	608	0.1925	403.8616	
	Poisson			0.25	0.25	AV	-0.0735	-0.3595	-0.0006			601				559
	fcomp			10	10	AS	0.2377	0.0006								
	B					BH	-0.2828	-0.0529	-0.0004	0.1871	0.2388	716				555
34	A	250	1000	AH	-0.2981	-0.0600	-0.0004	0.2014	0.2071	757	618	460.5438	687	0.2132	452.8156	
	Poisson			0.25	0.25	AV	-0.0835	-0.4030	-0.0006			757				618
	fcomp			10	10	AS	0.2679	0.0006								
	B					BH	-0.2979	-0.0601	-0.0004	0.2018	0.2423	751				621
35	A	500	1000	AH	-0.3452	-0.0820	-0.0004	0.2375	0.2119	869	815	624.6098	841	0.2341	610.5156	
	Poisson			0.25	0.25	AV	-0.1136	-0.5362	-0.0006			869				815
	fcomp			10	10	AS	0.3680	0.0006								
	B					BH	-0.3450	-0.0820	-0.0004	0.2378	0.2491	860				820
36	A	500	1000	AH	-0.3765	-0.0934	-0.0004	0.2481	0.2126	945	921	701.4139	932	0.2398	667.9090	
	Poisson			0.25	0.25	AV	-0.1292	-0.6076	-0.0006			945				921
	fcomp			10	10	AS	0.4141	0.0006								
	B					BH	-0.3764	-0.0935	-0.0004	0.2483	0.2503	936				928
37	A	1000	1000	AH	-0.4030	-0.1010	-0.0004	0.2506	0.2122	1011	992	757.2663	1001	0.2410	745.5052	
	Poisson			0.25	0.25	AV	-0.1389	-0.6546	-0.0006			1011				992
	fcomp			10	10	AS	0.4467	0.0006								
	B					BH	-0.4030	-0.1010	-0.0004	0.2506	0.2504	1001				1000
				BV	-0.1670	-0.6670	-0.0006			1001	1000					
				BS	0.4330	0.0006										

Data		Mortar	Brick	case	S_x	S_y	strain	v_x	v_y	E_x	E_y	G	Average E	Average ν	Average G	
38	A	2000	1000	AH	-0.4911	-0.1150	-0.0004	0.2342	0.2088	1238	1155	872.5703	1196	0.2307	860.5444	
	Poisson	0.25	0.25	AV	-0.1585	-0.7587	-0.0006			1238	1155					
	fcomp	10	10	AS	0.5112	0.0006										
	B			BH	-0.4911	-0.1149	-0.0004	0.2339	0.2458	1227	1165					848.5185
				BV	-0.1899	-0.7727	-0.0006			1227	1165					
39	A	3000	1000	BS	0.4960	0.0006						929.2949	1350	0.2182	936.1290	
	Poisson	0.25	0.25	AH	-0.5723	-0.1220	-0.0004	0.2131	0.2056	1450	1250					
	fcomp	10	10	AV	-0.1680	-0.8169	-0.0006			1450	1250					
	B			AS	0.5415	0.0006										
				BH	-0.5723	-0.1218	-0.0004	0.2127	0.2414	1439	1261					942.9631
40	A	4000	1000	BV	-0.2006	-0.8308	-0.0006			1439	1261	967.0119	1488	0.2072	956.7887	
	Poisson	0.25	0.25	BS	0.5480	0.0006										
	fcomp	10	10	AH	-0.6513	-0.1265	-0.0004	0.1942	0.2030	1658	1319					
	B			AV	-0.1742	-0.8581	-0.0006			1658	1319					
				AS	0.5614	0.0006										
41	A	5000	1000	BH	-0.6514	-0.1263	-0.0004	0.1939	0.2379	1647	1330	996.4464	1616	0.1979	987.5780	
	Poisson	0.25	0.25	BV	-0.2073	-0.8715	-0.0006			1647	1330					
	fcomp	10	10	BS	0.5480	0.0006										
	B			AH	-0.7293	-0.1299	-0.0004	0.1782	0.2008	1864	1374					978.7095
				AV	-0.1788	-0.8904	-0.0006			1864	1374					
			AS	0.5770	0.0006											
			BH	-0.7294	-0.1297	-0.0004	0.1779	0.2349	1852	1384						
			BV	-0.2121	-0.9030	-0.0006			1852	1384						
			BS	0.5651	0.0006											

APPENDIX B

Example calculation of FTM

Data

	<i>L</i>	<i>h</i>	<i>t</i>	<i>h/L</i>	<i>h/t</i>	<i>f_c</i>	<i>f_f</i>
E1	3.67	2.72	0.15	0.741144414	18.133333	14.79	2.89
E2	3.77	2.88	0.15	0.763925729	19.2	19.16	2.34
E3	3.77	2.88	0.12	0.763925729	24	19.8	2.47
E4	2.85	2.72	0.15	0.954385965	18.133333	15.31	2.79
E5	2.95	2.72	0.15	0.922033898	18.133333	17.39	2.66
E6	2.95	2.72	0.12	0.922033898	22.666667	21.67	2.26

<i>f_p</i>	<i>f_m</i>	<i>f_{pe}</i>	<i>f_{pa}</i>	<i>E_c</i>	<i>top</i>	<i>bottom</i>
5.47	2.84	0.14	0.44	9614	0.15x0.20	0.15x0.20
5.47	2.84	0.14	0.44	10943	0.15x0.40	0.15x0.20
4.09	2.45	0.11	0.36	11124	0.12x0.40	0.12x0.20
5.47	2.84	0.14	0.44	9782	0.15x0.20	0.15x0.20
5.47	2.84	0.14	0.44	10425	0.15x0.25	0.15x0.25
4.09	2.45	0.11	0.36	11638	0.12x0.25	0.12x0.20



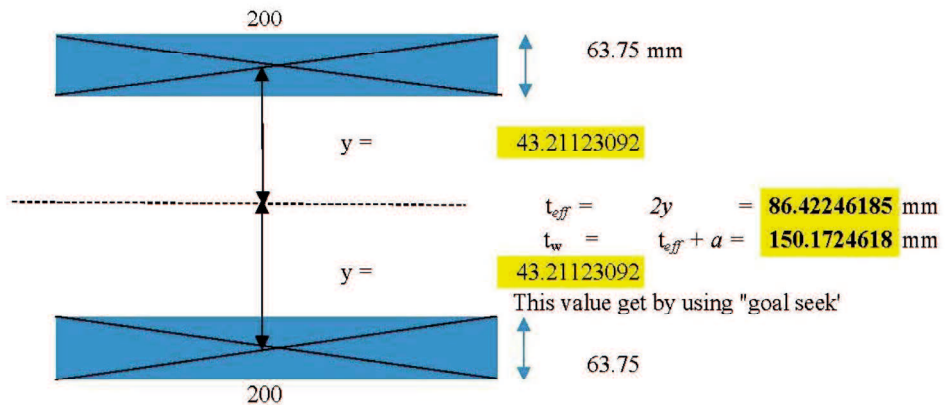
Wall dimension
2.88



$$\begin{aligned}
 I_{tot} &= 1/12 \cdot b \cdot t^3 &= 56250000 \text{ mm}^4 \\
 c &= 0.5 t &= 75 \text{ mm} \\
 b &= 0.85 \\
 a &= 63.75
 \end{aligned}$$

	<i>I</i>	<i>A - b_{eff} · a</i>	<i>y</i> ²
<i>I</i>	4318066.406	12750	?
2	4318066.406	12750	?
Σ	8636132.813		56250000 = <i>I_{ue}</i>

Use "goal seek" to find *y* in order to $I_{tot} = I_{ue}$



	I	$A (bt)$	y^2	$A \cdot y^2$
1	4318066.406	12750	43.21123092	23806934
2	4318066.406	12750	43.21123092	23806934
S	8636132.813			47613867
$SI + SAy^2 =$			$I_{ue} =$	56250000 mm ⁴

e_{crack}	Tension	0.00100 mm	
s		1.2 N/mm ²	
e_{crack}	Compression	0.00300 mm	
s		2.6 N/mm ²	
		E	
f_c	=	19.16	10943.00
$f_p (block)$	=	5.47	2735.00
f_j	=	2.34	877.50
f_m	=	2.84	877.50
f_{up}	average out of plane flexural tensile strength perpendicular		0.14
f_{tpa}	tensile paralel		0.44

A	200 mm	205 =	41000
	63.75 mm	200 =	12750
	210 mm	200 =	42000

P kN	P KPa	P N/mm ²	Analysis by SAP results		Stress	
			T	C	T	C
50	0.00119	1.19048	1587.6	1263.7	0.12452	0.09911
100	0.00238	2.38095	3175.2	2527.4	0.24904	0.19822
150	0.00357	3.57143	9525.7	7582.1	0.74712	0.59467
200	0.00476	4.76190	12701.0	10109.4	0.99615	0.79289
250	0.00595	5.95238	15876.2	12636.8	1.24519	0.99112
300	0.00714	7.14286	19051.5	15164.1	1.49423	1.18934
350	0.00833	8.33333	22226.7	17691.5	1.74327	1.38757
400	0.00952	9.52381	25402.0	20218.8	1.99231	1.58579
450	0.01071	10.71429	28577.2	22746.2	2.24135	1.78401
500	0.01190	11.90476	31752.4	25273.5	2.49039	1.98224
550	0.01310	13.09524	34927.7	27800.9	2.73943	2.18046
600	0.01429	14.28571	38102.9	30328.2	2.98846	2.37868
650	0.01548	15.47619	41278.2	32855.6	3.23750	2.57691
700	0.01667	16.66667	44453.4	35382.9	3.48654	2.77513

P	Tension	compression
50	0.000113 NO CRACK	0.00014 NO CRACK
100	0.000226 NO CRACK	0.00028 NO CRACK
150	0.000678 NO CRACK	0.00085 NO CRACK
200	0.000904 NO CRACK	0.00114 NO CRACK
250	0.001129 CRACK	0.00142 NO CRACK
300	0.001355 CRACK	0.00170 NO CRACK
350	0.001581 CRACK	0.00199 NO CRACK
400	0.001807 CRACK	0.00227 NO CRACK
450	0.002033 CRACK	0.00255 NO CRACK
500	0.002259 CRACK	0.00284 NO CRACK
550	0.002485 CRACK	0.00312 CRACK
600	0.002711 CRACK	0.00341 CRACK
650	0.002937 CRACK	0.00369 CRACK
700	0.003163 CRACK	0.00397 CRACK

Interpolation

y1	y2	x2	x1	x
4.76190476	5.952380952	0.001129	0.000904	0.00100
				5.27001979

y1	y2	x2	x1	x
11.9047619	13.0952381	0.003121853	0.002838048	0.00300
				12.5841013

NOMENCLATURE

AR	Aspect Ratio
A_n	the effective area n of element truss
A_c	the pressure effective area
A_r	the reinforcement effective area
AR	Aspect Ratio
A_t	the tension effective area
a	depth of the equivalent stress block
α'	constants representing contribution of bricks compressive strengths on f_m
α	shape factor of compressive area
b_{eff}	the width of the unit load to be used
β	ratio of brick's elastic modulus to the mortar elastic modulus
β'	constants representing contribution of mortar compressive strengths on f_m
β_l	function of strength class of materials
c	the distance from the center of thickness of masonry wall to the top
d_t	diagonal truss element
δ	geometric properties of cells
δ	displacement
E	Young Modulus
E_b	modulus of elasticity of bricks
E_m	modulus of elasticity of masonry

E_j	modulus of elasticity of mortar
E_{mor}	modulus of elasticity of mortar
\bar{E}_x	average modulus of elasticity in x-direction calculation
\bar{E}_y	average modulus of elasticity in y-direction calculation
E_x	modulus of elasticity in x-direction calculation
E_y	modulus of elasticity in y-direction calculation
E_b^i	modulus elastic moduli of brick in section i
E_m^i	modulus elastic moduli of mortar in section i
E_c	modulus of elasticity of concrete
ε	strain
ε_x	normal strain in x-direction
ε_y	normal strain in y-direction
$\bar{\varepsilon}_{xx}$	average normal strain in x-direction
$\bar{\varepsilon}_{yy}$	average normal strain in y-direction
$\bar{\varepsilon}_{ij}$	average strain vector
ε_{ij}	strain vector
ε'_m	peak strain in masonry, i.e., compressive strain corresponding to f_m _
ε_m	compressive strain in masonry
f_j	compressive strength of mortar
f'_m	compressive prism strength of masonry
f_m	the compressive strength of the mortar
f_b	the compressive strength of the brick

f_c	the compressive strength of the concrete
f'_{me}	the compressive strength of the member of truss
f_{ipe}	average out-of-plane flexural tensile strength perpendicular
f_p	compressive strength of unit masonry
FTM	fictitious truss method
FTMSD	fictitious truss method single diagonal
FTMDD	fictitious truss method double diagonal
G	shear Modulus
\bar{G}	average equivalent shear modulus
γ_{xy}	normal shear strain
$\bar{\gamma}_{xy}$	average normal shear strain
H	height of masonry wall
h_b	thickness of brick
h_t	horizontal truss element
I_{eq}	Inertia unit equivalent of the masonry element
I_n	inertia of element n equivalent of the masonry element
I_{tot}	Inertia unit of the masonry element
ξ	ratio of the height of bricks
θ_d	angle of diagonal truss
σ_u	Ultimate stress
L	length of masonry wall
l_b	long of brick

n	total number of data points
Ω	volume of RVE cell
P	joint load
p	joint load
P_{eq}	joint load equivalent
PoE	Percentage of Error
Poc	percentage of change
Q	uniform load
ρ_{mor}	volume ratio of mortar to the area of the cell
R_{mor}	ratio of mortar
$\bar{\sigma}_{ij}$	average stress vector
σ_{ij}	stress vector
σ_x	normal stress in x-direction
σ_y	normal stress in y-direction
$\bar{\sigma}_{xx}$	average normal stress in x-direction
$\bar{\sigma}_{yy}$	average normal stress in y-direction
t_{eff}	the effective width of a cross section of truss model
v_t	vertical truss
t	the thickness of masonry
t_w	the thickness of the masonry
θ	disparity value from geometric properties
t_m	thickness of mortar

τ_{xy}	normal shear stress
$\bar{\tau}_{xy}$	average normal shear stress
$\gamma_{eq(u)}$	the specific gravity equivalent of unit
$\gamma_{eq(m)}$	the specific gravity equivalent of mortar
ξ	specific gravity factor
γ_u	specific gravity factor unit
γ_m	specific gravity factor mortar
γ_{eq}	the specific gravity equivalent
t_w	the total height of the vertical truss elements
u	deformation in x direction
v	deformation in y direction
$\bar{\nu}_m$	average of Poisson's ratio of masonry
$\bar{\nu}$	average of Poisson's ratio
ν	Poisson Ratio
ν_x	Poisson ratio in x-direction calculation
ν_y	Poisson ratio in y-direction calculation
$\bar{\nu}_x$	average Poisson ratio in x-direction calculation
$\bar{\nu}_y$	average Poisson ratio in y-direction calculation
ν_t	vertical truss element
w_b	wide of brick
W_e	strength of masonry by using experimental
W_{ss}	strength of masonry by using spring–strut method

W_{yl}	strength of masonry by using yield-line method
W_{fl}	strength of masonry by using failure-line method
W_{cs}	strength of masonry by using compressive strut method
W_t	strength of masonry by using FTM in tension
W_c	strength of masonry by using FTM in compression
y	the distance from the center of effective width of a cross section of the masonry wall to the center of element top truss area.

REFERENCES

- Abrams D., Angel R. and Uzarski J. (1996), Out-of-plane strength of unreinforced masonry infill panels. *Earthq. Spectra* 12(4), pp.825–844.
- Abrams, D. P. (2001), Performance-based engineering concepts for unreinforced masonry building structures, *Prog. Struct. Eng. Mater.*, 3(1), pp.48–56.
- Agnihotri P., Singhal V., and Rai D. (2013), Effect of in-plane damage on out-of-plane strength of unreinforced masonry walls, *Eng. Struct.* 57 1–11.
- Alcocer, S.M. and Klinger, R.E., (1994), Masonry Research in the Americas, masonry in the Americas, *American Concrete Institute (ACI) Special Publication*, SP-147, pp.127-169
- Almeida J., Lourenco P., and Barros J. (2002), Characterization of brick and brick-mortar interface under uniaxial tension, *VII International Seminar on Structural Masonry for Developing Countries*.
- Andreus, U. (1996), Failure criteria for masonry panels under in-plane loading, *J. Struct. Eng.*, 122(1), pp.37–46.
- Anil Ö., Tatayoğlu M., and Demirhan M. (2012), Out-of-plane behavior of unreinforced masonry brick walls strengthened with CFRP strips, *Const. Build. Mat.*, 35, pp.614–624.
- Anthoine, A. (1995), Derivation of the in-plane elastic characteristics of masonry through homogenization theory, *Int. J. Solids and Struct.*, 32(2), pp.137-163.
- Anthoine, A. (1997), Homogenization of periodic masonry: plane stress, generalized plane strain or 3D modeling, *Communications in Numerical Methods in Engineering*, 13(5), pp.319-326.

- Anthoine, A., Magonette, G., and Magenes, G. (1994), Shear-compression testing and analysis of brick masonry walls, *Proc. 10th European Conference on Earthquake Engineering*, Vol. 3, pp.1657–1662.
- Arya, A. S., (1992), Masonry and timber structures including earthquake resistant design, Nem Chand & Bros., Roorkee, India.
- Ashihmin, V., N and Povyshev. I., A. (1995) Statistical distributional laws of stresses in polycrystals. *Mathematical modeling of systems and processes*, 3:11–18, Russian.
- Asteris P., Cavaleri L., Di Trapani F. and Tsaris A. (2017), Numerical modelling of out-of-plane response of infilled frames: State of the art and future challenges for the equivalent strut macro models, *Eng. Struct.* 132, pp.110–122.
- ASTM, (1984), Standard test method for splitting tensile strength of masonry units, *ASTM C1006-1984*, West Conshohocken, Pa.
- ASTM, (1989), Specification for aggregate for masonry mortar, *ASTM C114-1989*, West Conshohocken, Pa.
- ASTM, (1997), Specification for portland cement, *ASTM C150-1997*, West Conshohocken, Pa.
- ASTM, (1997), Test Method for young's modulus, tangent modulus, and chord modulus, *ASTM E111-1997*, West Conshohocken, Pa.
- ASTM, (1998), Standard method for constructing and testing masonry prisms used to determine compliance with specified compressive strength of masonry, *ASTM C1314-1998*, West Conshohocken, Pa.
- ASTM, (1998), Standard test methods of sampling and testing brick and structural clay tile, *ASTM C67-1998*, West Conshohocken, Pa.

- ASTM, (1998), Standard method for constructing and testing masonry prisms used to determine compliance with specified compressive strength of masonry, *ASTM C1314-1998*, West Conshohocken, Pa.
- ASTM, (1999), Specification for hydrated lime for masonry purposes, *ASTM C207-1999*, West Conshohocken, Pa.
- ASTM, (1999), Specification for mortar for unit masonry, *ASTM C270-1999*, West Conshohocken, Pa.
- ASTM, (2000), Standard test method for measurement of masonry flexural bond strength, *ASTM C1072-2000*, West Conshohocken, Pa.
- Badoux, M., Elgwady, M. A. and Lestuzzi, P., (2002), Earthquake simulator tests on unreinforced masonry walls before and after upgrading with composites, *Proc. of 12th European Conf. on Earthquake Eng.*, Paper Ref.862.
- Basoenondo, E. (2008), Lateral load response of Cikarang brick wall structures-an experimental study, *Build Environment: Disertasi*.
- Blondet, M. (2005). Construction and maintenance of masonry houses. Lima, Perú: Pontificia Universidad Católica de Perú.
- British Standards Institution, (1992), BS-3921: *Specifications for Clay Bricks*, BSI, London
- Bruneau, M. (1994), State-of-the-art report on seismic performance of unreinforced masonry buildings, *J. Struct. Eng.*, 120(1), pp.230–251.
- Bruneau, M., (1995), Damage to masonry buildings from the 1995 Hansin-Awaji Earthquake-Preliminary Report, *Proc. of the Seventh Canadian Masonry Symp.*, Vol.1, pp 84-95.

- Brunsdon, D. (1994), Study group on earthquake risk buildings 1993/94 report, in *Proc. Technical Conference of the New Zealand National Society for Earthquake Engineering*, pp.1–6.
- Bulsara, V., N., Talreja, R. and Qu, J. (1999) Damage initiation under transverse loading of unidirectional composites with arbitrarily distributed fibers. *Composites science and technology*, 59:673–682, 1999.
- Calvi, G. M. (1999), A displacement-based approach for vulnerability evaluation of classes of buildings, *J. Earthquake Eng.*, 3(3), pp.411–438.
- Cavaleri L., Fossetti M., and Papia M. (2009), Modeling of out-of-plane behavior of masonry walls, *J. Struct. Eng.*, 135(12), pp.1522–1532.
- Cecchi, A., and Di Marco, R. (2002), Homogenized strategy toward constitutive identification of masonry, *J. Eng. Mech.*, 128(6),688-697.
- Cecchi, A., Milani, G., and Tralli, A. (2004), In-plane loaded CFRP reinforced masonry walls: mechanical characteristics by homogenisation procedures, *Comp. Science and Tech.*, 64(13-14), pp.2097-2112.
- Cecchi, A., Milani, G., and Tralli, A. (2005), Out-of-plane loaded CFRP reinforced masonry walls: Mechanical characteristics by homogenization procedures, *Com. Science and Tech.*, 65(10), pp.1480-1500.
- CEN 1999. Eurocode 6: (2005), Design of masonry structures- Part-1-1: General rules for reinforced and unreinforced masonry structures, European Committee for Standardization, 1, 125.
- Cluni, F. and Gusella, V. (2004), Homogenization of non-periodic masonry structures. *Int. J. of Solids and Struct.*, 41(7), pp.1911-1923.

- Costigan, A., Pavia, S. and Kinnane, O. (2015). An experimental evaluation of prediction models for the mechanical behavior of unreinforced, lime-mortar masonry under compression. *Journal of Building Engineering*, 4, pp.283-294.
- Crisafulli, F.J., (1997), Seismic Behaviour of reinforced concrete structures with masonry infills, Ph.D thesis, Dep. of Civil Eng., Univ. of Canterbury, New Zealand, 404 p
- Crisafulli, F.J., Carr, A.J. and Park, R., (1995), Shear strength of unreinforced masonry panels, *Proc. of the Pacific Conf. on Earthquake Eng.*, Vol.3, pp.77-86, Melbourne, Australia.
- D.I.N. (2006). Eurocode 6: Bemessung und Konstruktion von Mauerwerksbauten. Deutschland: Deutsches Institut für Normung.
- Dassault Systèmes (2010), ABAQUS Documentation 6.10.
- Dawe J. and Seah C. (1989), Out-of-plane resistance of concrete masonry infilled panels, *Can. J. Civil Eng.*, 16(6), pp.854–864.
- De Buhan, P. and De Felice, G. (1997), Homogenization approach to the ultimate strength of brick masonry, *J. Mech. and Physics of Solids*, 45(7), pp.1085-1104.
- Dhanasekar M, Page, A.W. and Kleeman P.W. (1985), The failure of brick masonry under biaxial stresses, *Proc. Int. Civil Eng.*, Part 2, 79, pp.295-313.
- Dizhur D., Griffith M., and Ingham J. (2014), Out-of-plane strengthening of unreinforced masonry walls using near surface mounted fibre reinforced polymer strips, *Eng. Struct.*, 59, pp.330–343.
- Doherty, K. T. (2000), An investigation of the weaklinks in the seismic load path of unreinforced masonry buildings, Ph.D thesis, Faculty of Engineering, University of Adelaide, Australia.

- Doherty, K., Griffith, M. C., Lam, N., and Wilson, J. (2002), Displacement-based seismic analysis for out-of-plane bending of unreinforced masonry walls, *Earthquake Eng. Struct. Dyn.*, 31(4), pp.833–850.
- Drougkas, A., Roca, P. and Molins, C. (2015), Numerical prediction of the behavior, strength and elasticity of masonry in compression, *Eng. Struct.*, 90, pp.15-28.
- Drugan, W., J. and Willis, J., R., (1996), A micromechanics-based nonlocal constitutive equation and estimates of representative volume element size for elastic composite. *J. Mech. Phys. Solids*, 44(4). pp. 497–524.
- Drysdale R. and Essawy A. (1988), Out-of-plane bending of concrete block walls, *J. Struct. Eng.*, 114(1), pp.121–133.
- Drysdale, R.G., Hamid, A.A. and Baker, L.R., (1994), Masonry structures, behavior and design, *Prentice Hall Inc., Englewood Cliffs*, 784 p.
- ElGawady, M. A., Lestuzzi, P., and Badoux, M. (2006), Analytical model for the in-plane shear behavior of URM walls retrofitted with FRP, *Comp. Science and Tech.*, 66(3-4), pp.459-474.
- Elhusna, Wahyuni, A. and Gunawan, A. (2014), Performance of clay brick of Bengkulu. *Procedia Eng.*, 95, pp.504-509.
- Ewing, R. D., and Kariotis, J. C. (1981), Methodology for mitigation of seismic hazards in existing unreinforced masonry buildings: Wall testing, out-of-plane, *Tech. Rep.* ABK-TR-04, ABK, A Joint Venture, El Segundo, California.
- Fattal, S.G., and Cattaneo, L.E., (1977), Evaluation of structural properties of masonry in existing buildings, *National Bureau of Standards*, Department of Commerce, Washington.

- Federal Emergency Management Agency (1997), NEHRP commentary on the guidelines for the seismic rehabilitation of buildings, *FEMA Publication 274*, Washington D.C.
- Federal Emergency Management Agency (1997), NEHRP guidelines for the seismic rehabilitation of buildings, *FEMA Publication 273*, Washington D.C.
- Furtado A., Rodrigues H., Arêde A., and Varum H. (2016), Experimental evaluation of out-of-plane capacity of masonry infill walls, *Eng. Struct.*, 111, pp.48–63.
- Gabor, A., Bennani, A., Jacquelin, E. and Lebon, F. (2006), Modeling approaches of the in-plane shear behaviour of unreinforced and FRP strengthened masonry panels, *Comp. Str.*, 74(3), pp.277-288.
- Gere, J. M., & Timoshenko, S. (1986), *Mecánica de Materiales*. México: Grupo Editorial Iberoamérica.
- Gilstrap J. and Dolan C. (1998), Out-of-plane bending of FRP-reinforced masonry walls, *Comp. Sci.* 58(8), pp.1277–1284.
- Griffith M., Vaculik J. (2007), Out-of-plane flexural strength of unreinforced clay brick masonry walls, *TMS J.* Vol. 25 (1), pp. 63-62
- Griffith, M. C., Lam, N. T. K., Wilson, J. L., and Doherty, K. (2004), Experimental investigation of unreinforced brick masonry walls in flexure, *J. Struct. Eng.*, 130(3), pp.423–432.
- Gumaste, K., Nanjunda Rao, K., Venkatarama Reddy, B. and Jagadish, K. (2006), Strength and elasticity of brick masonry prisms and wallettes under compression. *Mater Struct*, 40(2), pp.241-253.
- Hamoush S., McGinley M., P. Mlakar, and M. Terro. (2002), Out-of-plane behavior of surface-reinforced masonry walls, *Constr. Build. Mater.* 16(6), pp.341–351.

- Hashin, Z., (1983), Analysis of composite materials – a survey. *Journal of Applied Mechanics*, 50 pp. 481–505.
- Henderson R., Fricke K., Jones W., Beavers J., and Bennett R. (2003), Summary of a large and small-scale unreinforced masonry infill test program, *J. Struct. Eng.*, 129(12), pp.1667–1675.
- Hendry, A. (1990), *Structural masonry*. Houndmills, Basingstoke: Macmillan.
- Hendry, A.W., Sinha, B.P and Davies, S.R. (1997), *Design of masonry structures*, third edition of load bearing brickwork design, E&FN Spon, UK
- Hilsdorf, H.K. (1967), Investigation into the failure mechanism of brick masonry loaded in axial compression, *Int. Conf. on Masonry Struct. Systems*, Univ. of Texas, Austin.
- I.N.N. (1993), NCh1928.Of93 Albañilería reforzada-requisitos de diseño estructural. norma chilena oficial. Chile: Instituto nacional de normalización.
- I.N.N. (1997), NCh2123.Of97 Albañilería armada-requisitos de diseño estructural. Chile: Instituto nacional de normalización.
- Indra, A., Elfina, S., Nurzal and Nofrianto, H. (2013), Development of making composite clay /silica rha application for improving the quality of red brick in order to create friendly earthquake building materials, *National Strategic Research*, Indonesia.
- Irmschler, H.-J., Schubert, P., and Jäger, W. (2004), *Mauerwerk kalender. deutschland*: Ernst & Sohn.
- Irsyam, M., Dangkoa D.T., Hendriyawan, Hoedajanto D., Hutapea B.M., Kertapati E.K., Boen T., Petersen M. D., (2008), Proposed seismic hazard maps of

Sumatra and Java island and microzonation study of Jakarta city, Indonesia,
J. Earth System Science, 117, S2, pp.865- 878.

Ismail N. and Ingham J. (2016), In-plane and out-of-plane testing of unreinforced masonry walls strengthened using polymer textile reinforced mortar, *Eng. Struct.*, 118, pp.167–177.

Jaramillo, J. D. (2002), Mecanismo de transmision de cargas perpendiculares al plano del muro en muros de mamposteria no reforzada, *Revista de Ingenieria Sismica*, 67, pp.53–78.

Khalaf, F. (2005). New test for determination of masonry tensile bond strength. *J. Mater. Civ. Eng*, 17(6), pp.725-732.

Kaushik H., Rai D. and Jain S. (2007), Stress-strain characteristics of clay brick masonry under uniaxial compression, *J. Mater. Civ. Eng.*, 19(9), pp.728–739.

König, G., Mann, W., and Ötes, A. (1988), Experimental investigations on the behaviour of unreinforced masonry walls under seismically induced loads and lessons derived, *Proc. 9th World Conf. on Earthquake Eng.*, Vol. 8, pp.1117–1122, Tokyo-Kyoto, Japan.

Kuczma, M., Wybranowska, K., (2005) Numerical Homogenization of Elastic Brick Masonry, *Civil and Environmental Engineering Report*, University of Zielona Góra Press, 1-2005, Zielona Góra. Poland

La Mendola L., Accardi M., Cucchiara C. and Licata V. (2014), Nonlinear FE analysis of out-of-plane behaviour of masonry walls with and without CFRP reinforcement, *Constr. Build. Mater.*, 54, pp.190–196.

Lee J., Pande, G., Middleton, J. and Kralj, B. (1996), Numerical modeling of brick masonry panels subject to lateral loadings, *Computers and Structures*, 61(4), pp.735-745.

- Lourenço P.B (1998), Experimental and numerical issues in the modelling of the mechanical behaviour of masonry, Structural Analysis of historical constructions II - P. Roca, J.L. González, E. Oñate and P.B. Lourenço (Eds.) CIMNE, Barcelona
- Lourenço P.B. (1996), Computational strategies for masonry structures, Delft University Press, Stevinweg 1, 2628 CN Delft, The Netherlands.
- Lourenço P.B. and Zucchini A. (2001), A homogenization model for stretcher bond masonry, Computer Methods in Structural Masonry - 5, Eds. T.G. Hughes and G.N. Pande, *Computers & Geotechnics*, UK, pp.60-67.
- Lourenço, P. (1996), Computational strategies for masonry structures, Delft, Netherlands: Delft University Press.
- Lourenço, P., Milani, G., Tralli, A. and Zucchini, A. (2007), Analysis of masonry structures: review of and recent trends in homogenization techniques, *Canadian J. Civil Eng.*, 34(11), pp.1443-1457.
- Lourenço, P., Rots, J. and Blaauwendraad, J. (1998), Continuum model for masonry: parameter estimation and validation, *J. Struct. Eng.*, 124(6), pp.642-652.
- Lu Y. and Panagiotou M.. (2014) Three-dimensional cyclic beam-truss model for nonplanar reinforced concrete walls. *J. Struct. Eng.*, 140(3), pp. 04013071
- Luccioni, B. M., Ambrosini, R. D., and Danesi, R. F. (2004), Analysis of building collapse under blast loads, *Eng. Struct.*, 26(1), pp.63-71.
- Luciano, R. and Sacco, E. (1997), Homogenization technique and damage model for old masonry material, *Int. J. Solids and Struct.*, 34(24), pp.3191-3208.
- Ma, G., Hao, H., and Lu, Y. (2001), Homogenization of masonry using numerical simulations, *J. Eng. Mech.*, 127(5), pp.421-431.

- Maffei, J., Comartin, C. D., Kehoe, B., Kingsley, G. R., and Lizundia, B. (2000), Evaluation of earthquake damaged concrete and masonry wall buildings, *Earthq. Spectra*, 16(1), pp.263–283.
- Magenes, G., and Calvi, G. M. (1997), In-plane seismic response of brick masonry walls, *Earthq. Eng. Struct. Dyn.*, 26(11), pp.1091–1112.
- Martini, K. (1997), Finite element studies in the out-of-plane failure of unreinforced masonry, *Proc., 7th Int. Conf. on computing in Civil and Building Eng.*, C. K. Choi, ed., Korea, pp.179–184.
- McCaffrey, R. (2009), The tectonic framework of the Sumatran subduction zone, *The Annual Review of Earth and Planetary Science*, 37, pp.345–66.
- Milani, G., Lourenço, P. and Tralli, A. (2006), Homogenization approach for the limit analysis of out-of-plane loaded masonry walls, *J. Struct. Eng.*, 132(10), pp.1650-1663.
- Milani, G., Lourenco, P. B., and Tralli, A. (2006a), Homogenised limit analysis of masonry walls, Part I: Failure surfaces, *Computers and Structures*, 84(3-4), pp.166-180.
- Milani, G., Lourenco, P. B., and Tralli, A. (2006b), Homogenised limit analysis of masonry walls, Part II: Structural examples, *Computers and Structures*, 84(3-4), pp.181-195.
- Mistler, M. (2006), Verformungs-basiertes seismisches Bemessungskonzept für Mauerwerksbauten. Aachen, Deutschland: Univ.-Prof. Dr.-Ing. Konstantin Meskouris.
- Mistler, M., Anthoine, A. and Butenweg, C. (2007), In-plane and out-of-plane homogenization of masonry, *Computers and Structures*, 85(17-18), pp.1321-1330.

- Moharrami M., Koutromanos I. and Panagiotou M. (2015), Nonlinear truss modeling method for the analysis of shear failures in reinforced concrete and masonry structures, *Improving the Seismic Performance of Existing Buildings and Other Structures*, pp.74–85.
- Mohebkah, A., Tasnimi, A. and Moghadam, H. (2008), Nonlinear analysis of masonry-infilled steel frames with openings using discrete element method, *J. Const. Steel Res.*, 64(12), pp.1463-1472.
- Moreno-Herrera J., Varela-Rivera J. and Fernandez-Baqueiro L. (2016), Out-of-plane design procedure for confined masonry walls. *J. Struct. Eng.*, 142(2), p.04015126
- Natawidjaja, D.H. (2002), Neotectonics of the Sumatran fault and paleogeodesy of the Sumatran subduction, Ph.D Thesis, California Institute of Technology, USA.
- NEHRP (2000), Recommended provisions for seismic regulations for new buildings and other structures, 2000 edition.
- Noor-E-Khuda S., Dhanasekar M., and Thambiratnam D. (2016), An explicit finite element modelling method for masonry walls under out-of-plane loading, *Eng. Struct.*, 113 pp.103–120.
- Okazaki, K., Pribadi, K. S., Kusumastuti, D. & Saito, T., 2012. Comparison of current construction practices of non-engineered buildings in developing countries. *15th WCEE*, Lisboa,
- Ömer Aydan, Fumihiko Imamura, Tomoji Suzuki, Ismail Febrin, Abdul Hakam, Mas Mera and Patras Rina Devi (2007), A Reconnaissance Report on The Bengkulu Earthquake of September 12, 2007, *Japan Society of Civil Engineers (JSCE)-Japan Association for Earthquake Engineering (JAEE)*, Japan.

- Ostoja, M., Starzewski, (2001), The use, misuse, and abuse of stochastics in mechanics of random media. In Z. Waszczyszyn and J. Pamin, editors, *Eur. Conf. Comp. Mech.*
- Oyguc, R. and Oyguc, E. (2017). 2011 Van Earthquakes: Lessons from Damaged Masonry Structures. *Journal of Performance of Constructed Facilities*, 31(5), p. 062.
- Page A.W. (1981) The biaxial compressive strength of brick masonry, *Proc. Intsn. Civ. Eng.*, Part 2, Vol.71, pp.893-906.
- Pande G. N., Liang J. X. and Middleton J. (1989), Equivalent elastic moduli for brick masonry, *Computers and Geotechnics*, pp.243-265.
- Paquette, J., and Bruneau, M. (2003), Pseudo-dynamic testing of unreinforced masonry building with flexible diaphragm, *J. Struct. Eng.*, 129(6), pp.708–716.
- Paulay, T., and Priestley, M. J. N. (1992), *Seismic Design of Reinforced Concrete and Masonry Buildings*, John Wiley and Sons, New York.
- Pegon, P. and Anthoine, A. (1997), Numerical strategies for solving continuum damage problems with softening: application to the homogenization of masonry., *Computers and Structures*, 64(1-4), pp.623-642.
- Pietruszczak, S. and Niu, X. (1992), A mathematical description of macroscopic behaviour of brick masonry, *Int. J. Solids and Struct.*, 29(5), pp.531-546.
- Putri, P. (2014), Quality study in the reconstruction of brick houses that built after earthquake 2009 in Koto Tengah Sub-district-Padang, *Procedia Eng.*, 95, pp.510-517.
- Rekik, A., Allaoui, S., Gasser, A., Blond, E., Andreev, K. and Sinnema, S. (2015), Experiments and nonlinear homogenization sustaining mean-field theories for

refractory mortar-less masonry: The classical secant procedure and its improved variants, *Euro. J. Mech. - A/Solids*, 49, pp.67-81.

Rots J.G. (1991), Numerical simulation of cracking in structural masonry, *Heron*, 36(2), pp.49-63.

Sahlin, S. (1971), Structural masonry, Prentice-hall inc., Englewood cliffs, New Jersey, 290 p.

Salamon M.D.G. (1968), Elastic moduli of stratified rock mass, *Int. J. Rock. Mech. Min. Sci.*, 5, pp.519-527.

SAP2000, Version 17.3.0 Build 1158. (2015), Structural analysis program, Berkeley, (CA), Computer and Structure, Inc..

Simsir, C.C., Aschheim, M.A. and Anrams, D.P. (2004), Out-of-plane dynamic response of unreinforced masonry bearing walls attached to flexible diaphragms, *Proc. 13th World Conf. on Earthquake Eng.*, Vancouver – Canada, Paper N0. 2045.

SNI 15-2094-1991, Mutu dan Cara Uji - Bata Merah Pejal (in Indonesian), Departemen Perindustrian.

SNI 15-2094-2000, Mutu dan Cara Uji - Bata Merah Pejal (in Indonesian), Departemen Perindustrian

Standards Australia, (2001), Masonry Code, AS3700-2001, Standards Australia, Sydney

Standart Nasional Indonesia SNI 03-2847-2013. (2013), Persyaratan beton struktural untuk bangunan gedung, Badan standarisasi nasional (BSN), Jakarta.

- Stefanou, I., Sab, K. and Heck, J. (2015), Three dimensional homogenization of masonry structures with building blocks of finite strength: a closed form strength domain, *Int. J. Solids and Struct.*, 54, pp.258-270.
- Tomažević, M., and Klemenc, I. (1997), Seismic behaviour of confined masonry walls, *Earthquake Eng. Struct. Dyn.*, 26(10), pp.1059–1071.
- Tomazevic, M. (1999), Earthquake-Resistant Design of Masonry Buildings, Series on Innovation in Structures and Construction, Vol.I, Chapter 3, Masonry Materials and Construction Systems, Imperial College Press.
- Trusov, P., V., and Keller, I., E., (1997) Theory of constitutive relation. Part I. *Perm State Technical University, Perm.*, in Russian.
- Tu Y., Chuang T., Liu P. and Yang Y. (2010), Out-of-plane shaking table tests on unreinforced masonry panels in RC frames, *Eng. Struct.* 32(12), pp.3925–3935.
- Tzamtzis A.D., (2003), Finite element modeling of cracks and joints in discontinuous structural systems, 16th ASCE Engineering Mechanics Conference, July 16-18 2003, University of Washington, Seattle.
- United Nations Industrial Development Organization (UNIDO) (1978a), First Progress Report on Improved Brickwork: Mortar And Bricklaying, Technical Paper No. 11, Bandung, 43 p.
- United Nations Industrial Development Organization (UNIDO) (1978b), Second Progress Report on Improved Brickwork: Testing of Brickwork I, *Technical Paper* No. 12, Bandung, 58 p.
- Van Mier. J.G.M (1997), Fracture processes of concrete. *CRC Press, Inc.*, USA,

- Varela-Rivera J., Moreno-Herrera J., Lopez-Gutierrez I. and Fernandez-Baqueiro. L. (2012a), Out-of-plane strength of confined masonry walls, *J. Struct. Eng.*, 138(11), pp.1331–1341.
- Varela-Rivera J., Navarrete-Macias D., Fernandez-Baqueiro L. and Moreno E. (2011), Out-of-plane behaviour of confined masonry walls, *Eng. Struct.*, 33(5), pp.1734–1741.
- Varela-Rivera J., Polanco-May M., Fernandez-Baqueiro L., and Moreno E. (2012b), Confined masonry walls subjected to combined axial loads and out-of-plane uniform pressures, *Can. J. Civil Eng.*, 39(4), pp.439–447.
- Vasconcelos, G., and Lourenço, P. B. (2009), In-plane experimental behavior of stone masonry walls under cyclic loading, *J. Struct. Eng.*, 135(10), pp.1269–1277.
- Wang, G., Li, S., Nguyen, H. and Sitar, N. (2007), Effective elastic stiffness for periodic masonry structures via eigens train homogenization. *J. Mater. Civ. Eng.*, 19(3), pp.269-277.
- Willis C., Seracino R., and Griffith M. (2010), Out-of-plane strength of brick masonry retrofitted with horizontal NSM CFRP strips. *Eng. Struct.*, 32(2), pp.547–555.
- Wisnumurti, Dewi, S. and Soehardjono, A. (2014), Strength reduction factor (R) and displacement amplification factor (Cd) of confined masonry wall with local brick in Indonesia, *Procedia Eng.*, 95, pp.172-177.
- Wu, C. Q. and Ha, H. (2006), Derivation of 3D masonry properties using numerical homogenization technique, *Int. J. Numerical Methods in Eng.*, 66(11), pp.1717-1737.
- Wu, C. Q. and Hao, H. (2007), Safe scaled distance for masonry infilled RC frame structures subjected to airblast loads, *J. Performance of Constructed Facilities*, 21(6), pp.422-431.

- Zachariasen, M., Sieh, K., Taylor, F. W., Edwards, R. L. and Hantoro, W. S. (1999), Submergence and uplift associated with the giant 1833 Sumatran subduction earthquake: evidence from coral micro - atolls. *J. Geophysical Res.*, 104, pp.895-919.
- Zavalis, R., Jonaitis, B. and Lourenco, P. (2014), Analysis of bed joint influence on masonry modulus of elasticity, *9th Int. Masonry Conf.*, pp.1-11.
- Zhang X., Singh S., Bull D., and Cooke N. (2001), Out-of-plane performance of reinforced masonry walls with openings, *J. Struct. Eng.*, 127(1), pp.51–57.
- Zucchini, A. and Lourenco, P. B. (2002), A micro-mechanical model for the homogenization of masonry, *Int. J. Solids and Struct.*, 39(12), pp.3233-3255.
- Zucchini, A. and Lourenco, P. B. (2004), A coupled homogenisation-damage model for masonry cracking, *Computers and Structures*, 82(11-12), pp.917-929.

RESEARCH ACHIEVEMENT

Research Article

Proposal of Design Formulae for Equivalent Elasticity of Masonry Structures Made with Bricks of Low Modulus

Muhammad Ridwan,¹ Isamu Yoshitake,² and Ayman Y. Nassif³

¹Department of Civil Engineering, Padang Institute of Technology, Jalan Gajah Mada Kandis Nanggalo, Padang, Indonesia

²Department of Civil and Environmental Engineering, Yamaguchi University, Tokiwadai 2-16-1, Ube, Yamaguchi 755-8611, Japan

³School of Civil Engineering and Surveying, University of Portsmouth, Portsmouth PO1 3AH, UK

Correspondence should be addressed to Muhammad Ridwan; mhd.rid.wan.itp@gmail.com

Received 14 August 2016; Revised 20 October 2016; Accepted 20 December 2016; Published 17 January 2017

Academic Editor: Gianmarco de Felice

Copyright © 2017 Muhammad Ridwan et al. This is an open access article distributed under the Creative Commons Attribution License, which permits unrestricted use, distribution, and reproduction in any medium, provided the original work is properly cited.

Bricks of low elastic modulus are occasionally used in some developing countries, such as Indonesia and India. Most of the previous research efforts focused on masonry structures built with bricks of considerably high elastic modulus. The objective of this study is to quantify the equivalent elastic modulus of lower-stiffness masonry structures, when the mortar has a higher modulus of elasticity than the bricks, by employing finite element (FE) simulations and adopting the homogenization technique. The reported numerical simulations adopted the two-dimensional representative volume elements (RVEs) using quadrilateral elements with four nodes. The equivalent elastic moduli of composite elements with various bricks and mortar were quantified. The numerically estimated equivalent elastic moduli from the FE simulations were verified using previously established test data. Hence, a new simplified formula for the calculation of the equivalent modulus of elasticity of such masonry structures is proposed in the present study.

1. Introduction

Brick masonry (BM) is a building construction method in which a two-phase composite material is formed of regularly distributed brick and mortar [1]. Usually, the bricks show higher values for compressive strength and stiffness than the mortar. However, the opposite is true in some of the developing countries. For example, the mechanical properties of bricks in some areas of Indonesia show significantly lower values than those of mortar because construction materials are sometimes manufactured in family-run industries [2]. In spite of the use of low-quality bricks, the design code for masonry structures in Indonesia (SNI-2094-2000) is based on the design code of other countries, namely, the DIN 105 standard of Germany and the ASTM C 67-94 standard of the USA.

Hence, most investigations are focused on bricks showing higher strength and when compared to the mortar used in masonry structures. However, as mentioned above, this is not always the case ([2, 3]) in some developing countries. It was reported in [2] that bricks in Payakumbuh, located in

the West Sumatera Province of Indonesia, had a significantly low compressive strength of 2.9 MPa on an average. Similarly, Putri [4] reported a brick strength of 2.5 MPa in Padang city. Elhusna et al. [5] observed that the compressive strength of bricks in Bengkulu Province was within the range of 2.4–6.7 MPa. Wisnumurti et al. [6] investigated the strength of bricks from four different areas in East Java. According to their investigations, the compressive strength was within the range of 0.55–0.9 MPa, and the modulus of elasticity of the low-quality bricks was within the range of 279–571 MPa. In addition, Basoenondo [7] reported that the compressive strength and the modulus of elasticity of bricks in the West Java Province were 0.5–2.87 MPa and 220–540 MPa, respectively. It is noteworthy that the test was based on the American standard ASTM E-111 owing to the lack of an Indonesian standard for the evaluation of the elastic modulus of bricks.

General-purpose bricks in western countries have higher strength and stiffness than mortar, as discussed by [3]. They reported that bricks in India have a relatively lower strength (3–20 MPa) and elastic modulus (300–15000 MPa). Similarly [7], Indonesian bricks have lower strength and stiffness.

The general theory is based on the assumption that mechanical properties of brick elements are higher than those of mortar (Paulay and Priestly [8]). In most cases, the ideal elasticity used in the design refers to formulae specified in overseas regulation. These assumptions may result in inappropriate design for the construction of masonry structures using Indonesian bricks.

Finite element (FE) simulations are often used to analyze and design such masonry structural systems. The challenges in numerical modeling of the behavior of large-scale masonry systems have led to the development of techniques such as homogenization [22]. Lourenço et al. [22] reviewed the recent trends in homogenization techniques. They discussed different homogenization techniques available in published literature, and special attention was paid to the micromechanical-based model and the one based on polynomial expansion of the microstress field.

The homogenization techniques are based on establishing constitutive relations in terms of averaged stresses and strains from the geometry and constitutive relations of the individual components. The popularity of such techniques has increased in the masonry community during the last decade ([1, 12, 14, 15, 21–25]).

The techniques of masonry homogenization can be classified into three types: traditional homogenization, numerical homogenization, and micromechanical and microstructural models. Pande et al. [14], Hendry [26], and Pietruszczak and Niu [21] used the traditional homogenization with an empirical approach to estimate the volume ratio effects on the physical and the mechanical properties of bricks and mortar. Equivalent elastic properties were determined for a brick-mortar system made with equally spaced layers. In addition, a simplified geometry to represent the complex geometry of the representative cell was adopted so that a close-form solution to the homogenization problem would be possible. This method is suitable for modeling the linear elastic behavior and for a relatively simple modeling of the nonlinear behavior of masonry structures.

Anthoine [15], Mistler et al. [19], Pegon and Anthoine [23], Luciano and Sacco [24], Ma et al. [1], Zucchini and Lourenço [12], and Anthoine [25] developed the numerical homogenization theory, which is applicable to FE simulations of masonry wall structures. It is used to apply the homogenization theory for masonry wall consisting of the periodic arrangement of unit and mortar as cell. Owing to the complexity of a masonry basic cell, it is necessary to use the finite element method to obtain a numerical solution to problems. This approach is suitable for analyzing the nonlinear behavior of the complex masonry basic cell by solving the problem for all possible macroscopic loading histories.

Luciano and Sacco [24], Ma et al. [1], and Zucchini and Lourenço [12] proposed a theory based on the micromechanical and macrostructural concepts. Their model contained representative volume elements and constitutive elements for all geometries. Although this approach is very useful, its applications are limited because it is difficult to determine several parameters in the micromechanical model for macroscopic analysis.

TABLE 1: Moduli of elasticity for homogenization.

Author(s)	E_{brick} (MPa)	E_{mortar} (MPa)
Stefanou et al. [9]	6740	1700
Cluni and Gusella [10]	12500	1200
Cecchi and Di Marco [11]	1000	$E_{\text{mortar}}/E_b < 1$
Zucchini and Lourenço [12]	20000	$1 < E_b/E_{\text{mortar}} < 1000$
Rekik et al. [13]	10000	0.49
Pande et al. [14]	11000	$E_b/E_{\text{mortar}} = 1.1-11$
Anthoine [15]	11000	2200
Lee et al. [16]	22000	7400
Gabor et al. [17]	13000	4000
Lourenço [18]	20000	2000

Homogenization typically has two different models, namely, discrete and continuum models. Mohebbkhah et al. [27] used discrete models for nonlinear static analysis. They performed simulations using the model for analyzing the fracture behavior of small laboratory panels and verified the model with experimental data. Lourenço et al. [28] used continuum models to analyze masonry structures. The model is appropriate for analyzing anisotropic elastic and inelastic behaviors; it is also suitable for nonlinear static analysis, such as in case of large-scale masonry walls.

The generalization of the homogenization procedure for out-of-plane behavior of masonry [29] can be applied to periodic composite materials. There are two or more units of masonry, such as stones, bricks, and hollow bricks. Mistler et al. [19] examined the effect of the elastic properties on a brick masonry structure. They used the numerical homogenization technique to confirm the effectiveness of the generalization of the homogenization procedure. Pegon and Anthoine [23] developed a homogenization theory for studying the macroscopic nonlinear behavior of masonry. Lourenço [18] used a micromechanical model of homogenization for three-dimensional numerical simulations. The study developed a representative volume element system using multiparametrical representations of the elastic properties of masonry. It was observed that typical mortar has a lower elasticity than bricks in the homogenization process (Table 1).

The purpose of the present study is to numerically determine the equivalent elastic modulus of a brick masonry construction, assuming that the elastic modulus of mortar (E_{mor}) is higher than that of bricks (E_b). The analysis in the present study was based on a numerical simulation using the homogenization technique. The fundamental model is a two-dimensional (2D) representative volume element (RVE) formulation. The proposed analytical approach can significantly contribute to a safer analysis and design of masonry structural systems built with low-quality bricks in various developing countries, such as Indonesia.

2. Approach of the Solution

2.1. Representative Element. The representative volume element (RVE) is a typical unit of masonry; it was selected to represent brick masonry. We considered a masonry wall Ω ,

consisting of a periodic arrangement of masonry units and mortar joints, as shown in Figure 1. The periodicity allows Ω to be regarded as the repetition of the RVE [22].

Ma et al. [1] stated that a masonry RVE should include all the participating materials, constitute the entire structure in a periodic and continuous distribution, and be the minimum unit satisfying the first two conditions.

The RVE cell is classified into two types: RVE-1 and RVE-2. The cell dimensions of these two types of cells are the same; however, the arrangement of bricks and mortar in the cells are different. Ma et al. [1] compared both RVEs and observed that their stress-strain curves under the condition of vertical compression without applying horizontal restrains are the same. Figure 1 shows an RVE. It provides a valuable dividing boundary between the discrete and continuum models. Equivalent stress-strain relations of the RVE were homogenized by applying a compatible, distributed displacement loading along the vertical and horizontal directions and a positive-negative horizontal displacement loading on the top and bottom of the RVE surfaces [1].

The average stress and strain can be calculated via the following equations:

$$\begin{aligned}\bar{\sigma}_{ij} &= \frac{1}{|\Omega|} \int_{\Omega} \sigma_{ij} d\Omega, \\ \bar{\varepsilon}_{ij} &= \frac{1}{|\Omega|} \int_{\Omega} \varepsilon_{ij} d\Omega,\end{aligned}\quad (1)$$

where Ω is volume of the RVE cell.

The elastic parameters of the RVE can be derived from the simulated stress-strain relation.

2.2. Constitutive Equation. Isotropic, linear elastic materials were used for both the brick and mortar. The constitutive stress-strain relations are presented in the following matrix:

$$\begin{Bmatrix} \sigma_x \\ \sigma_y \\ \tau_{xy} \end{Bmatrix} = \frac{E}{1-\nu^2} \begin{bmatrix} 1 & \nu & 0 \\ \nu & 1 & 0 \\ 0 & 0 & \frac{1-\nu}{2} \end{bmatrix} \begin{Bmatrix} \varepsilon_x \\ \varepsilon_y \\ \gamma_{xy} \end{Bmatrix}. \quad (2)$$

Here, E and ν are Young's modulus and Poisson's ratio, respectively, which were applied for each material, individually. Five independent material properties (E_x , E_y , ν_x , ν_y , and G) are used to constitute the equation for the isotropic material under the plane stress condition, which is expressed as

$$\begin{Bmatrix} \bar{\sigma}_{xx} \\ \bar{\sigma}_{yy} \\ \bar{\tau}_{xy} \end{Bmatrix} = \begin{bmatrix} \frac{\bar{E}_{11}}{1-\bar{\nu}_{12}\bar{\nu}_{21}} & \frac{\bar{E}_{11}\bar{\nu}_{21}}{1-\bar{\nu}_{12}\bar{\nu}_{21}} & 0 \\ \frac{\bar{E}_{22}\bar{\nu}_{12}}{1-\bar{\nu}_{12}\bar{\nu}_{21}} & \frac{\bar{E}_{22}}{1-\bar{\nu}_{12}\bar{\nu}_{21}} & 0 \\ 0 & 0 & \bar{G} \end{bmatrix} \begin{Bmatrix} \bar{\varepsilon}_{xx} \\ \bar{\varepsilon}_{yy} \\ \bar{\gamma}_{xy} \end{Bmatrix}. \quad (3)$$

The effective properties of the brick masonry structure can be calculated from (3), and a set of numerical solutions were derived under certain boundary conditions. The numerical simulation results were combined using a nonlinear regression process.

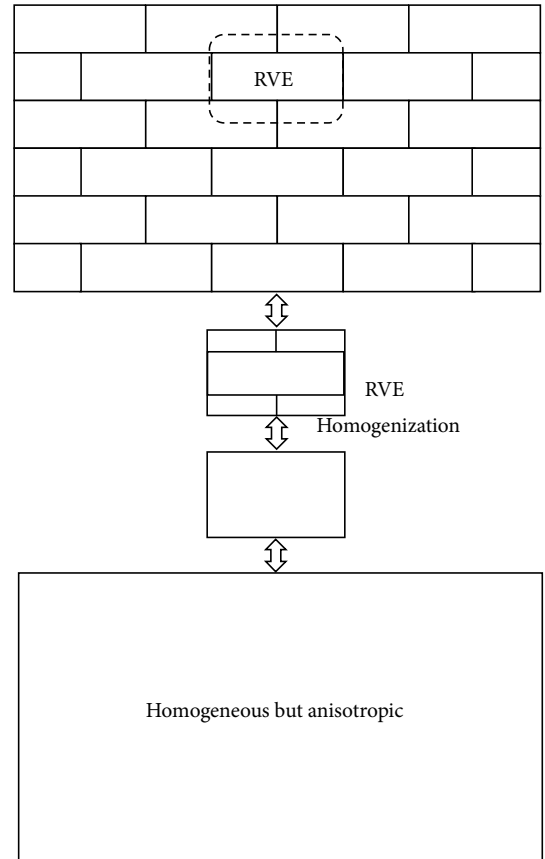


FIGURE 1: Homogenization of masonry material.

3. Numerical Simulations

3.1. Simulation Model. The physical models of the RVEs (RVE-1 and RVE-2) used in the present numerical simulation are shown in Figure 2. Both were used to obtain the differences in elasticity, Poisson's ratio, and shear moduli between the RVE-1 and RVE-2. For each RVE cell, three boundary conditions (BCs) and a displacement load were applied; the FE simulation was realized through the FE program SAP2000-V17. The three BCs will be explained in Section 3.3. Then, the values of E , ν , and G were calculated using (4)–(7). The elasticity and Poisson's ratio were used as baseline data, and various data measurements for elasticity were obtained from the FE simulation.

Figure 3 shows the quadrilateral (Q4) finite element with four nodes and eight degrees of freedom (DOF) used to discretize the problem in the numerical investigation.

The RVE-1 and RVE-2 cells consisted of 3,360 elements, 3,485 nodes, and 6,970 DOF. The brick and the mortar were discretized individually. The dimensions of the cell were $250 \times 120 \times 65$ mm, and the assumed thickness of the mortar was 15 mm.

Ma et al. [1] also applied both the models and obtained the same numerical results. The numerical results in the present study indicated that the RVE was able to represent the material properties at the unit volume level. Thus, all

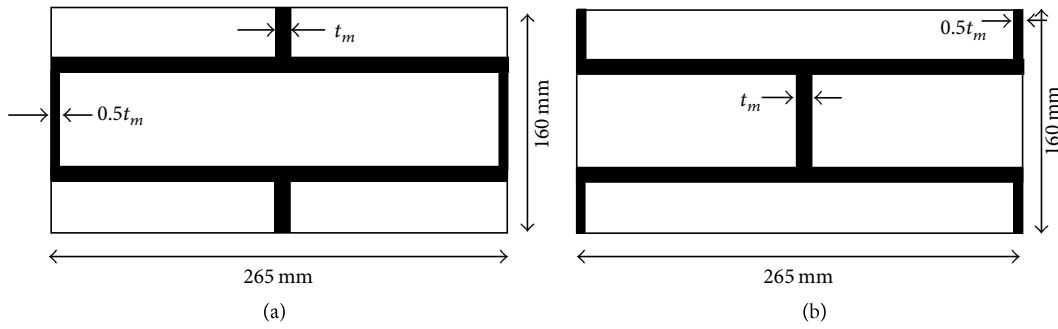


FIGURE 2: Model of masonry cells: (a) RVE-1; (b) RVE-2.

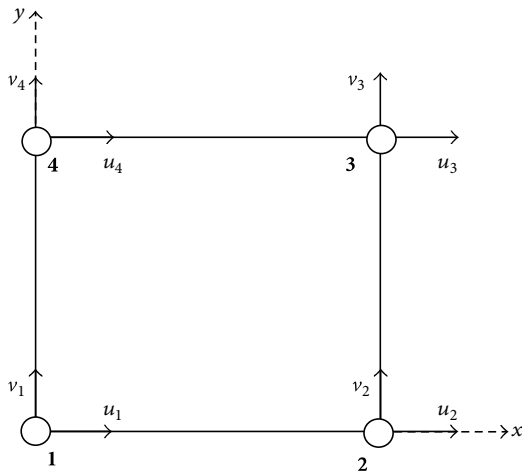


FIGURE 3: Finite element Q4 used in numerical analysis.

TABLE 2: Material parameter for brick and mortar.

Material	$E_x = E_y$ (MPa)	$\nu_x = \nu_y$	$G = E/2(1 + \nu)$ (MPa)
Brick	11000	0.2	4580
Mortar	2200	0.25	880

E_x, E_y = Young's modulus [MPa], G = Kirchhoff's modulus [MPa], ν_x, ν_y = Poisson's ratios.

subsequent calculations were performed with the RVE-1 model as the RVE.

3.2. Materials. The material properties for the validation of the model were obtained from the experimental and simulation results published by Pegon and Anthoine [23] and Ma et al. [1] (Table 2). These material properties are used to ensure applying FE program for the RVE model. Then, the material properties of mortar have higher and lower elasticity than the brick which can be used to the simulation.

3.3. Boundary Condition. Ma et al. [1] simulated various BCs. Three state groups of BCs were applied to the RVE model. These included the compression-compression stress state, the compression-tension state, and the compression-tension-shear stress state. Each group had six BC cases. Ma et al. [1]

stated that the elastic modulus could be obtained from the abovementioned groups using three BC cases. Figure 4 shows the three load cases and the boundary displacements that were used in present study. There were certain displacement boundary conditions: (1) $u \neq 0, v = 0, \bar{\epsilon}_{xx} \neq 0, \bar{\epsilon}_{yy} = 0,$ and $\bar{\gamma}_{xy} = 0$ were used for horizontal compression, (2) $v \neq 0, u = 0, \bar{\epsilon}_{yy} \neq 0, \bar{\epsilon}_{xx} = 0,$ and $\bar{\gamma}_{xy} = 0$ were used for vertical compression, and (3) $u \neq 0, v = 0, \bar{\epsilon}_{xx} = 0, \bar{\epsilon}_{yy} = 0,$ and $\bar{\gamma}_{xy} \neq 0$ were used for horizontal shear. A displacement of approximately 0.05 mm was applied to the nonzero side of the cell. The zero-displacement side was constrained to achieve simplicity in calculations and homogenization of the linear static materials.

3.4. Equivalent Elastic Modulus Calculation. The average values of stress and strain can be calculated by employing (1) as well as the FE simulation results. The effective material parameters of the masonry structure can be estimated as these for an equivalent, homogeneous orthotropic material by using (4)–(7) [1]:

$$\bar{\nu}_{yx} = \frac{\bar{\sigma}_{xx}^{(2)}}{\bar{\sigma}_{yy}^{(2)}}, \quad (4)$$

$$\bar{\nu}_{xy} = \frac{\bar{\sigma}_{yy}^{(1)}}{\bar{\sigma}_{xx}^{(1)}},$$

$$\bar{E}_{xx} = \frac{\bar{\sigma}_{xx}^{(1)}(1 - \bar{\nu}_{xy}\bar{\nu}_{yx})}{\bar{\epsilon}_{xx}^{(1)}} \quad (5)$$

$$= \bar{\sigma}_{xx}^{(1)} \frac{1 - (\bar{\sigma}_{xx}^{(2)}/\bar{\sigma}_{yy}^{(2)}) (\bar{\sigma}_{yy}^{(1)}/\bar{\sigma}_{xx}^{(1)})}{\bar{\epsilon}_{xx}^{(1)}},$$

$$\bar{E}_{yy} = \frac{\bar{\sigma}_{yy}^{(2)}(1 - \bar{\nu}_x\bar{\nu}_y)}{\bar{\epsilon}_y^{(2)}} \quad (6)$$

$$= \bar{\sigma}_{xx}^{(2)} \frac{1 - (\bar{\sigma}_{xx}^{(2)}/\bar{\sigma}_{yy}^{(2)}) (\bar{\sigma}_{yy}^{(1)}/\bar{\sigma}_{xx}^{(1)})}{\bar{\epsilon}_{yy}^{(2)}},$$

$$\bar{G} = \frac{\bar{\tau}_{xy}^{(3)}}{\bar{\gamma}_{xy}^{(3)}}. \quad (7)$$

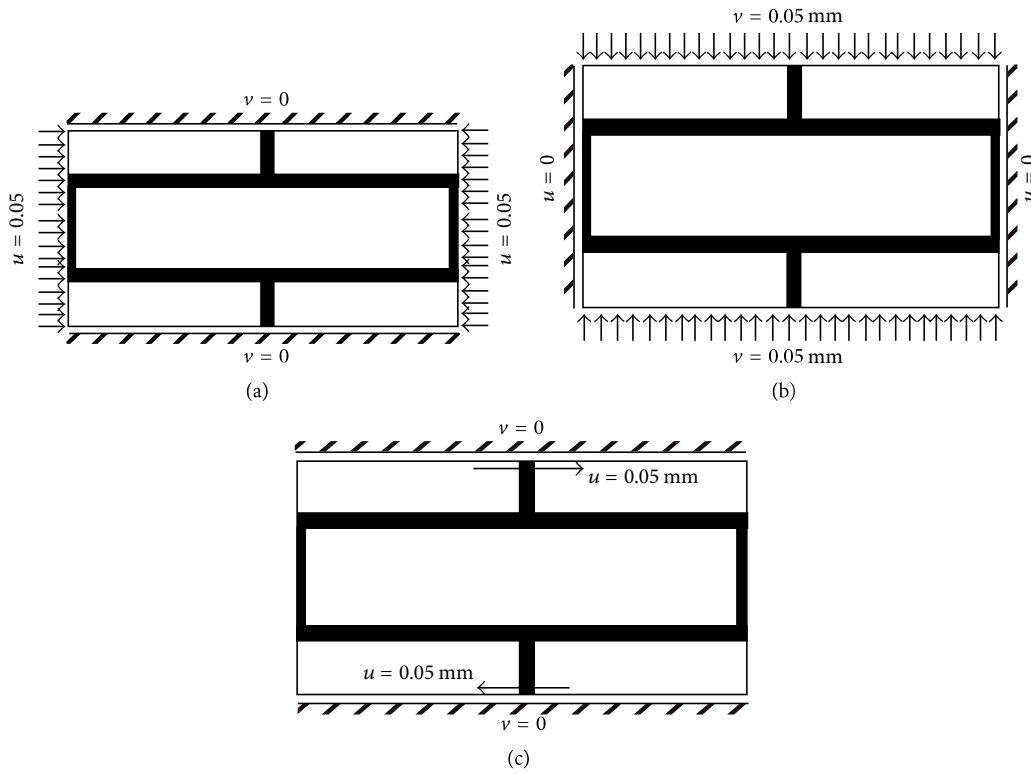


FIGURE 4: Load cases of imposed boundary displacement: (a) load case 1: horizontal compression; (b) load case 2: vertical compression force; (c) load case 3: horizontal shear force.

The superscript index ($i = 1, 2$) denotes the BC case. Subsequently, the simulations were performed with a wide range of elasticity and Poisson's ratio values. Then, nonlinear regression was applied to determine the trend line of the simulation and the basis of the formulation. The formula can represent the case $E_{mor} > E_b$ as well as the case where $E_{mor} < E_b$. The equivalent elastic modulus is the average value of E_{xx} and E_{yy} in the simulation (see (5) and (6)).

To ensure the accuracy of the results, the validation and verification were performed by comparing the results with the numerical and experimental results obtained in other research works [1, 19, 30]. The simulation results were analyzed to develop the empirical formula proposed in this work.

4. Results and Discussion

4.1. Equivalent Elastic Modulus. In this study, the elasticity values of the brick are 1,000 MPa, 2,000 MPa, 5,000 MPa, and 10,000 MPa. The elasticity values of mortar are 0.2 to 5 times the elasticity of the brick. Poisson's ratio was assumed to be 0.25, where $\nu_x = \nu_y$. Each of these data was applied to every load case (RVE-1 and RVE-2).

The elastic modulus of the mortar and brick are the main input data in the numerical simulation. The ratio of the elastic modulus of mortar to that of the brick is called the ratio of mortar (R_{mor}). The value of R_{mor} changes depending on the elasticity of both the materials, bricks, and mortar, in the unit cell.

Additionally, the value of R_{mor} was also influenced by the dimensions of the two elements. The Indonesian code for masonry (SNI 15-2094-2000) regulates the dimensions of bricks with diverse sizes, which are 65 ± 2 to 80 ± 3 mm in height, 92 ± 2 to 110 ± 2 mm in width, and 190 ± 4 to 230 ± 5 mm in length. Changes in the thickness of either the brick or mortar t affect the value of R_{mor} . Here, the thickness of the mortar is set to $t_m \leq 0.5h_b$, where h_b is the thickness of brick. Therefore, by using a mortar thickness of $0.5h_b$, the ratio of the volume of the mortar would reach its maximum value. It could reach up to 47% if volume of mortar divided by RVE unit when the dimensions of bricks are $h_b = 65$ mm, $l_b = 250$ mm, and $w_b = 110$ mm.

The change in the volume ratio influences the stress-strain distribution in the unit cell.

Therefore, it will affect the value of Poisson's ratio and that of the equivalent elasticity of the masonry structure. Thus, for the case $E_{mor} > E_b$ or $R_{mor} > 1$, higher mortar elasticity increases the equivalent elastic modulus of the masonry structure.

Figure 5 shows the simulation results and regression curves between the R_{mor} and E_m where E_m is the equivalent elastic modulus of the masonry structure. It is remarkable that the coefficient of correlation is established at a value of 0.9974. The best equation of R_{mor} is power trend line with the power value is 0.2798. This value did not change for various E_b ; however, there is only a slight difference in the elasticity value of the brick. Based on the results, the proposed

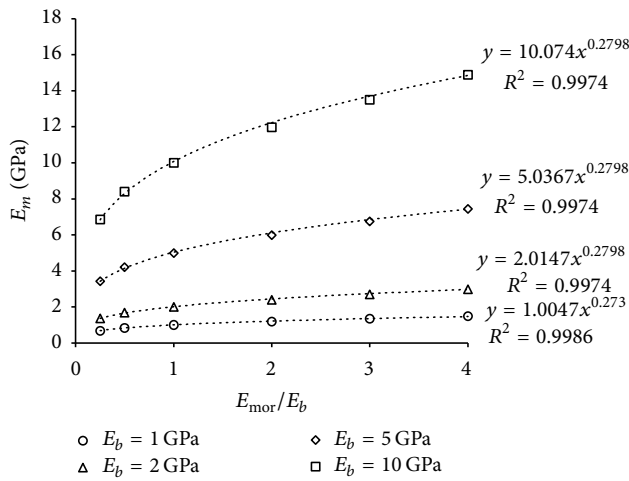


FIGURE 5: Simulation results of equivalent elastic moduli of brick masonry.

equations for the equivalent elastic modulus in the simulation are presented as follows:

$$E_m = E_b (R_{mor})^{\delta+\theta}, \quad (8)$$

where $R_{mor} = E_{mor}/E_b$.

The superscript δ denotes the geometric properties of the cells and θ is a disparity value from the geometric properties to the ratio of the elastic modulus of mortar.

The value δ is given by the following equation:

$$\delta = 0.33 \left(\rho_{mor} + \bar{\nu} + \frac{t_m}{h_b} \right), \quad (9)$$

where ρ_{mor} is the volume ratio of mortar to the area of the cell, $\rho_{mor} = t_m(t_m + h_b + l_b)/(t_m(t_m + h_b + l_b) + (h_b l_b))$; $\bar{\nu}$ is the average Poisson's ratio (brick and mortar); $\bar{\nu} = 0.5(\nu_{mor} + \nu_b)$; t_m/h_b is the ratio of the thickness of the mortar to that of the brick

The disparity value θ can be calculated as follows:

If $R_{mor} > 1$, the following expression can be used:

$$\theta = 0.002 (R_{mor}^2 + R_{mor} + 1). \quad (10)$$

If $R_{mor} < 1$, the following expression can be used:

$$\theta = 0.002 \left(\left(\frac{1}{R_{mor}} \right)^2 + \frac{1}{R_{mor}} + 1 \right). \quad (11)$$

The simulation results obtained from using this formula are suitable for cases of ratios from 0.2 to 5.0. Figure 5 shows simulation results using brick elasticity values of 1, 2, 5, and 10 GPa. The result confirms that the elasticity of the masonry structure increases in accordance with the mortar ratio R_{mor} . Figure 5 also shows that the gradient of each curve is different for each R_{mor} .

The percentage of change (Poc) was applied to quantify the changes of gradient in each curve. The Poc is an index of how much a quantity has increased or decreased with respect

to the original amount. Therefore, the Poc can be obtained from

$$Poc = \frac{E_m - E_b}{E_b} 100\%. \quad (12)$$

Table 4 provides the percentage of change for the curves in Figure 5, where for any change in R_{mor} for each E_b , it remains the same. To obtain the equivalent elastic modulus of the masonry structure with a different gradient, (13) can be employed:

$$E_{m,(poc)} = E_b (1 + Poc). \quad (13)$$

This illustrates that the elasticity of the masonry structure will increase linearly with an increase in R_{mor} for each E_b . Table 5 lists some examples of E_m . The results indicate that the gradient for each value of E_b and R_{mor} is different, but at the same R_{mor} , the Poc is the same. This indicates that an increase in the R_{mor} value influences the stress distribution of the elements in the cells and increases the equivalent elastic modulus of the masonry structure. Conversely, a decrease in the elasticity of mortar would minimize the equivalent elastic modulus of the masonry structure. From the above discussion, we can conclude that it is beneficial to increase the elasticity of the bricks if the elasticity of mortar is higher than the elasticity of the bricks.

4.2. Poisson's Ratio and Shear Modulus. Poisson's ratio describes the transverse strain; therefore, it is obviously related to shear. The shear modulus, usually abbreviated as G , plays the same role in describing shear as Young's modulus does in describing the longitudinal strain. It is defined as $G = \text{shear stress}/\text{shear strain}$.

The shear modulus G can be calculated in terms of E and ν : $G = E/2(1 + \nu)$. As ν ranges from 1/4 to 1/3 for most rocks, therefore that G is approximately calculated as $0.4E$.

The average Poisson's ratio decreased linearly as the R_{mor} value increased. The t equivalent Poisson's ratio can be expressed as follows.

If $R_{mor} < 1$, the following expression can be used:

$$\bar{\nu}_m = \bar{\nu} - 0.015 \left(\frac{1}{R_{mor}} \right). \quad (14)$$

If $R_{mor} > 1$, the following expression can be used:

$$\bar{\nu}_m = \bar{\nu} - 0.015 R_{mor}. \quad (15)$$

Poisson's ratio of the masonry structure decreased by approximately 0.015 times the R_{mor} value owing to the assumption that Poisson's ratio of the brick is smaller than that of mortar.

In present study, the shear modulus was obtained from the simulation results using (7). The range of the estimated G was 60–70% of E_m because of the lower Poisson's ratio estimated in the simulation.

The vertical deformation (y direction) and the lateral deformation (x direction) are different owing to Poisson's effect. The effect may lead to the increase of the equivalent

\bar{G} . Using (14) and (15), the equivalent shear modulus \bar{G} can be expressed as in

$$\bar{G} = \frac{E_m}{1.3(1 + \bar{\nu})}. \quad (16)$$

4.3. Verification and Validation. The numerical simulation results were compared to the results of the simulation conducted by Wang et al. [20], Ma et al. [1], and Mistler et al. [19], as given in Table 3. It is evident that the 2D plane stress analysis results reported by Mistler et al. [19] are similar to those in the present work. However, \bar{E}_y , $\bar{\nu}_y$, and \bar{G} present slight differences because the input data used were different. It should be noted that the average horizontal elastic modulus of the masonry structure was greater than that in the vertical direction. The calculated average value of the equivalent elasticity agreed very well with the experimental data obtained by Mistler et al. [19] on the 2D plane stress and by and Ma et al. [1]. By employing the same input data, listed in Table 2, the value of \bar{E}_x is equal to Mistler's result and slightly different from Ma's result. The differences in the results value range are 7.5% while the value of Poisson's ratio ν_x is relatively similar. The value of G is different and is slightly increase, because of the diminution of Poisson's ratio value.

4.4. Formula Comparison. In the previous investigations, many formulae have been proposed for the determination of material parameters. These formulae addressed isotropic materials. Zavalis et al. [30] have cited some formulae developed by Matysek [1999] (such as (17)), Brooks [1999] (see (18)), and Ciesielski [1999] (see (19)). However, they were originally derived to be used in the modeling of masonry structures. It is noteworthy that the values of elastic moduli obtained from other researchers are similar to the results obtained in the numerical simulations reported in the present study

$$E_m = \frac{1.25\xi + 1}{1.25\xi + \beta} E_b, \quad (17)$$

where ξ is the ratio of the height of bricks to the thickness of the mortar joints and β is the ratio of brick's elastic modulus to that of the mortar

$$\frac{1}{E_m} = \frac{0.86}{E_b} + \frac{0.14}{E_{\text{mor}}}, \quad (18)$$

where E_b and E_{mor} are the elastic moduli of the bricks and mortar, respectively,

$$E_m^i = \frac{1.20E_b^i E_{\text{mor}}^i}{0.2E_b^i + E_{\text{mor}}^i}, \quad (19)$$

where E_b^i and E_{mor}^i are the medium elastic moduli of the brick and mortar in section i , respectively.

The equivalent elasticities (E_m) estimated through the proposed formula were compared to the modulus derived from the previous formulae, (17)–(19). Figure 6 shows that

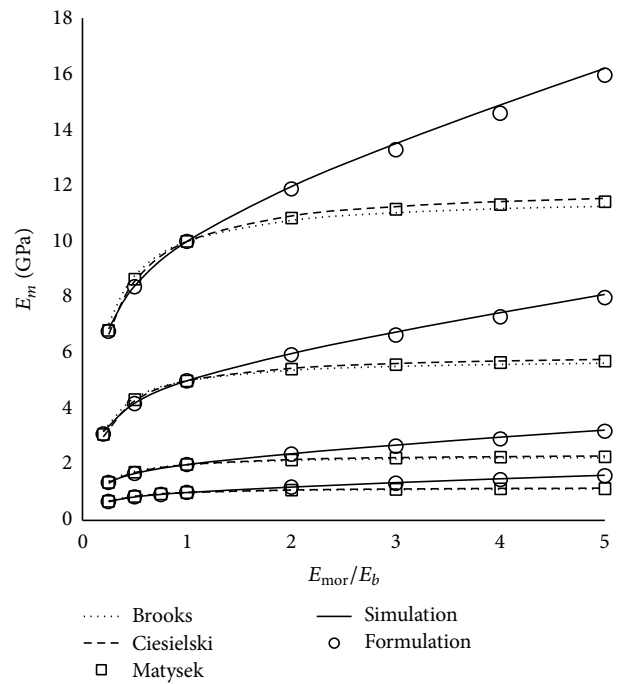


FIGURE 6: Equivalent elasticity of brick masonry.

these previous formulae underestimate the equivalent elasticity of the masonry structures with low-modulus bricks. It is noteworthy that the proposed formula is applicable for the elasticity ratio of $R_{\text{mor}} < 1$.

Equations (17)–(19) have a Poc behavior similar to that of the simulation results (Table 4). There same percentage of change can be observed for any E_b , as presented in Table 6. However, there are differences for the case of $R_{\text{mor}} > 1$. By using (17)–(19), when $R_{\text{mor}} = 2$, the E_m value has only increased by approximately 7.53% to 9.09% and for $R_{\text{mor}} = 5$, the E_m value has increased by approximately 12.6% to 15.38%. For the case of $R_{\text{mor}} = 2$, E_m increased by approximately 19.48–19.79%, and when $R_{\text{mor}} = 5$, E_m increased by approximately 61.68–62.71%.

For $R_{\text{mor}} < 1$, the Poc presents similar values between the proposed and the previous formulae, particularly with the Ciesielsky and Matysek formula; however, there was a slight difference with respect to the Brooks formula. This indicates that for the case of $R_{\text{mor}} < 1$, the proposed formula can be used as well.

Any increase in the ratio of mortar increased the elasticity of masonry. This is consistent with the data obtained by Drougkas et al. [31] and Gumaste et al. [3] who also examined the $E_{\text{mor}} > E_b$ case as shown in Table 6.

Table 8 and Figure 7 illustrate the comparison results of the equivalent elastic moduli based on data obtained by Gumaste et al. [3] (see Table 7). Table 8 and Figure 7 also demonstrate a comparison between the equivalent elastic moduli results derived from the proposed formula to those derived from the formulae proposed by Gumaste, Brooks, Matystek, and Ciesielsky.

Results from the Gumaste formula were almost similar to the simulation; the difference was lower than 1%. On the

TABLE 3: Homogenization model result from various researcher.

Model (MPa)	\bar{E}_x	\bar{E}_y	$\bar{\nu}_x$	$\bar{\nu}_y$	$\bar{G}(0.4\bar{E}_m)$
This research					
RVE-2	7882	6120	0.1600	0.2046	4520 (2450)
RVE-1	7882	6121	0.1604	0.2044	4441 (2450)
Ma et al. [1]	7899	6274	0.270	0.310	2884
Mistler et al. [19]					
3D model	7958	6777	0.164	—	2583
2D Plane Stress	7882	6592	0.159	—	2682
2D generalized plane strain	7971	6811	0.165	—	2584
2D plane strain	8157	6963	0.194	—	2584
Wang et al., [20]					
FEM, stack bond [15]	8530	6790	0.196	—	2580
FEM, running bond [15]	8620	6770	0.2	—	2620
Periodic model stack bond	8568	6850	0.191	—	2594
Periodic model stack bond	8574	6809	0.197	—	2620
Periodic model running bond	8574	6809	0.197	—	2620
Multilayer method [14]	8525	6906	0.208	—	2569
Wo-step method [21]	9,187	6,588	0.215	—	2658

TABLE 4: Percentage of change of simulation.

E_b (MPa)	Percentage of change (Poc)%					
	R_{mor}					
	0.25	0.5	1	2	3	4
1000	-31.42	-15.98	0	19.62	35.05	61.98
2000	-31.42	-15.98	0	19.62	35.05	61.98
5000	-31.42	-15.98	0	19.62	35.05	61.98
10000	-31.42	-15.98	0	19.62	35.05	61.98

TABLE 5: Examples of the calculations E_m .

Case	R_{mor}	Poc (%)	E_b (MPa)	Calculation $E_m = E_b \times (1 + Poc\%)$ MPa
$R_{mor} > 1$	4	61.98	1000	1620
			2000	3240
			5000	8099
			10000	1698
	3	35.05	1000	1351
			2000	2701
			5000	6753
			10000	13505
	2	19.62	1000	1196
			2000	2392
			5000	5981
			10000	11962
$R_{mor} < 1$	0.5	-15.98	1000	840
			2000	1680
			5000	4201
			10000	8402
	0.25	-31.42	1000	686
			2000	1372
			5000	3429
			10000	6858

TABLE 6: Percentage of change of formula comparison.

Ref.	E_b (MPa)	Percentage of change (Poc) %						
		0.25	0.50	1.00	R_{mor} 2.00	3.00	4.00	5.00
Brooks	1000	-29.58	-12.28	0.00	7.53	10.29	11.73	12.61
Ciesielski		-33.33	-14.29	0.00	9.09	12.50	14.29	15.38
Matysek		-31.86	-13.48	0.00	8.45	11.59	13.24	14.24
Simulation		-31.41	-16.00	0.00	19.48	34.85	48.68	61.68
Formulation		-33.34	-16.99	0.00	19.79	34.60	48.34	62.71
Brooks	2000	-29.58	-12.28	0.00	7.53	10.29	11.73	12.61
Ciesielski		-33.33	-14.29	0.00	9.09	12.50	14.29	15.38
Matysek		-31.86	-13.48	0.00	8.45	11.59	13.24	14.24
Simulation		-31.43	-15.98	0.00	19.62	35.05	48.94	61.98
Formulation		-33.34	-16.99	0.00	19.79	34.60	48.34	62.71
Brooks	5000	-29.58	-12.28	0.00	7.53	10.29	11.73	12.61
Ciesielski		-33.33	-14.29	0.00	9.09	12.50	14.29	15.38
Matysek		-31.86	-13.48	0.00	8.45	11.59	13.24	14.24
Simulation		-31.60	-15.98	0.00	19.62	35.05	48.94	61.98
Formulation		-32.23	-16.99	0.00	19.79	34.60	48.34	62.71
Brooks	10000	-29.58	-12.28	0.00	7.53	10.29	11.73	12.61
Ciesielski		-33.33	-14.29	0.00	9.09	12.50	14.29	15.38
Matysek		-31.86	-13.48	0.00	8.45	11.59	13.24	14.24
Simulation		-31.43	-15.98	0.00	19.65	35.05	48.93	61.98
Formulation		-33.34	-16.99	0.00	19.79	34.60	48.34	62.71

TABLE 7: Gumaste data and experiment and numerical results.

Ref.	Data								Results	
	E_b (MPa)	E_{mor} (MPa)	ν_b	ν_{mor}	h_b (mm)	l_b (mm)	t_b (mm)	t_{mor} (mm)	E_{ex} (MPa)	E_{num} (MPa)
Gumaste et al. [3]	3370	8570	0.15	0.2	75	230	105	12	3317	4005
	3370	5450	0.15	0.2	75	230	105	12	3789	3684
	3370	7080	0.15	0.2	75	230	105	12	3677	3865

TABLE 8: Comparison of equivalent elastic moduli based on Gumaste data ($E_{mor} > E_b$).

E_{mor}/E_b	Numeric		Formula			
	Gumaste	Proposed	Brooks	Matysek	Ciesielski	
1.62	3.68	3.67	3.56	3.58		3.60
2.10	3.87	3.86	3.64	3.67		3.69
2.54	4.01	4.01	3.68	3.72		3.75

other hand, the estimation using the proposed formula was 3–8% higher than the results of Ciesielski, (19), Brooks, (18), and Matysek, (17). Although numerical values obtained by Gumaste were very similar to those of the proposed formula, the experimental research is still required. To compensate for the lower brick strength in some countries, such as Indonesia and India, the proposed formula resulting from the investigation could be employed. The formula is appropriate for the calculation of the variable elasticity of low-quality masonry structures. In addition, the proposed formula is suitable for numerical applications on further large-scale masonry structures.

5. Conclusions

Most of the design formulae for calculating the equivalent elasticity of brick masonry structures are applicable only for the case where $E_{mor} < E_b$. The present study was focused on masonry structures with low-quality bricks; that is, $E_{mor} > E_b$. This paper presented numerical simulations to derive formulae for the equivalent elasticity of brick masonry structures. The accuracy of the formulae was discussed and verified by using experimental secondary data. The equivalent elasticity obtained using the newly developed formulae was estimated with high accuracy, resulting in a

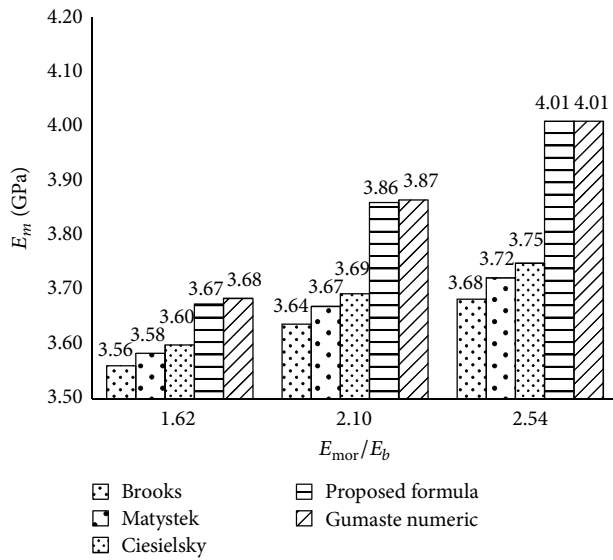


FIGURE 7: Comparison of equivalent elastic moduli based on Gumaste data ($E_{mor} > E_b$).

discrepancy of less than 1% compared to the numerical results derived by Gumaste. The conclusions of this investigation are summarized as follows:

- (i) The proposed formula is a new, simplified formula; we performed finite element (FE) simulations, adopting the homogenization technique. It can be used to calculate the equivalent modulus of elasticity of such brick masonry structures.
- (ii) The conventional formula may underestimate the equivalent elasticity of the masonry structures made with mortar that has a higher modulus than bricks.
- (iii) The proposed formula is applicable in various calculations of the equivalent elasticity of masonry structures. In particular, the formula can be suitable for the estimation of the equivalent elasticity of bricks with low elastic modulus. Furthermore, the proposed formula can be applied for bricks with high elastic modulus.
- (iv) The equivalent elasticity estimated via the proposed formula increases in accordance with the increase in elastic modulus ratio of mortar.
- (v) The proposed formula can be employed for masonry structures in countries that use bricks of low elastic moduli.

In further studies, it is suggested that the experimental research be extended, particularly to masonry structures that are composed of mortar with a higher modulus of elasticity than that of bricks.

List of Symbols

- β : Ratio of brick's elastic modulus to the mortar elastic modulus
 δ : Geometric properties of cells

- E : Young's modulus
 E_b : Modulus of elasticity of brick
 E_m : Modulus of elasticity of masonry
 E_{mor} : Modulus of elasticity of mortar
 \bar{E}_x : Average modulus of elasticity in x -direction calculation
 \bar{E}_y : Average modulus of elasticity in y -direction calculation
 E_x : Modulus of elasticity in x -direction calculation
 E_y : Modulus of elasticity in y -direction calculation
 E_b^i : Modulus elastic moduli of brick in section i
 E_m^i : Modulus elastic moduli of mortar in section i
 ε_x : Normal strain in x -direction
 ε_y : Normal strain in y -direction
 $\bar{\varepsilon}_{xx}$: Average normal strain in x -direction
 $\bar{\varepsilon}_{yy}$: Average normal strain in y -direction
 $\bar{\varepsilon}_{ij}$: Average strain vector
 ε_{ij} : Strain vector
 G : Shear modulus
 \bar{G} : Average equivalent shear modulus
 γ_{xy} : Normal shear strain
 $\bar{\gamma}_{xy}$: Average normal shear strain
 h_b : Thickness of brick
 ξ : Ratio of the height of bricks
 l_b : Long of brick
 Ω : Volume of RVE cell
 Poc : Percentage of change
 ρ_{mor} : Volume ratio of mortar to the area of the cell
 R_{mor} : Ratio of mortar
 $\bar{\sigma}_{ij}$: Average stress vector
 σ_{ij} : Stress vector
 σ_x : Normal stress in x -direction
 σ_y : Normal stress in y -direction
 $\bar{\sigma}_{xx}$: Average normal stress in x -direction
 $\bar{\sigma}_{yy}$: Average normal stress in y -direction
 θ : Disparity value from geometric properties
 t_m : Thickness of mortar
 τ_{xy} : Normal shear stress
 $\bar{\tau}_{xy}$: Average normal shear stress
 u : Deformation in x -direction
 v : Deformation in y -direction
 $\bar{\nu}_m$: Average of Poisson's ratio of masonry
 $\bar{\nu}$: Average of Poisson's ratio
 ν : Poisson ratio
 ν_x : Poisson ratio in x -direction calculation
 ν_y : Poisson ratio in y -direction calculation
 $\bar{\nu}_x$: Average Poisson ratio in x -direction calculation
 $\bar{\nu}_y$: Average Poisson ratio in y -direction calculation
 w_b : Wide of brick.

Additional Points

Research highlights are as follows: (i) a proposed new formula for calculating the equivalent modulus of elasticity of masonry structures, built with low-modulus bricks; (ii) extensive finite element simulations by using representative volume elements (RVEs); (iii) verification of finite element

models by using experimental data; and (iv) quantification of the elastic properties of lower-stiffness bricks used with higher stiffness mortar.

Competing Interests

The authors declare that they have no competing interests.

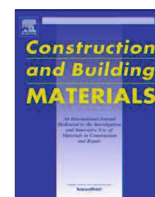
References

- [1] G. Ma, H. Hao, and Y. Lu, "Homogenization of Masonry using numerical simulations," *Journal of Engineering Mechanics*, vol. 127, no. 5, pp. 421–431, 2001.
- [2] A. Indra, S. Elfina, Nurzal, and H. Nofrianto, *Development of Making Composite Clay/Silica Rha Application for Improving the Quality of Red Brick in Order to Create Friendly Earthquake Building Materials*, National Strategic Research, Bogor, Indonesia, 2013.
- [3] K. S. Gumaste, K. S. N. Rao, B. V. V. Reddy, and K. S. Jagadish, "Strength and elasticity of brick masonry prisms and wallettes under compression," *Materials and Structures*, vol. 40, no. 2, pp. 241–253, 2007.
- [4] P. Putri, "Quality Study in the reconstruction of brick houses that built after earthquake 2009 in Koto Tengah Sub-district-Padang," *Procedia Engineering*, vol. 95, pp. 510–517, 2014.
- [5] Elhusna, A. S. Wahyuni, and A. Gunawan, "Performance of clay brick of Bengkulu," *Procedia Engineering*, vol. 95, pp. 504–509, 2014.
- [6] Wisnumurti, S. M. Dewi, and A. Soehardjono, "Strength reduction factor (R) and displacement amplification factor (Cd) of confined masonry wall with local brick in Indonesia," *Procedia Engineering*, vol. 95, pp. 172–177, 2014.
- [7] E. Basoendondo, *Lateral load response of Cikarang brick wall structures—an experimental study [Disertasi]*, Build Environment, 2008.
- [8] T. Paulay and M. J. Priestly, *Seismic Design of Reinforced Concrete and Masonry Buildings*, Wiley-Interscience, New York, NY, USA, 1992.
- [9] I. Stefanou, K. Sab, and J.-V. Heck, "Three dimensional homogenization of masonry structures with building blocks of finite strength: a closed form strength domain," *International Journal of Solids and Structures*, vol. 54, pp. 258–270, 2015.
- [10] F. Cluni and V. Gusella, "Homogenization of non-periodic masonry structures," *International Journal of Solids and Structures*, vol. 41, no. 7, pp. 1911–1923, 2004.
- [11] A. Cecchi and R. Di Marco, "Homogenized strategy toward constitutive identification of masonry," *Journal of Engineering Mechanics*, vol. 128, no. 6, pp. 688–697, 2002.
- [12] A. Zucchini and P. B. Lourenço, "A micro-mechanical model for the homogenisation of masonry," *International Journal of Solids and Structures*, vol. 39, no. 12, pp. 3233–3255, 2002.
- [13] A. Rekić, S. Allaoui, A. Gasser, E. Blond, K. Andreev, and S. Sinema, "Experiments and nonlinear homogenization sustaining mean-field theories for refractory mortarless masonry: the classical secant procedure and its improved variants," *European Journal of Mechanics, A/Solids*, vol. 49, pp. 67–81, 2015.
- [14] G. N. Pande, J. X. Liang, and J. Middleton, "Equivalent elastic moduli for brick masonry," *Computers and Geotechnics*, vol. 8, no. 3, pp. 243–265, 1989.
- [15] A. Anthoine, "Derivation of the in-plane elastic characteristics of masonry through homogenization theory," *International Journal of Solids and Structures*, vol. 32, no. 2, pp. 137–163, 1995.
- [16] J. S. Lee, G. N. Pande, J. Middleton, and B. Kralj, "Numerical modelling of brick masonry panels subject to lateral loadings," *Computers & Structures*, vol. 61, no. 4, pp. 735–745, 1996.
- [17] A. Gabor, A. Bennani, E. Jacquelin, and F. Lebon, "Modelling approaches of the in-plane shear behaviour of unreinforced and FRP strengthened masonry panels," *Composite Structures*, vol. 74, no. 3, pp. 277–288, 2006.
- [18] P. Lourenço, *Computational Strategies for Masonry Structures*, Delft University Press, Delft, The Netherlands, 1996.
- [19] M. Mistler, A. Anthoine, and C. Butenweg, "In-plane and out-of-plane homogenisation of masonry," *Computers & Structures*, vol. 85, no. 17–18, pp. 1321–1330, 2007.
- [20] G. Wang, S. Li, H.-N. Nguyen, and N. Sitar, "Effective elastic stiffness for periodic masonry structures via eigenstrain homogenization," *Journal of Materials in Civil Engineering*, vol. 19, no. 3, pp. 269–277, 2007.
- [21] S. Pietruszczak and X. Niu, "A mathematical description of macroscopic behaviour of brick masonry," *International Journal of Solids and Structures*, vol. 29, no. 5, pp. 531–546, 1992.
- [22] P. B. Lourenço, G. Milani, A. Tralli, and A. Zucchini, "Analysis of masonry structures: review of and recent trends in homogenization techniques," *Canadian Journal of Civil Engineering*, vol. 34, no. 11, pp. 1443–1457, 2007.
- [23] P. Pegon and A. Anthoine, "Numerical strategies for solving continuum damage problems with softening: application to the homogenization of masonry," *Computers and Structures*, vol. 64, no. 1–4, pp. 623–642, 1997.
- [24] R. Luciano and E. Sacco, "Homogenization technique and damage model for old masonry material," *International Journal of Solids and Structures*, vol. 34, no. 24, pp. 3191–3208, 1997.
- [25] A. Anthoine, "Homogenization of periodic masonry: plane stress, generalized plane strain or 3D modelling?" *Communications in Numerical Methods in Engineering*, vol. 13, no. 5, pp. 319–326, 1997.
- [26] A. Hendry, *Structural Masonry*, Macmillan, Basingstoke, UK, 1990.
- [27] A. Mohebbkhah, A. A. Tasnimi, and H. A. Moghadam, "Non-linear analysis of masonry-infilled steel frames with openings using discrete element method," *Journal of Constructional Steel Research*, vol. 64, no. 12, pp. 1463–1472, 2008.
- [28] P. B. Lourenço, J. G. Rots, and J. Blaauwendraad, "Continuum model for masonry: parameter estimation and validation," *Journal of Structural Engineering*, vol. 124, no. 6, pp. 642–652, 1998.
- [29] G. Milani, P. Lourenço, and A. Tralli, "Homogenization approach for the limit analysis of out-of-plane loaded masonry walls," *Journal of Structural Engineering*, vol. 132, no. 10, pp. 1650–1663, 2006.
- [30] R. Zavalis, B. Jonaitis, and P. Lourenço, "Analysis of bed joint influence on masonry modulus of elasticity," in *Proceedings of the 9th International Masonry Conference*, pp. 1–11, Guimarães, Portugal, July 2014.
- [31] A. Drougkas, P. Roca, and C. Molins, "Numerical prediction of the behavior, strength and elasticity of masonry in compression," *Engineering Structures*, vol. 90, pp. 15–28, 2015.



Contents lists available at ScienceDirect

Construction and Building Materials

journal homepage: www.elsevier.com/locate/conbuildmat

Two-dimensional fictitious truss method for estimation of out-of-plane strength of masonry walls



Muhammad Ridwan^{a,*}, Isamu Yoshitake^b, Ayman Y. Nassif^c

^a Department of Civil Engineering, Padang Institute of Technology, Jalan Gajah Mada Kandise Nanggalo, Padang, Indonesia

^b Department of Civil and Environmental Engineering, Yamaguchi University, Tokiwadai 2-16-1, Ube, Yamaguchi 755-8611, Japan

^c School of Civil Engineering and Surveying, University of Portsmouth, Portsmouth PO1 3AH, United Kingdom

HIGHLIGHTS

- A new truss model is proposed for analyzing out-of-plane strength of masonry walls.
- The evolution of crack patterns of masonry walls is identified numerically.
- The fictitious truss model was experimentally verified for various masonry walls.

ARTICLE INFO

Article history:

Received 8 March 2017

Received in revised form 20 June 2017

Accepted 22 June 2017

Keywords:

Fictitious truss method

Masonry structure

Out-of-plane strength

ABSTRACT

The truss method is rarely used to analyze a masonry wall, especially a masonry wall under a load in the out-of-plane direction. The present study proposes a model called the fictitious truss method (FTM) to determine the ability of masonry structures to withstand a lateral load within their elastic deformation capacities, and introduces a two-dimensional linear static model for masonry walls. The model represents the effect of flexural interaction by computing the stress and strain in the axial direction of the material and by considering uniaxial force effects on masonry elements. Pressure is applied to the surface area of the wall sequentially to predict the ultimate tension and compression cracking. FTM modeling is validated using previously obtained results for confined and unconfined masonry walls and for reinforced and unreinforced masonry walls. The FTM is a reliable method of assessing the out-of-plane strength of masonry structures owing to its conceptual accuracy, simplicity, and computational efficiency.

© 2017 Elsevier Ltd. All rights reserved.

1. Introduction

The masonry wall is widely used for its low cost in low-rise construction in various countries. Additionally, a ring beam around a masonry structure (confined masonry) wall is recommended for the prevention of injuries and casualties that might occur in the unexpected collapse of a masonry wall. One form of masonry wall collapse is due to loading in the out-of-plane direction, which can occur, for example, in an earthquake or a flood. However, there is no indication that many masonry walls have collapsed under wind pressure after the completion of their construction [4], which can be considered evidence of the adequacy of their construction.

There is a connection between walls and reinforced concrete, given the different deformations of the two materials in response to loading. This is strongly dependent on the type of masonry used

for infill. Masonry can be built using different kinds of units (e.g., solid or hollow), unit materials (e.g., clay or concrete), and mortar, depending on the region. The infill wall and the confinement are usually connected with mortar (unreinforced masonry) using an anchor and reinforcement (reinforced masonry).

Research on out-of-plane loading has included experiments and theoretical analysis using different analytical methods, but there has been far less research on out-of-plane loading of masonry walls than on in-plane loading of masonry walls. Some experimental studies have been performed on out-of-plane behavior of masonry reinforced walls [1–3], unreinforced masonry walls [4,5], infill masonry walls [6–8] and confined masonry walls [9–11]. Based on these studies the main variables that affect the out-of-plane behavior of masonry walls are the aspect ratio (height divided by length), wall support conditions, wall slenderness ratio (height divided by thickness), axial load, in-plane stiffness of surrounding elements, wall openings, and unit type. Moreover, the out-of-plane behavior of confined walls is different than that observed for unreinforced, reinforced, and infill walls. The difference is mainly asso-

* Corresponding author.

E-mail addresses: mhd.rid.wan.itp@gmail.com (M. Ridwan), yoshtake@yamaguchi-u.ac.jp (I. Yoshitake), ayman.nassif@port.ac.uk (A.Y. Nassif).

Nomenclature

A_n	effective area n of element truss	H	height of masonry wall
A_c	pressure effective area	h_t	horizontal truss element
A_r	reinforcement effective area	I_{eq}	inertia unit equivalent of masonry element
AR	aspect ratio	I_n	inertia of element n equivalent of masonry element
A_t	tension effective area	I_{tot}	inertia unit of masonry element
a	depth of the equivalent stress block	θ_d	angle of diagonal truss
α'	constants representing contribution of bricks compressive strengths on f_m	σ_u	ultimate stress
α	shape factor of compressive area	L	length of masonry wall
b_{eff}	width of unit load to be used	n	total number of data points
β'	constants representing contribution of mortar compressive strengths on f_m	P	joint load
β_t	function of strength class of materials	p	joint load
c	distance from center of thickness of masonry wall to the top	P_{eq}	joint load equivalent
d_t	diagonal truss element	PoE	percentage of error
δ	displacement	Q	uniform load
E	Young's modulus	t_{eff}	effective width of a cross section of truss model
E_b	modulus of elasticity of bricks	u_t	vertical truss
E_m	modulus of elasticity of masonry	t	thickness of masonry
E_j	modulus of elasticity of mortar	t_w	thickness of masonry
ϵ'_m	peak strain in masonry, i.e., compressive strain corresponding to f_m	$\gamma_{eq(u)}$	specific gravity equivalent of unit
ϵ_m	compressive strain in masonry	$\gamma_{eq(m)}$	specific gravity equivalent of mortar
ϵ	strain	ξ	specific gravity factor
E_c	modulus of elasticity of concrete	γ_u	specific gravity factor unit
f_j	compressive strength of mortar	γ_m	specific gravity factor mortar
f'_m	compressive prism strength of masonry	γ_{eq}	specific gravity equivalent
f_m	compressive strength of mortar	t_w	total height of vertical truss elements
f_b	compressive strength of brick	u_t	vertical truss element
f_c	compressive strength of concrete	W_e	strength of masonry by using experimental method
f_{me}	compressive strength of member of truss	W_{ss}	strength of masonry by using spring–strut method
f_{tpe}	average out-of-plane flexural tensile strength perpendicular	W_{yl}	strength of masonry by using yield-line method
f_p	compressive strength of unit masonry	W_{fl}	strength of masonry by using failure-line method
FTM	fictitious truss method	W_{cs}	strength of masonry by using compressive strut method
FTMSD	fictitious truss method single diagonal	W_t	strength of masonry by using FTM in tension
FTMDD	fictitious truss method double diagonal	W_c	strength of masonry by using FTM in compression
		y	distance from center of effective width of a cross section of the masonry wall to center of element top truss area

ciated with construction procedures and wall reinforcement details. The differences between infill and confined walls are as follows. Firstly, confined walls consist of unreinforced panels surrounded by flexible reinforced concrete confining elements. The wall panels are constructed first, and later the confining elements are constructed. Infill walls consist of unreinforced or reinforced masonry walls surrounded by stiff concrete or structural steel frames [12]. The frames are constructed first, and later the masonry panels are constructed. This type of construction causes gaps between the frames and the masonry panels. Construction gaps delay the formation of arching action [6,13].

The aspect ratio and slenderness ratio [4,10,12,14] have been shown to affect the strength of unreinforced masonry (URM). Some researchers have used finite element (FE) theory and software to analyze masonry walls under out-of-plane loading. Drysdale et al. [4] used FE elastic plate analysis, Noor-E-Khuda et al. [1] used the explicit FE method and a layered shell model, and La-Mendola et al. [15] and Milani et al. [16] used commercial FE software. The FE method is very helpful, but it is complex and requires considerable cost.

On the other hand, numerical modeling of the out-of-plane response of infill frames was reviewed by Asteris et al. [17], whose in-depth literature review included some models of out-of-plane

responses for infill frames. There are flexural-action-based models and arching-action-based models.

Cavalery et al. [18] investigated modeling of the out-of-plane behavior of masonry walls. They proposed analytical modeling of the moment curvature law and a numerical procedure to determine the flexural response of masonry cross sections, including nonlinearity owing to the σ - ϵ law in compression and the assumption of limit-tension material. This investigation simplifies the solution to a problem in which the bending moment increases because of increases in the eccentricity of the constant compressive axial load. This investigation used previous calcarenite and clay brick wall experimental data to validate the analytical model of the moment-curvature curve. This approach can be used for various classes of materials and structures, and is easy to apply means of the analytical moment-curvature law, allowing a fitted “exact” numerical result to be defined. In this investigation, the tensile strength was negligible.”

Some researchers have also investigated near-surface-mount-reinforced masonry walls. [15,19–22]. They used fiber-reinforced polymer (FRP), carbon-fiber-reinforced polymer (CFRP) strips, and polymer-textile-reinforced mortar to reinforce a masonry wall. These materials are used to improve the out-of-plane performance of a URM wall. Near-surface-mount-reinforced masonry walls are

very helpful in increasing the strength of masonry but are strongly affected by the type of reinforcement used.

URM panels in reinforced concrete frames were investigated by Tu et al. [8] and Furtado et al. [23]. Tu et al. investigated the out-of-plane behavior of URM walls in shaking table tests. They used an analytical model for analysis. Furtado et al. evaluated the combination of in-plane and out-of-plane behaviors by comparing two infill masonry walls subjected to monotonic out-of-plane loading and cyclic out-of-plane loading.

Many theories have been proposed to investigate the strength and behavior of masonry structures in the out-of-plane direction, as shown in Table 1. However, these theories are based on and limited to certain experimental configurations. Most studies on the out-of-plane behavior of masonry walls have been experimental works and thus time-consuming and expensive [1]. It has been concluded that the method that most accurately predicts the out-of-plane strength of confined walls is the bidirectional strut method. This method is an iterative procedure based on two-way arching action.

The truss model is rarely used in calculations for a masonry wall structures, but several truss models have been extensively used for analysis of the nonlinear behavior of masonry infills. A truss model for masonry structures was proposed by Lu et al. [24] in research on a nonplanar reinforced concrete wall. Recently, Moharrami et al. [25] used the truss model for the analysis of masonry structures employing nonlinear truss modeling, which was used in the analysis of shear failure in the in-plane direction of the wall.

The present study proposes a new method of using a truss as a structural element of a masonry wall in order to analyze the out-of-plane strength of a masonry structure. The aim of present study is a model oriented to the determination of out of-plane resistance. The proposed fictitious truss method (FTM) provides practitioners and academics with analytical results and can be modified for a variety of masonry walls.

2. Material and methods

The FTM creates patterns of stress distribution in a flexural element structure. The geometry of the FTM is obtained by centralizing and simplifying the force acting on a wall. The elements establish truss blocks and then configure the truss structure as indicated in Fig. 1.

2.1. Determination of truss geometry

A truss model requires cross-sectional dimensions and determination of the geometry of truss elements as well as applicable material models. The first step is establishing the dimensions of the truss and of the truss elements considering

Table 1
Methods of analyzing masonry structures under out-of-plane loading.

Analysis Method		Reference
Yield line method	Unreinforced wall	[4,30]
	Reinforced wall	[3]
	Confined wall	[9–11]
The failure line method	Unreinforced wall	[4]
	Unconfined wall	[9–11]
The modified yielding line method	Surrounded by steel frame	Dawe and Seah [13] cited from [12]
The compressive strut method	Confined wall	[9,10]
	Infill walls	[6]
The spring-strut and the bidirectional strut method	Confined walls	[9–12]

the real dimensions of the masonry structure. In the cross section of the masonry structure, t is the thickness of the masonry and is not directly used in the FTM models.

The FTM makes the following assumptions. The thickness of the masonry wall is the initial height of the truss model (t). The effective cross section of the truss element is a square shape ($a \times b_{eff}$), the cross section is the effective area of compression stress in a flexural beam, the aspect ratio is less than one (i.e., $H/L < 1$), and the truss is fictitious. The truss can be calculated as a numerical value until early fracture, and buckling can be ignored. If reinforcement is used, its arrangement must be regular.

The shape of the truss model is shown in Fig. 2. There are three types of shapes: v_t is a vertical truss, h_t is a horizontal truss, and d_t is a diagonal truss. A diagonal truss can be a single diagonal or double diagonal truss.

The truss geometry defines the geometry of the vertical cross section of the brick and determines the height of the masonry wall. Each block truss is the representative geometry of the brick and mortar. The height of the truss (v_t) is the effective width of a cross section of the masonry wall (t_{eff}), while the width (h_t) of the truss is the effective thickness of the mortar or unit masonry. b_{eff} is the assumed width of the unit load to be used. It is obtained from the length of the brick unit. t_{eff} is the effective height of a cross section of the truss model. It is obtained from the equivalent inertia of the effective cross section as shown in Fig. 3 and by solving Eq. (1) below:

$$I_{tot} = I_{eq}, \quad (1)$$

where $I_{tot} = \frac{1}{12} b_{eff} t^3$ and I_{eq} is the inertia unit equivalent of the masonry element which can be solved with the provision that $A_1 = A_2$ and the equation

$$I_{eq} = \sum_1^n I_n + \sum_1^n (A_n y_n^2) \quad (2)$$

y is thus obtained if $n = 2$ as

$$y = \sqrt{\frac{I_{tot} - 2I_n}{2A_n}} \quad (3)$$

The result is that t_{eff} is $2y$

The total height of the vertical truss elements is $t_w = 2y + a$; however, the height used in the analysis (t_{eff}) is $2y$ as indicated in Fig. 4. Fig. 3 shows the determination of the effective height of a truss element that has parameters for the equivalent stress of the block parameter.

The total stress area in compression is $A_c = a b_{eff}$. In accordance with SNI 03-2847-2013 [32], the depth of the equivalent stress block (a) is obtained as $a = \beta_1 c$, where c is the distance from the center of mass to the top and $\beta_1 = 0.85$. β_1 is a function of the strength class of materials: $\beta_1 = 0.85$ for $f_{me} < 30$ MPa, and is reduced by 0.008 for every increase of 1 MPa in compressive strength; it should not be less than 0.65. Therefore, $a = 0.85c$ and $\alpha = 1$ for actual compressive strength, and 0.85 for the compressive strength equivalent. b_{eff} is the length of the brick or the length of the effective area of pressure used as the effective width. $A_c = A_t = a b_{eff}$ is used for a masonry wall without reinforcement and $A_t = A_r$ is used for a masonry wall with reinforcement, where A_t is the area of tension, A_c is the area of compression, and A_r is the area of reinforcement. Typical cross-sectional dimensions used in the FTM are shown in Fig. 1.

The geometric dimension of the mortar part is the same for the brick and unit parts. The material parameters should be set according to the properties of each material, and the material modeling assumption in tension and compression is isotropic, linear, elastic material. An elastic material may show linear or nonlinear behavior. In this study, we assume linear behavior. For linear elastic materials, stresses are linearly proportional to strains ($\sigma = E\varepsilon$) as described by Hooke's law. The law is applicable for material properties that are independent of coordinates (homogeneous) and material properties that are independent of the rotation of the axes at any point in a body or structure (isotropic materials). Here only two elastic constants (modulus of elasticity E and Poisson's ratio ν) are needed for linear elastic materials.

The FTM can be used to determine the strength of a confined or unconfined masonry structure in the out-of-plane direction.

2.2. Schematic of the FTM

The FTM determines the out-of-plane strength of a masonry wall structure and involves the following steps:

- Check that the aspect ratio (H/L) of the masonry structure is less than 1.0.
- Provide material properties including the elasticity, specific gravity, Poisson's ratio, compressive strength, tensile strength, and others.
- Determine the widely assumed pressure area (b_{eff}).
- Determine the effective height of the element truss ($a = \beta_1 c$).
- Arrange $A_c = A_t = a b_{eff}$ to obtain y (Eqs. (1)–(3)).
- Determine the effective thickness of the truss structure $t_{eff} = 2y$.
- Obtain the model and its dimensions by determining the boundary conditions of the masonry structure.
- Analyze the FTM structure to obtain the element truss force.

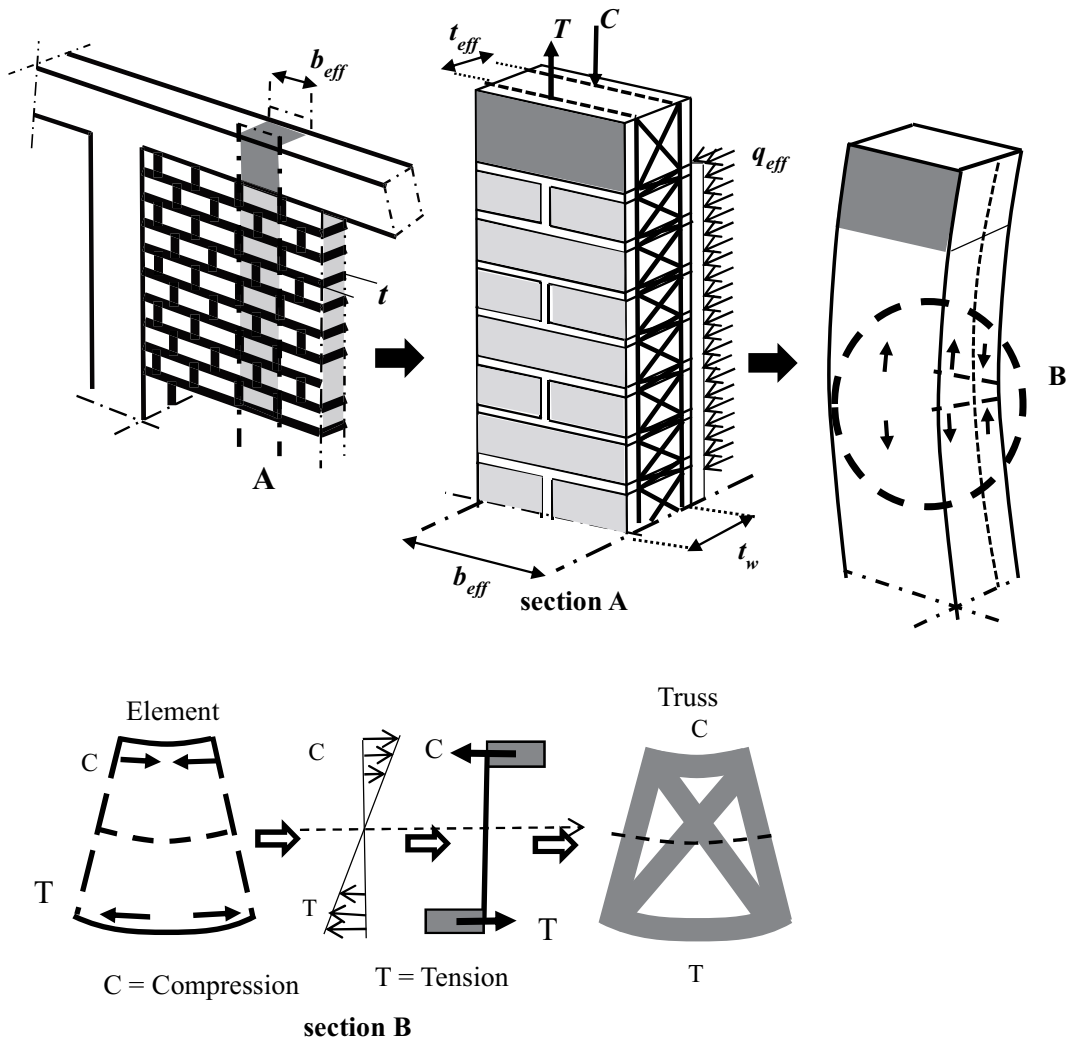


Fig. 1. Establishing truss blocks and configuring the truss structure.

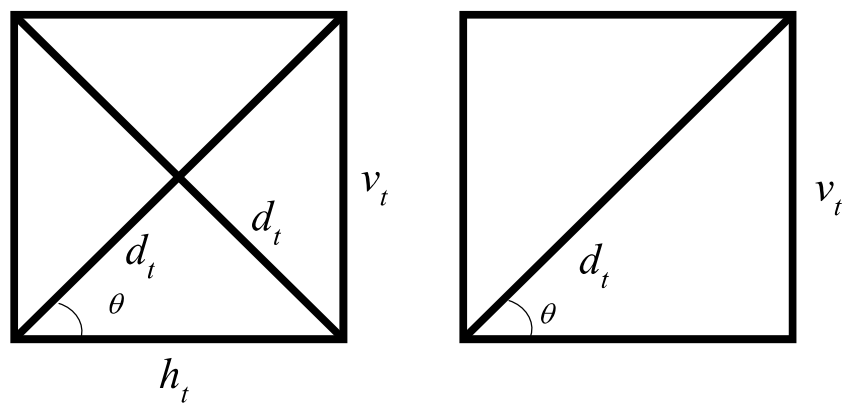


Fig. 2. Truss shapes.

- Apply the load (P_{eq}) gradually until there is cracking in areas of tension and compression.

All loads are applied as concentrated equivalent loads acting on the truss joints. The FTM is schematically shown in Fig. 5.

The FTM may not be applicable physically, but it can be performed numerically. The element truss force can be analyzed using classical mechanics methods, other methods typically used to calculate truss structures, or using FE software. After determining the truss element and truss structure, the loading can be applied gradually while checking the strain in compression and the tension truss element condition.

2.3. Material models

The stress-strain relationship of truss elements representing masonry walls is shown in Fig. 6. The tensile strength and compressive strength of the mortar and the units are interconnected. In the present study, the vertical and horizontal truss elements are the studied variables while the diagonal truss element distributes forces to the vertical and horizontal truss elements.

The material model of masonry is linear and elastic for brittle material; likewise for units and mortar. The failure criterion of the FTM model is the maximum principal strain by uniaxial loading on a truss member. The Hooke's law concept $\epsilon = \frac{\sigma}{E}$

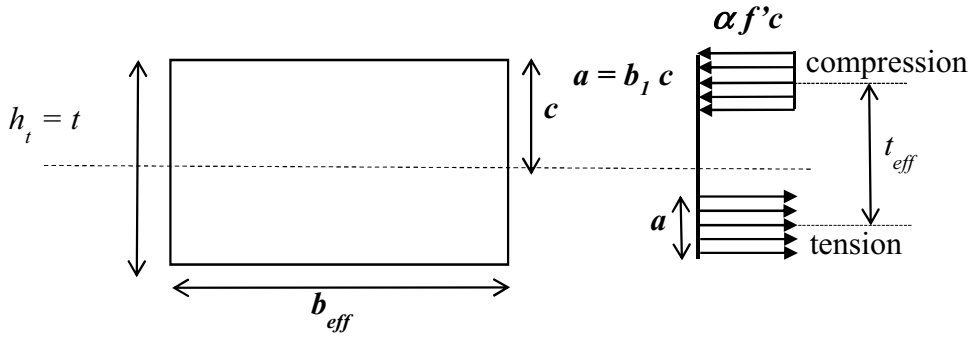


Fig. 3. Determination of the effective height of a truss element.

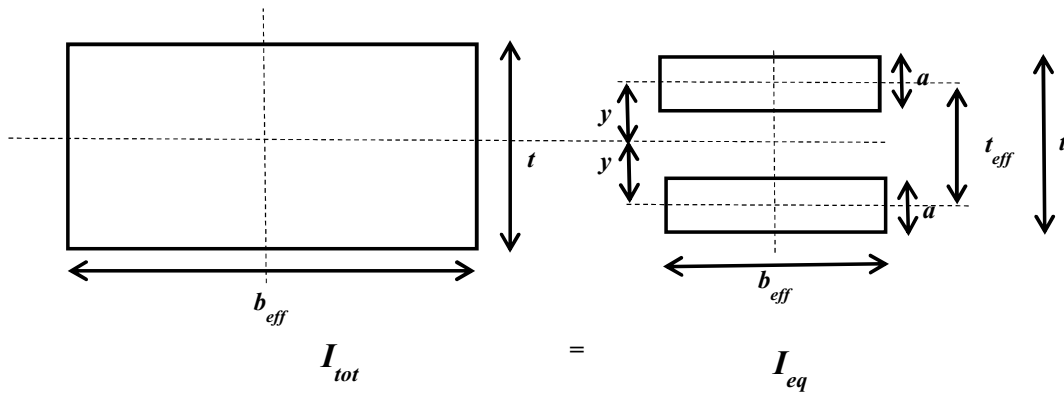


Fig. 4. Equivalent inertia of the effective cross section.

can be applied to predict when either of the principal strains resulting from the principal stresses ($\sigma_{1,2}$) meets or exceeds the maximum strain corresponding to the yield strength (σ_y) of the material in uniaxial tension or compression.

The FTM requires the force acting on a truss element to be in the critical region of the mid-span of the truss structure, where there is tension and compression on either side. Tension and compression may occur in mortar and brick in structural elements. It is therefore necessary to choose either brick or mortar as the material when determining the strength of masonry structures.

Almeida et al. [26] investigated hollow bricks and the brick–mortar interfaces under uniaxial tension for hollow bricks sourced from Portugal and Spain. Testing various brick types revealed a similar uniaxial response in tension and compression (Fig. 6). Fig. 6a shows the relationship between tension stress and strain. Stress increases linearly to a peak value before gradually and nonlinearly decreasing. The present paper focuses only on the behavior until the peak tensile load is reached. The same behavior is seen for both raw materials and materials such as FRP, CFRP, and steel. Almeida et al. [26] found that elongation values for hollow brick obtained with different peak tensile loads ranged from 3 to 10 μ while those for mortar were less than 5 μ . The tensile stress values ranged over 2.75–3.82 and 1.93–2.25 N/mm², respectively, for the hollow brick and mortar. In the present study, the tensile stress was assumed to be 3 and 2 N/mm², respectively, for the hollow brick and mortar, and the tensile strain was assumed to be 0.001. Fig. 6b shows the relationship between compression stress and strain.

Kaushik et al. [27] found cracking at strain values from 0.0023 to 0.00375. Based on these data, the present study used 0.003 as the cracking point for masonry elements. Kaushik et al. stated that the values of E_b , E_j , and E_m for masonry walls are approximately

$$E_b \approx 300f_b, \tag{4}$$

$$E_j \approx 200f_j, \tag{5}$$

$$E_m = 550f'_m. \tag{6}$$

Corresponding coefficients of variance were 0.35, 0.32, and 0.3 respectively. These results are in line with the basic formula used by Eurocode 6 [28] regarding the characteristic compressive strength of masonry. Following the above research, E_b , E_j , and E_m for masonry can be used in the present study; however, the present study considers the elastic linear range.

2.4. Aspect ratio, slenderness ratio, and weight reduction

A masonry structure comprising multiple walls subjected to out-of-plane loading has an aspect ratio (AR). The present study does not consider $AR \geq 1$ except for the case of the one-way vertical wall (with a plane of failure parallel to the bed joints). This is because several previous studies [14] revealed that structural rigidity is higher in the horizontal direction than in the vertical direction if $AR \geq 1$. However, the approach of using $P = (0.3AR + 0.7) P$ can be invoked for $AR > 1$.

The slenderness ratio also affects the masonry structure. The thickness of a masonry wall (t) affects the stiffness and strength of the wall. In the present study, t is a variable that has been resolved in various stages used in determining the stiffness and strength of a masonry wall. The stages seek the equivalent thickness of the wall (t_{eff}), which represents the truss.

In structural analysis using, for example, FE software, self-weight is calculated automatically. A solid element is used as the truss element. Therefore, the specific gravity of the truss must be adapted to the specific gravity of the solid masonry elements. This can be achieved by multiplying the specific gravity by a factor ξ for masonry elements:

$$\gamma_{eq(u)} = \xi \gamma_u \tag{7}$$

$$\gamma_{eq(m)} = \xi \gamma_m \tag{8}$$

where $\xi = \frac{b_{eff}t}{2\alpha \frac{t_{eff}^2}{\sin^2\theta} + t_{eff} + b_{eff}}$, γ_{eq} is the specific gravity equivalent of a unit or of mortar, ξ is the specific gravity factor, γ_u is the specific gravity of the unit, and γ_m is the specific gravity of the mortar. Geometrically, the self-weight of a truss element affects the behavior of masonry structures. The load given to the structure is therefore an additional external load. For instance, if the thickness of the wall is (t) = 120 mm, the width of the unit load to be used is (b_{eff}) = 210 mm, the depth of the equivalent stress block is (a) = 51 mm, and the effective width of a cross section of the truss model is (t_{eff}) = 69.13 mm, then the value of the specific gravity factor (ξ) is 0.655. This value has a significant influence on the self-weight of a masonry structure.

3. Results

The FTM was validated using the results of analysis of out-of-plane masonry structures conducted in previous studies. Truss analysis can be performed by using matrix methods as for a two-

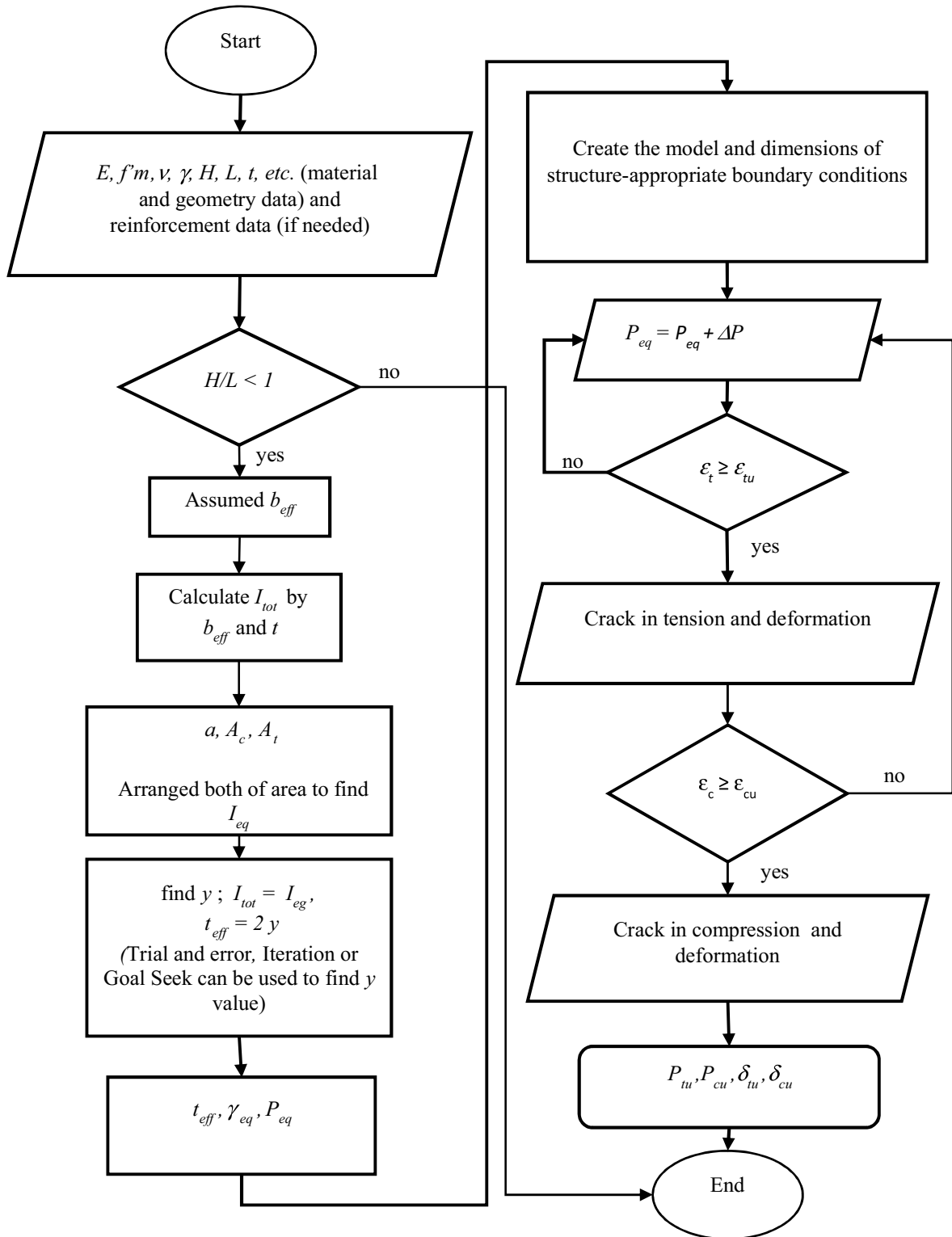


Fig. 5. Schematic of the proposed FTM.

dimensional truss using the direct stiffness method. In this study, this is performed using SAP2000 software [31]. The basic data are entered in accordance with the constitutive modeling approach. Both truss shapes were used and validated for masonry wall structures subject to out-of-plane loading. Material properties from the literature were used as input data in analyzing the FTM structure with FE software.

3.1. Validation 1

The first validation of the FTM was conducted for a model used by Varela-Rivera et al. [9], namely six confined masonry walls with reinforced concrete. The specifications of the materials and dimensions of the walls are given in Table 2. Each wall was comprised of hollow blocks in a half-running bond pattern. The dimensions of

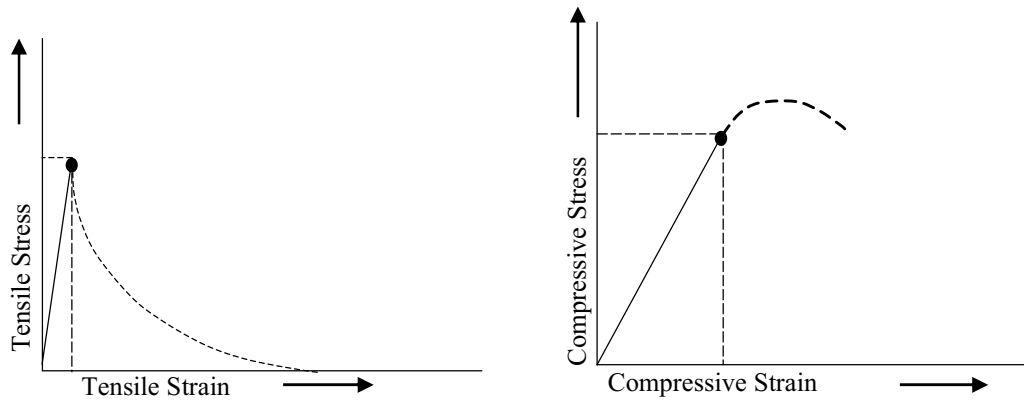


Fig. 6. Stress–strain relationship of truss elements representing masonry walls.

the concrete confining elements were $0.15 \times 0.2 \text{ m} \times 0.4 \text{ m}$ for E-1, E-2, E-4, and E-5, and $0.12 \text{ m} \times 0.2 \text{ m} \times 0.4 \text{ m}$ for E-3 and E-6. Each wall was confined by reinforced concrete around its perimeter. A load was applied to the masonry wall using air bags with dimensions of $1.2 \text{ m} \times 3 \text{ m}$ (Fig. 7).

The air bags were filled gradually until the ultimate cracking of the masonry walls. The thickness of mortar connecting the blocks of masonry units was 10 mm.

The results of this numerical experiment (W_e) were compared with those obtained by Varela et al. [10,11] using the spring–strut method (W_{ss}), and were previously compared with the results of previous studies conducted by Varela-Rivera et al. [9] using the yield-line method (W_{yl}), failure-line method (W_{fl}), and compressive strut method (W_{cs}). The yield-line method (W_{yl}) is theoretically not recommended for brittle materials such as masonry, but is still used to predict the out-of-plane strength of walls [4]. The failure-line method (W_{fl}) is a modification of the yield line method based on the idea that, prior to the formation of the final failure cracking pattern, some cracks are already formed, and their contribution to the internal work should not be included. For this reason, the failure line method predicts lower strength than the yield line method. The compressive strut method (W_{cs}) was proposed by Abrams et al. [6] for infill walls surrounded by concrete frames. In Abrams' work, an infill wall was subjected to uniform pressures. It was assumed that, after the formation of a given cracking pattern, a wall was divided into segments.

The structure and description of the walls and the FTM model proposed here are presented in Fig. 8. Results of FTM analysis are denoted by W_t and W_c . FTM results are presented and incorporated in Fig. 9.

The example calculations of b_{eff} and t_{eff} are as follows:

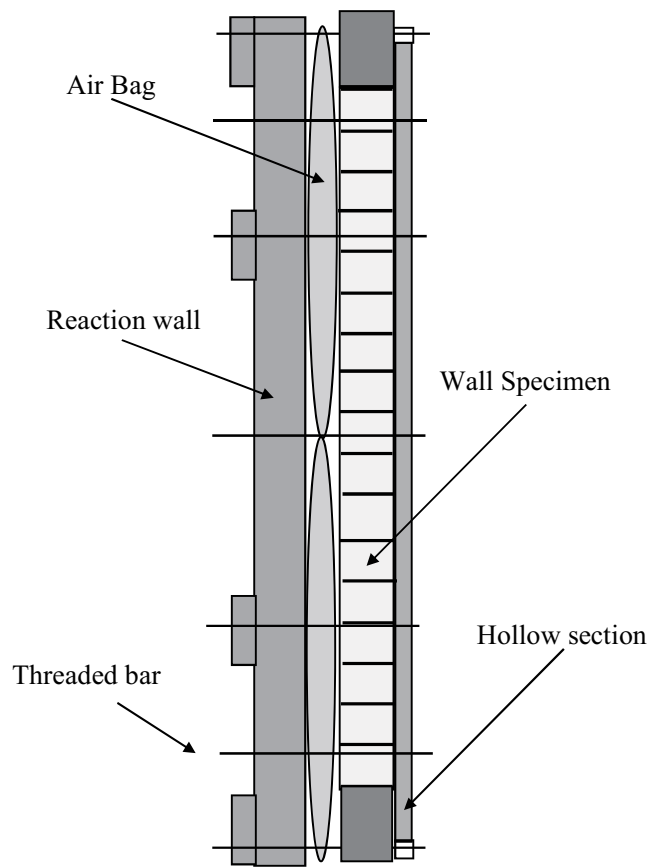
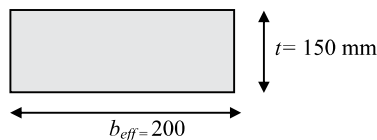


Fig. 7. Setup of air bag (source Herrera et al. [12]).

Table 2
Geometry, aspect ratio, and slenderness ratio of wall specimens.

Wall specimen	f_c (MPa)	f_j (MPa)	f_p (MPa)	f_m (MPa)	f_{tpe} (MPa)	f_{tpa} (MPa)	E_c (MPa)	Length L (m)	Height H (m)	Thickness t (m)	H/L	H/t
E-1	14.79	2.89	5.47	2.84	0.14	0.44	9614	3.67	2.72	0.15	0.74	18.13
E-2	19.16	2.34	5.47	2.84	0.14	0.44	10,943	3.77	2.88	0.15	0.76	19.20
E-3	19.80	2.47	4.09	2.45	0.11	0.36	11,124	3.77	2.88	0.12	0.76	24.00
E-4	15.31	2.79	5.47	2.84	0.14	0.44	9782	2.85	2.72	0.15	0.95	18.13
E-5	17.39	2.66	5.47	2.84	0.14	0.44	10,425	2.95	2.72	0.15	0.92	18.13
E-6	21.67	2.26	4.09	2.45	0.11	0.36	11,638	2.95	2.72	0.12	0.92	22.67

Data taken from Varela-Rivera et al. [9].

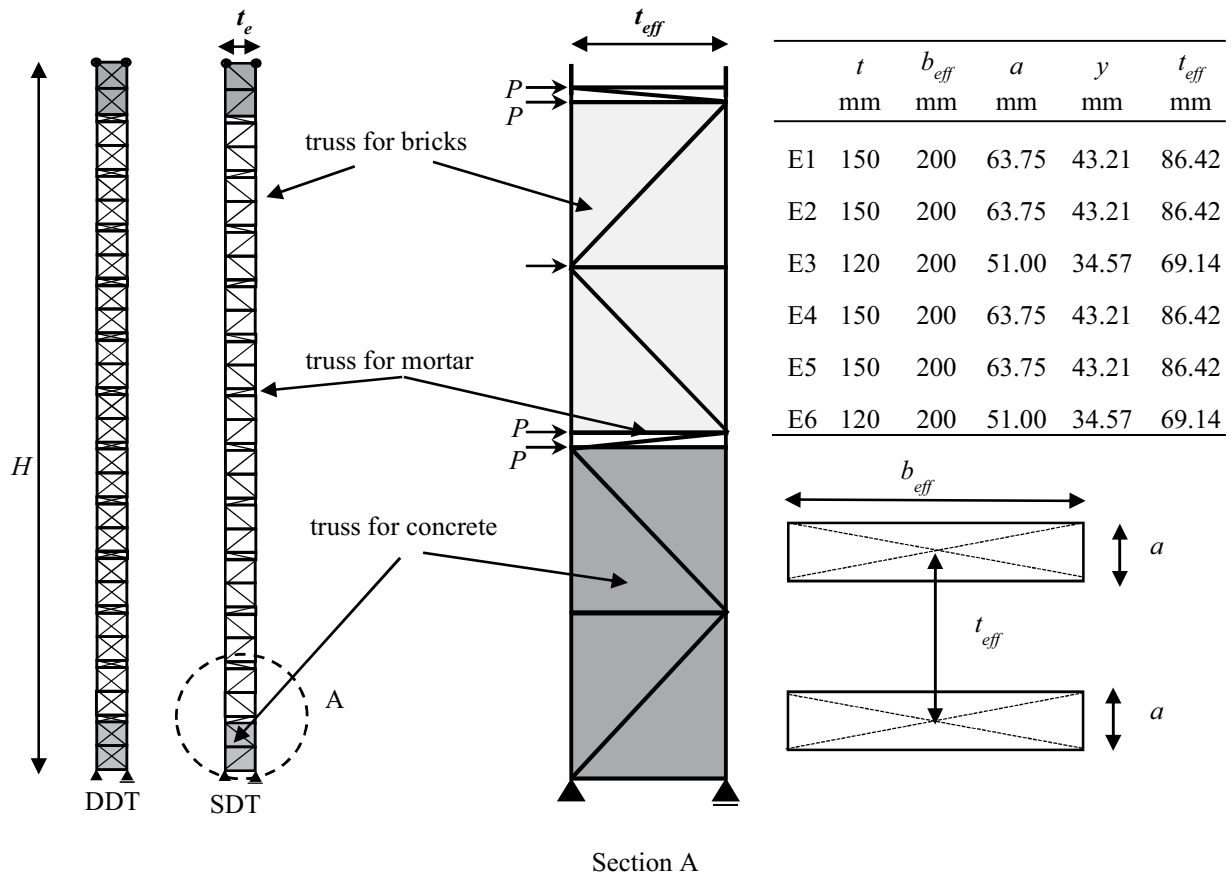


Fig. 8. FTM model for Varela Rivera's setup.

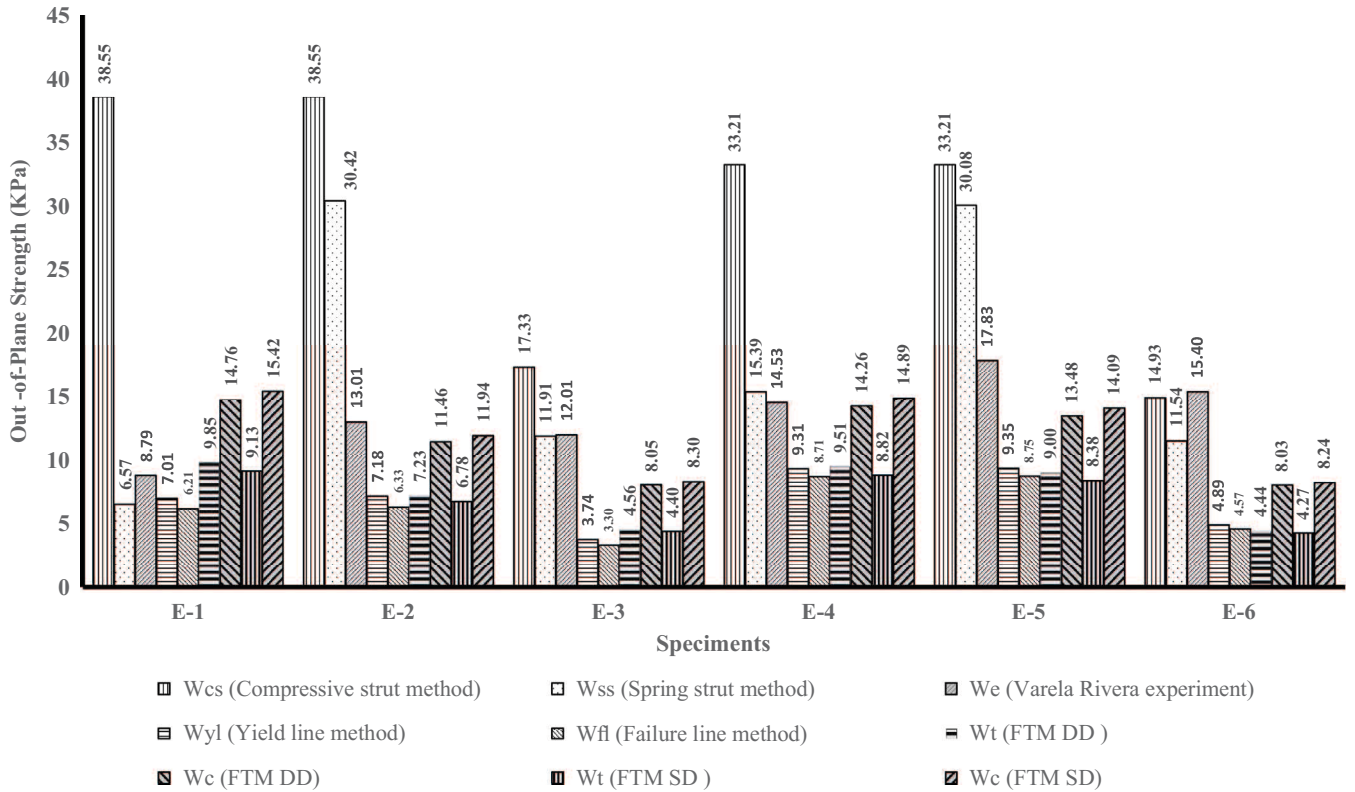
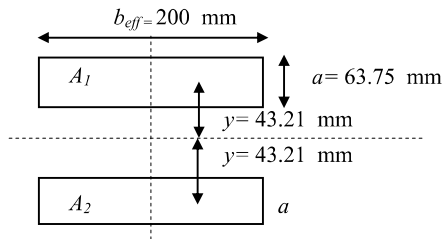


Fig. 9. Comparison of results for the first validation experiment.

$$I_{tot} = \frac{1}{12} b_{eff} t^2 = 56,250,000 \text{ mm}^4$$

$$c = 0.5 t, \beta = 0.85 \rightarrow a = c\beta = 75 \times 0.85 = 63.75 \text{ mm}$$



$$I_{eq} = \sum I_n + \sum A_n y^2$$

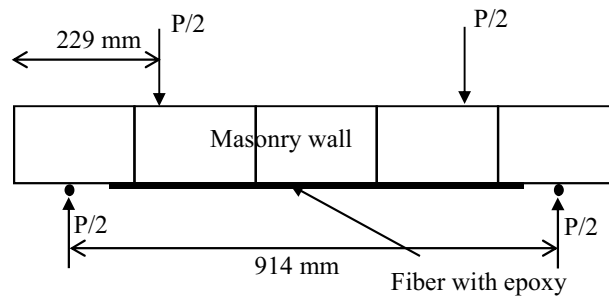
$$I_{eq} = 56,250,000 = I_{tot}$$

n	$I_n = 1/12 b_{eff} a^3$ (mm^4)	$A_n = b_{eff} a$ (mm^2)	y^2	(mm^4)
1	4,318,066.406	12,750	1,867.21	28,125,000
2	4,318,066.406	12,750	1,867.21	28,125,000
Σ	8,636,132.813		$I_{eq} =$	56,250,000

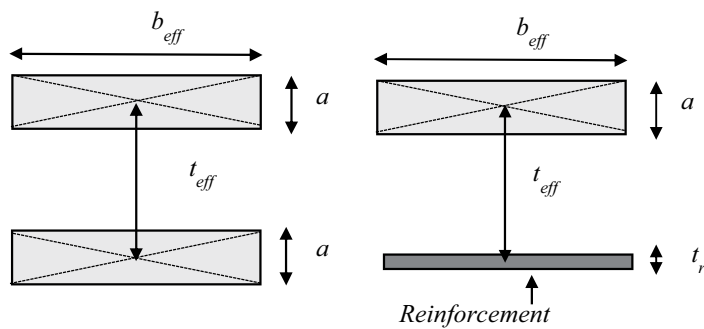
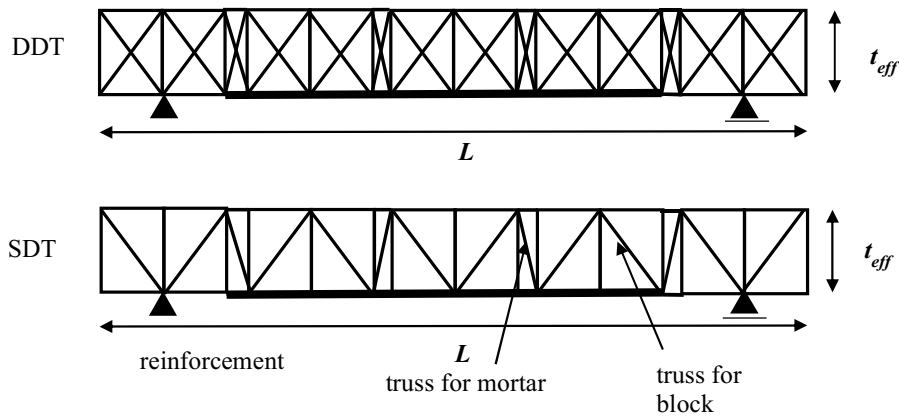
y is calculated by using the “goal seek” command in Microsoft Excel software or by Eq. (3):

$$y = \sqrt{\frac{I_{tot} - 2I_n}{2A_n}} = 43.21 \text{ mm}$$

The result is that $y = 43.21 \text{ mm}$; hereafter, $t_{eff} = 2y = 86.42 \text{ mm}$ and $t_w = 150.17 \text{ mm}$.FTM results are explained further in the Section 4.



(a) Hamoush test setup



L (mm)	H (mm)	t (mm)	b_{eff} (mm)	a (mm)	y (mm)	t_{eff} (mm)
600	900	200	200	85.00	38.89	77.78

(b) FTM model

Fig. 10. Hamoush's test setup and FTM model.

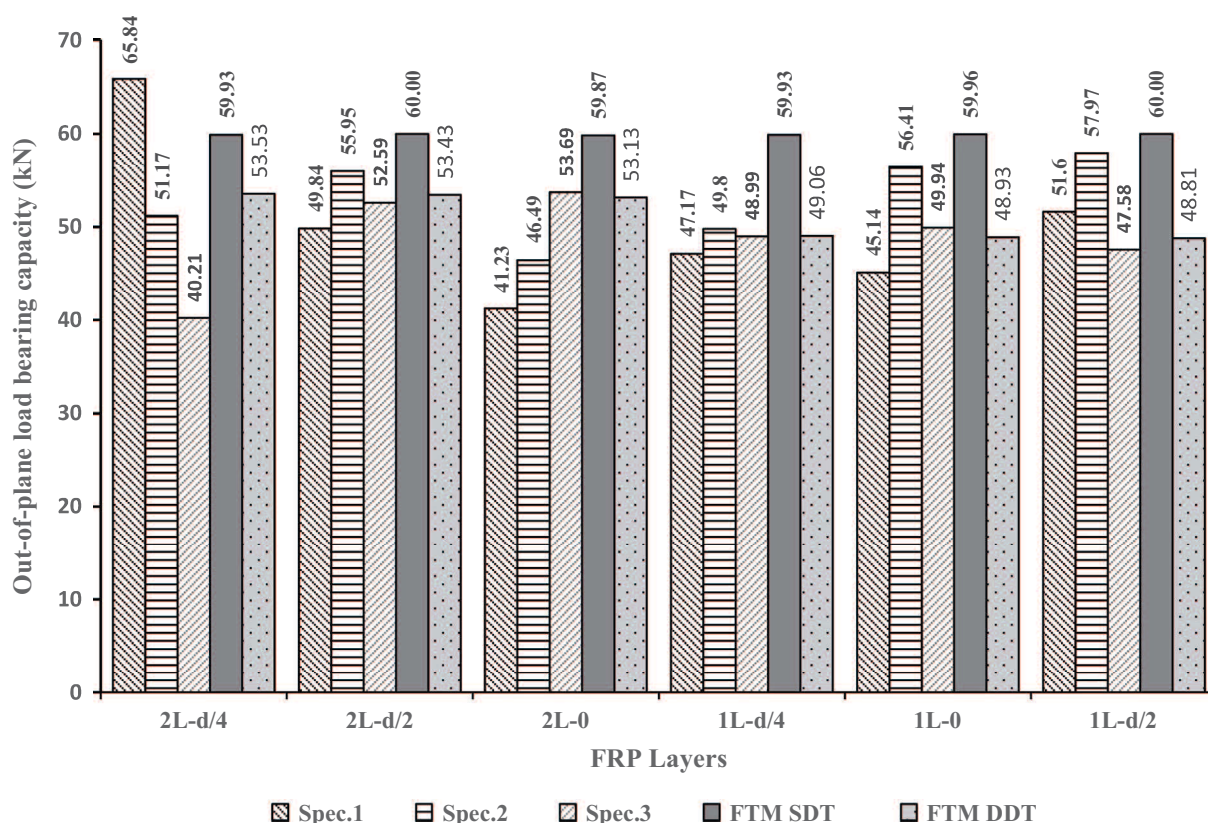


Fig. 11. Comparison of results for the second validation experiment.

Table 3
Properties of SikaWrap 230-C (unidirectional) CFRP and Sikadur 330 resin.

Properties of CFRP	Remarks of CFRP
Thickness (mm)	0.12
Tensile strength (MPa)	4100
Elastic modulus (MPa)	231,000
Ultimate tensile strain (%)	1.7%
Properties of resin	Remarks of resin
Tensile strength (MPa)	30
Elastic modulus (MPa)	3800

Data taken from Anil et al. [21].

3.2. Validation 2

The second validation of the FTM was conducted for a model used by Hamoush et al. [29], who investigated the behavior of a surface-reinforced masonry wall under out-of-plane loading. The wall was reinforced with FRP and had dimensions of 900 mm × 600 mm × 200 mm. There were 18 specimens in total. Specimens had a single or double layer of FRP and a distance from the fiber to the support of 0, $d/2$, or $d/4$, where d is the span from the support to the first of point load on the masonry wall specimen. Specimens were constructed with hollow bricks made from mortar with a thickness of 25 mm. A single hollow block unit had two holes. The dimensions of a hollow block were 400 mm × 200 mm × 200 mm. The thickness of the HB was the effective compressed zone in this validation. The web fiber used in the validation was constructed with Tyfo Hi-Clear epoxy resin with an ultimate tensile strength of 414 MPa, ultimate elongation of 2.0%, elastic modulus of 27,580 MPa, and design thickness of 0.4 mm per layer. The Hamoush test setup and FTM model are shown in Fig. 10.

The height (t_{eff}) of the truss was the center distance between the top and bottom of the hollow block.

Several methods can be used to analyze the FTM, such as the consistent deformation method, matrix method, finite element method, or FE software. Here, we analyzed the FTM structure using FE software using material properties taken from the literature as input data. The results of this validation are presented in Fig. 11. The FTM results compared with the three experimental specimen results are explained in the Section 4.

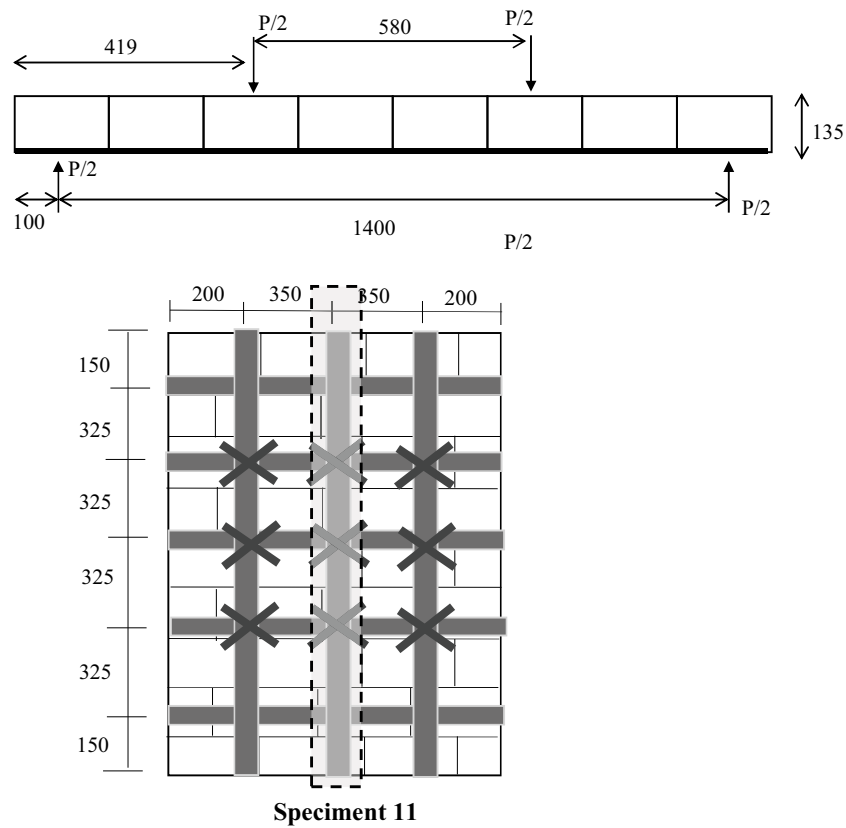
3.3. Validation 3

The third validation of the FTM was conducted for low-quality brick considered by Anil et al. [21]. The brick had a strength of 2.5 MPa, hollow ratio of 65%, and dimensions of 185 mm × 185 mm × 135 mm. The mortar was of higher strength (5.2–7.1 MPa). The dimensions of the masonry walls were 1600 mm × 1100 mm × 135 mm. CFRP was coated on the side adjacent to the load side to retrofit the walls. The properties of the CFRP are given in Table 3. The test setup is presented in Fig. 12.

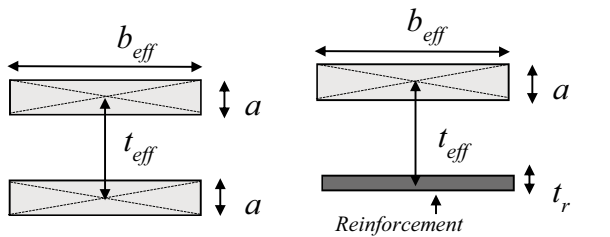
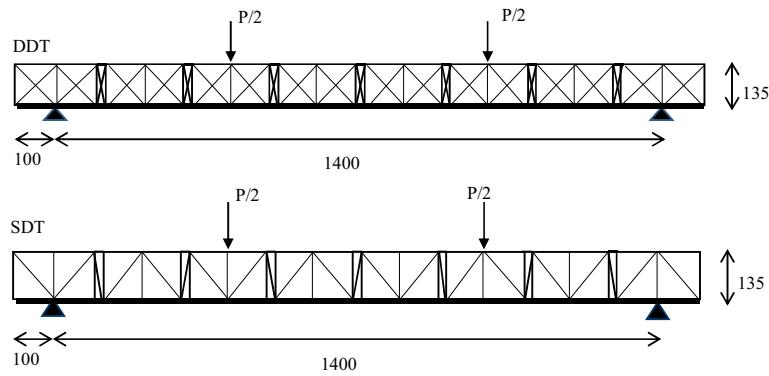
The CFRP was used in diverse arrays with different anchor arrangements and different combinations of vertical, horizontal, and diagonal arrangements. The CFRP arrangements were applied to 11 samples. Five sample results obtained using the FTM in this validation were satisfactory, as presented in Fig. 13. The results are close to the experimental values.

4. Discussion

The use of FTM to analyze a confined masonry wall under out-of-plane loading was convincing in the first validation. The maximum pressure generated by the FTM (i.e., the strength of the wall) is given in Fig. 9 and on Table 4. W_t and W_c are the pressures



(a) Anil's test setup



L (mm)	H (mm)	t (mm)	b_{eff} (mm)	a (mm)	y (mm)	t_{eff} (mm)
1100	1600	135	185	37.29	52.50	105.00

(b) FTM model

Fig. 12. Anil's test setup and FTM model.

required to produce forces on the tension truss and compression truss, respectively, that cause the wall to fail. Experimental results obtained by Varela-Rivera et al. [9] and displayed in Fig. 9 revealed

that specimens with similar aspect and slenderness ratios (E-1 and E-2; E-4 and E-5) have a lower out-of-plane strength than specimens with lower in-plane stiffness (E-1 and E-4). In the case of

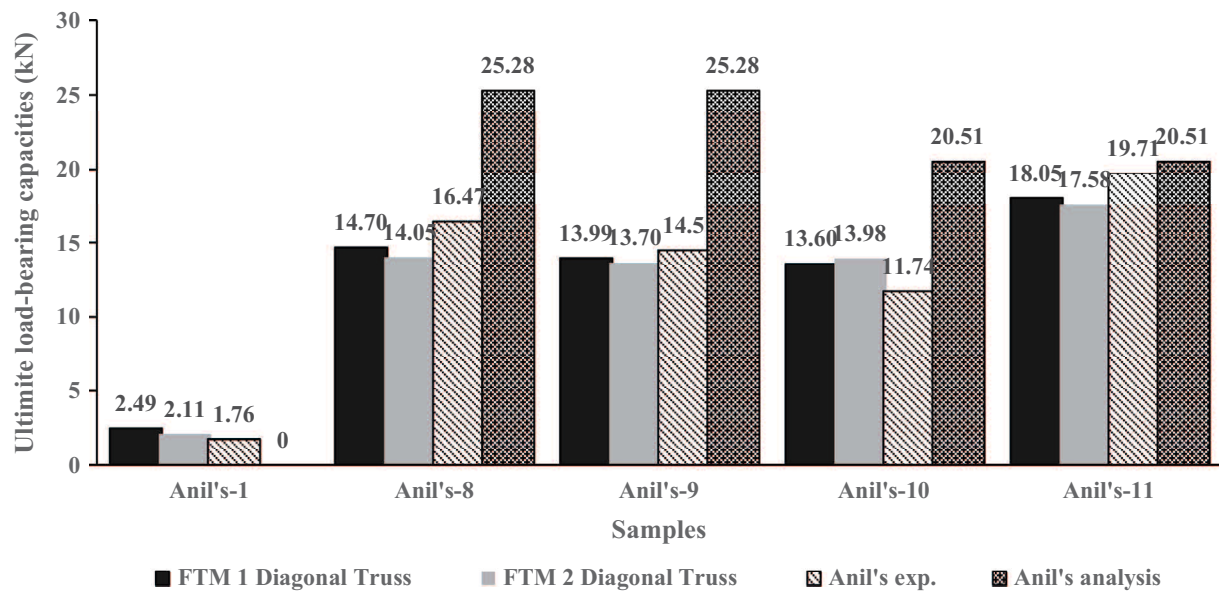


Fig. 13. Comparison of results for the third validation experiment.

Table 4
Comparison of FTM with Varela Rivera's experimental results and various analysis methods.

Wall specimen (kPa)	E-1	E-2	E-3	E-4	E-5	E-6	
W_e (Varela Rivera experiment)	8.79	13.01	12.01	14.53	17.83	15.40	
W_{yl} (Yield line method)	7.01	7.18	3.74	9.31	9.35	4.89	
W_{fl} (Failure line method)	6.21	6.33	3.30	8.71	8.75	4.57	
W_{cs} (Compressive strut method)	38.55	38.55	17.33	33.21	33.21	14.93	
W_{ss} (Spring strut method)	6.57	30.42	11.91	15.39	30.08	11.54	
Double Diagonal	W_t (FTMDD)	9.85	7.23	4.56	9.51	9.00	4.44
	δ (mm)	13.22	14.89	18.72	12.82	12.26	15.07
	W_c (FTMDD)	14.76	11.46	8.05	14.26	13.48	8.03
	δ (mm)	19.81	23.60	33.08	19.21	18.37	27.30
Single Diagonal	W_t (FTMSD)	9.13	6.78	4.40	8.82	8.38	4.27
	δ (mm)	12.67	14.29	17.08	12.28	11.81	14.88
	W_c (FTMSD)	15.42	11.94	8.30	14.89	14.09	8.24
	δ (mm)	21.40	25.15	32.27	20.74	19.85	28.73

specimens with similar aspect ratios and in-plane stiffness (E-2 and E-3; E-5 and E-6), W_e is greater for specimens with smaller slenderness ratios (E-2 and E-5). The difference is related to the greater axial compressive strength of the block. The same behavior is seen in the above results obtained using the FTM. In contrast, the yield-line method and failure-line method underestimate W_e .

The FTM provides the strength resulting from a compression crack W_c and the strength resulting from a tension crack W_t . W_c represents the value of the strength resulting from an experimental crack W_e (E-2, E-3, E-4 and E-5); W_e is similar to W_c . The strength of masonry using W_{cs} (the compressive strut method) and W_{ss} (the spring-strut-method) overestimated W_e ; this comparison is similar to that for W_t and W_c obtained in FTM analysis. These results are consistent with the effects of the slenderness ratio of a masonry structure in that the thickness of the masonry structure affects the pressure needed for the structure to fail. W_t and W_c were slightly greater than W_{yl} and W_e .

The FTM provided a value close to the experimental result (W_e) and the result of the spring-strut method (W_{ss}). However, W_c was a greater than W_e while W_t was lower than W_e for specimen E-1 owing to the difference in the rigidity of confinement. The rigidity of confinement depends on the reinforcement factor; this will be considered in the next FTM study.

W_t appears almost identical to W_{yl} and W_{fl} . This indicates that the previous method of obtaining W_{yl} and W_{fl} can only be used at one stage of cracking. The previous method can be applied only to a confined masonry wall. The above comparison reveals that FTM is useful in analyzing the strength of confined masonry walls.

The percentage of error (PoE) comparison between FTM and experimental and analysis results can be seen in Table 5. It is shown that for W_e (E-1) relative to FTM (W_t), PoE values are 3.9–12.1%; for E-2, E-4, and E-5 relative to W_c , PoE values are 1.9–20.9%; for W_{yl} relative to W_t , PoE values are 0.7–21.8%; for W_{fl} (E-2, E-4, E-5 and E-6) relative to W_t , the PoE values are 1.2–14.2%; for W_{ss} (E-4 and E-6) relative to W_c , PoE values are 3.3%, 7.4%, and 28.6%, and only W_{cs} relative to W_t or W_c have PoE values greater than 30%." From these results it is seen that the first crack of a masonry structure can be caused by tensile stress or compressive stress.

In the second validation, FRP was used to provide tension on the truss element. Results obtained with FTM show that the addition of FRP strengthens masonry structures, which is in line with the results of experiments. The FRP would fail before cracking appears in the area of compression [29]. The FTM reveals that the tensile load does not reach a maximum and that there is cracking as a result of compressive strain.

Table 5
Percentage of error of FTM method relative to Varela Rivera's experiment and analysis method results.

Wall specimen (kPa)	E-1	E-2	E-3	E-4	E-5	E-6
We (Varela Rivera experiment)	8.79	13.01	12.01	14.53	17.83	15.40
Wt (FTMDD)	9.85	7.23	4.56	9.51	9.00	4.44
% of error	12.06	44.41	62.06	34.53	49.53	71.20
Wt (FTMSD)	9.13	6.78	4.40	8.82	8.38	4.27
% of error	3.85	47.88	63.40	39.33	52.98	72.27
Wc (FTMDD)	14.76	11.46	8.05	14.26	13.48	8.03
% of error	67.95	11.88	32.95	1.88	24.38	47.83
Wc (FTMSD)	15.42	11.94	8.30	14.89	14.09	8.24
% of error	75.4	8.3	30.9	2.5	20.9	46.5
Yield line method						
Wall specimen	E-1	E-2	E-3	E-4	E-5	E-6
Wyl (Yield line method)	7.01	7.18	3.74	9.31	9.35	4.89
Wt (FTMDD)	9.85	7.23	4.56	9.51	9.00	4.44
% of error	40.52	0.72	21.83	2.18	3.76	9.29
Wt (FTMSD)	9.13	6.78	4.40	8.82	8.38	4.27
% of error	30.22	5.56	17.54	5.31	10.33	12.69
Wc (FTMDD)	14.76	11.46	8.05	14.26	13.48	8.03
% of error	110.60	59.67	115.33	53.13	44.20	64.30
Wc (FTMSD)	15.42	11.94	8.30	14.89	14.09	8.24
% of error	119.95	66.23	122.06	59.92	50.75	68.52
Failure line method						
Wall specimen	E-1	E-2	E-3	E-4	E-5	E-6
Wfl (Failure line method)	6.21	6.33	3.30	8.71	8.75	4.57
Wt (FTMDD)	9.85	7.23	4.56	9.51	9.00	4.44
% of error	58.62	14.25	38.08	9.22	2.84	2.94
Wt (FTMSD)	9.13	6.78	4.40	8.82	8.38	4.27
% of error	47.00	7.13	33.21	1.22	4.18	6.57
Wc (FTMDD)	14.76	11.46	8.05	14.26	13.48	8.03
% of error	137.73	81.11	144.04	63.68	54.09	75.80
Wc (FTMSD)	15.42	11.94	8.30	14.89	14.09	8.24
% of error	148.28	88.55	151.66	70.94	61.08	80.32
Compressive strut method						
Wall specimen	E-1	E-2	E-3	E-4	E-5	E-6
Wcs (Compressive strut method)	38.55	38.55	17.33	33.21	33.21	14.93
Wt (FTM DD)	9.85	7.23	4.56	9.51	9.00	4.44
% of error	74.4	81.2	73.7	71.4	72.9	70.3
Wt (FTM SD)	9.13	6.78	4.40	8.82	8.38	4.27
% of error	76.3	82.4	74.6	73.5	74.8	71.4
Wc (FTM DD)	14.76	11.46	8.05	14.26	13.48	8.03
% of error	61.7	70.3	53.5	57.1	59.4	46.2
Wc (FTM SD)	15.42	11.94	8.30	14.89	14.09	8.24
% of error	60.0	69.0	52.1	55.2	57.6	44.8
Spring strut method						
Wall specimen	E-1	E-2	E-3	E-4	E-5	E-6
Wss (Spring strut method)	6.57	30.42	11.91	15.39	30.08	11.54
Wt (FTM DD)	9.85	7.23	4.56	9.51	9.00	4.44
% of error	49.93	76.23	61.74	38.19	70.08	61.56
Wt (FTM SD)	9.13	6.78	4.40	8.82	8.38	4.27
% of error	38.95	77.71	63.09	42.72	72.13	63.00
Wc (FTM DD)	14.76	11.46	8.05	14.26	13.48	8.03
% of error	124.70	62.31	32.38	7.37	55.18	30.38
Wc (FTM SD)	15.42	11.94	8.30	14.89	14.09	8.24
% of error	134.68	60.76	30.27	3.26	53.14	28.59

Table 6
Comparison of FTM relative to Hamoush's experiment.

	Distance of fiber to support											
	2L-d/4		2L-d/2		2L-0		1L-d/4		1L-0		1L-d/2	
	Max. load kN	δ , mm	Max. load kN	δ , mm	Max. load kN	δ , mm	Max. load kN	δ , mm	Max. load kN	δ , mm	Max. load kN	δ , mm
Spec.1	65.84	2.47	49.84	3.33	41.23	2.69	47.17	2.87	45.14	4.05	51.6	2.75
Spec.2	51.17	2.10	55.95	2.71	46.49	3.22	49.80	3.76	56.41	2.60	57.97	3.23
Spec.3	40.21	1.75	52.59	4.49	53.69	3.53	48.99	3.25	49.94	3.05	47.58	2.76
Average	52.41	2.11	52.79	3.51	47.14	3.15	48.65	3.29	50.50	3.23	52.38	2.91
FTMSD	59.93	3.17	60.00	3.38	59.87	3.34	59.93	3.17	59.96	5.36	60.00	5.48
% of error	14.35	50.43	13.65	3.62	27.01	6.13	23.17	3.77	18.75	65.71	14.55	88.08
FTMDD	53.53	2.62	53.43	2.63	53.13	2.63	49.06	3.67	48.93	3.69	48.81	3.72
% of error	2.15	24.15	1.21	25.20	12.72	16.50	0.83	11.42	3.10	14.22	6.82	27.84

Table 7

Comparison of FTM to Anil' experiment and analysis results.

	Anil's-1		Anil's-8		Anil's-9		Anil's-10		Anil's-11	
	Load kN	δ . mm								
Anil's experiment	1.76	0.91	16.47	8.14	14.50	5.83	11.74	7.10	19.71	10.93
Anil's Analysis	–		25.28		25.28		20.51		20.51	
FTMSD	2.16	3.72	16.48	24.56	16.71	23.32	10.10	20.77	17.70	33.15
% of error	22.67		0.07		15.22		13.98		10.18	
FTMDD	1.84	3.58	16.28	29.05	16.86	22.66	9.60	22.75	16.14	31.19
% of error	4.27		1.16		16.28		18.21		18.09	

Fig. 11 and Table 6 shows that cracking, as a result of the truss tension obtained with the FTM, is similar to the experimental result. The percentage of error in this validation for all comparisons was between 0.82 and 27.01%.

The addition of the FRP layer provides a peak load before cracking that is higher than that for a single layer along with an increase in the loading capacity. Similarly, the two layers reduce the deformation of the structure. Apparently, retrofitting using a single layer and retrofitting using a double layer are similar under tension of the truss element, but the double layer provides different compressive strengths for the compression of the truss element. A double layer of FRP increases structural integrity, especially when the FRP layers extend to the supports [29]. Various installations of a single layer of FRP strengthen the system only slightly.

Fig. 13 and Table 7 compare the results obtained using FTM with the experimental and analytical results of Anil et al. [21] in the third validation experiment. The FTM was used in cases with and without CFRP.

The diagonal modeling of CFRP in this validation is not applicable because the diagonal combination of CFRP strips is not handled in the two-dimensional FTM; it could be applied in three-dimensional FTM. Therefore, only certain reinforcements are used in this case, namely the reinforcements of samples 1, 8, 9, 10, and 11.

Sample 1 did not use CFRP and cracked at low load in sample 10. FTM values overestimated the load capacities compared with experimental values. For sample numbers 8, 9, and 11, FTM underestimated the load capacity results found by analysis. The average overestimation of samples 1 and 10 were around 4.27% (FTMDD) and 13.98% (FTMSD) of the load capacity values, and the average underestimation of samples 8, 9, and 11 were between 0.07% (FTMSD) and 130.0.98% (FTMSD) of the load capacity values. The load capacity then increased as CFRP was applied and the truss element was compressed. FTM provided results similar to the experimental results, although there were slight differences owing to the modeling of the anchor in the FTM models. The analysis of Anil et al. [21] overestimated the results obtained using FTM and the results obtained in experiments. Anil et al. did not record an analysis of sample 1.

5. Conclusions

FTM was applied to a wide variety of planar masonry structures, both confined and unconfined as well as both with and without reinforcement. The structures corresponded to a simple beam, cantilever, distributed load, and concentrated load. The following conclusions are drawn from the results of validation tests on FTM.

- FTM can be applied to various conditions of masonry structure models subject to out-of-plane loading. Specifically, FTM can be applied to a structure having an aspect ratio less than 1.
- FTM produces satisfactory results if the reinforcement of the masonry structure is uniform in direction and runs parallel to the span of the structure. However, diagonal reinforcement is difficult to model using FTM.

- FTM overcomes problems faced by previous methods because it reproduces compression and tension failures.

FTM is expected to serve as a tool for evaluating the strength of a masonry wall under out-of-plane loading. The FTM's effectiveness in three-dimensional modeling of walls will be investigated further in future work. The FTM will thus be of use to both academics and practitioners.

References

- [1] S. Noor-E-Khuda, M. Dhanasekar, D. Thambiratnam, An explicit finite element modelling method for masonry walls under out-of-plane loading, *Eng. Struct.* 113 (2016) 103–120.
- [2] J. Gilstrap, C. Dolan, Out-of-plane bending of FRP-reinforced masonry walls, *Compos. Sci.* 58 (8) (1998) 1277–1284.
- [3] X. Zhang, S. Singh, D. Bull, N. Cooke, Out-of-plane performance of reinforced masonry walls with openings, *J. Struct. Eng.* 127 (1) (2001) 51–57.
- [4] R. Drysdale, A. Essawy, Out-of-plane bending of concrete block walls, *J. Struct. Eng.* 114 (1) (1988) 121–133.
- [5] M. Griffith, J. Vaculik, Out-of-plane flexural strength of unreinforced clay brick masonry walls, *TMS J.* (2007).
- [6] D. Abrams, R. Angel, J. Uzarski, Out-of-plane strength of unreinforced masonry infill panels, *Earthq. Spectra* 12 (4) (1996) 825–844.
- [7] R. Henderson, K. Fricke, W. Jones, J. Beavers, R. Bennett, Summary of a large and small-scale unreinforced masonry infill test program, *J. Struct. Eng.* 129 (12) (2003) 1667–1675.
- [8] Y. Tu, T. Chuang, P. Liu, Y. Yang, Out-of-plane shaking table tests on unreinforced masonry panels in RC frames, *Eng. Struct.* 32 (12) (2010) 3925–3935.
- [9] J. Varela-Rivera, D. Navarrete-Macias, L. Fernandez-Baqueiro, E. Moreno, Out-of-plane behaviour of confined masonry walls, *Eng. Struct.* 33 (5) (2011) 1734–1741.
- [10] J. Varela-Rivera, J. Moreno-Herrera, I. Lopez-Gutierrez, L. Fernandez-Baqueiro, Out-of-plane strength of confined masonry walls, *J. Struct. Eng.* 138 (11) (2012) 1331–1341.
- [11] J. Varela-Rivera, M. Polanco-May, L. Fernandez-Baqueiro, E. Moreno, Confined masonry walls subjected to combined axial loads and out-of-plane uniform pressures, *Can. J. Civil Eng.* 39 (4) (2012) 439–447.
- [12] J. Moreno-Herrera, J. Varela-Rivera, L. Fernandez-Baqueiro, Out-of-plane design procedure for confined masonry walls, *J. Struct. Eng.* 142 (2) (2016) 04015126.
- [13] J. Dawe, C. Seah, Out-of-plane resistance of concrete masonry infilled panels, *Can. J. Civil Eng.* 16 (6) (1989) 854–864.
- [14] P. Agnihotri, V. Singhal, D. Rai, Effect of in-plane damage on out-of-plane strength of unreinforced masonry walls, *Eng. Struct.* 57 (2013) 1–11.
- [15] L. La Mendola, M. Accardi, C. Cucchiara, V. Licata, Nonlinear FE analysis of out-of-plane behaviour of masonry walls with and without CFRP reinforcement, *Constr. Build. Mater.* 54 (2014) 190–196.
- [16] G. Milani, M. Pizzoloto, A. Tralli, Simple numerical model with second order effects for out-of-plane loaded masonry walls, *Eng. Struct.* 48 (2013) 98–120.
- [17] P. Asteris, L. Cavaleri, F. Di Trapani, A. Tsaris, Numerical modelling of out-of-plane response of infilled frames: state of the art and future challenges for the equivalent strut macromodels, *Eng. Struct.* 132 (2017) 110–122.
- [18] L. Cavaleri, M. Fossetti, M. Papia, Modeling of out-of-plane behavior of masonry walls, *J. Struct. Eng.* 135 (12) (2009) 1522–1532.
- [19] D. Dizhur, M. Griffith, J. Ingham, Out-of-plane strengthening of unreinforced masonry walls using near surface mounted fibre reinforced polymer strips, *Eng. Struct.* 59 (2014) 330–343.
- [20] C. Willis, R. Seracino, M. Griffith, Out-of-plane strength of brick masonry retrofitted with horizontal NSM CFRP strips, *Eng. Struct.* 32 (2) (2010) 547–555.
- [21] Ö. Anil, M. Tatayoglu, M. Demirhan, Out-of-plane behavior of unreinforced masonry brick walls strengthened with CFRP strips, *Constr. Build. Mater.* 35 (2012) 614–624.
- [22] N. Ismail, J. Ingham, In-plane and out-of-plane testing of unreinforced masonry walls strengthened using polymer textile reinforced mortar, *Eng. Struct.* 118 (2016) 167–177.

- [23] A. Furtado, H. Rodrigues, A. Arêde, H. Varum, Experimental evaluation of out-of-plane capacity of masonry infill walls, *Eng. Struct.* 111 (2016) 48–63.
- [24] Y. Lu, M. Panagiotou, Three-dimensional cyclic beam-truss model for nonplanar reinforced concrete walls, *J. Struct. Eng.* 140 (3) (2014) 04013071.
- [25] M. Moharrami, I. Koutromanos, M. Panagiotou, Nonlinear truss modeling method for the analysis of shear failures in reinforced concrete and masonry structures, *Improving the Seismic Performance of Existing Buildings and Other Structures*, 2015, 74–85.
- [26] J. Almeida, P. Lourenco, J. Barros, Characterization of brick and brick-mortar interface under uniaxial tension, in: VII International Seminar on Structural Masonry for Developing Countries, 2002.
- [27] H. Kaushik, D. Rai, S. Jain, Stress-strain characteristics of clay brick masonry under uniaxial compression, *J. Mater. Civ. Eng.* 19 (9) (2007) 728–739.
- [28] CEN 1999, Eurocode 6: Design of Masonry Structures-Part-1-1: General Rules for Reinforced and Unreinforced Masonry Structures, European Committee for Standardization, 2005. 125.
- [29] S. Hamoush, M. McGinley, P. Mlakar, M. Terro, Out-of-plane behavior of surface-reinforced masonry walls, *Constr. Build. Mater.* 16 (6) (2002) 341–351.
- [30] K. Martini, Finite element studies in the out-of-plane failure of unreinforced masonry, in: C.K. Choi (Ed.), Proc., 7th Int. Conf. on Computing in Civil and Building Engineering, Korea, 1997, pp. 179–184.
- [31] SAP2000, Version 17.3.0 Build 1158, Structural Analysis Program, Berkeley, (CA), Computer and Structure, Inc., 2015.
- [32] Standart Nasional Indonesia SNI 03-2847-2013, Persyaratan Beton Struktural untuk Bangunan Gedung. Badan Standarisasi Nasional (BSN), Jakarta, 2013.